SOME ASPECTS OF THE SEDIMENTOLOGY OF THE SUPERFICIAL DEPOSITS OF THE EDEN ESTUARY, FIFE, SCOTLAN

Keith M. Eastwood

A Thesis Submitted for the Degree of PhD
at the
University of St. Andrews

1977

Full metadata for this item is available in
Research@StAndrews:FullText
at:
http://research-repository.st-andrews.ac.uk/

Please use this identifier to cite or link to this item:
http://hdl.handle.net/10023/2692

This item is protected by original copyright

SOME ASPECTS OF THE SEDIMENTOLOGY OF THE SUPERFICIAL DEPOSITS OF THE EDEN ESTUARY, FIFE, SCOTLAN

Keith M. Eastwood

A Thesis Submitted for the Degree of PhD
at the
University of St. Andrews

1977

Full metadata for this item is available in
Research@StAndrews:FullText
at:
http://research-repository.st-andrews.ac.uk/

Please use this identifier to cite or link to this item:
http://hdl.handle.net/10023/2691

This item is protected by original copyright

SOME ASPECTS OF THE SEDIMENTOLOGY OF THE SUPERFICIAL DEPOSITS OF THE EDEN ESTUARY, FIFE, SCOTLAND

being a thesis presented by

KEITH M. EASTWOOD

to the University of St. Andrews

in application for the degree of

Doctor of Philosophy

BIBLIOTHECA UNIVERSITATIS ST. ANDREAS

BEST COPY

AVAILABLE

Variable print quality

VOLUME CONTAINS CLEAR OVERLAYS

OVERLAYS SCANNED SEPERATELY AND OVER THE RELEVANT PAGE.

CERTIFICATION

I certify that Keith M. Eastwood has been engaged in research for the equivalent of 13 full terms at the University of St. Andrews, that he has fulfilled the conditions of Ordinance No. 16 and that he is qualified to submit the accompanying thesis in application for the degree of Doctor of Philosophy.

[redacted]

DECLARATION

I certify that the following thesis is based on the results of research carried out by me, that it is my own composition and that it has not previously been presented for [illegible] degree.

[redacted]

CAREER

In 1970 I obtained the degree of B.Sc. (Hons) from the University of Newcastle-upon-Tyne.

I was then employed as a mine geologist by Consolidated Gold Fields until 1972.

I registered as a research student at the University of St. Andrews in September 1972 and performed research for this thesis until December 1975.

I am now employed as a Petroleum Engineer by the Nederlandse Aardolie Maatschappij B.V. in the Netherlands.

CONTENTS

FIGURES

Text figures have been inserted in groups at the ends of sections within chapters:

PREFACE

Little attention has previously been given to the sediments of the Eden estuary, Fife, Scotland. This research was performed in order to identify, delineate and account for the observed sedimentary facies in the superficial sediments of the intertidal zone.

The research was carried out whilst I was in the receipt of a N.E.R.C. research studentship for which I am grateful.

I should like to thank Professor E.K. Walton for his supervision of the work. Thanks are due also to Dr. W.E. Stephens for help with computing and statistical matters. Special thanks go to George Tacker for his excellent untiring assistance in the field, and to Jim Allen for photographic work.

I am also grateful to the following institutions: the Tay Estuary Research Centre, Newport-on-Tay, for the loan of equipment; the Royal Air Force, Leuchars, for taking air photographs of the estuary; and the Radiography Department of the Memorial Cottage Hospital, St. Andrews, for allowing me to use their facilities.

Final thanks go to my wife, Freda, for constant encouragement and for typing the manuscript.

SUMMARY

The stratigraphic framework of the superficial sediments of the Eden estuary consists of the post-Glacial Carse sequence as defined by Chisholm (1971).

Coastal processes affect a redistribution of sediment in the lower estuary which, historically, has produced dramatic changes in the areal distribution of land and sea. In the middle and upper estuary sediment redistribution is limited, and the distribution of land and water is relatively stable. At the entrance to the Eden estuary the north shore tends to be retreating landwards, whereas the south shore is prograding seawards.

Measurements and observation of water circulation patterns in the estuary showed that sediment redistribution in the lower estuary may be explained by the importance of wave action to the south of the Eden channel and flood-tidal current activity to the north of the channel.

Measurements of velocity and salinity profiles showed that:

(a) an asymmetry exists between the time of maximum flood and ebb currents relative to high water. Maximum flood currents occurred consistently between 1.5 and 1.8 hours before high water and maximum ebb currents between 3 and 4 hours after high water. In general, maximum ebb velocities were greater than those of the flood.

(b) the time of occurrence of maximum salinities relative to high water varies systematically throughout the estuary. In the lower estuary maximum salinities occurred before high water, in the middle estuary the time of maximum salinity and high water were coincident, and in the upper estuary maximum salinities occurred after high water.

(c) no single classification could be assigned to the Eden estuary, although it may be stated that it is tide-dominated, and under 'average'

conditions it would be a Pritchard type C or 'vertically homogeneous' estuary.

The superficial sediments of the middle estuary are dominated by structures of biogenic origin. Primary sedimentary structures are almost completely obliterated. Shell concentrates are widespread and in origin may be related to the living habits of the lugworm Arenicola marina.

Two major intertidal sand bodies, termed flood and ebb-tidal deltas, occur in the lower estuary. These topographic features bear smaller bedforms which record the response of sediment to reversing current flow. On the flood-tidal delta both flood and ebb-orientated bedforms were present. Flood-orientated bedforms were sand-waves, whereas ebb-orientated bedforms were megaripples. Certain topographic features within the flood-tidal delta serve to divert ebb-tidal currents around the delta and this, coupled with the asymmetry in time of maximum flood and ebb-tidal currents, allows flood-orientated bedforms to be preserved. On the ebb-tidal delta, which effectively terminates the Eden channel, all bedforms are ebb-orientated and sand-waves predominate. Internal sedimentary structures of the flood-tidal delta show a prominent flood orientation. This is at variance with the surface expression of the bedforms which exhibit subequal numbers of flood- and ebb-orientated features. The internal structures illustrate the importance of flood-tidal currents in the formation of this sand-body and the secondary nature of the ebb-tidal currents which serve only to modify the surface features.

As a group the estuary sands may be classified as sublitharenites with quartz averaging 62.45%, orthoclase 14.45%, plagioclase 4.47% and lithic fragments 18.63%. Heavy minerals average $\frac{1}{2}$ wt% of the fine sand fraction, but this value increases rapidly in the vicinity of the Eden channel. Detrital calcium carbonate in the form of shell

fragments may account for up to 16.8 wt% of some samples from the middle estuary, which may be considered the factory area for carbonate detritus. Quartz grain-surface microtextures showed great variety, but types which might be considered of glacial origin with aqueous overtones are predominant.

The clay fraction of the estuary sediments consists of illite 56%, kaolinite and chlorite in subequal amounts totalling 41%, and montmorillonite 3%. Clay mineral suites are polluted by kaolinite-bearing effluent from Guardbridge paper mill.

Textural analysis showed that eight sediment sub-populations control the textural variation in the superficial sediments of the Eden estuary. Fine sand is the basic sub-population with which all others are mixed in varying proportions. Intertidal flat textural variation is primarily produced by the addition of medium sand and/or silt and clay to the fine sand sub-population.

Seven textural facies were identified in the Eden estuary: four in the sediments of the intertidal flats and three in the channel sediments. Each facies has textural attributes which are believed to have originated in the depocentre, that is, they are a response to transportational and depositional processes within the estuary.

Chapter 1 INTRODUCTION

I. AREA OF RESEARCH

The estuary of the River Eden is situated on the north-east coast of Fife, Scotland, between the town of St. Andrews and the mouth of the Firth of Tay (Fig. 1.1).

The general shape of the intertidal zone is triangular with a north-south trending base 5.6 km long and the apex 7 km to the west. The north, south and west boundary points are defined by the national grid co-ordinates NO 500 230, NO 505 174, and NO 430 170 respectively. The basic shape is modified by several landforms which protrude into the intertidal zone. Out Head (NO 493 198), Coble Shore (NO 468 194), Coble House Point (NO 465 199), Shelly Point (NO 474 200) and Sanctuary Spit (NO 485 204) are prominent (Fig. 1.2).

From the Pouch (NO 430 170) to Guardbridge (NO 450 190) the estuary has a sinuous and north-east trending course. To the east of Guardbridge the trend becomes more easterly and the width of the intertidal zone increases rapidly to a maximum of 2.2 km across the flats in a north-south direction immediately west of Sanctuary Spit. The total area of the intertidal zone is approximately 8 km^2.

At Guardbridge a minor stream, Motray Water, discharges into the estuary, although flow in its lower reaches is impeded by weirs constructed by Guardbridge Paper Mill (NO 451 196).

At low-water the whole estuary becomes sub-aerially exposed except for the narrow channel of the River Eden.

For convenience of description the estuary has been divided arbitrarily into upper, middle and lower sections. The upper section extends from the Pouch to Guardbridge, the middle section from Guardbridge to Sanctuary Spit and the lower section eastwards from Sanctuary Spit.

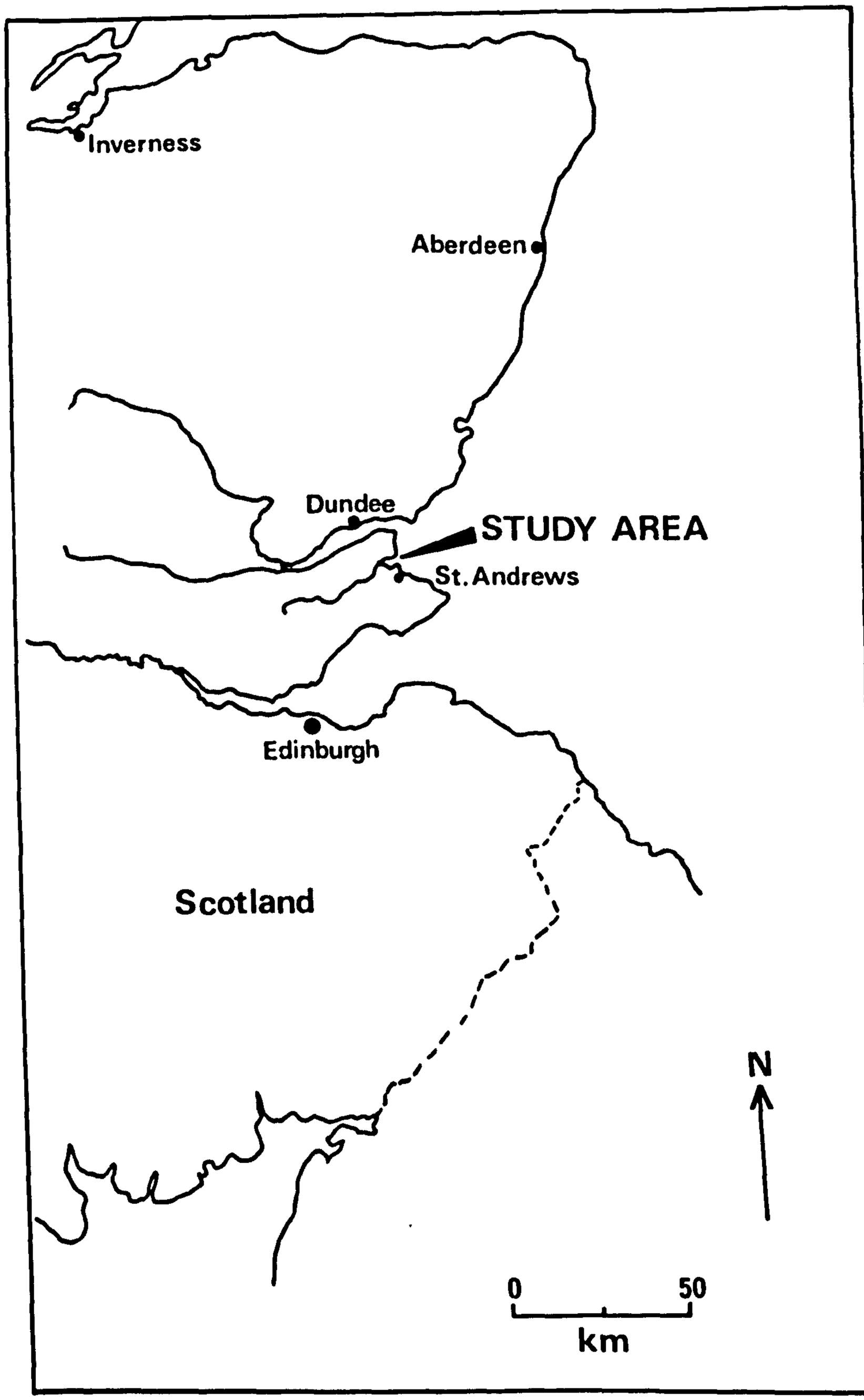

Fig. 1.1. The location of the study area.

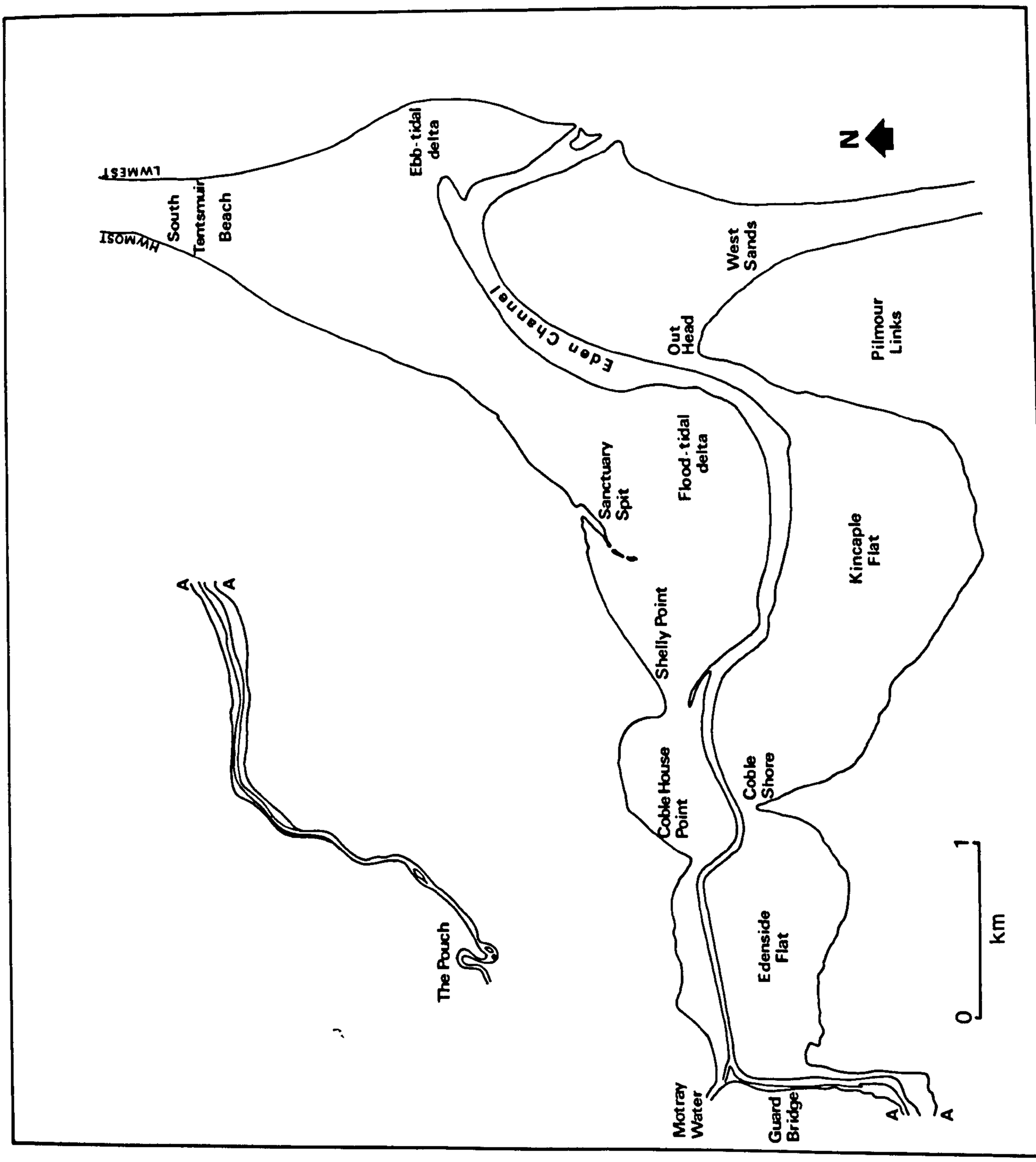

Fig. 1.2. The locations of named features within the Eden estuary.

II. PREVIOUS WORK

The Eden estuary has been the subject of very little geological research.

Geikie (1902) made brief reference to the estuary, stating that:

> "At the mouth of the Eden ... the sea has spread out, over an area some three miles long and a mile broad, a tract of sand and silt, largely the gift of the river."

Wilson (1910) described certain features of the sediments of the West Sands and the Eden Bar (Ebb-tidal delta). Of the West Sands he said:

> "The sand is firm and forms a pleasant promenade, until the 'Outhead' is reached, where a part of it is unpleasantly soft."

This is probably the first reference to the development of 'bubble' or cavernous sand within the sediments between Out Head and the Eden channel. Wilson also commented on the significance of the Eden Bar:

> "The broad spit of sand between the river and the sea, known as the 'bar of Eden', is a continuation of the West Sands of St. Andrews. The bar is covered to no great depth at high water. It suffices to break the violence of the waves in stormy weather, rendering the wide estuary inside a place of comparative quiet. When the tide recedes from the bar, it is usual to find there ripple-marks well worthy of more than a passing study, by reason of their variety of design."

Perkins (1960), in a study of the diurnal rhythm of littoral diatoms, referred to the cohesive nature of the sediments of the middle estuary.

Chisholm (1971) described the stratigraphic sequences developed during the Flandrian marine transgression and the subsequent regression in the Tentsmuir and Strathedon areas of Fife.

Adams and Grierson (1974) reported measurements of water movement, temperature and salinity over the period of a tidal cycle at one station in the estuary.

III. GEOLOGICAL SETTING

The area of north Fife which contributes drainage to the Eden estuary is underlain by Lower and Upper Old Red Sandstone and the Carboniferous Calciferous Sandstone Measures (Fig. 1.3). Late-Glacial and post-Glacial sediments form a veneer over the Palaeozoic bedrock.

The NE-SW regional strike of the Palaeozoic controls the present-day drainage system, and was presumably of similar or enhanced importance in pre-Pleistocene times. The valley of the River Eden is coincident with the narrow strip of Upper Old Red Sandstone arenaceous sediments (Chisholm and Dean, 1974) which lies between the andesites and basalts of the Lower Old Red Sandstone (Chisholm, 1964; MacGregor, 1968) to the north and the Calciferous Sandstone Measures (Greensmith, 1965; Belt, 1975), with associated intrusives, to the south.

The distribution of drift is extensive (Fig. 1.4) and only the highest areas of the Ochill Hills and the Lomond Hills are drift free. Boulder clay covers the high ground of the North Fife Hills (Eastern Ochills), East Fife Uplands and the upper reaches of the Eden valley in the Middle Ochills. The lowlands are associated with sands and gravels of fluvio-glacial or marine origin. Sands and gravels in the Eden valley may be attributed to out-wash from the Stratheden glacier (MacGregor, 1968). Windblown sand is important in the coastal zone of Tentsmuir and Pilmour Links.

Evidence of late-Glacial and post-Glacial sea-level changes in east and north-east Fife is provided by associations of raised beaches (Chisholm, 1966; Sissons, Smith and Cullingford, 1966). In east Fife Sissons et al. recognised six late-Glacial shorelines which were formed during a period of westward retreat of the ice-margin at a time prior to 13000 BP, the age of a supposed Perth Readvance (Sissons,

1967). In north-east Fife a late-Glacial shore-line is indicated at 36 m (120') OD (Chisholm, 1966) with associated sediments ranging from gravels and sands to laminated reddish-brown clays.

The 15.8 m raised beach at Leuchars may be an easterly continuation of the Main Perth Shoreline which was related to a proposed Perth Readvance between 13 500 and 13 000 BP (Sissons et al., 1966). Paterson (1974), however, contends that the readvance was a local event and the Main Perth Shoreline reflects abundant sedimentation at a time when rapid eustatic sea-level rise, accompanying an abrupt climatic amelioration, kept pace with the isostatic response by the land.

In the Forth valley, around Menteith, relative sea-level changes which post-date the Main Perth Shoreline are recorded by buried shorelines and outwash deposits. Three buried beaches, the High, Main and Low Buried Beaches, indicate an irregular fall in sea-level which culminated in the exposure of the Low Buried Beach. Minimum sea-level probably occurred at about 8500 BP (Sissons et al., 1966).

The succeeding post-Glacial or Flandrian transgression and subsequent regression produced a stratigraphic sequence in north-east Fife which forms the framework for the present-day Eden estuary (Chisholm, 1971). The general post-Glacial sequence is one of peat which accumulated on a raised beach (an equivalent of the Lower Buried Beach of Sissons) succeeded by silts and clays and/or sand and shingle (Geikie, 1902). Radiocarbon dating of peat from the St. Michael's Wood area of Fife suggests that peat accumulation began during the pre-Boreal period at about 10,000 BP and continued into the Boreal period up to 7,630 BP.

The succeeding Carse sequence was differentiated by Chisholm (1971) into sediments deposited in protected coastal inlets and those

deposited in exposed coastal areas (Fig. 1.5). The relationships between the two were also established. The post-Glacial sequence developed in Stratheden is representative of deposition in protected localities. Chisholm gives the succession as:

Silty soil	0.30m
Soil plus very fine grained sand, mottled grey and yellow, passing down into	0.75m
Silt and very fine sand, light grey, laminated	0.15m
Lenticular alternations of silt and fine to coarse grained sand	0.20m
Gravel, fine grained, well-rounded, ferruginous cement.	0.30m
..... EROSION SURFACE	
Clay, silty, grey, with numerous remains of reedswamp vegetation	2.00m
Peat with tree stumps and branches; base at 1.3m OD	0.30m
Clay, grey, soft, with plant remains	0.15m
Sand, clayey, pinkish grey, mottled; some plant remains.	0.30m

A constant feature of the sequence is the erosion surface above the 2m thick clay with reedswamp vegetation.

The post-Glacial sequence of Tentsmuir is representative of deposits formed in areas exposed to wave action and borehole sections show that the major part of the succession is of sand. In places, as at Morton Quarry (Fig. 1.5), the sand is 13m thick and rests directly on bedrock. In most boreholes, however, and in exposures on the north side of the Eden estuary a thin development of fine-grained deposits is preserved between the base of the sand and the late-Glacial or earlier deposits. The fine-grained sediments have been equated with those of the lower part of the post-Glacial sequence of Stratheden. Their diminished thickness is due to erosion during the later stages of the transgression under high-energy, intertidal conditions.

On the north side of the Eden estuary between Coble House Point and Guardbridge a sequence showing characteristic deposits of both protected and exposed areas was described by Chisholm:

Silt and very fine sand, mottled grey and yellow, no bedding visible. Top surface forms part of the 'Low Raised Beach' platform. Basal contact not exposed	0.90m
Gap	
Sand, pale yellow, massive, soft; irregular grey silty lenses at the top and a few small pebbles at the base	1.80m
..... EROSION SURFACE	
Clay, silty, grey, with remains of reedswamp vegetation on poorly marked bedding planes; the deposit thickens eastwards	0.90 - 2.60m
Clay, grey, abundant remains of reedswamp vegetation on bedding planes. Some plants in growth position	0.30m
Peat, dark brown, with woody fragments. Dips and thickens eastwards	0.10m
Sand, muddy, pinkish grey; passes down into orange sand and reddish-brown, laminated clay	0.30m

The sequence is again divided by an erosion surface where the early transgressive deposits are truncated and overlain by a bed of sand which is continuous with the sand which covers the Tentsmuir area. The sand was interpreted by Chisholm as a high-energy intertidal deposit.

The transgression reached its fullest extent between 7,600 and 5,800 BP, and the maximum water level attained during the period was 8.9m OD.

The regression has been accompanied by the incision of rivers and streams and the partial erosion of the post-Glacial sequence. On Tentsmuir and Pilmour Links the topography of the post-Glacial or Lower Raised Beach has been reworked into a series of dune ridges.

Fig. 1.3. The solid geology of Fife.

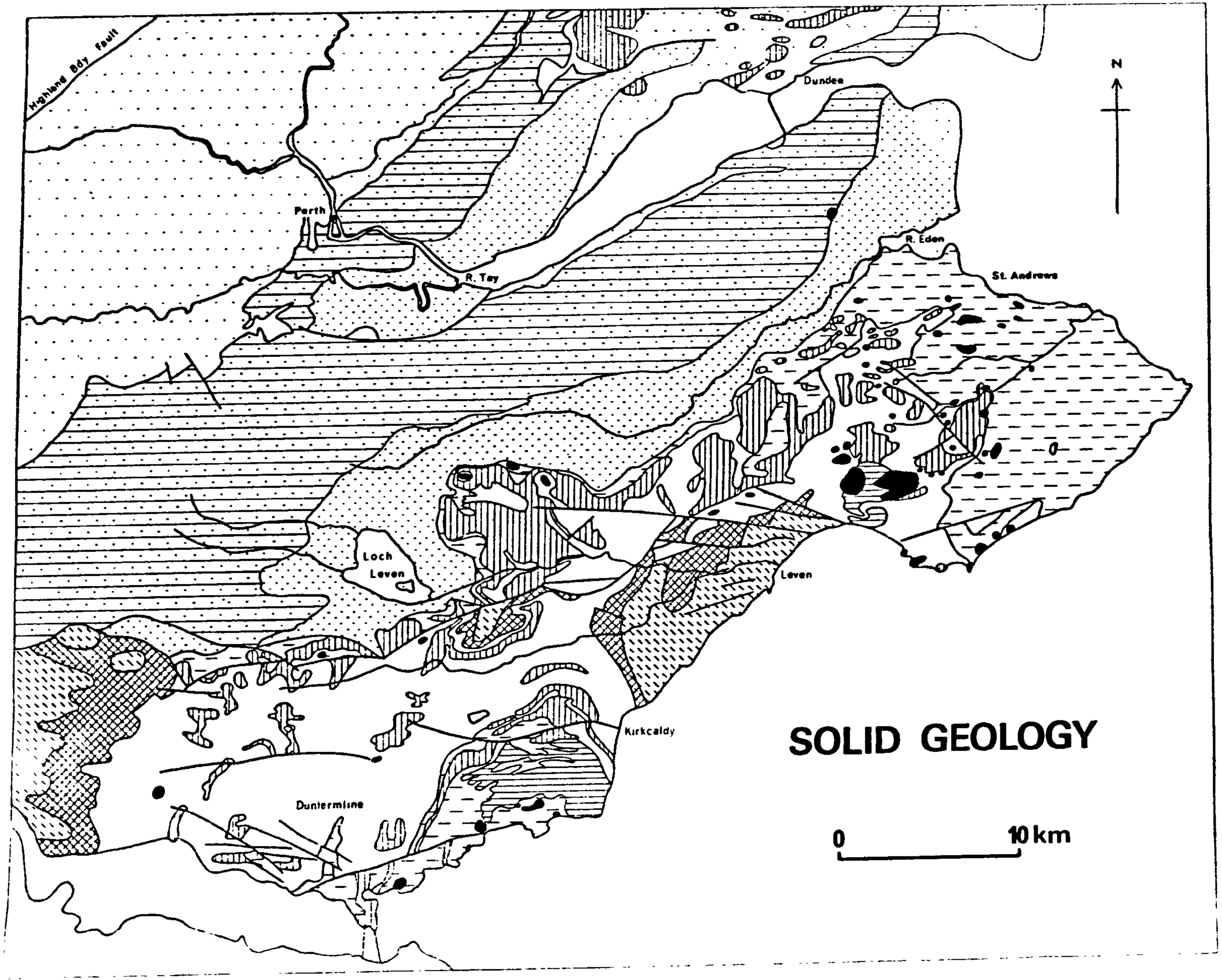

EXPLANATION

CARBONIFEROUS

- Coal Measures
- Millstone Grit
- Carboniferous Limestone
- Calciferous Sandstone

DEVONIAN

- Upper Old Red Sandstone
- Lower

- Carboniferous Basalts & Tuffs
- Lower O.R.S. Basalts, Andesites & Tuffs
- Agglomerate etc. in Vents
- Carboniferous Dolerite Sills
- Lower O.R.S. Dolerite Sills

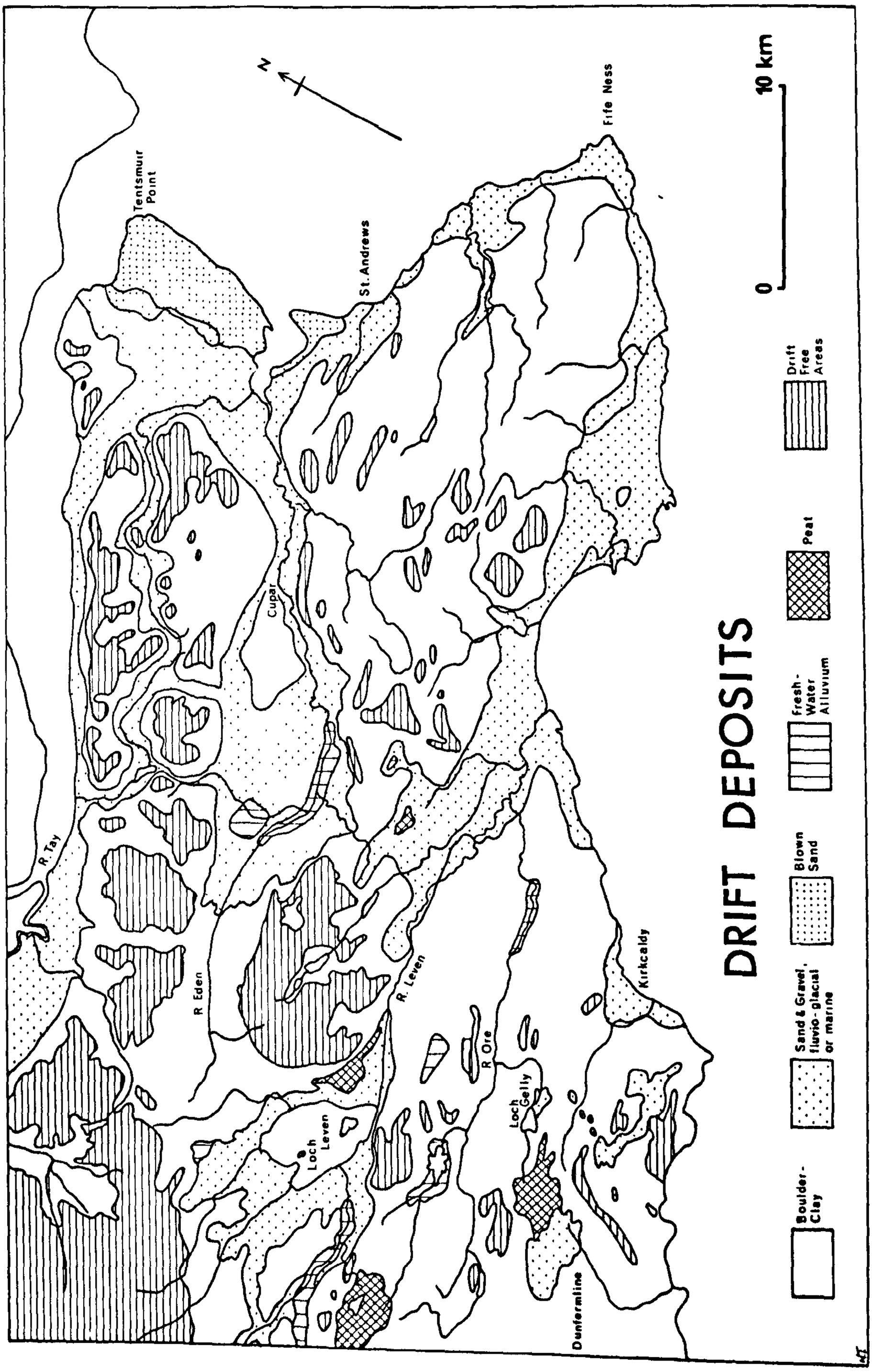

Fig. 1.4. Drift deposits in Fife.

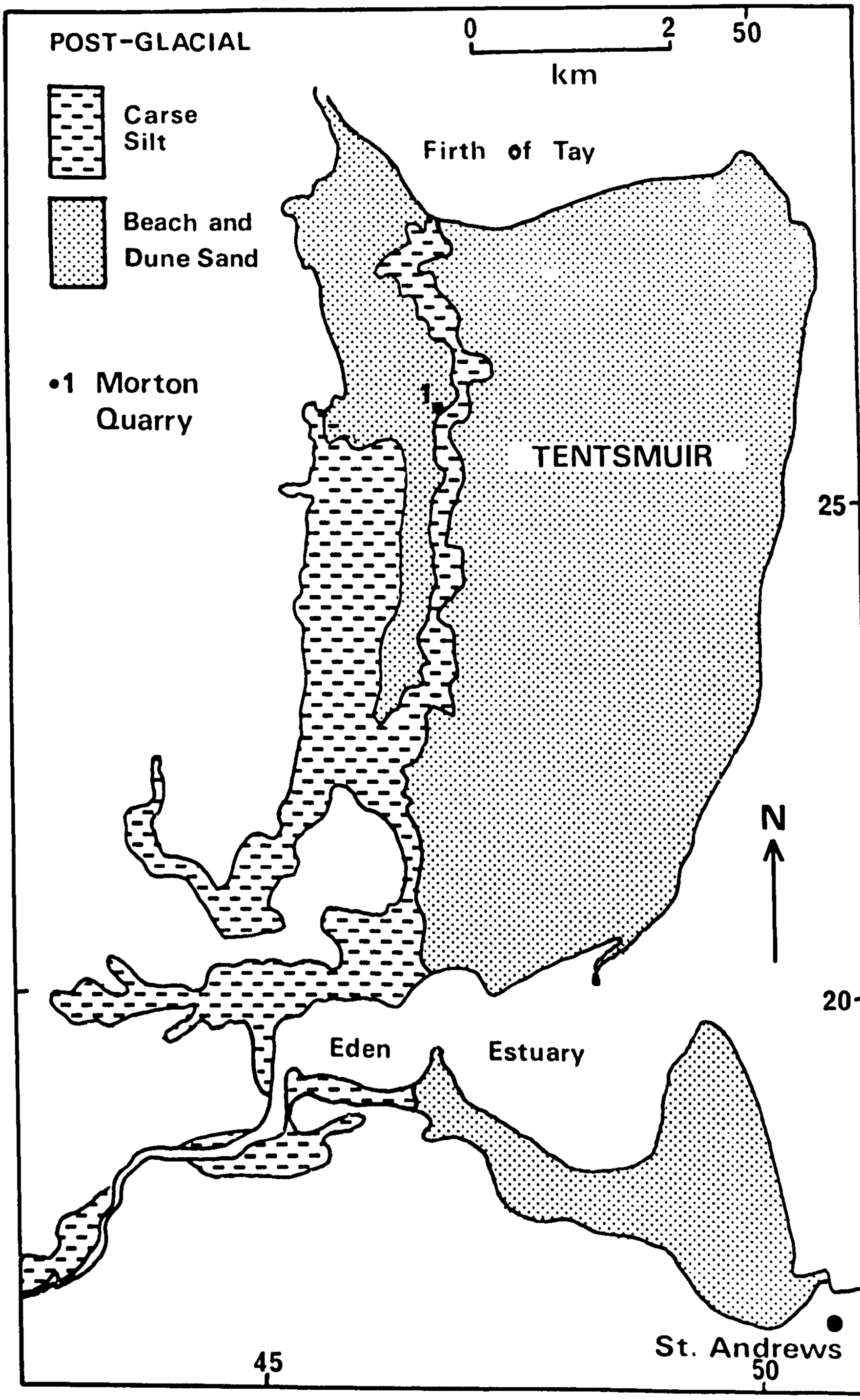

Fig. 1.5. Post-Glacial deposits in the Tentsmuir area of Fife (after Chisholm, 1971).

IV. CHANGES IN COASTAL MORPHOLOGY 1855 - 1975

Sources of Data

The redistribution of sediment by coastal processes during the past 120 years has produced dramatic changes in the areal distribution of land and sea at the entrance to the Eden estuary. Since 1855 the area has been surveyed periodically by the Ordnance Survey, and changes on the north and south shores of the estuary may be considered on the basis of the movement of the line of High Water Mark Ordinary Spring Tide (HWMOST) as indicated on the various editions of the 1:10,560 Ordnance Survey maps. The use of HWMOST as a criterion for the recognition of sediment redistribution is justified, because average sea-level in this area has remained constant for the past two centuries (MacGregor, 1968). During the same period the position of the Low Water Mark Ordinary Spring Tide (LWMOST) has not changed radically.

The position of the Eden channel in the lower estuary has not remained stable. The various positions of the centre-line of the channel as shown on the O.S. maps indicate a channel migration belt in the lower estuary with a maximum width of 1km. The geographic limits of the migration belt are defined by the 1855 and 1919 channel positions (Fig. 1.6).

In addition to Ordnance Survey maps, air photographs of the Eden estuary are available for the years 1948, 1953, 1964 and 1973. These photographs were invaluable in determining minor changes in coastal morphology and in providing detailed information on the configuration of intertidal sediment bodies, major and minor drainage channels and, in some instances, wave refraction patterns.

Coastline Changes

The variation in HWMOST as shown by O.S. maps published in 1855, 1895, 1919, and 1959 (Fig. 1.6) suggests that the following changes

have occurred:

1. a progressive easterly and northerly migration of Pilmour Links and Out Head,
2. a net westward (landward) movement of HWMOST on the northern part of South Tentsmuir Beach,
3. a net south-eastward (seaward) movement of HWMOST on the south-western part of South Tentsmuir Beach,
4. a northward migration of the Eden channel between 1855 and 1919, followed by a rapid movement to the south before 1948.

These changes have been quantified by the calculation of the net landward (negative) or seaward (positive) displacements of HWMOST and the centre-line of the channel along selected lines of latitude (Table 1.1).

Table 1.1. Summary of the Movement of HWMOST on Specific Lines of Latitude

Latitude	1855–1895	1895–1919	1919–1959	Net	
56°23'15"	No data	−70	−350	−420	
56°23'00"	+310	−310	−320	−320	
56°22'45"	+630	−490	−20	+120	South Tentsmuir
56°22'30"	+240	+130	−130	+240	
56°22'45"	−720		+630	−90	
56°22'30"	−460	−260	+190	−530	Eden Channel
56°22'15"	−150	−30	+80	−100	
56°21'45"	+190	+20	+270	+480	
56°21'30"	+60	+40	+210	+310	Pilmour Links

+ indicates a seaward movement, i.e. a net gain of land
− indicates a landward movement, i.e. a net loss of land
Distances given to the nearest 10 metres.

The development of Pilmour Links and Out Head

The eastern or seaward margin of Pilmour Links has progressively migrated to the east and north. The growth has been accomplished by the accretion of dune ridges, several of which have attached themselves to the coastline of 1855 (Fig. 1.7). Up to 1919 a calculated net seaward movement of HWMOST of 210m on latitude $56^{o}21'45"$ and 100m on latitude $56^{o}21'30"$ had occurred. The easterly progression of HWMOST continued to 1959, by which time 480m had been gained on the northern line of latitude and 310m on the southern one.

Since the early 1960's the natural balance between deposition and erosion has been upset by the interference of man. A refuse tip was initiated on the north-east coastal strip of Pilmour Links and material was dumped there for about a decade. Although a certain amount of land was gained from the sea by this exercise, the sea is now in the process of re-establishing equilibrium, and the easily eroded refuse is periodically redistributed along the shore at Out Head, much to the detriment of the local beach.

Little change has taken place on the western side of Pilmour Links, except for a small amount of erosion in the period 1919 to 1959 (Fig. 1.6).

The shape of Out Head prior to the period of man's interference was moulded by two sets of dune ridges. The first, and major set, trended NNW-SSE and was a continuation of the dunes on the east side of Pilmour Links (Fig. 1.7, features c, part of d, e). The second set trended between N-S and NNE-SSW and infilled a small convex-southward embayment on the north-west side of the promontory (Fig. 1.7, feature a).

The embayment is a constant feature of Out Head and, as the promontory migrates to the east and north, so does the embayment. The

feature is maintained by ebb-tidal currents which approach the shore of the embayment at acute angles before being diverted into the Eden channel. Within the embayment blown sand driven by persistent south-westerly winds is able to accumulate. The dune ridges so formed are skewed in plan with long narrow tails to the south-west.

The configuration of Out Head at the present time is controlled by the refuse tip constructed in the 1960's and dune ridges in an embayment to the west of the refuse tip (Fig. 1.7, feature b). The development of the dune ridges has been rapid with an average annual accretion rate of 2.3m in the west-north-westerly direction (calculated from air photographs dated 1948 and 1973). The emplacement of anti-tank blocks in 1941 and the protection offered by the refuse tip from easterly and north-easterly winds have enhanced the stability of sediment deposited in the embayment.

Changes on the North Shore

Between 1855 and 1895 the position of HWMOST in the South Tentsmuir area moved rapidly eastwards over distances of between 240 and 630m (Table 1.1). A Royal Commission on Coast Erosion (1911) was given evidence by the Ordnance Survey to the effect that between St. Andrews and the Tay 534 acres of land were gained and only 23 acres lost in the years 1855 to 1895.

The seaward accretion was not, however, maintained, and a rapid northward migration of the Eden channel between 1895 and 1919 resulted in the erosion of much of the land gained during the previous 40 years. (Compare the 1895 and 1919 shorelines, Fig. 1.6.)

In the subsequent 40 years (1919 to 1959) erosion in the north of the area continued with landward movements of HWMOST of 420 and 320m on latitudes $56^{o}23'15"$ and $56^{o}23'00"$ respectively. In the south of the area erosion was less severe during this period, and since 1855

there has been a net seaward advance of 120 and 240m on latitudes $56^{o}22'45"$ and $56^{o}22'30"$ respectively.

The development of Sanctuary Spit, located to the south-west of South Tentsmuir Beach (Fig. 1.2), has resulted in a net gain of land from the sea. The structure was initiated between 1855 and 1895, and its spit-like elongate form was enhanced by the period of erosion on South Tentsmuir between 1895 and 1919. The history of the spit since 1919 has been one of south-westerly migration and, during the last 30 years, shape inversion.

Between 1919 and 1948 the spit moved to the south-west over a distance of 0.7km (Fig. 1.6). The tip of the feature has since remained in the same position where, presumably, there is maintained a balance between flood- and ebb-orientated sediment transport processes.

Air photographs record the variation in spit configuration since 1948 (Fig. 1.8, drawn from air photographs). After the cessation of south-westerly spit migration during or before 1948 there occurred a gradual inversion of the shape of the spit. Between 1948 and 1943 the spit suffered erosion which changed the shape of its seaward side from a relatively straight NE-SW trending feature to one with a slight north-westwards concavity.

In 1953 the tip of the spit had a strong clockwise curvature, but in the succeeding 7 years there was a rapid north-westerly migration of the main body of the spit whilst the tip remained in the same position. This movement produced the shape inversion with the whole spit becoming convex north-westwards in plan. It also gave the tip a slight anti-clockwise curvature (Fig. 1.8, c).

During the north-westerly movement the spit used the compacted vegetative remains which had previously accumulated in its lee as a

base over which to migrate (Fig. 1.8, stippled area of the 1948 map). This peat deposit is now exposed to the east of the spit and is subject to erosion (Fig. 1.9). During an early stage in the breakdown of the peat discoidal blocks are produced (Fig. 1.10). These blocks may be transported considerable distances and have been found to the south of the Eden channel on the West Sands.

Since 1964 the shape of the spit has changed slightly with the tip becoming fully recurved. The recurved portion has assumed the form of an ebb-orientated sand-wave which may indicate that the balance between sediment transport processes has shifted in the favour of ebb currents.

The Movements of the Eden Channel

The Eden channel has changed its position frequently since 1855. The most important period of movement was from 1895 to 1919, when the channel moved northwards by 880m, and in so doing contributed to the destruction of land at the south end of Tentsmuir which had only recently been gained from the sea.

By 1948 the river had moved southwards again towards its 1895 position. The presence of a relict channel in the 1919 position, adjacent to the north shore of the estuary (Fig. 1.8, 1948 map), suggests that the southerly movement of the Eden channel might have been the result of avulsion rather than of a gradual migration. To the east of the relict channel is a topographically high beach bar which continues to the south of the Eden channel as a spit-platform extending southwards to Out Head. The beach bar and platform together may constitute the structure built to the south-east of the Eden channel during the 1895-1919 northward migration. They probably constituted the 'Eden Bar' of Wilson (1910). Since 1948 the relict channel has gradually diminished in size, but it still forms an important topographic feature.

The Eden channel is now moving northwards again, and an average movement of 9m a year has been calculated for the past 27 years.

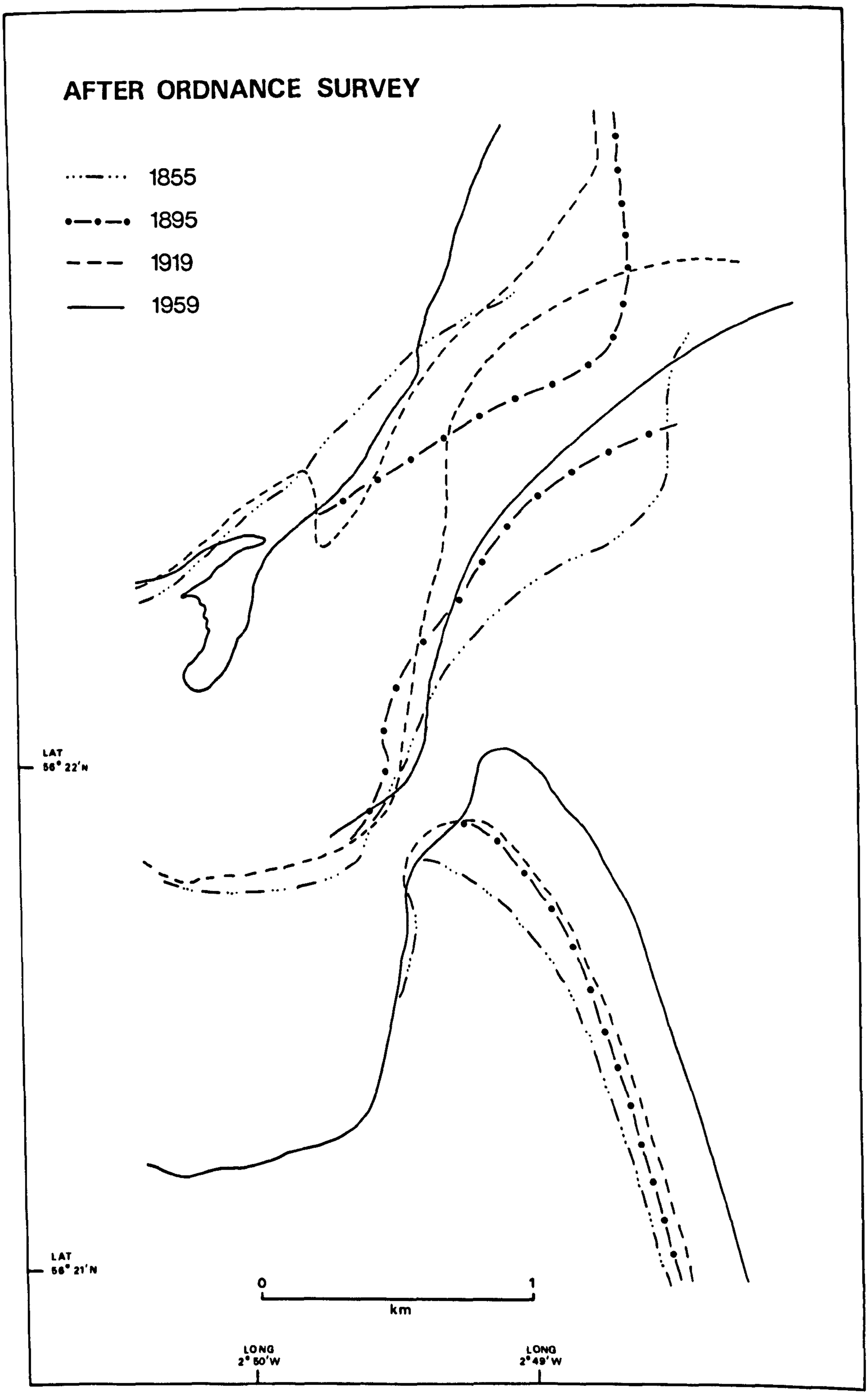

Fig. 1.6. The historic positions of HWMOST and the centre-line of the Eden channel, drawn drom the 6":1 mile editions of Ordnance Survey maps.

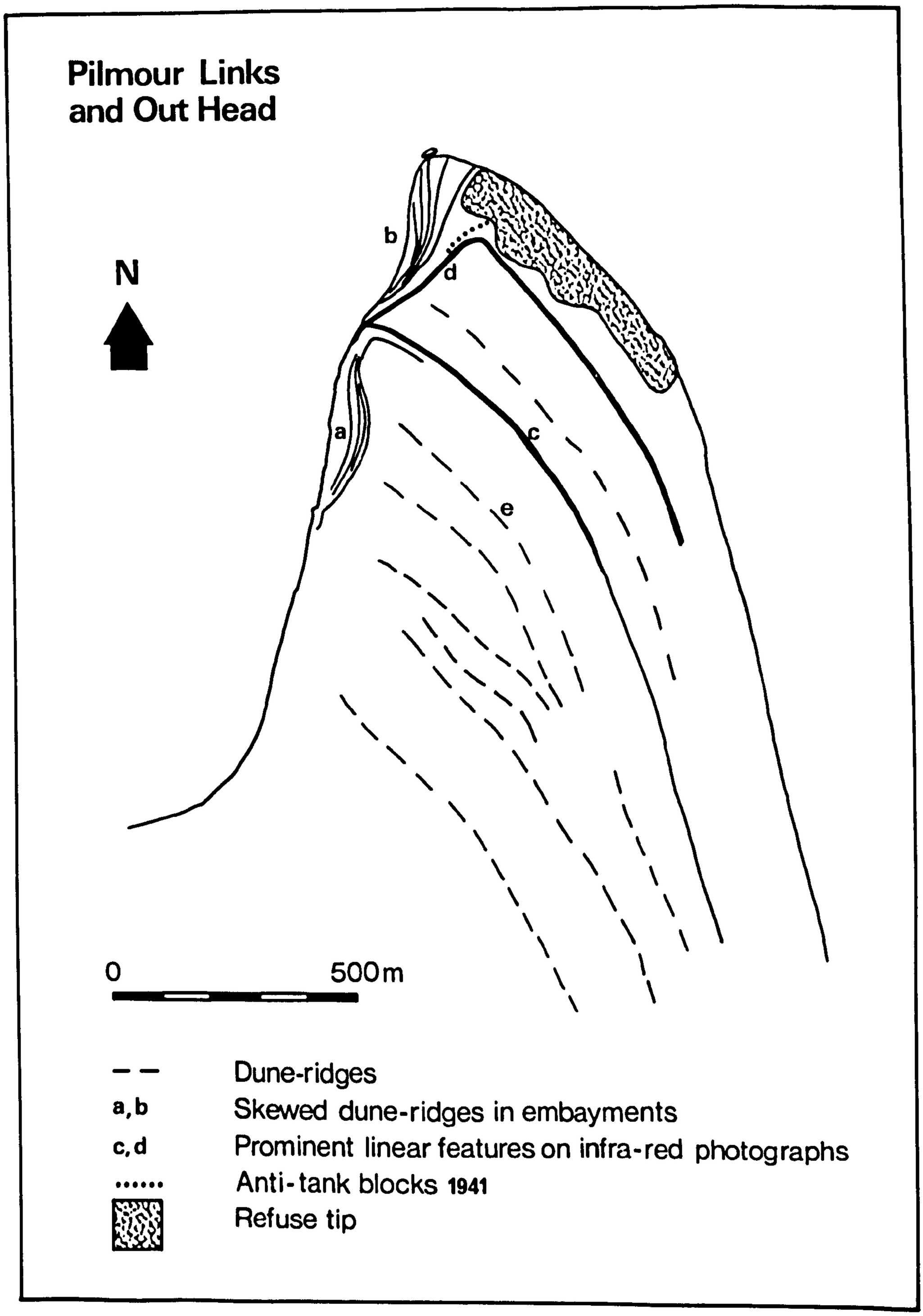

Fig. 1.7. Structural elements of Pilmour Links and Out Head. (Drawn from an air photograph.)

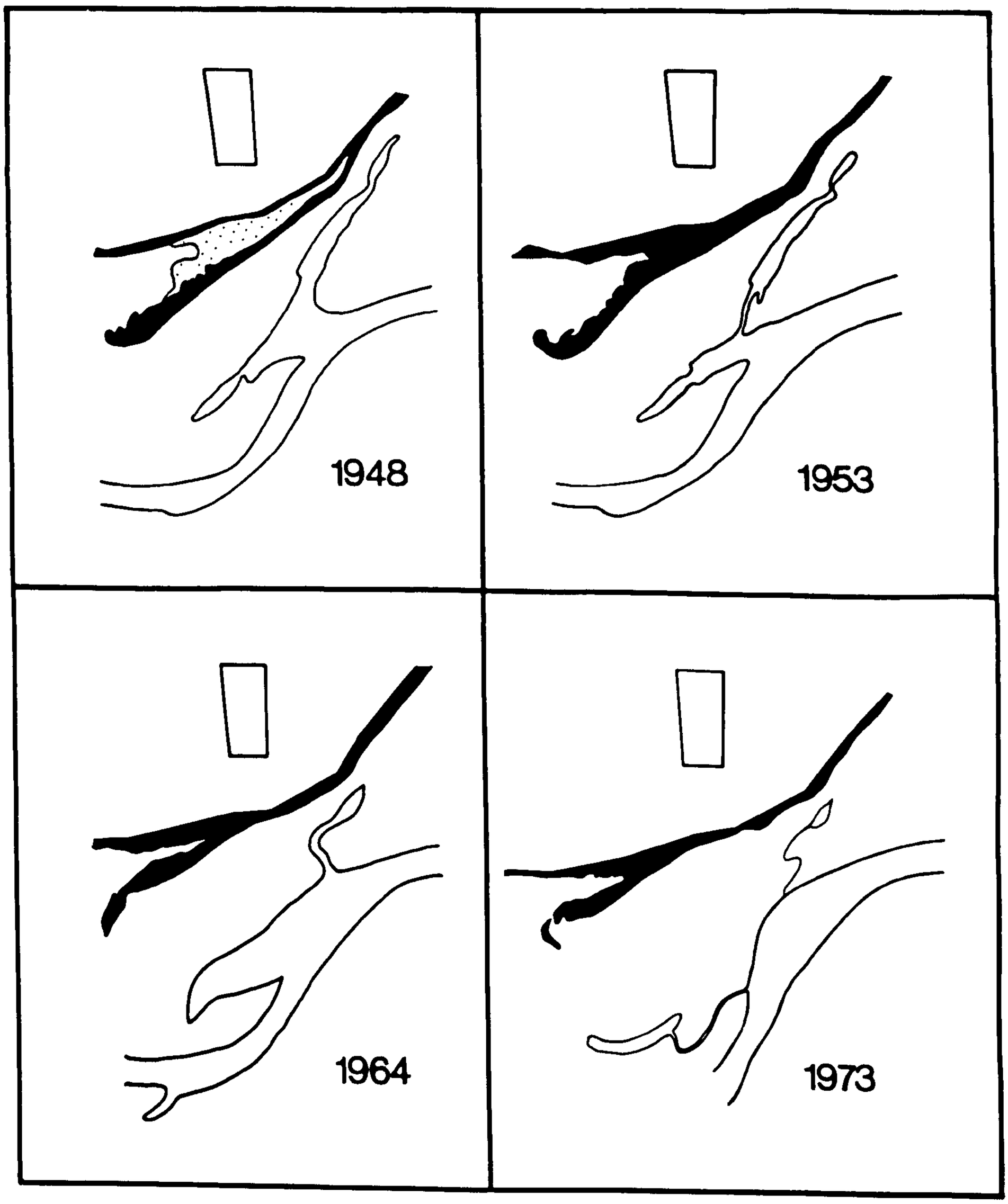

Fig. 1.8. The development of Sanctuary Spit, 1948–1973. Note the shape inversion between 1953 and 1964 and the re-curving of the tip between 1964 and 1973. (Drawn from air photographs.)

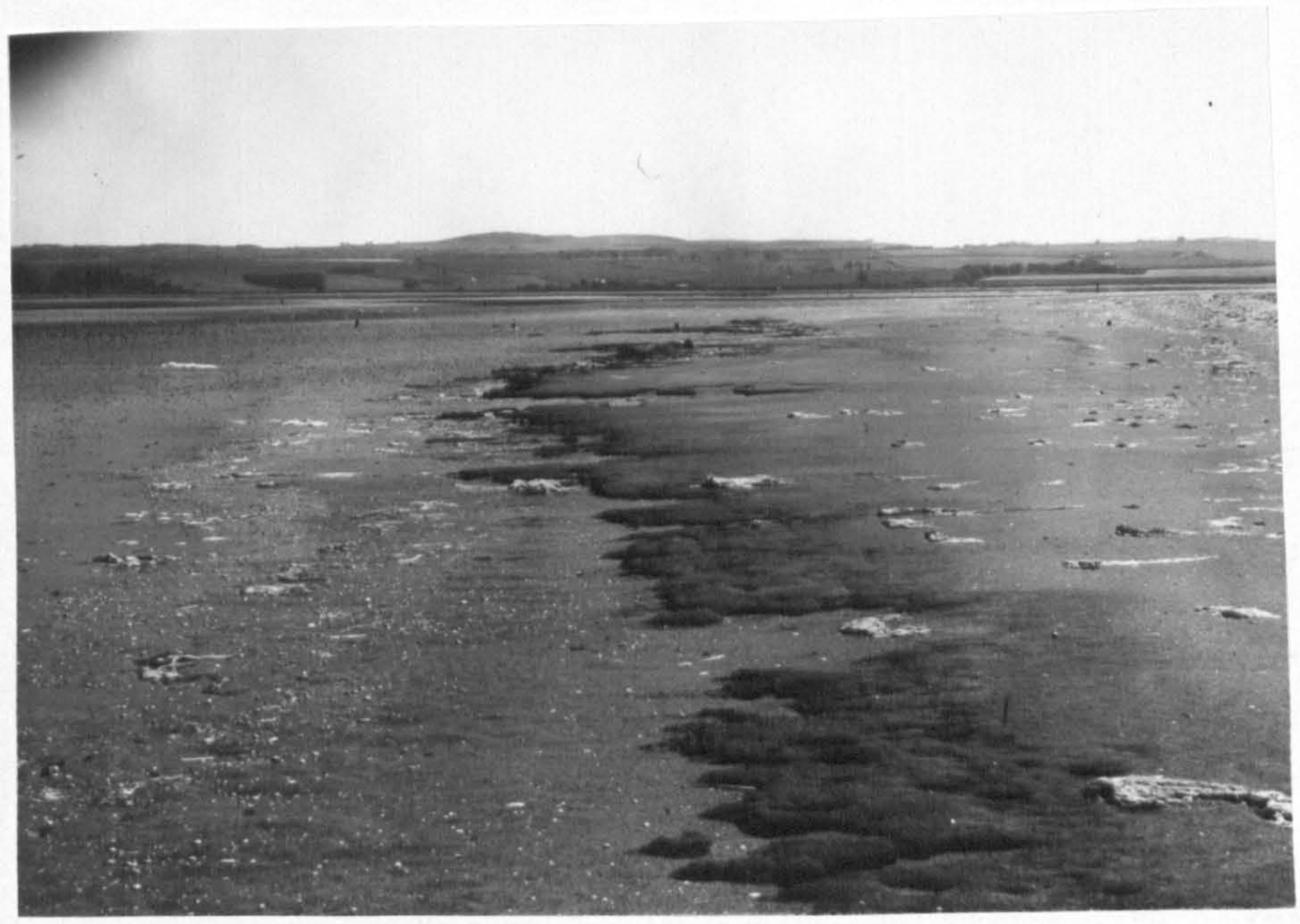

Fig. 1.9. The peat accumulation over which Sanctuary Spit migrated between 1948 and 1973.

Fig. 1.10. Discoidal peat fragments produced by erosion of the deposit shown in Fig. 1.9.

Chapter 2 WATER CIRCULATION

I. PHYSICAL FACTORS IN ESTUARINE CIRCULATION

The major physical factors which influence estuarine circulation patterns are the relative magnitudes of river and tidal flow and the morphology of the estuary (Pritchard, 1955; Schubel, 1971).

River Discharge

Two rivers discharge into the Eden estuary. The River Eden drains the southern slopes of the North Fife Hills and the northern slopes of the Lomond Hills and has a drainage area of 307km^2. Motray Water, a minor stream, which enters the estuary to the north of Guardbridge, rises in the North Fife Hills and drains an area of 52km^2.

The relationship of areal rainfall to river discharge (Table 2.1, p. 15) shows that the high precipitation of the winter months (November to March) promotes a high river discharge of between 4 and 5.5 cumecs. Summer discharge is normally low (1 to 2 cumecs), even though rainfall in the months of July and August is on average in excess of 80mm.

The discharge of the River Eden is monitored by the Tay River Purification Board at the guaging station at Kemback (NO 415158). Between October 1967 and September 1974 the mean daily discharge was 3.04 cumecs. The maximum recorded flow was 38.54 cumecs (5 May 1968), and the minimum 0.64 cumecs (30 August 1973).

The discharge of Motray Water over the period October 1969 to September 1972 averaged 0.38 cumecs with a range of 0.06 to 4.08 cumecs.

Tidal Flow

Tidal flow is absolutely dominant over river flow in terms of the amounts of saline water and fresh water entering the intertidal zone during the period of a flood tide. The mean spring-tidal range is

Table 2.1. Average rainfall in the Eden catchment (1916–1950) and the monthly averages of rainfall, run-off and mean river flow for 1974.

	Av. Rain mm	Areal Rain mm	Run-Off mm	Mean Flow cumecs
January	85	89	38	4.37
February	57	50	35	4.45
March	54	88	39	4.47
April	49	19	17	1.99
May	66	50	15	1.70
June	55	45	11	1.34
July	82	52	8	0.91
August	82	47	7	0.81
September	73	85	9	1.08
October	86	40	9	1.03
November	80	106	38	4.47
December	70	88	48	5.54

Average rainfall figures supplied by the Meteorological Office and the remainder by the Tay River Purification Board.

approximately 4.3m, and that of the neap tides 2.2m. If a conservative estimate of 1m is taken for the average water-depth in the estuary at high-water, the total volume of water is of the order of $8 \times 10^6 m^3$. Of this amount, under average river discharge conditions, approximately $7.7 \times 10^4 m^3$ will be supplied by the River Eden and Motray Water. The ratio of the volume of fresh-water to the total volume of water entering the estuary during the period of a flood-tide (Schubel, 1971) may be used as a mixing index which is a crude guide to the classification of the estuary in terms of Pritchard's (1955) categories. The mixing index for average flow conditions in the Eden estuary is 0.009, a value which places the estuary in Pritchard's Type C or 'vertically homogeneous' category. Under maximum flood conditions the estuary would become a Type B or 'partially-mixed' body of water with a mixing index of 0.12.

The theoretical mixing index applies to the estuary as a whole, but in the natural state of affairs the degree of mixing between fresh and salt water varies from section to section within the estuary, and, as pointed out by Hansen and Rattray (1966), no single value of a mixing or circulation parameter can adequately characterise an estuary.

Estuary Morphology

The mixing indices previously mentioned took no account of the morphology of the estuary which in fact is rather complex and of major influence in the control of current flow directions. A major feature of the estuary is the extreme shallowness, a fact which is expressed by the emergence of the whole intertidal zone at low-water except for the narrow Eden channel. Maximum water-depth over the intertidal flats at high-water probably does not exceed 3m.

Although the general trend of the estuary is east-west, the upper estuary is off-set to the south of the middle and lower estuary by approximately 1km. This off-set introduces two 90 degree bends into the course of the estuary, both of which must serve to generate structures within the flow capable of enhancing the degree of mixing and altering the velocity profiles.

Flow patterns in the middle and lower estuary are profoundly influenced by the intertidal sand-bodies termed flood- and ebb-tidal deltas, beach bars and spit-platforms. The sandy promontories of Out Head, Sanctuary Spit, Coble Shore also influence flow directions.

II. WATER CIRCULATION MEASUREMENT

The water circulation pattern in the estuary was determined by direct measurement and by inference based on natural and artificial indicators of flow direction. Direct measurement included eulerian and lagrangian methods of flow determination; direct-reading current meters were employed at several channel stations and path-time methods were used over the intertidal flats when water depth permitted. Observation of orientated features on the bed such as asymmetric ripples, drag-marks and algal filaments allowed certain flow directions to be inferred and hence complemented the eulerian and lagrangian data. In areas where direct measurement of the flow was impracticable and where natural indicators of flow direction and sediment movement were absent or of a complex nature, for example, where multiple interfering bedforms appeared, the direction of sediment movement, deduced from the dispersal of a fluorescent sand, was used as a flow direction indicator.

Eulerian Methods

The variation in current velocity and direction, salinity and temperature over a tidal cycle was measured at seven stations in the estuary. Five stations were over the Eden channel and two in the flood-tidal delta system.

Velocity, averaged over a 60 second period, and direction of current flow relative to magnetic north ($\pm 5^{o}$) were measured with a Braystoke directional current meter. Salinity and temperature were measured with an Electronic Switchgear Ltd. Salinity-Temperature Bridge Type MC5. Where practicable, readings of velocity, direction, salinity and temperature were recorded each half-hour at 0.5m depth intervals. This interval was increased to 1m in water deeper than 4m because of the time period required to complete the profiles (10 to 15 min.).

Due to a combination of factors (tidal state, inclement water conditions, equipment non-availability and failure) six of the data sets are from a period extending over 5 months and the seventh set was obtained some six months later. The results are not, therefore, directly comparable. One of the main inconsistencies is the discharge of the River Eden. The TRPB records for the guaging station at Kemback show that discharges on the days when measurements were taken ranged from 0.906 cumecs to 4.904 cumecs. Successful recordings were obtained on three pairs of days: 20/21 June 1974, 30 September/1 October 1974 and 28/29 November 1974, and therefore only data for areas studied on these consecutive days may be directly comparable. No attempts have been made to depict longitudinal profiles of velocity or salinity.

Lagrangian Methods

In Lagrangian methods of flow determination an object is placed in the flow and is carried along by it - the path-time history of the object gives the average flow speed and direction.

In practice there are two main problems associated with path-time methods. Firstly, the need to suspend a drogue at the required depth, and secondly, the accurate geographic fixing of points on the path-time curve. Ideally the drogue should be neutrally buoyant (Swallow, 1965) and consequently held in position with no connection to the surface. Drogues are, however, frequently suspended from floats. The surface areas of the float and suspension chord are kept to a minimum, in order to reduce the frictional drag. Knauss (1963) showed that a square-law relationship exists between the ratio of velocity differences and the ratio of the surface areas of the drogue and float.

Geographic location on the open sea of points on the path-time curve could be a major source of error in the calculation of average velocities, but in a coastal setting with several fixed reference points

significant inaccuracies should not occur.

The drogues used in this survey consisted of two sheets (30 x 30cm) of 18 guage aluminium, folded at right-angles and argon-welded into the form of a cross. The vane was suspended from a small float (10 x 10 x 4cm) of expanded polystyrene by a 1mm thick nylon chord. A 50 gramme weight was suspended below the vane to help maintain a vertical attitude.

The surveys were confined to the 6-hour period around the time of high-water because of inadequate water-depth over the flats during the early-flood and late-ebb stages of the tide. Drogue positions were fixed periodically by Ebbco sextant using simultaneous horizontal angles to three reference points. Positions were plotted using an Ebbco station pointer - a plastic, precision 3-arm protractor. The interval between fixes was determined by the time taken to travel by dinghy between adjacent drogues.

Average flow velocities were calculated on the basis of straight-line distances between adjacent points on the individual flow-paths and, as such, are minimum values.

Indirect Methods

Lagrangian and eulerian methods of flow determination have the advantages of measuring the rates and directions of flow directly, but under certain circumstances their use is restricted. It was found that drogues were not very successful in water less than 1m deep, mainly because of the obstruction to flow provided by the buoyant fronds of several varieties of seaweed which cover extensive areas of the middle estuary. The design of the Braystoke current meter makes its use in shallow water very cumbersome, and flow measurements cannot be taken more closely than 10cm to the bed even with the streamlined weight removed from the instrument.

Indirect measurements of flow direction were made through the study of (a) sedimentary structures, (b) tracer sand dispersal patterns, (c) historic coastal morphological changes, and (d) air photography of wave-refraction patterns.

Sedimentary Structures

The non-cohesive sediments of the lower estuary were moulded into a hierarchy of bedforms ranging from parting lineations to tidal deltas. The most common bedforms on the sand-flats were small-scale asymmetrical ripples, whereas adjacent to the Eden channel large-scale asymmetrical ripple-type bedforms occurred. Measurements of ripple chord, span, height, plan-form, foreset dip and strike were routinely taken at each sediment sampling site (Fig. 2.1). Also recorded were other flow indicators, such as imbricate structures in shell-beds, drag-marks produced by seaweed scrolls, and the orientation of filamentous strands of fixed green algae.

Tracer Sand Dispersal Patterns

A sediment tracing technique was applied in areas where direct measurement of the flow was impracticable and where natural indicators were absent or of a complex nature. The technique was most effective on the West Sands and was also applicable to the beach north-west of Out Head, the south-east and south-west parts of Kincaple Flat, to east and west of Coble Shore, and in areas of the flood-tidal delta to the north of the Eden channel (Fig. 2.2).

1. The Tracer Sand

The tracer was fluorescent-dye-coated sand, Fesglo FG12, produced by British Industrial Sand Ltd., to a formula supplied by the Hydraulics Research Association for Great Britain.

The base sand was 'Redhill T', a moderately-well sorted, medium

to fine sand with a near-symmetrical and mesokurtic grain size distribution (Fig. 2.3).

2. Tracer Sand Release

At each release point approximately 25kg of tracer sand were substituted for the natural sand. The substitute sand was prepared for incorporation into the sediment by 'wetting' with 0.5l of Teepol (an industrial detergent) and 1l of salt water. This served to reduce the aggregation of the finer particles in the tracer and ensured that the individual grains behaved in as near a natural manner as possible.

The sand was then placed in a 25 x 25 x 15cm deep hollow, and the surface was made level with that of the surrounding sediment. All tracer samples were emplaced at a time of low-water: no sample was introduced under water.

3. Tracer Sand Recovery

In the experiments of January and February 1975 samples were collected on 15 x 15cm sheets of 'Fablon' - a plastic sheet coated on one side with a uniform thickness of adhesive (TERC, 1971). Recovery was good from dry and moist sand, but poor from wet sand.

In the experiments of May 1975 samples were not collected, but grains were counted <u>in situ</u> with the aid of a pyramid-shaped box in which one of the narrow sides was of glass which transmitted ultra-violet light (Fig. 2.4). The sun was used as an ultra-violet light source, and the arrangement of the glass and the viewing aperture in the box allowed a 4 x 10cm area of sediment to be illuminated. Fluorescent grains were readily identified and counted.

Samples were collected and/or grains counted on a grid set up around the release point. Normally a square grid with 2m between samples was used. The extent of the grid was predetermined in the case of samples collected on Fablon but was controlled by the observed

grain concentrations when counts were made in the field.

The counting of fluorescent grains on Fablon sheets was done under ultra-violet light in the laboratory. If few grains were present, all were counted. If numerous grains were present, ten random squares of area 6.25cm^2 were observed and the average number of fluorescent grains counted. The average multiplied by 36 gave the number of grains per card.

The counting of grains in the field was preferred to the collection of samples. It had the advantages of flexibility, rapidity and cheapness, but was subject to a decrease in accuracy in the grain counts and was dependent upon the sun's being unclouded. The increased flexibility of being able to follow paths of high grain-concentration far outweighed the loss in accuracy of the grain counts when directional attributes of the grain distribution were the object of study.

Coastal Morphological Changes

The data presented in Chapter 1 (IV) were used as indicators of gross sediment-transport directions, and, by inference, the predominant flow directions in the lower estuary.

Air Photography of Wave Refraction Patterns

Air photographs taken by Fairey Surveys Ltd. in August 1973 showed in considerable detail the distribution of wave-fronts and wave refraction patterns in the lower estuary during the late stages of a flood-tide. Data from this source complemented bedform and tracer sand data.

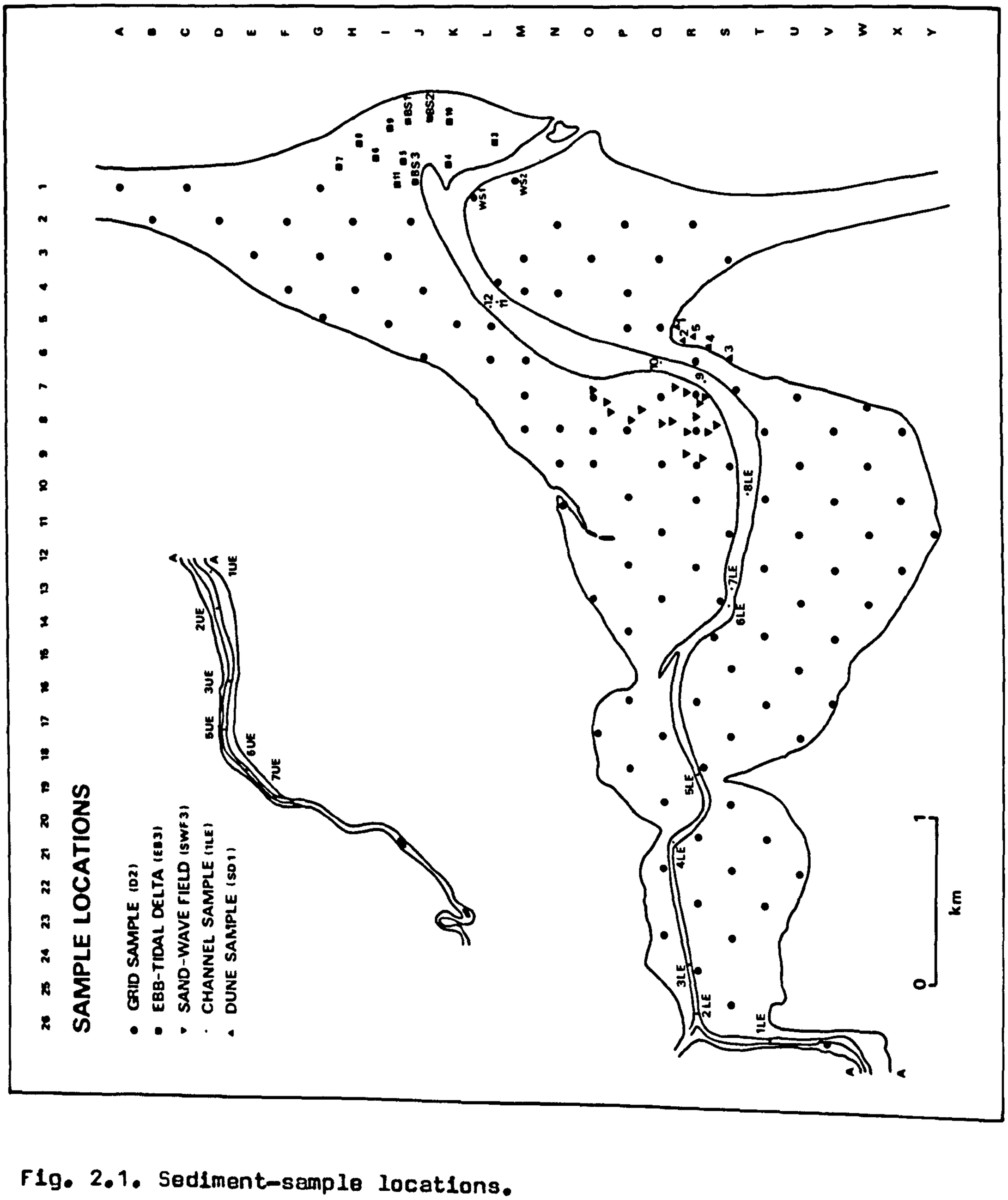

Fig. 2.1. Sediment-sample locations.

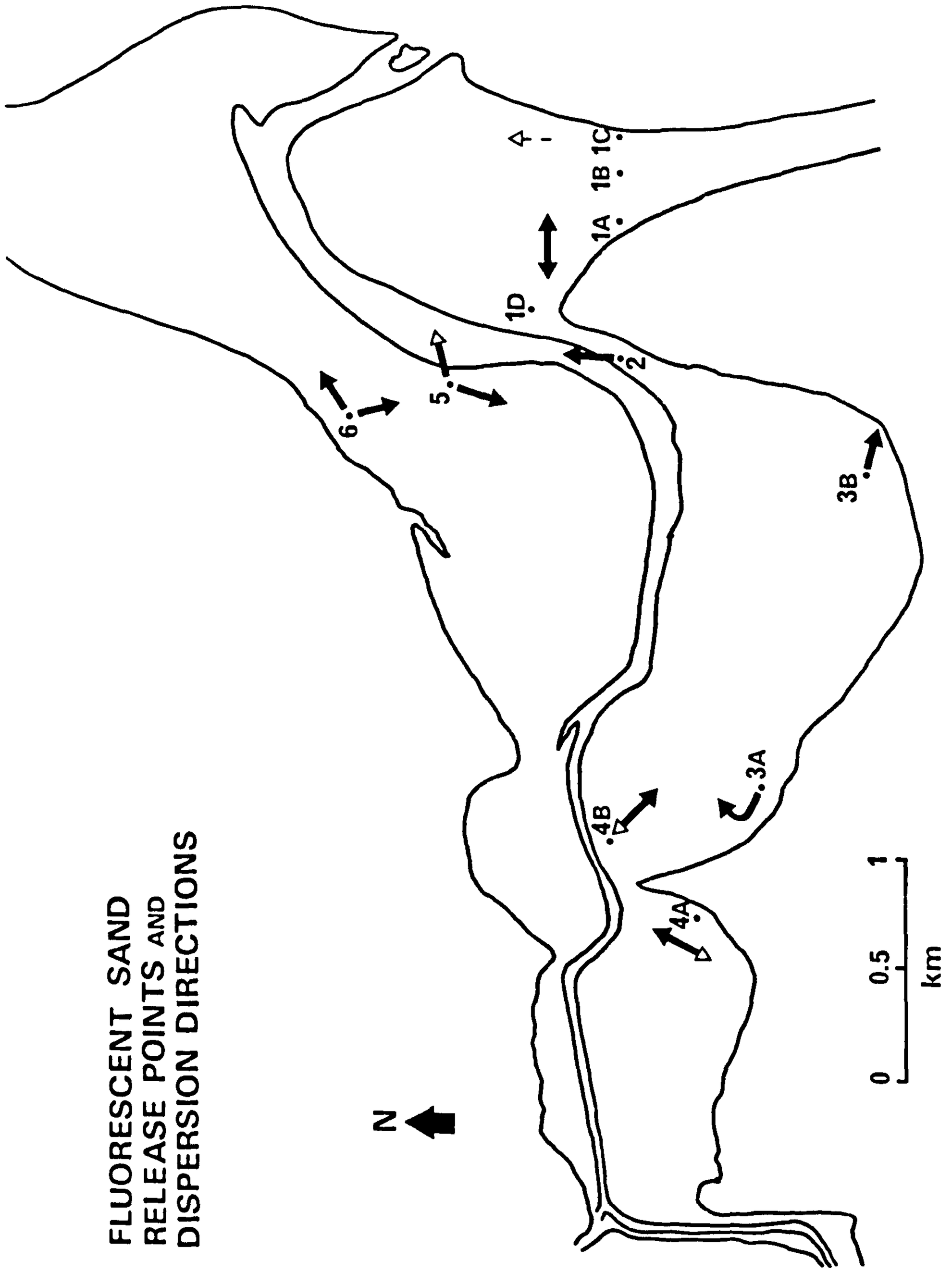

Fig. 2.2. The release points of fluorescent tracer sand and the prominent dispersion directions. Secondary dispersion directions are indicated by the open arrow-heads.

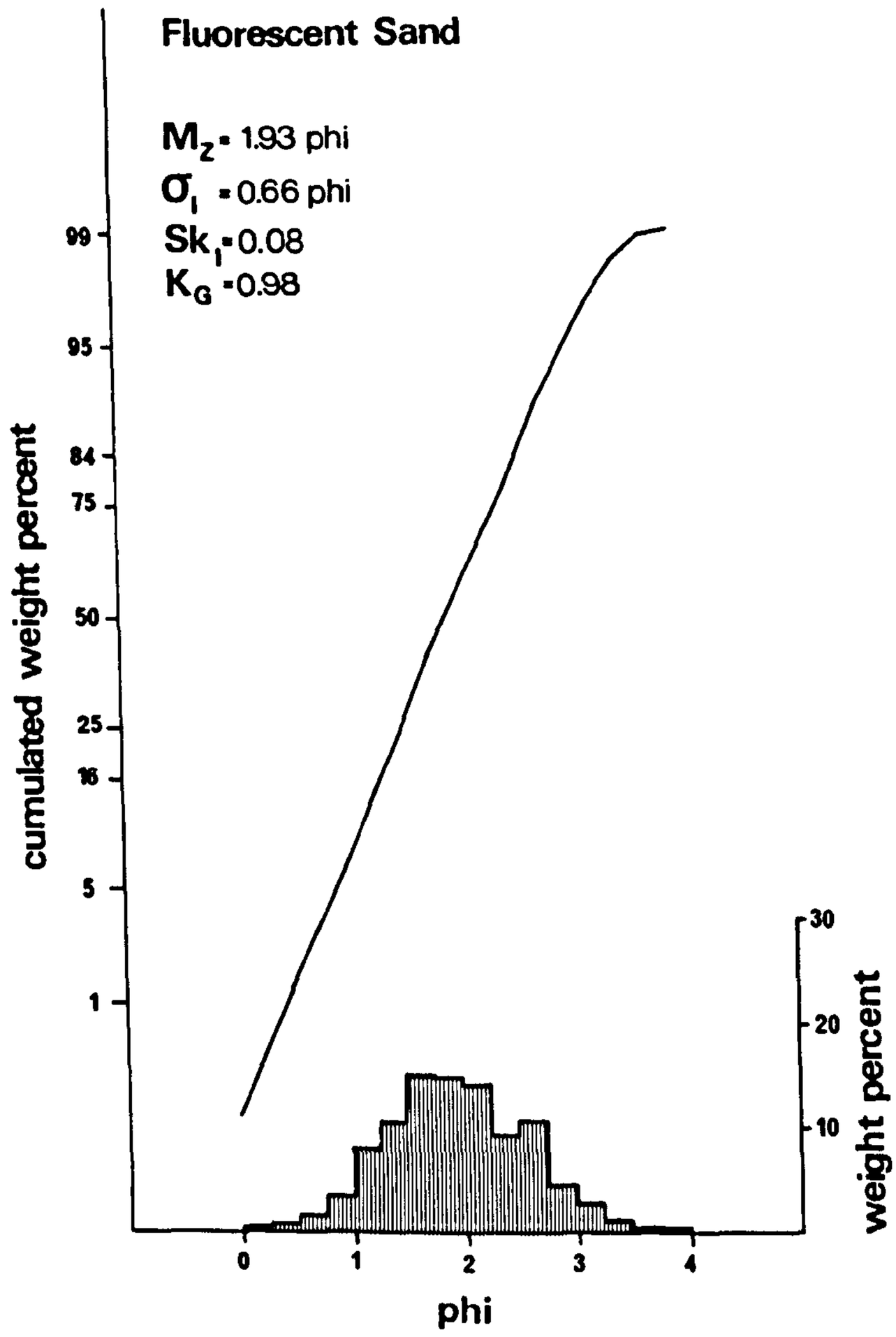

Fig. 2.3. Cumulative curve and histogram of the size distribution of the fluorescent sand.

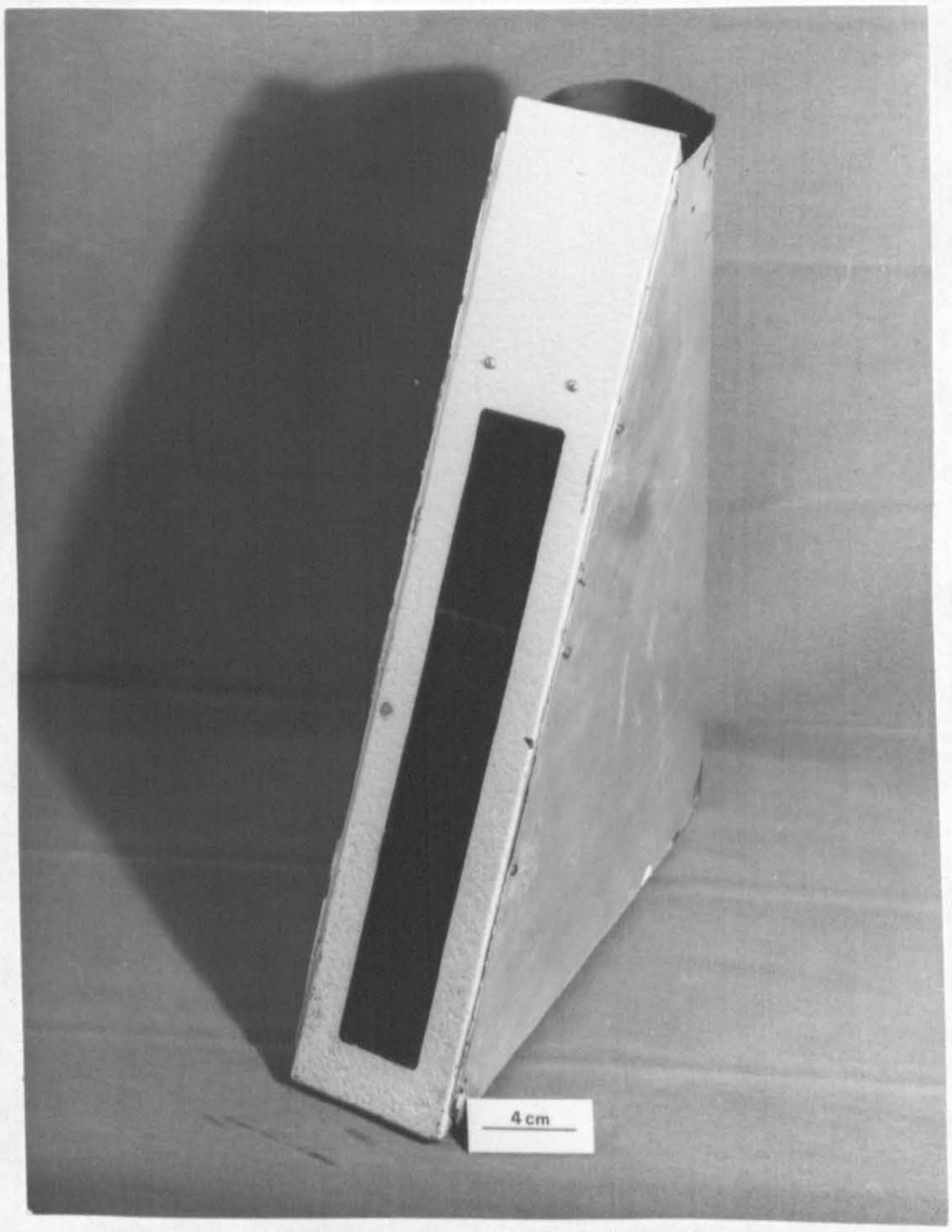

Fig. 2.4. The device used for illuminating fluorescent sand grains in the field. Grains were illuminated through the glass on the sloping side and were viewed through the semi-circular aperture at the top.

III. WATER CIRCULATION - FLOW PATTERNS

Eulerian Results

The variation in direction and magnitude of tidal currents, over the period of a tidal cycle, was measured at six stations in the estuary (Fig. 2.5a, b). The velocity data are discussed further in Section IV of this chapter. Directional variation between near-surface (surface minus 1m) and near-bottom (bed plus 0.4m) waters at a particular station (Table 2.2, page 24) is attributable to three factors: (a) the interaction of flood- and ebb-tidal currents or flood-tidal currents and river flow, (b) the development of spiral flow where water depth and channel geometry allow, and (c) the conflict between water confined to a channel in the lower part of a column and water free to move directly landward or seaward in the upper part of a column.

Surface and bottom currents with opposite flow directions occurred for short periods at the beginning of the flood- and ebb-stage of each tide. This effect became more important in the upstream direction, and at the most landward station (Fig. 2.5, 5), where river water and flood-tidal currents met, there was a distinctly layered flow for a period of 3.5 hours (see Fig. 2.27(a)).

The Out Head station (Fig. 2.5, 1) was situated on a convex-southward meander of the Eden channel. Whilst flood-waters remained within the confines of the channel, the surface currents trended slightly to the south of the channel axis, whereas near-bottom currents were directed towards the inner bank of the meander. The maximum recorded deviation between near-surface and near-bottom currents was 60^{o}, at which time transverse velocities were 21cm sec^{-1} (northwards) near the bed and 15cm sec^{-1} (southwards) at 2.5m below the surface.

Table 2.2. Directional variation between non-surface and near-bottom waters at the Eden channel stations. Figures accurate to $\pm 5^{o}$.

	1. Out Head			2. Coble Shore			3. Paper Mill		
Time	a	b	c	a	b	c	a	b	c
0	270	200	070	280	300	020	260	250	010
+1	200	240	040	280	300	020	250	260	010
+2	210	240	030	250	260	010	250	260	010
+3	210	230	020	240	330	090	170	070	100
+4	210	210	000	070	150	080	100	110	010
+5	020	180	160	110	120	010	090	090	000
+6	030	020	010	120	090	030	070	090	020
+7	040	020	020	100	100	000	090	090	000
+8	040	020	020	090	090	000			
+9	040	020	020						

	4. Guardbridge			5. Upper Estuary		
Time	a	b	c	a	b	c
0	010	010	000	120	120	000
+1	170	190	020	300	100	160
+2	160	150	010	270	310	040
+3	360	350	010	080	280	160
+4	030	020	010	100	220	120
+5	360	010	010	120	250	130
+6	020	360	020	130	110	020

Time 0 taken at low water, then hourly readings.
a: Near-surface flow direction in degrees, relative to magnetic north.
b: Near-bed flow direction in degrees, relative to magnetic north.
c: Directional variation.

The deviation in flow direction between near-surface and near-bottom currents was particularly marked when the tide-height was adequate to allow water to flow over the intertidal flats. Bottom currents, confined to the channel, tended to move in the direction of channel elongation, whereas near-surface currents took a direct route to landward or seaward. At the two lower estuary stations (Fig. 2.5, 1 and 6) late-stage, flood-tidal currents stabilised at 200-210° and 228-240° respectively, thereby maintaining an angular relationship with the channel. Similarly, at Coble Shore (station 2) near-bottom currents flowed in the direction 280-290°, whilst near-surface currents took a direct route landwards (240-260°) (Fig. 2.5a, b).

During the early stages of the ebb-tide surface-flow was unaffected by the channel, and water drained directly seawards. At Coble Shore (Fig. 2.5a, b) surface currents varied between 070°and 110° in direction, whereas bottom-currents trended 120° to 150°. In the lower estuary the early ebb-flow was to the NNE (020-030°), but this gradually turned to a north-easterly flow as topographic features became exposed and confined flow to the vicinity of the channel. In the upper estuary also, at stations 3, 4 and 5 (Fig. 2.5a,b) the ebb-flow was characterised by a gradual alignment with the channel as water-level fell.

Lagranoian Results

Actual path-time histories for the drogues used in this study are given in Appendix 1.

Flood Tide

As the water-level rises under the influence of the flooding-tide, surface-currents leave the confines of the Eden channel and take direct routes landward. The outer, or convex, banks of meanders tend to suffer erosion during this phase, and channels which shoal and terminate west-

wards are formed at points of maximum meander curvature. Such channels ('flood-channels' of Van Straaten (1954); Robinson (1960)) serve to carry flood-water in a direction tangential to the main Eden channel. Drogues A, Q_1 and, over the latter three sections of its course, Q_2, flowed through such channel systems (Fig. 2.6).

The second stage of flow over the intertidal flats begins about 1.5 hours before high-water. By this time the major sand-bodies of the lower estuary are submerged and surface-currents flow unimpeded into the estuary from the NNE and NE. The currents take an acute path across the flood-tidal delta, cross the Eden channel, and progress over Kincaple Flat in a SSW direction. The flow over Kincaple Flat is shown by drogues A, B, C, D, E and F (Fig. 2.6).

Over Kincaple Flat and its equivalent to the north of the Eden channel the last phase of flood-tidal flow is directed sub-parallel to the estuary margins with components to both east and west (Fig. 2.6, drogues A-F and L). This movement may simply be related to the filling of the estuary and the halting of the landward progression of water by the natural and artificial estuary boundaries. Continued application of tidal pressure from the NE would cause the water-level to rise and lateral flow might be expected to ensue.

Ebb Tide

Ebb tide flow directions are more uniform than those of the flood tide, and over most of the ebb period flow is basically a tidal-drain with water taking the most direct route to the narrow outlet to the sea, east of Out Head (Fig. 2.7).

From the vicinity of Coble Shore the early-ebb currents flowed eastwards to join the Eden channel to the south of Sanctuary Spit (Fig. 2.7, drogues D, E, F, G, H). From the eastern part of Kincaple Flat and the flood-tidal delta the flow was towards the north-east

(Fig. 2.7, drogues A, B, C, K, L) until the Out Head was reached, when it became north-easterly under the influence of the Eden channel (Fig. 2.7, drogues M, N, P).

To the east of Out Head the Eden channel dominates the ebb-flow patterns as water is effectively confined to it very soon after the turn of the tide. The emergence of elongate, north-south trending sand-bodies in the lower estuary forces water to converge on the narrow outlet (Fig. 2.7, drogues M, N, P).

Isotachs for one hour after the time of high-water (Fig. 2.7) show a velocity increase from west to east and from marginal areas of the estuary towards the Eden channel. Flow convergence on the narrow tidal outlet results in high current velocities with a maximum recorded value of 130cm sec^{-1} (2.6 knots).

Bedform Orientations

Internally consistent bedform orientations were obtained from measurements of large-scale bedforms (megaripples and sand-waves, see Chapter 3,III) on the flood- and ebb-tidal deltas of the lower estuary (Fig. 2.8).

Bedforms of the flood-tidal delta exhibited both flood and ebb orientations with distinct lee-slope orientation modes (dip directions) of 210-240^{o} for the former and 000-030^{o} for the latter. These figures show a good general agreement with the stable flood- and ebb-flow directions measured by eulerian methods (page 23).

The ebb-tidal delta carried only ebb-orientated, large-scale bedforms with the majority having lee-slope orientations between 060^{o} and 090^{o}. The overall variation between 030^{o} and 120^{o} is related to flow divergence as currents leave the restriction of the tidal outlet.

Small-scale bedforms, being sensitive to temporal current direction changes, showed orientations more variable than those of large-scale

bedforms. The vast majority of structures were ebb-orientated, and on the West Sands two or three ripple-trains were frequently present at one site. It may be shown by reference to photographs of wave-fronts over the West Sands that there is close correspondance between wave-front orientation and bedform orientation. The presence of up to three wave-fronts at any one time suggests that three ripple trains may form virtually simultaneously, although there is generally one dominant orientation which on the West Sands strikes NNW-SSE.

Imbricate Structures, Drag-marks and Filamentous Algae

Flow directions in the later stages of the ebb-flow were inferred from the orientation of movable objects on the bed. Of the above three direction-indicating features, imbricate structures were of very limited occurrence, filamentous algae were abundant in the middle estuary, and drag-marks were important in the lower estuary.

Imbricate structures were observed in a shell-pavement (Shäfer, 1972) consisting of the valves of Mytilus edulis (Fig. 2.9). The valves were concentrated in a channel situated 400m to the east of Coble Shore. The majority of valves rested with their convex side uppermost and were aligned with their long axes parallel to the flow direction with the anterior border (umbo) facing in the flood direction.

Drag-marks produced on the sediment surface by scrolls of Chaeto-morpha sp., which were carried along by tidal currents have been traced over distances of more than 200m (Fig. 2.10). The main area of occurr-ence of these structures was to the north of the Eden channel in the vicinity of the flood-tidal delta. The trails were remarkably straight, and the scroll which produced the trail was often left stranded at the seaward end of the feature as water-level fell (Fig. 2.11). The ebb flow direction given by the trails was 030°.

Filamentous green algae of the genus Chaetomorpha were sufficient-

ly abundant during the summer months to form algal mats over large areas of the middle estuary. The orientation of the filamentous strands, which are attached to the substrate at one end only, is an excellent indicator of the flow direction just prior to exposure (Fig. 2.12). To the south of the Eden channel flow in the late stage of the ebb tide was to the north-east and north north-east. Local variations were caused by water flowing into the drainage systems of minor channels. To the north of the channel the flow direction was to the east south-east and was directed around the margins of the flood-tidal delta.

Sediment Tracer Results

Contour maps (Fig. 2.13-18) show the dispersal of fluorescent grains about the release points. In some cases repeat sampling illustrated the changing grain distribution with time.

1. The West Sands

Of the four release points on the West Sands three were on a W-E traverse at intervals of 200m (Fig. 2.2, 1A-C) and the fourth was situated to the north of Out Head (Fig. 2.2, 1D).

The grain-size distribution of the tracer sand differed from that of the natural sand in this area with respect to mean grain-size and sorting. The natural sand was predominantly fine sand (~80%), whereas the tracer sand contained up to 50% of medium and coarse sand.

Sediment dispersal patterns at points 1A, B and D were very similar and showed an onshore-offshore couplet with very little lateral, i.e. N-S dispersion (Fig. 2.13). In each instance the onshore component was greater, in terms of grain concentrations, than the offshore component. Release points 1A, B and D have a common factor in that they are situated on the topographically high spit-platform

associated with Pilmour Links and Out Head. Water depths over the platform are very shallow, and the dominant sediment transporting agents are the swash and backwash created by breaking waves during the advance and retreat of the tide. There is little evidence of any longshore movement, although point A shows a NW-SE secondary elongation at grain concentrations between 10 and 50. At the same concentrations point B shows a minor elongation to the north.

At points A and B the transport direction conformed with the lee-slope azimuths of the small-scale ripples which were present on the bed. Although the ripple-tops were planed off by the ebb, a flood-orientated asymmetry was clearly present.

The relationship of the dispersal pattern to bedforms at release point D was not so simple. This was due to the fact that the interference of waves at Out Head produces refraction and several wave-fronts with different orientations may pass over the area simultaneously (Fig. 2.1). Two sets of ripples perpendicular to each other were present at the sampling site, and the grain dispersal pattern was elongate in the direction bisecting the angle between the two ripple trains. In Figure 2.13,D sample points are aligned on the two ripple trains with strikes of 022^{o} and 112^{o}. The sediment transport direction is that of the vector resultant of the velocities and directions of the two wave-fronts.

Release point C, on the lower foreshore, exhibited a slightly different dispersal pattern (Fig. 2.13,C) which was characterised by a predominant onshore north-westerly movement. This distribution suggests that seawards of the spit-platform transport in the offshore direction is very minor and that a weak northerly component exerts an influence on the sediment motion. The resulting direction of dispersion is WNW.

2. Out Head

At the Out Head release point (Fig. 2.2, location 2) sediment movement was observed over a two week period. As at the previous locality the tracer sand was slightly coarser and more poorly sorted than the natural sand.

After two tides the grain distribution was characterised by north-eastern and eastern components, i.e. an onshore flood dispersion (Fig. 2.14,A). Over the next week however the onshore-flood components were lost and the trend became northerly (Fig. 2.14,B-D), which suggests that ebb-tidal currents draining into the Eden channel are responsible for the observed distribution.

Small-scale ripples in the area showed two trends. Adjacent to the low-water mark of the Eden channel ripples were orientated in the ebb-direction and had lee-slope azimuths of approximately 030°. To the south-east, i.e. shorewards, the azimuths became 120° to 140°. The two trends, at approximately 90° to each other, represent ripples formed by tidal currents (the former case) and by the lapping of waves on the shore as water-level falls (the latter case). Neither set of ripples corresponded with the measured grain dispersal direction, and it is possible that most sediment movement occurs prior to the bedform formation at an early stage in the ebb tide when tidal currents are draining towards the tidal outlet north-east of Out Head.

3. Kincaple Flat

On west Kincaple Flat the release point was in an area of cohesive sediment (Fig. 2.2,3A). Consequently the nature of the tracer sand was not comparable to that of natural sediment which contained approximately 20 wt% of silt and clay-size material. This discrepancy was in fact advantageous as the tracer was capable of responding to water movement as a sediment donor and by the generation of bedforms. The

results were interesting in that the distribution of grains around the release point bore little relation to the orientation of small-scale asymmetric ripples which were produced on the surface of the supply of tracer sand.

The fluorescent grains were dispersed to the west and north of the release point (Fig. 2.15) with maximum concentrations occurring in a N-NNE trending zone offset to the west of the release point. This suggests that sediment transport was in a direction roughly parallel to the estuary margin - a conclusion also derived from drogue studies in this area of the estuary.

The strike of the ripples formed in the tracer sand was 136°, and slip-face dips were to the south-west, thus inferring that the sediment transport direction was also to the south-west.

The east Kincaple Flat release point was also in an area of cohesive sediment (Fig. 2.2, 3B). The grain distribution, mapped after 2, 4 and 14 tidal cycles, indicated that the dispersion direction was to the ESE (Fig. 2.15). Eight metres to the east of the release point a small tidal channel carried grains seaward and so distorted the original pattern. The resulting distribution was to the ESE and NNE. The east-south-easterly direction is in general agreement with that suggested by drogue studies over East Kincaple Flat.

4. Coble Shore

To the west of Coble Shore (Fig. 2.2, 4A) grain dispersal was parallel to the western margin of the promontory. Movement was greater in the ebb (N) than in the flood direction (Fig. 2.16). The dispersal pattern was related to tidal current flow in a channel which lay to the west of the release point. A very minor onshore easterly component was also produced.

To the east of Coble Shore (Fig. 2.2, 4B) a lobate grain

distribution was observed after 14 tidal cycles (Fig. 2.16). The major transport direction was to the SE and would appear to be the result of early-stage ebb flow, which drogue studies indicated was in the direction which afforded the shortest route to the Eden channel at a point to the south of Sanctuary Spit. The release point was on the platform associated with Coble Shore and was affected by currents which were themselves influenced by the emergence of the platform. Once the platform is exposed, the area to the south of it is protected from the strong ebb currents of the Eden channel, and water continues to drain from it to the south-east and east.

5. The Flood Channel (within the flood-tidal delta)

The dispersal of grains in this setting on the northern margin of a flood channel (Fig. 2.17,5) was in accord with the dominant transport direction indicated by the asymmetry of large-scale bedforms. Grains moved to the SSW and into the deeper parts of the flood channel. This was probably aided by late stage flow in the troughs between the sand-waves. A similar flow direction was also recorded in the early stage of the flood tide at current-meter station 6 (Table 2.2, page 24).

Grain dispersion in the ebb direction had a prominent ENE component which may be indicative of flow down the stoss-side of the bedform into the adjacent trough.

6. The North Shore

At the North Shore station (Fig. 2.2,6) two separate areas with concentrations of over 100 grains per card were produced (Fig. 2.18). These were to the NE and SSE of the release point and are related to the ebb and flood-tidal current directions respectively.

Conclusions

1. On the West Sands there is a predominant onshore transport of

sediment, which, over the lower foreshore, is coupled with a northerly drift.

2. Tracer experiments appear to confirm the presence of lateral sediment transport in the marginal areas of the middle estuary.

3. Small-scale ripples are not reliable indicators of the direction of sediment transport in this environment. Where only one ripple train is present, however, its strike generally parallels the adjacent shoreline.

4. Large-scale bedforms faithfully indicate flow and sediment transport directions.

Historic Coastal Morphological Changes

The data presented in Chapter 1 (IV) showed that three major coastal changes have occurred since 1855:

1. a progressive easterly and northerly migration of Pilmour Links and Out Head,
2. a net landward movement of HWMOST on the northern part of South Tentsmuir Beach,
3. a net seaward movement of HWMOST on the southern part of South Tentsmuir Beach.

The progression of Pilmour Links and Out Head to both the north and east is related to the accumulation of wind-blown sand, as dunes, upon a base or spit-platform generated by the combined effects of wave-action and tidal currents. As the spit-platform extends northwards from Out Head, it might be assumed that there exists a balance between on- and offshore sediment transport processes, that is, between flood-tidal currents combined with wave-action, and ebb-tidal currents. However, flood-tidal currents appear to have very little influence to the south of the Eden channel in the lower estuary and the balance must be between wave-action and ebb-tidal currents.

To the north of the Eden channel, however, the gross coastal changes indicate a predominantly landward transport of sediment. At least a part of the material eroded from the north part of South Tents-muir Beach may have accumulated on the south part of the same area. The south-westerly migration of Sanctuary Spit also testifies to the dominance of onshore-directed processes.

Wave Induced Flow Patterns

The spit-platform to the north of Out Head is often covered by interference ripples consisting of two or three ripple trains of sub-equal development but different orientation. The orientation of these structures is related to wave refraction patterns developed in the entrance of the estuary.

Air photographs taken on 11th. August 1973 during the late stage of a flood tide show three prevalent directions of wave propagation to the north of Out Head (Fig. 2.19, a, b). These are:

1. wave-fronts associated with water moving up the Eden channel in a SSW direction (Fig. 2.19b, 1). Due to the shape of the inlet the wave-fronts have a strong westward convexity.
2. wave-fronts approaching from the West Sands in the direction of 260^{o} (Fig. 2.19b, 2).
3. a refracted portion of the Eden channel wave travels down the eastern margin of the spit-platform in the direction of 215^{o} (Fig. 2.19b, 3).

The wave-fronts converge on the platform and intersect at approx-imately right-angles to produce diamond-shaped areas between wave crests. In such a situation sediment may accumulate on the platform during both the flood and ebb parts of the tidal cycle, as described by Oertel (1972). Oertel concluded that where wave crests interfered, surges of water towards the shoreline were produced, and waves which

'broke' at interference points created bores which carried sediment shoreward. He also found that, during the ebbing tide, sediment being transported seaward by tidal currents was diverted landward in gyral paths created by the interference of tidal currents and wave surge. The resultant 'sediment gyres' acted as sediment traps which caused sediment to accumulate on the swash-platform.

In the Eden entrance waves approach the spit-platform from the east and east south-east during the early stages of the flood tide due to wave refraction around the ebb-tidal delta (Fig. 2.20). The waves break on the eastern margin of the platform and sediment is transported westwards. As the tide rises and submerges the major intertidal sand-bodies, waves are alloued to enter the estuary from the north-east as well as from the east. At this stage the process of interference and cell formation over the spit-platform begins, and it continues up to the time of high-water. The formation of sediment gyres may be important in the retention of sediment on the spit-platform during the early stage of the ebb tide, but as the spit-platform emerges with two hours of high-water, they are relatively short-lived phenomena.

The mean direction of the wave-front which enters the estuary from the north-east is 213°, and, once inside the inlet, the main wave-front travels over the flood-tidal delta system, that is, to the north of the Eden channel (Fig. 2.19b, 4). A second wave (Fig. 2.19b, 5)is split from the first and travels up the Eden channel, interfering with the first wave over the ridge on the south side of the flood-tidal delta as it does so.

Topographic features on the east side of the spit-platform associated with Sanctuary Spit cause waves to interfere and approach the shore at varying angles (Fig. 2.19b, 6). Sediment which accumulates in this area during the flood-stage by wave and tidal-current processes is subject to very little erosion by ebb-tidal currents.

Ebb-flow from the middle estuary is diverted southwards by the western margin of the spit-platform.

A Summary of Flood- and Ebb-Tide Flow Patterns

During the flood tide four phases of tidal-current flow were recognised (Fig. 2.21).

Phase 1 consists of tidal-current flow restricted to the Eden channel. The general flow direction is to the west, but the flow follows the sinuous course set by the Eden channel. Within the flow a single helicoid spiral structure may develop.

Phase 2 is marked by flow in a direction tangential to the Eden channel. As the water-level rises, the flow leaves the confines of the channel and takes a more direct route to the west, utilising landward shoaling flood channels.

Phase 3 begins about two hours before high-water and is characterised by a uniform flow direction in the lower estuary, with a considerable angular relationship to the Eden channel of the middle estuary.

Phase 4 consists of flow sub-parallel to the estuary margins on Kincaple Flat and its opposite number to the north of the Eden channel.

Superimposed on the tidal-current flow patterns are the wave-induced flow patterns which are especially important in the lower estuary during phase 3.

Ebb-flow directions are more uniform than those of the flood, and for most of the ebb-flow period there is a tidal drain with water taking the most direct route to the tidal outlet (Fig. 2.22a).

The emergence of major sand-bodies in the lower estuary is a strong influence on flow directions during the intermediate stage of the ebb tide (Fig. 2.22b). The two north-south trending structures to the north of Out Head effectively restrict flow to the Eden channel

and the flow convergence at the tidal outlet results in high current velocities. Beyond the outlet flow divergence occurs over the ebb-tidal delta. The exposure of the western margin of the flood-tidal delta has the pronounced effect of diverting ebb-currents to the south of the structure, hence reducing flow velocities over the delta itself.

Late-stage ebb-flow is controlled by the dendritic drainage pattern in the middle estuary and by topographic features and bedforms in the lower estuary. Flow directions are therefore extremely variable. Water in the Eden channel at low-tide only maintains contact with the water of St. Andrews bay via a very shallow south-east trending distributary on the southern margin of the ebb-tidal delta.

Fig. 2.5a. Velocity vectors of near-surface currents.

Surface - Current Velocity Vectors
Stations 1 - 6

Directions relative to true north

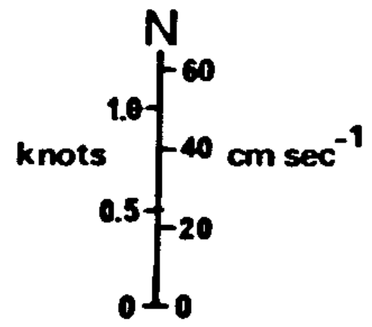

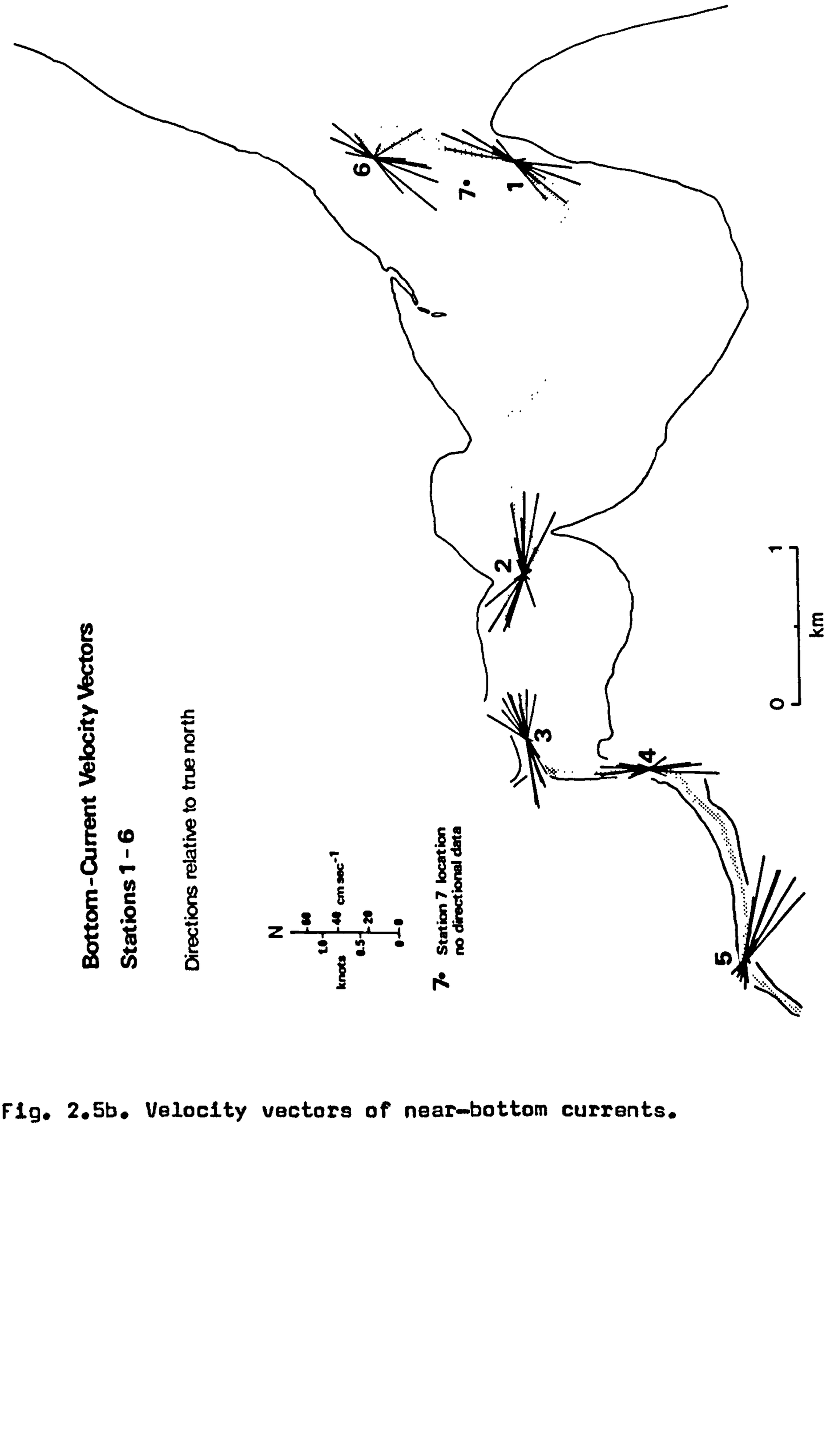

Fig. 2.5b. Velocity vectors of near-bottom currents.

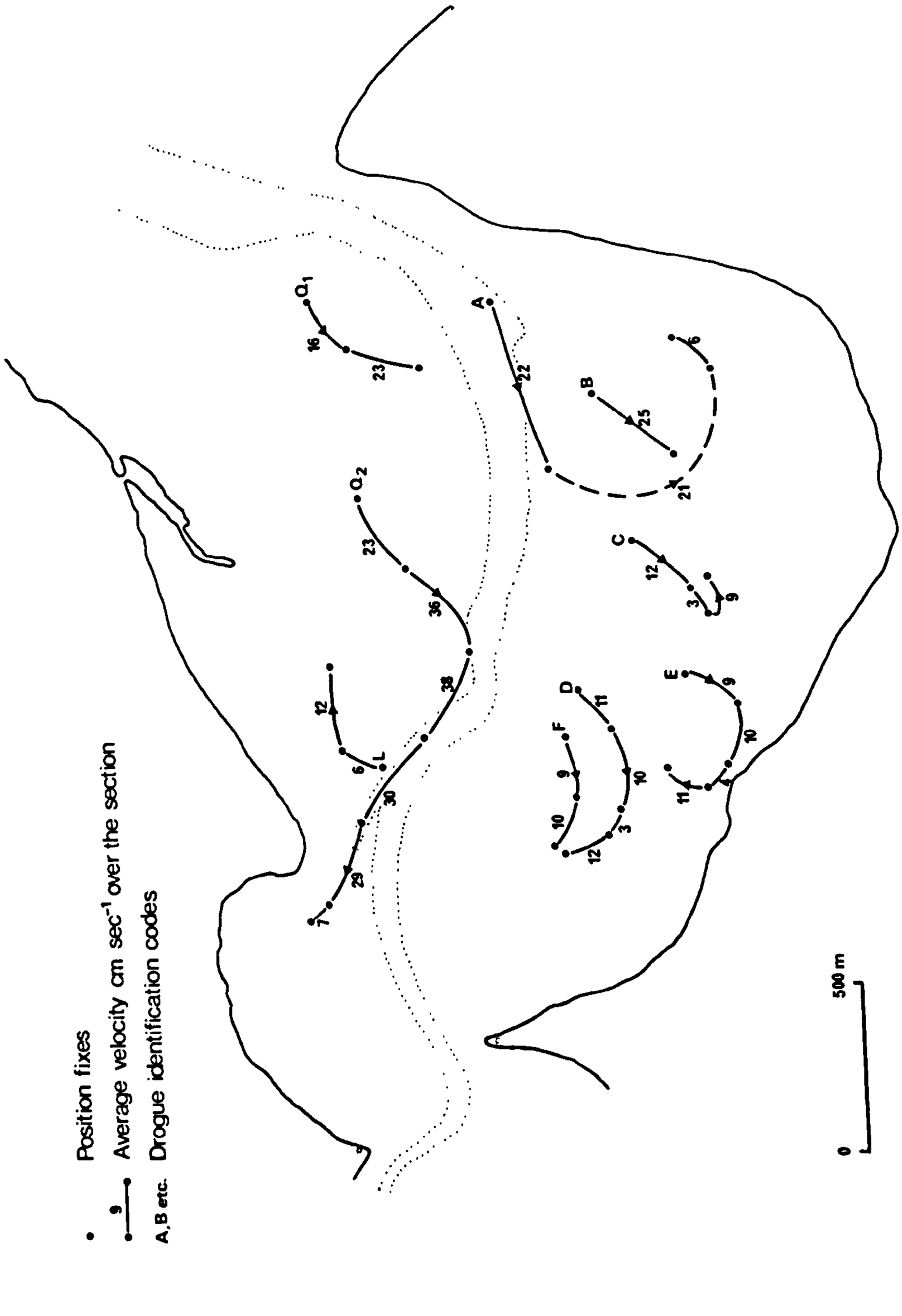

Fig. 2.6. Flood-tidal current flow paths as indicated by drogues suspended 0.5 to 1.0m below the water surface.

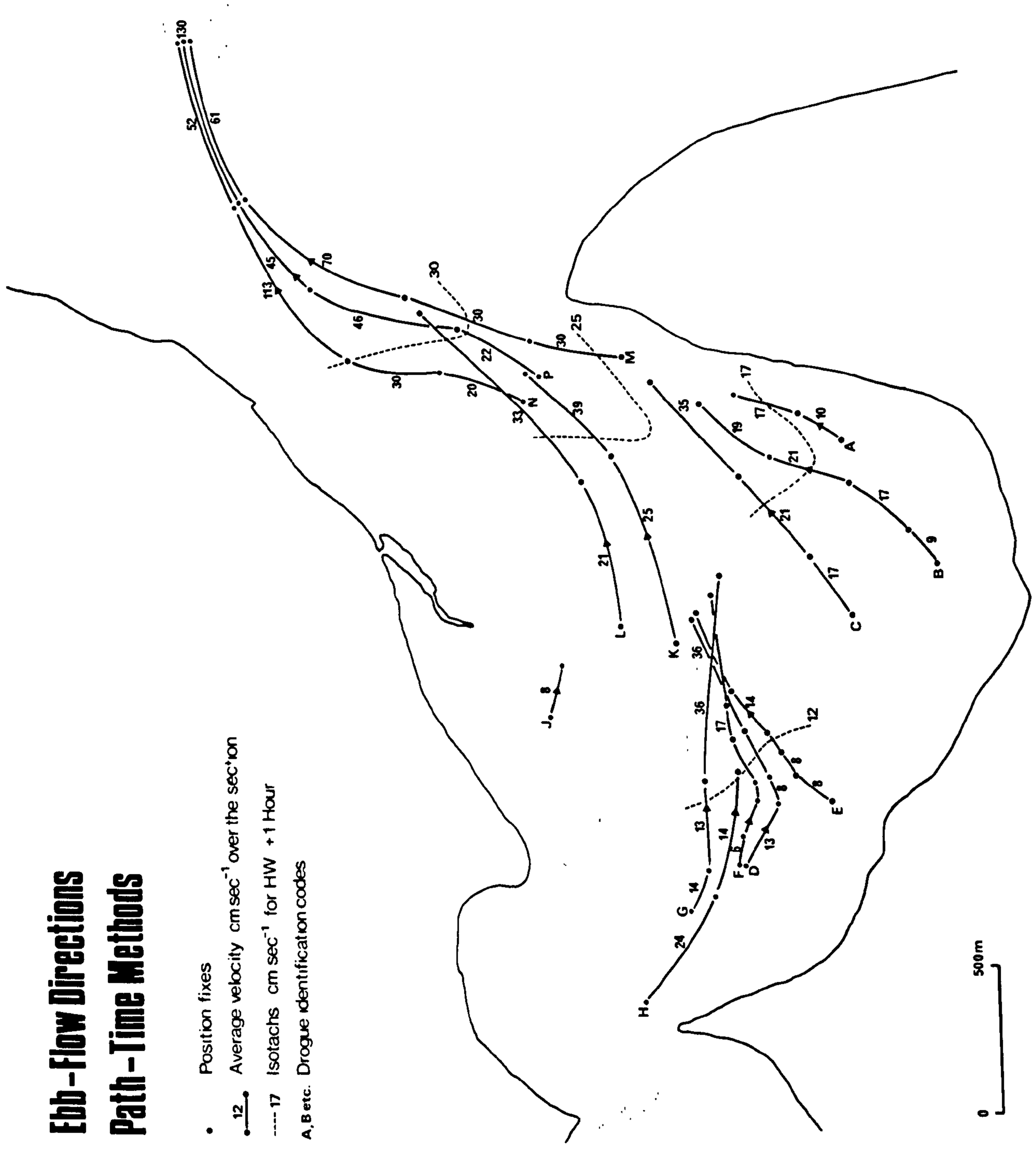

Fig. 2.7. Ebb-tidal current flow paths as indicated by drogues suspended 0.5 to 1.0m below the water surface.

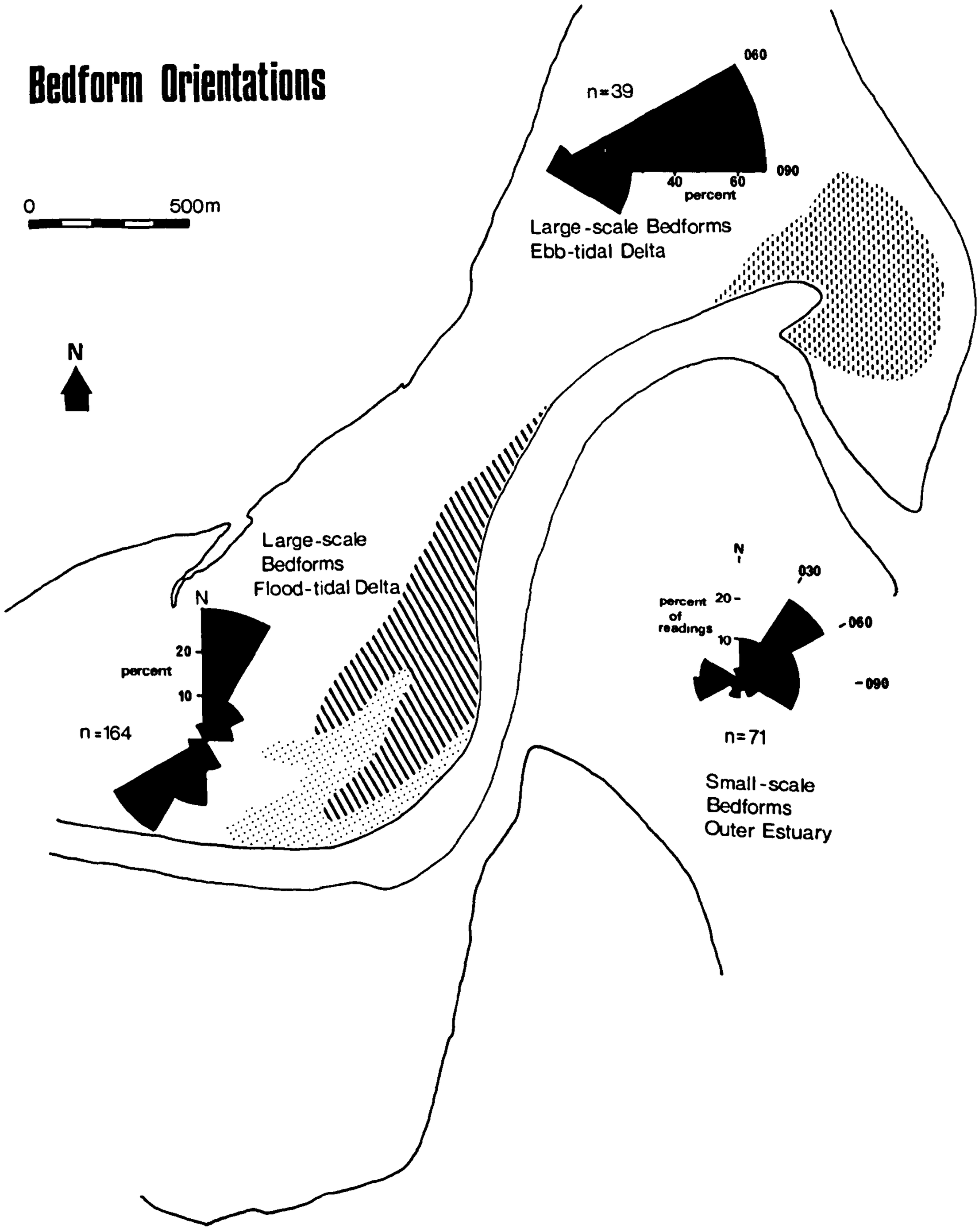

Fig. 2.8. Bedform orientations (lee-slope azimuths) in the lower estuary.

Broken lines : large-scale bedforms on ebb-tidal delta
Diagonal lines : flood-orientated large-scale bedforms on flood-tidal delta
Dots : ebb-orientated large-scale bedforms on flood-tidal delta.

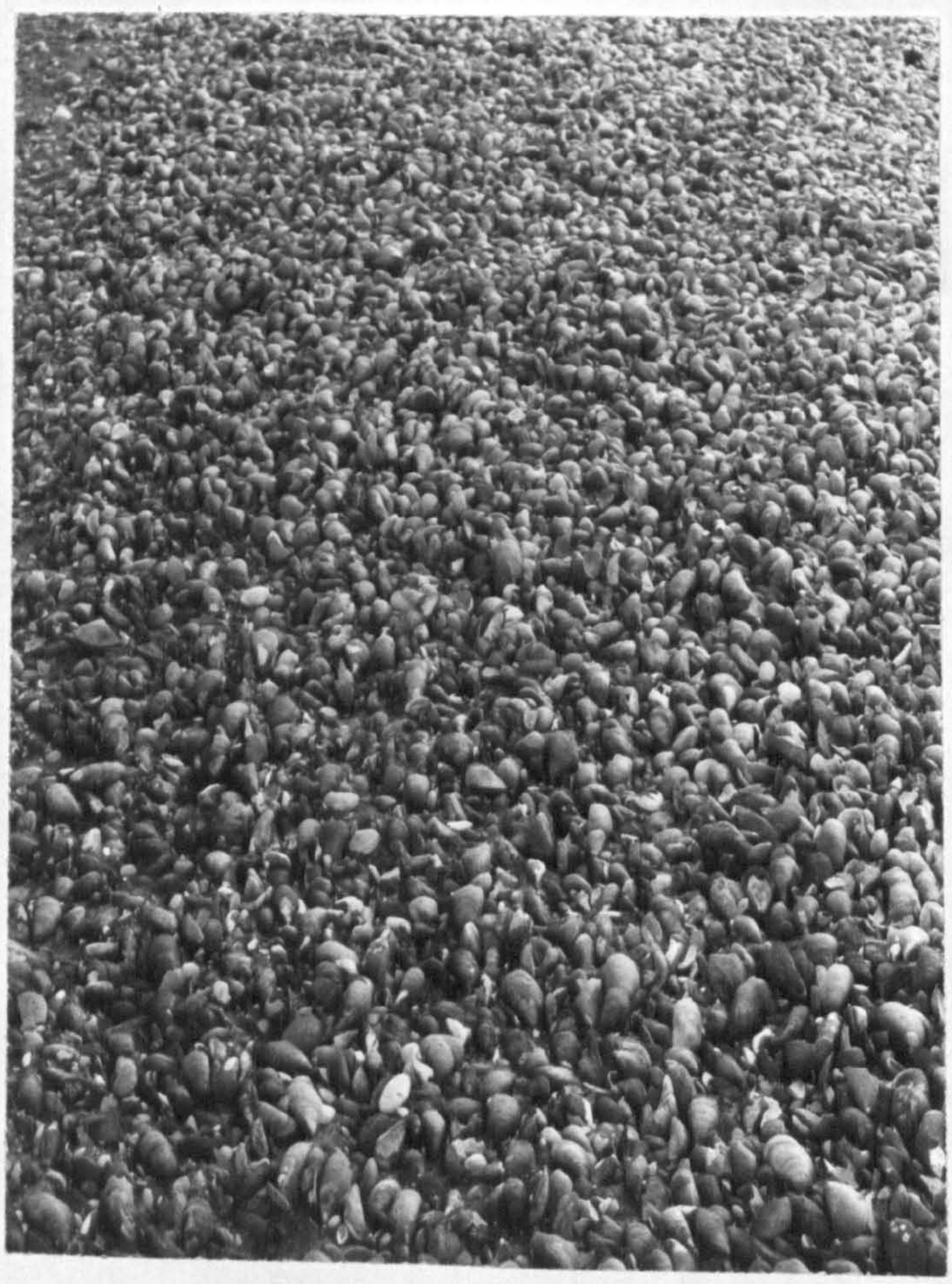

Fig. 2.9. A shell pavement composed of the disarticulated valves of Mytilus edulis. Note the convex-upward attitude of the valves and the preferred orientation of the umbones. Current direction was towards the top of the page.

Fig. 2.10. Ebb-tidal current flow paths as indicated by the trails left by algal scrolls. Flow towards the observer.

Fig. 2.11. The seaward end of a trail with the actual algal scroll which produced it.

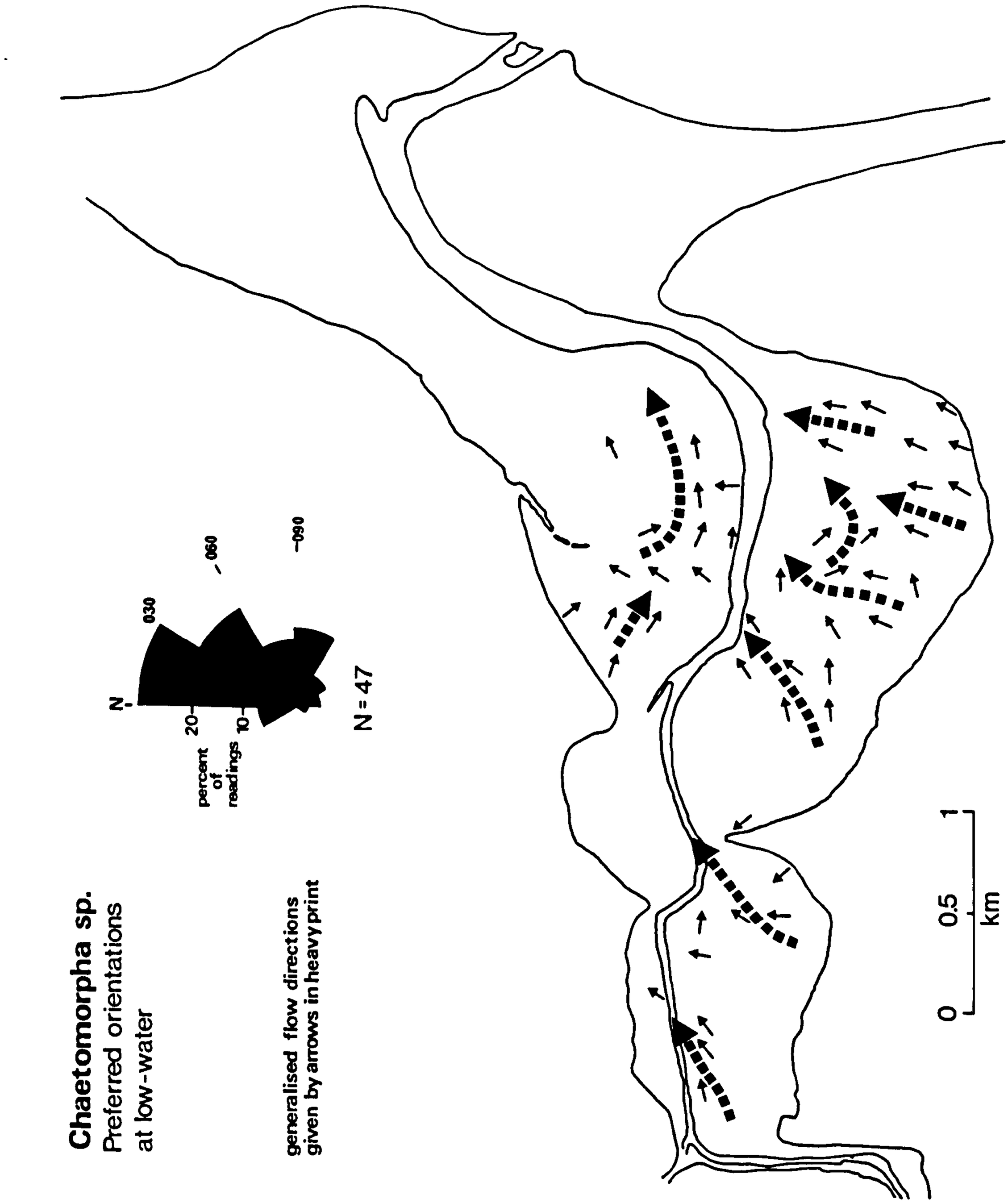

Fig. 2.12. The preferred orientations of strands of the filamentous green alga Chaetomorpha sp.. Inferred ebb-flow directions are shown by the large arrows.

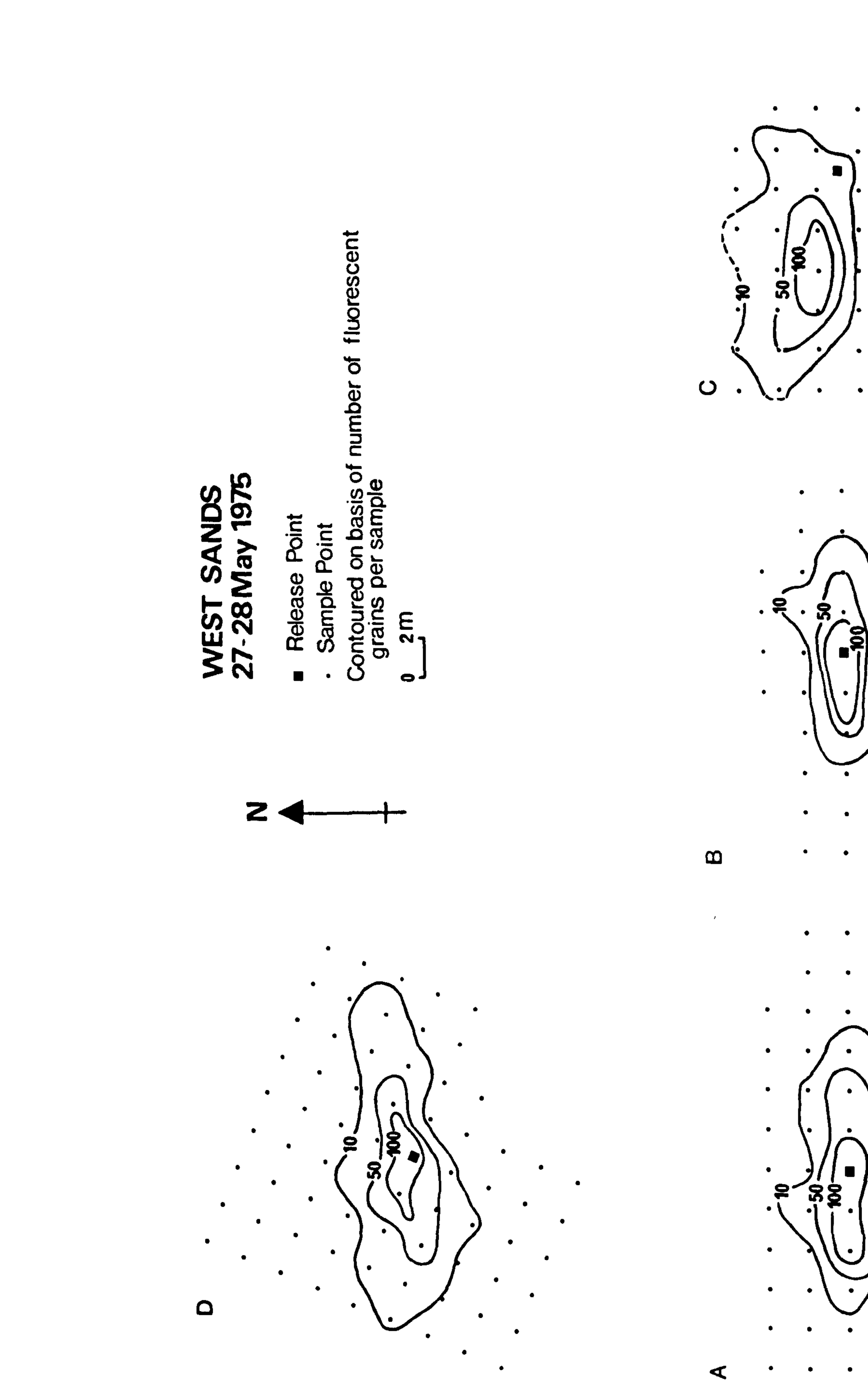

Fig. 2.13. Tracer sand dispersal patterns for the stations on the West Sands. Each grid pattern has been rotated in order to conform with the orientation of true north shown. The locations of A, B, C and D were given in Figure 2.2.

OUT HEAD

Sand released 21-1-75

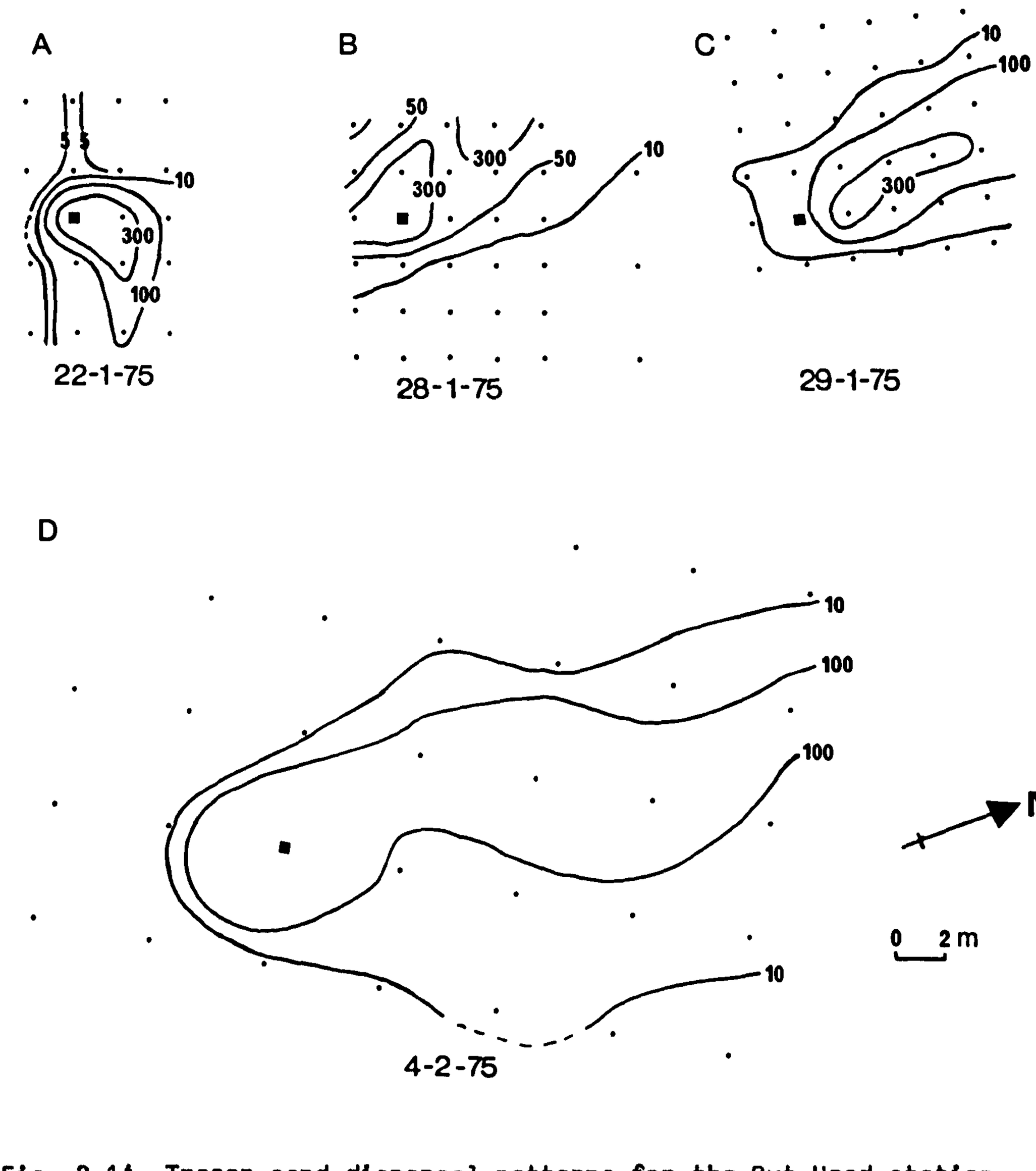

Fig. 2.14. Tracer sand dispersal patterns for the Out Head station. Contour values are of the number of fluorescent grains per sample.

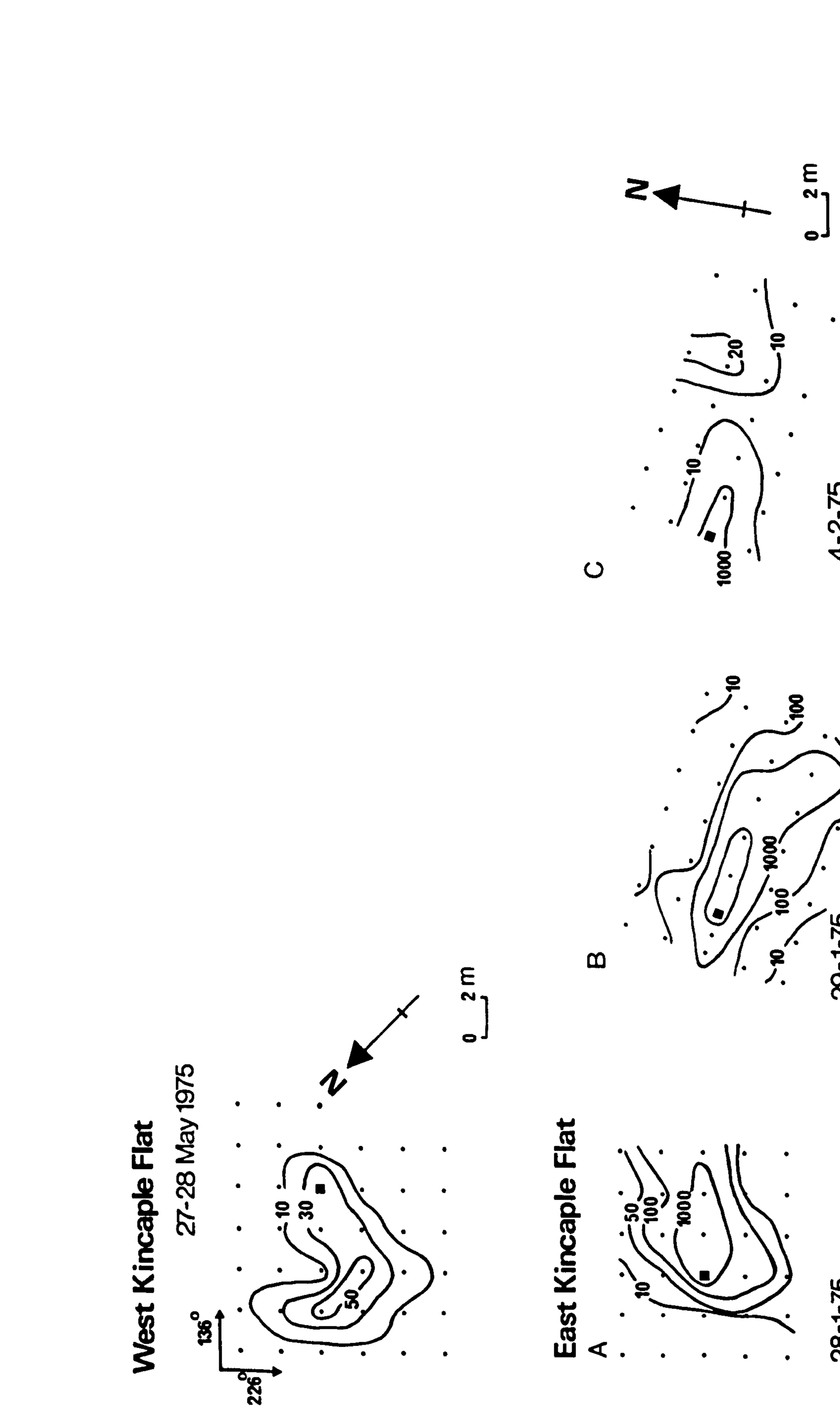

Fig. 2.15. Tracer sand dispersal patterns on west and east Kincaple Flat. Contour values are of the number of fluorescent grains per sample.

COBLE SHORE

West

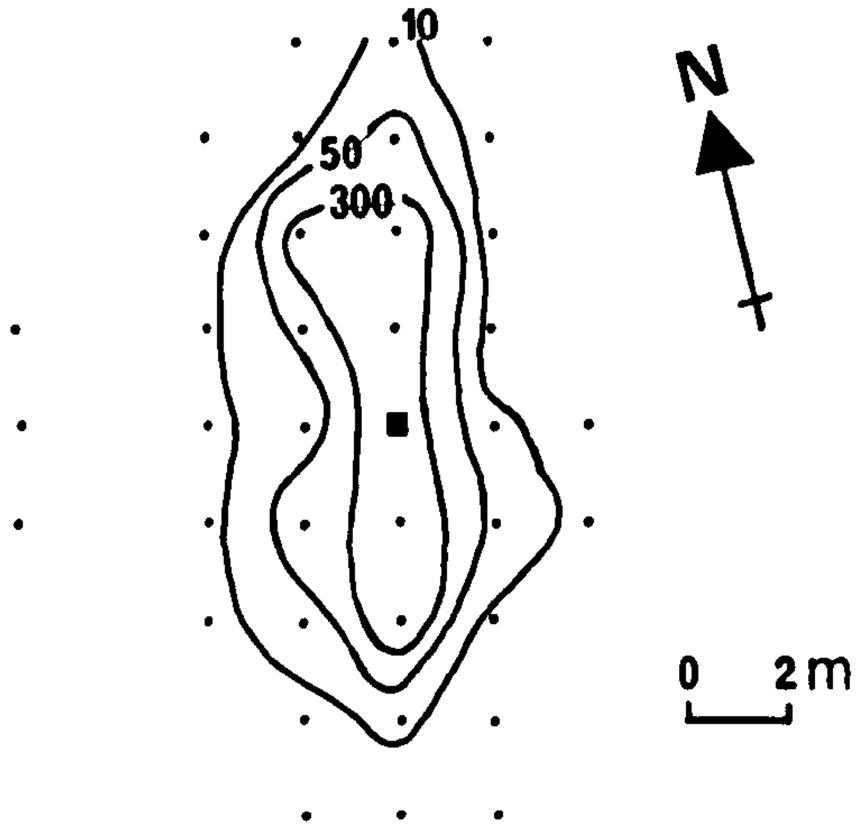

27-28 May 1975

East

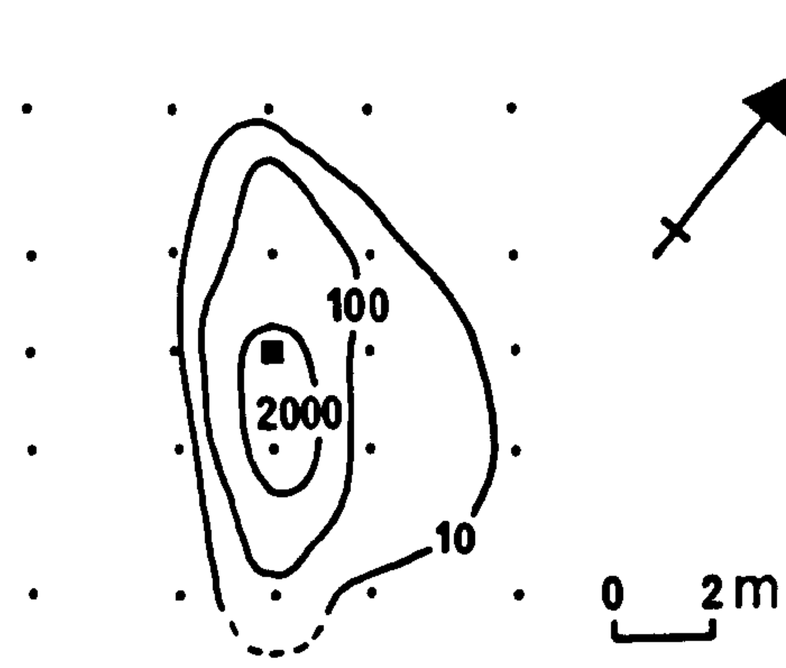

13-21 January 1975

Fig. 2.16. Tracer sand dispersal patterns to west and east of Coble Shore.

FLOOD CHANNEL

4-5 March 1975

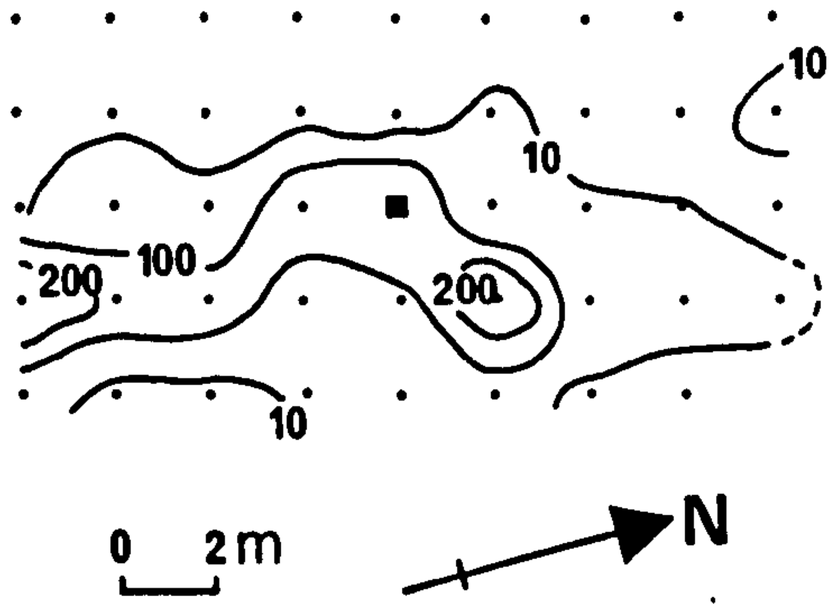

Fig. 2.17. Tracer sand dispersal pattern in the flood channel.

NORTH SHORE

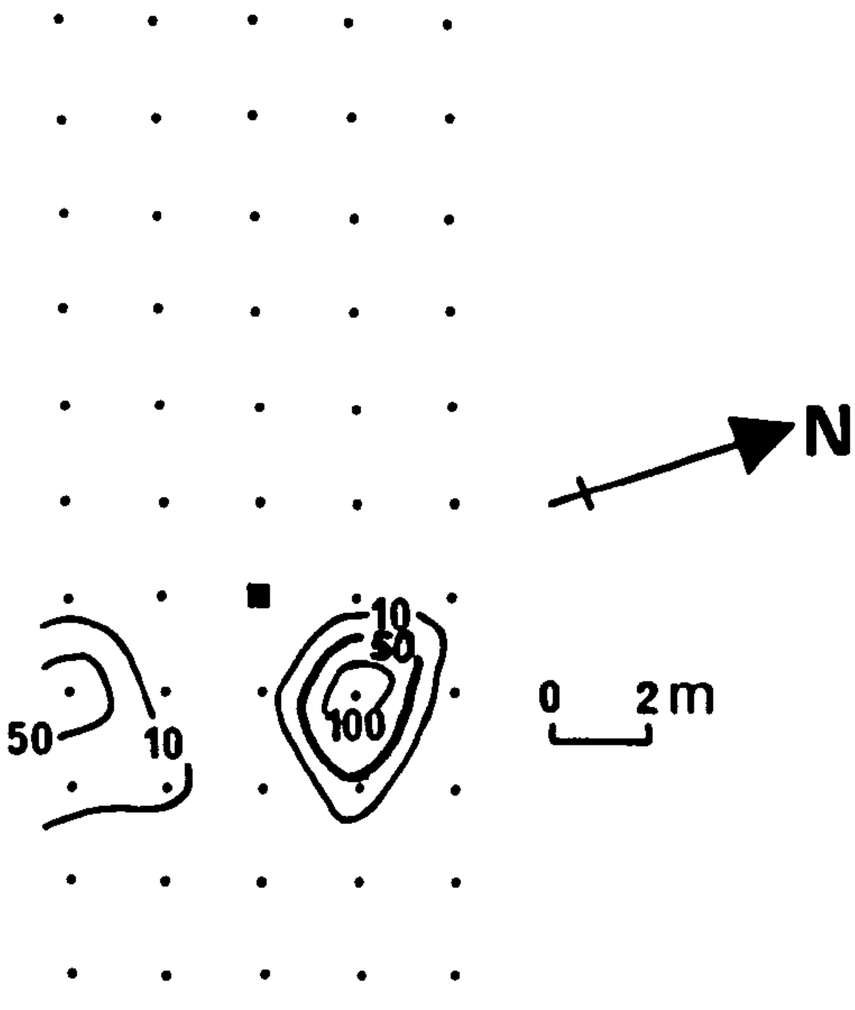

Fig. 2.18. Tracer sand dispersal pattern on a part of the north shore of the estuary.

All contour values are of the number of fluorescent grains per sample.

Fig. 2.19a, Air photograph 11 August 1973, (Fairey Surveys Ltd) showing wave refraction and interference at the entrance to the Eden estuary.
See also Fig. 2.19b.

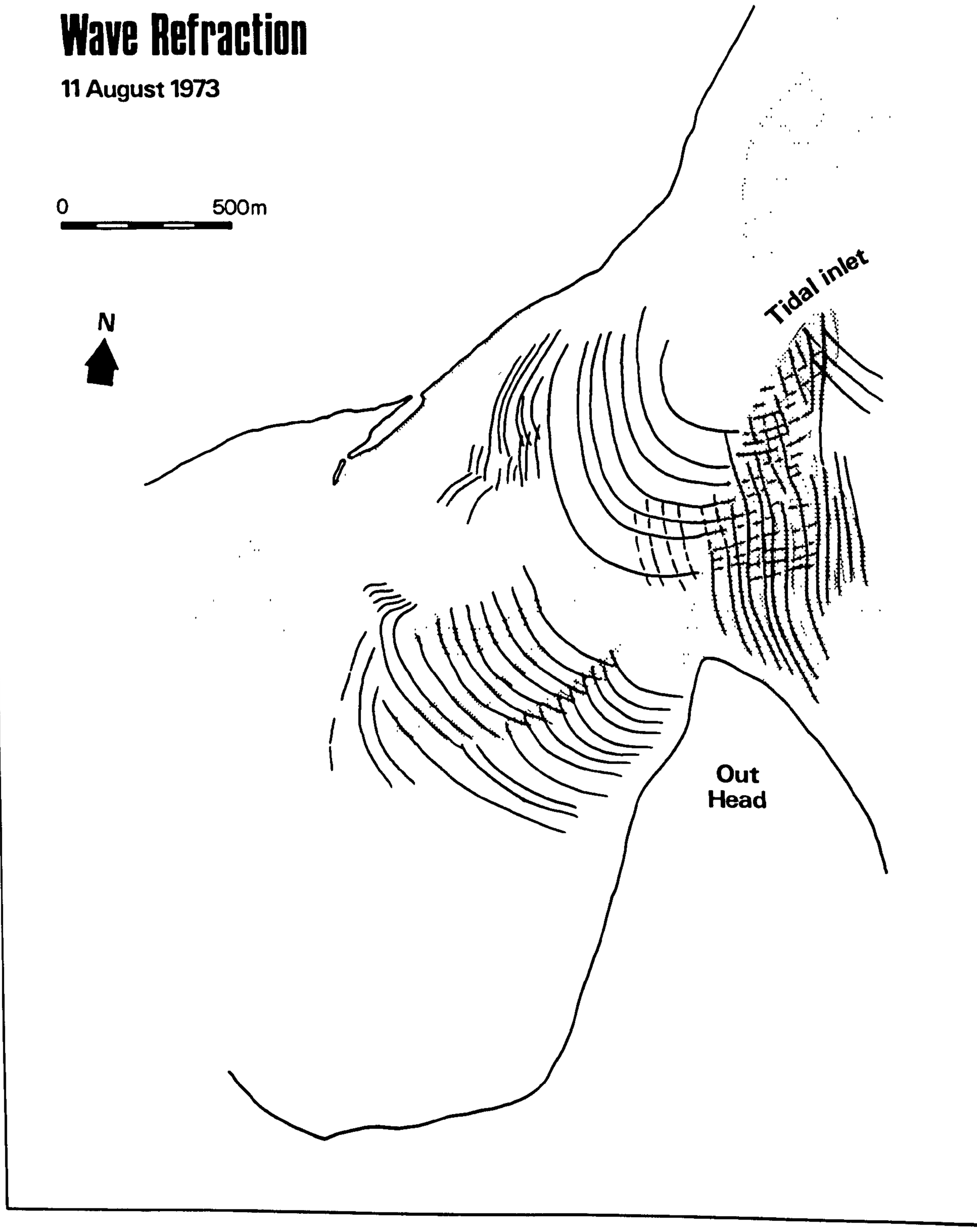

Fig. 2.19b. Wave refraction in the vicinity of Out Head, 11 August 1973. Note the formation of diamond-shaped cells over the spit-platform to the north of Out Head by the interference of two wave-fronts. (Drawn from an air photograph.)

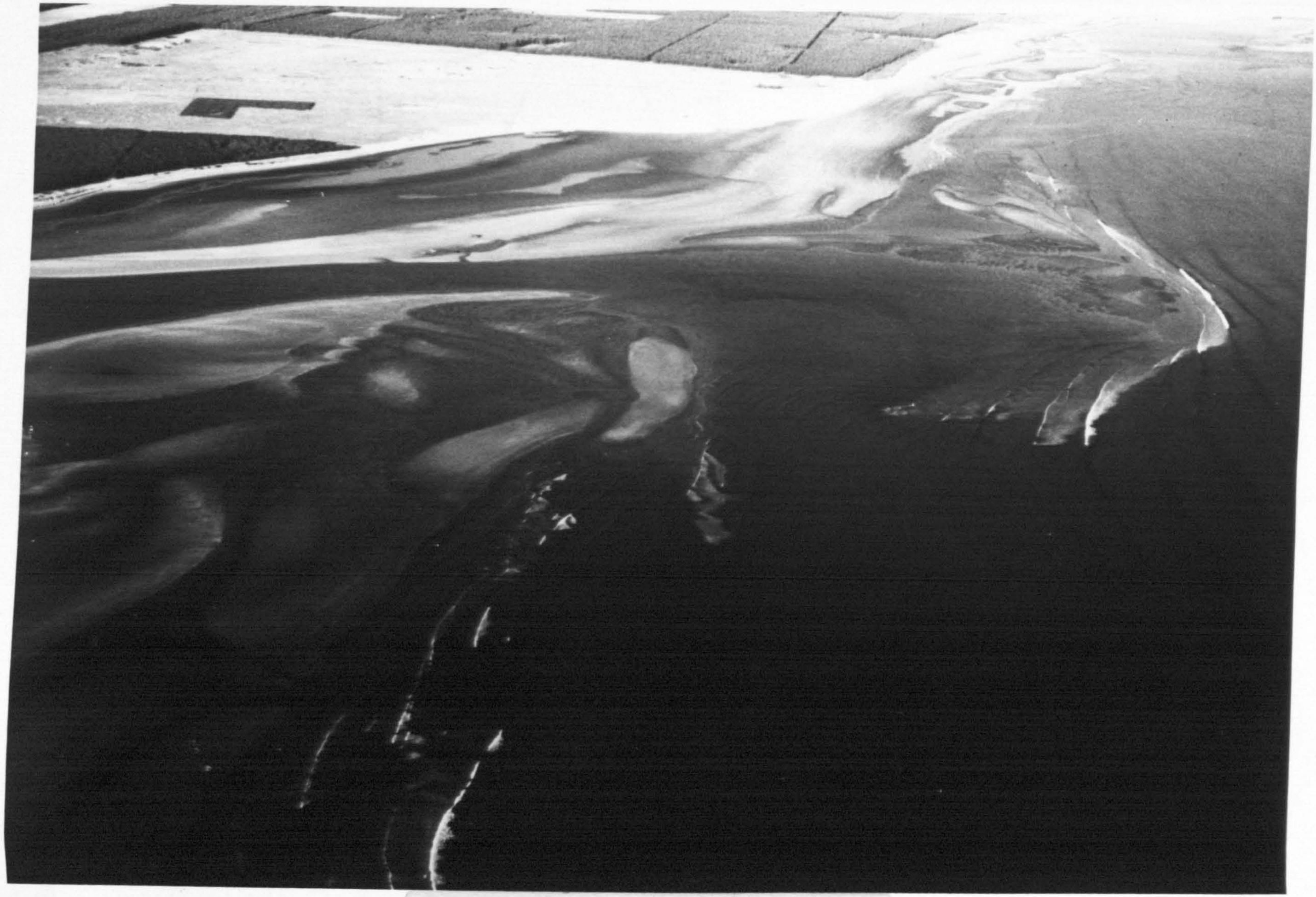

Fig. 2.20. Wave refraction around the ebb-tidal delta during the early stages of the flood tide.

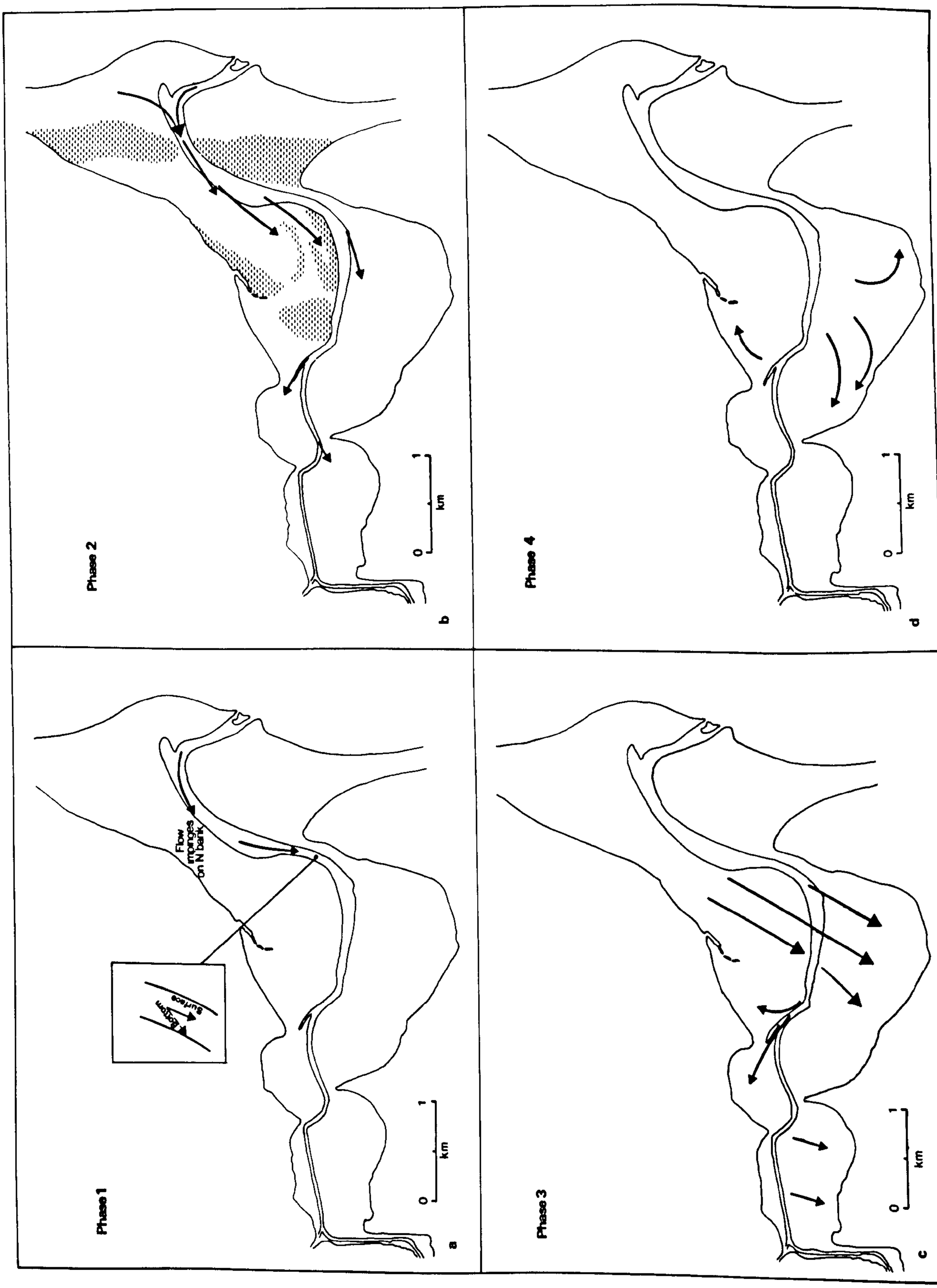

Fig. 2.21. The four directional phases of flow during the flood tide based on a combination of eulerian and lagrangian data.

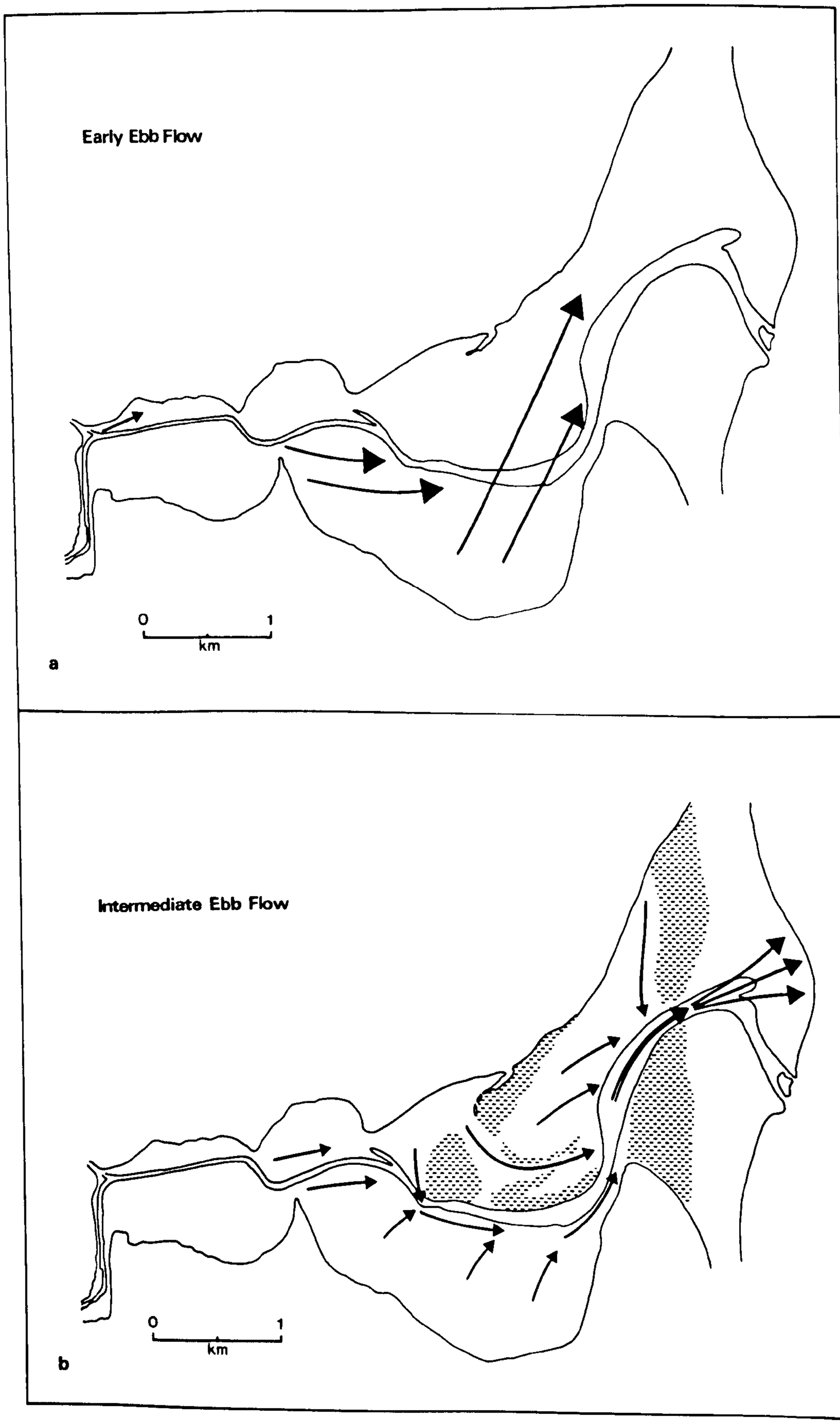

Fig. 2.22. The early and intermediate stages of ebb-tidal flow based on eulerian and lagrangian data. Shaded areas on b are major intertidal sand-bodies.

IV. VELOCITY-SALINITY RELATIONSHIPS

Station 1: Out Head (Fig. 2.23)

a. Velocity

In the upper 60% of the water column ebb-flow continued for 1.5 to 2 hours after the flood had begun near the bed. In the first hour after the flood was established throughout the water column the highest velocities were at approximately two-thirds depth. During the remainder of the flood part of the cycle, however, the maximum velocities occurred near to the surface. The maximum recorded velocity was 96cm sec^{-1} at 1m below the surface 1.5 hours before high-water.

During the ebb tide surface velocities were always in excess of these on the bed, and maximum velocities occurred 3.5 hours after high-water. Surface currents were of the order of 100cm sec^{-1}, and those near the bed 30-40cm sec^{-1}.

b. Salinity

From the time of high-water to 1.5 hours before low-water the water column was well mixed with respect to salinity with a maximum variation of 0.2‰ (0.63%). During the same period there was a general decrease in salinity from 31.6‰ to 28.5‰. Salinity stratification developed during the last hour of the ebb and the first two hours of the flood. During this period the surface salinity continued to decroase, whereas the bottom salinity began to increase under the influence of flood-directed currents. Stratification was at a maximum 4 hours before high-water when the top to bottom salinity difference was 5.5‰. Three hours before high-water the column was of almost uniform salinity (31.1 to 31.4‰), and one hour later a consistent salinity of 32.3‰ was recorded. Between this time of maximum salinity (32.3‰) and the time of high-water salinity decreased by 0.8‰.

c. Mean Velocity

The cycle was divided into 12 lunar hours and the mean velocities calculated for each interval of 0.2 x total water depth. The net non-tidal flow for the station (Fig.2.23c) shows that the upper 40% of the column is characterised by a net seaward flow of up to 0.08m sec^{-1} and the lower 60% by a net landward flow of up to 0.05m sec^{-1}.

d. Mean Salinity

Mean salinity (Fig.2.23d) shows only slight variation between the surface and lower layers. Mean stratification is 3.6% which represents a salinity variation of 1.2‰.

Station 2: Coble Shore (Fig. 2.24)

a. Velocity

Flow velocities at low-water were of the order of 10cm sec^{-1} in the ebb direction. Within the first half-hour of the flood tide the flow direction was reversed and velocities increased rapidly: 77cm sec^{-1} was recorded at 0.5m below the surface and 44cm sec^{-1} within 20cm of the bed. This initial surge was not maintained and velocities of less than 60cm sec^{-1} characterised the second hour of the flood. A second period of high velocities occurred 1.7 hours before high-water. In the last hour before high-water velocities decreased and the velocity stratification was much reduced.

Ebb flow velocities were less than 30cm sec^{-1} for the first 2.25 hours, after which they increased rapidly. The flow became stratified and a velocity of 97cm sec^{-1} was recorded at the surface 3.75 hours after high water.

b. Salinity

The depth-salinity-time diagram illustrates the abrupt increase

in salinity which the initial surge of flood water generated. Salinity stratification increased to a maximum of 10.41% some 1.2 hours before high-water, and then the column became homogeneous at a salinity of 33‰. Maximum stratification (7.5%) in the ebb part of the cycle occurred 2.2 hours after high-water.

c. Mean Velocity

Mean velocity (Fig.2.24c) was seaward at all depths and varied between 6 and 10cm sec^{-1}.

d. Mean Salinity

The range of mean salinity (Fig.2.24d) was from 23.6‰ at the surface to 24.3‰ at the bed.

Station 3: Paper Mill (Fig. 2.25)

The features of the velocity and salinity distributions at this station are similar to those at Coble Shore. The period of maximum flood velocities, which were located in the upper part of the water column, occurred 1.5 hours before high-water, and maximum ebb velocities were recorded 4 hours after high-water (Fig. 2.25a). In comparison with Coble Shore, however, the period of rising water associated with the flood tide was of shorter duration, 3 hours as opposed to 4.

Salinity stratification was always more marked at the Mill station than at Coble Shore and, even over the high-water period, a variation of 3.2% was present (Fig. 2.25b). Maximum stratification occurred at the beginning of the flood (12.5%) and a secondary peak of 11.11% developed during the ebb, 2 hours after high-water.

The salinity range at the Mill station was considerable. During the low-water period salinity decreased from 10‰ to 1‰, but with the influx of flood tidal currents 4 hours before high-water salinity increased rapidly to 20‰ and then more slowly to 31‰, which value

was maintained near the bed for the 2-hour period around high-water. The maximum surface salinity was 30.2‰.

Mean velocity was seaward at all depths and varied between the narrow limits of 10.7 and 12.1cm sec^{-1} (Fig. 2.25c).

Mean salinity (Fig.2.25d) shows a slight stratification with the surface layer of 17.2‰ and the bottom layer of 17.81‰.

Station 4: Guardbridge (Fig. 2.26)

a. Velocity

Ebb flow velocities of the order of 20cm sec^{-1} were reduced rapidly by the flood tide, and within a 20-minute period a flood directed flow of the same magnitude had been established. The flood tide, which lasted for 2.5 hours, was characterised by one period of high velocities (50 to 60cm sec^{-1}) which occurred 1.5 hours before high-water. Half an hour after high-water an ebb flow with maximum velocities of 36cm sec^{-1} was observed. The high velocities occurred only in the upper part of the column and were a short-lived phenomenon, as within half an hour ebb velocities of only 2cm sec^{-1} characterised the whole water column. The ebb-flow was then re-established and gradually increased to a maximum of 73cm sec^{-1} 3.5 hours after high-water.

b. Salinity

Salinity increased gradually during the period of the flood tide resulting in salinities of 24‰ on the bottom and 21‰ near the surface at the time of high-water. A slight stratification characterised the flood with water in the surface layer approximately 3‰ less saline than the remainder of the column which tended towards uniform salinity.

Immediately after high-water salinity in the surface layer decreased rapidly (21‰ to 9‰ in 0.5 hour), whereas in the lower

layers salinity values remained at 22 to 24‰ for 2 hours after high-water. In the halocline salinity changes of 9.5‰ to 15.9‰ occurred over a depth interval of 0.5m.

Mean velocity (Fig.2.26c) was in the seaward direction at all depths. Figures based on flow over a 8.25 hour period show that the net velocity in the upper layer is 16.27cm sec^{-1} and 5.87cm sec^{-1} in the lower layer.

Average salinity (Fig.2.26d) over the same period showed a stratification from 3.33‰ at the surface to 7.63‰ near the bed.

Station 5: Upper Estuary (Fig. 2.27)

The tidal curve for this station was strongly asymmetrical with the rise in water-level associated with the flooding tide, taking only 2.25 hours and the period of falling water-level being 3.5 hours

At the surface of the flow flood-orientated currents were evident for only 1.25 hours (Fig.2.27c). At the beginning of this period ebb velocities of 60 to 70cm sec^{-1} were rapidly halted and water of zero salinity was forced to move landward by tidal pressure. Fresh-water flow velocities in the landward direction reached 30cm sec^{-1}. The flow direction at the surface reversed to an ebb flow about 1 hour before high-water and velocities gradually increased to 22cm sec^{-1} at the time of high-water and 40cm sec^{-1} 30 minutes after high-water.

At the same time as the ebb flow established itself at the surface, the first traces of a saline intrusion were observed near the bed (Fig. 2.27a, b). Salinity increases near the bed during the last 0.5 hour before high-water were accompanied by increased flood flow velocities. In the first hour after high-water flood directed velocities in the lower 60% of the water column decreased whilst ebb directed velocities in the upper part of the column increased. Salinity throughout the

column also increased during this time, and saline water was entrained into the seaward flowing upper layer to the extent of 0.3‰. During the next hour salinities in the upper 60% of the column decreased, whereas on the bed the increase continued and a maximum salinity of 20‰ was recorded 2 hours after high-water. Salinity decreased to zero in the succeeding hour, and seaward directed fresh-water with velocities of 60 to 70cm sec^{-1} occupied the whole column.

The graph of mean velocity (Fig.2.27c) shows that the net flow is seaward at all depths with values ranging from 21.12cm sec^{-1} near the bed to 38.35cm sec^{-1} at the surface.

The mean salinity for the station (Fig.2.27d) shows that a fresh-water surface layer overlays a uniform salinity gradient to the bottom.

Current Velocities over the Flood-Tidal Delta

Current velocity profiles were measured at two station on the flood-tidal delta. In each case the area became dry at low-water.

Station 6: Flood Sand-Wave Field (Fig. 2.28a)

Current velocities increased gradually during the flood, which lasted 3.5 hours, and were at their peak between 2 and 1.5 hours before high-water. Surface currents were in the excess of 70cm sec^{-1} and those near the bed 30 to 50cm sec^{-1}.

Ebb velocities reached 20cm sec^{-1} near the surface about 1 hour after high-water and the same near the bed some 0.7 hours later. Maximum ebb velocities of 35cm sec^{-1} were recorded in the upper part of the column 2 to 2.5 hours after high-water. Velocities in excess of 30cm sec^{-1} were noted near the bed during the same time interval.

It is evident that a marked asymmetry exists between the maximum velocities of flood and ebb currents and also between the times of occurrence of these maximum velocities relative to high-water.

Net mean velocity (Fig.2.28c) shows a landward residual of 3.36cm sec^{-1} near the bed and 14.05cm sec^{-1} near the surface.

Station 7: Channel in Flood-Tidal Delta (Fig. 2.28b)

The tidal curve at this station was more symmetrical than that recorded at the flood sand-wave field station which was characterised by a flood period of shorter duration than the ebb. The distribution of velocities was, however, similar in both cases, and there occurred a single period of high flood current velocities. At station 7 these occurred 1.3 hours before high-water and near surface velocities were 70 to 76cm sec^{-1}, whilst those near the bed were 40 to 50cm sec^{-1}.

Ebb velocities reached maximum values of 50 to 60cm sec^{-1} near the surface and 30 to 40cm sec^{-1} near the bed about 2.7 hours after high-water.

Net mean velocity (Fig.2.28d) was in the landward direction at all depths and varied between 7.3 and 9.3cm sec^{-1}.

The fact that the station was sited on a channel used by both flood and ebb currents explains the occurrence of higher ebb velocities than were observed at the previous station. Relative to the flood sand-wave field station the differential between flood- and ebb-current velocities is reduced, whereas the time asymmetry is enhanced.

General Features

In so far as generalisations may be drawn from the data presented, the following features are of note:

1. the degree of asymmetry of the tidal curve increases in the landward direction with the period of rising water-level becoming shorter, eg. 5.5 hours at Out Head, 3.75 hours at Coble Shore and 2.4 hours at the Upper Estuary station;

2. the time of maximum flood currents is consistently between 1.5

and 1.8 hours before high-water. A secondary flood peak may occur at the beginning of the flood period when water is confined to the Eden channel;

3. maximum ebb-tidal currents occur late in the cycle between 3 and 4 hours after high-water when water is confined to the Eden channel;

4. maximum ebb-tidal current velocities are generally greater than maximum flood-tidal current velocities;

5. the time of occurrence of maximum salinities relative to high-water varies systematically throughout the estuary. At the Out Head station salinity was at a maximum on the bed between 2.5 and 1 hour before high-water. At the Paper Mill station maximum salinity was in-phase with the water-level maximum. At the Upper Estuary station maximum salinity occurred 2 hours after high-water. The Coble Shore station showed the highest salinities near the bed over a 1.6 hour period which spanned the time of high-water, and at Guardbridge salinities were at a peak for 1.2 hours beginning at the time of high-water;

6. the three sections of the estuary represented by the Upper Estuary station and Guardbridge, the Paper Mill and Coble Shore, and the Out Head station may be classified according to the stratification and circulation parameters of Hansen and Rattray (1966). The stratification-circulation diagram (Fig. 2.29) shows that the part of the estuary west of Guardbridge, under the conditions of a river discharge of 4.1 to 4.9 cumecs and an intermediate tide (predicted 5.1m at Leith), is characterised by moderate to high stratification with the development of a distinct salt-wedge in the westernmost part of the section. The two middle estuary stations, Paper Mill and Coble Shore, at a time of low river discharge (1.4 cumecs) are classified as Type 2a - a well mixed section in which salinity stratification is slight. The Out Head station was categorised as Type 2a showing only slight salinity stratification and a reversal of the net flow at depth;

7. over the flood-tidal delta a tidal current time-velocity asymmetry exists; the degree of asymmetry varies with location within the delta.

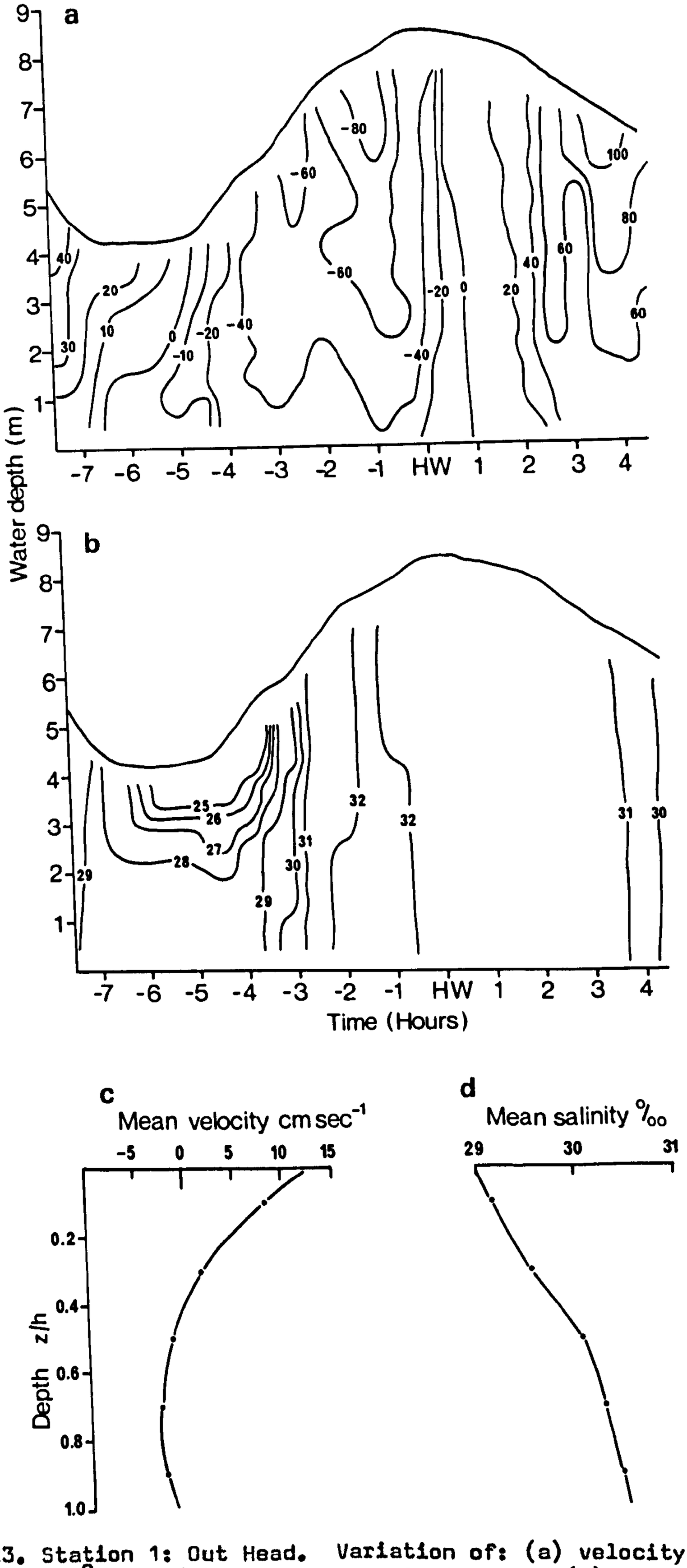

Fig. 2.23. Station 1: Out Head. Variation of: (a) velocity (cm sec^{-1}); (b) salinity ($^{o}/oo$); (c) tidal mean velocity, and (d) tidal mean salinity.

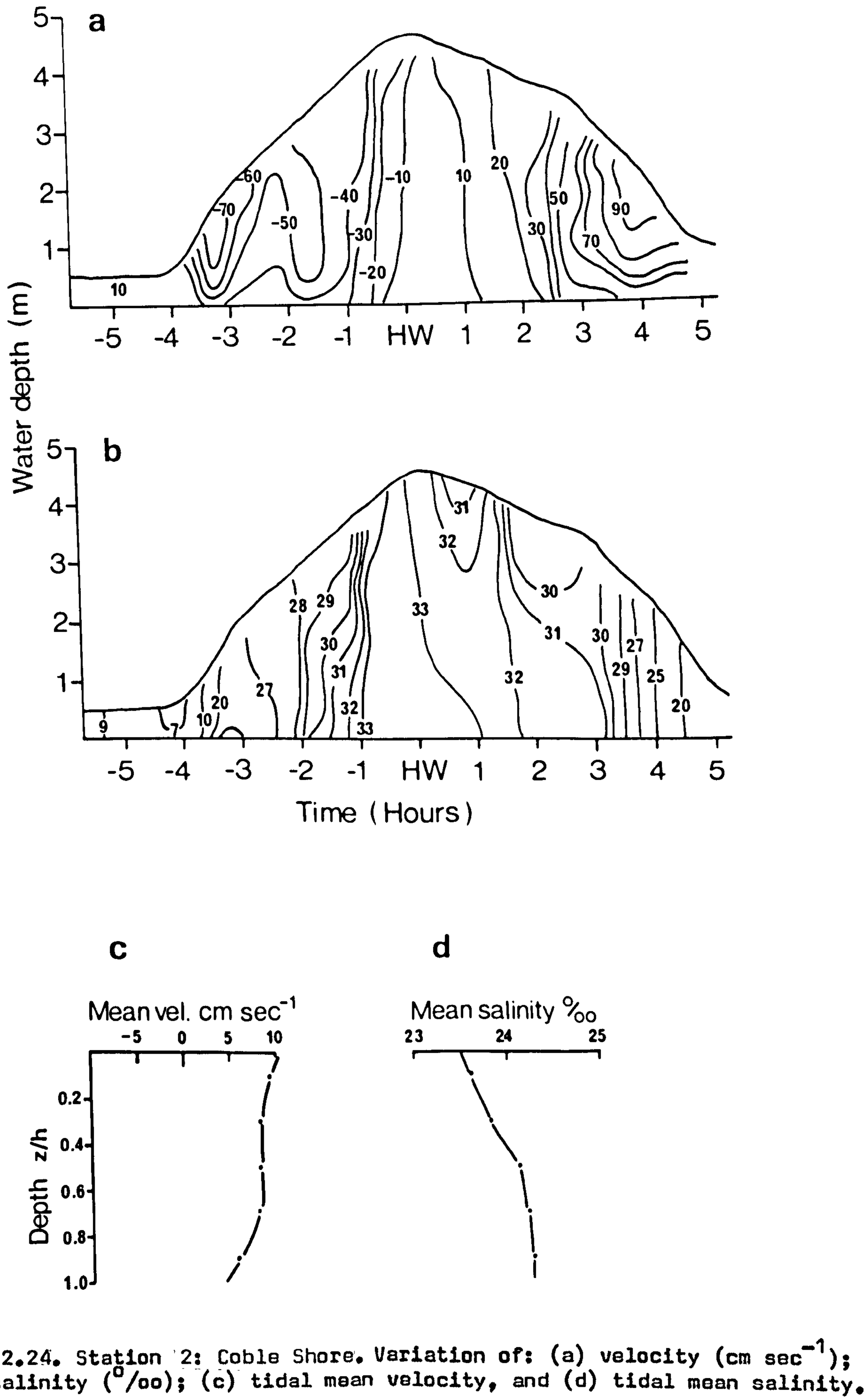

Fig. 2.24. Station 2: Coble Shore. Variation of: (a) velocity (cm sec^{-1}); (b) salinity ($^{o}/oo$); (c) tidal mean velocity, and (d) tidal mean salinity.

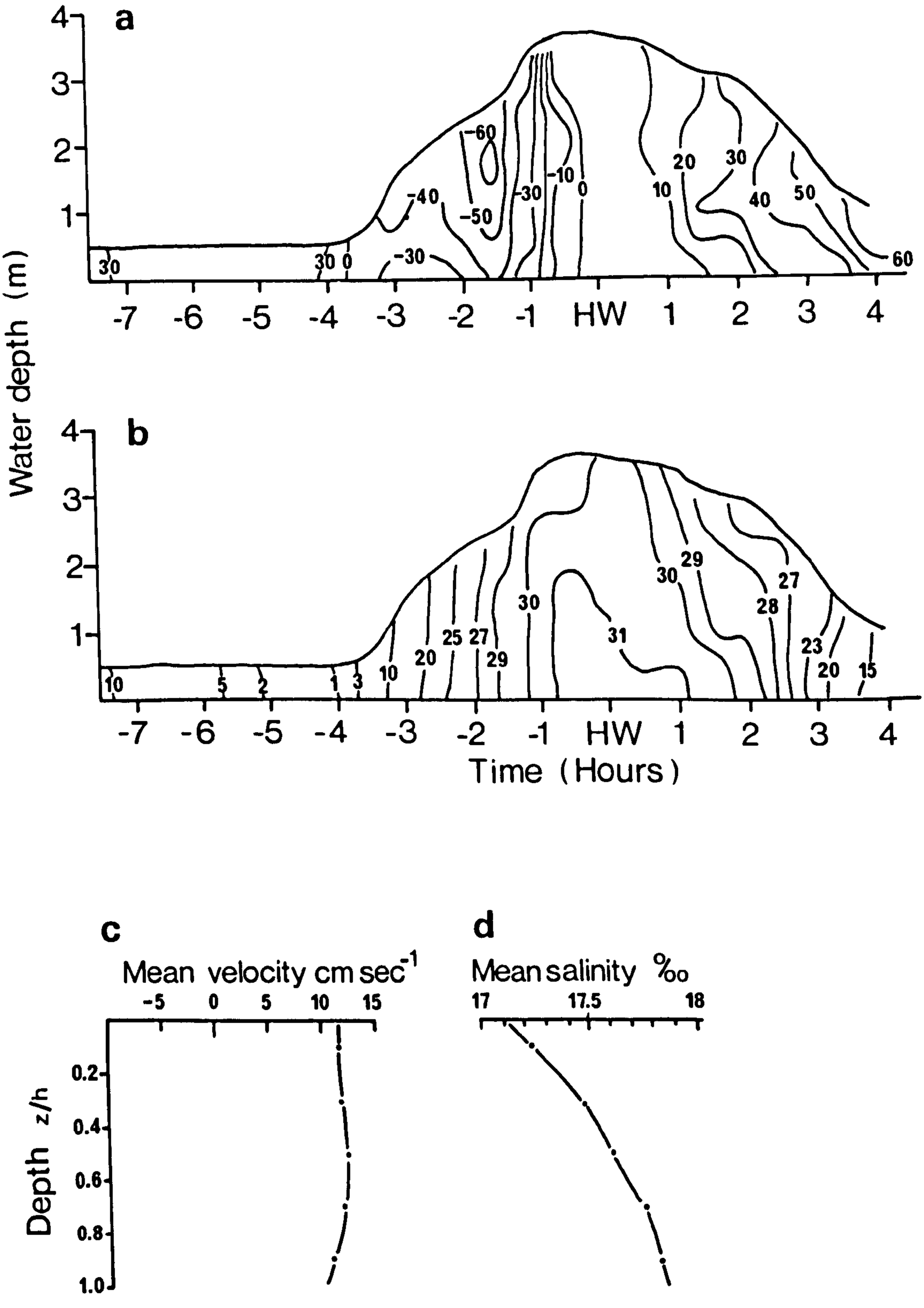

Fig. 2.25. Station 3: Paper Mill. Variation of: (a) velocity (cm sec^{-1}); (b) salinity ($^{o}/oo$); (c) tidal mean velocity, and (d) tidal mean salinity.

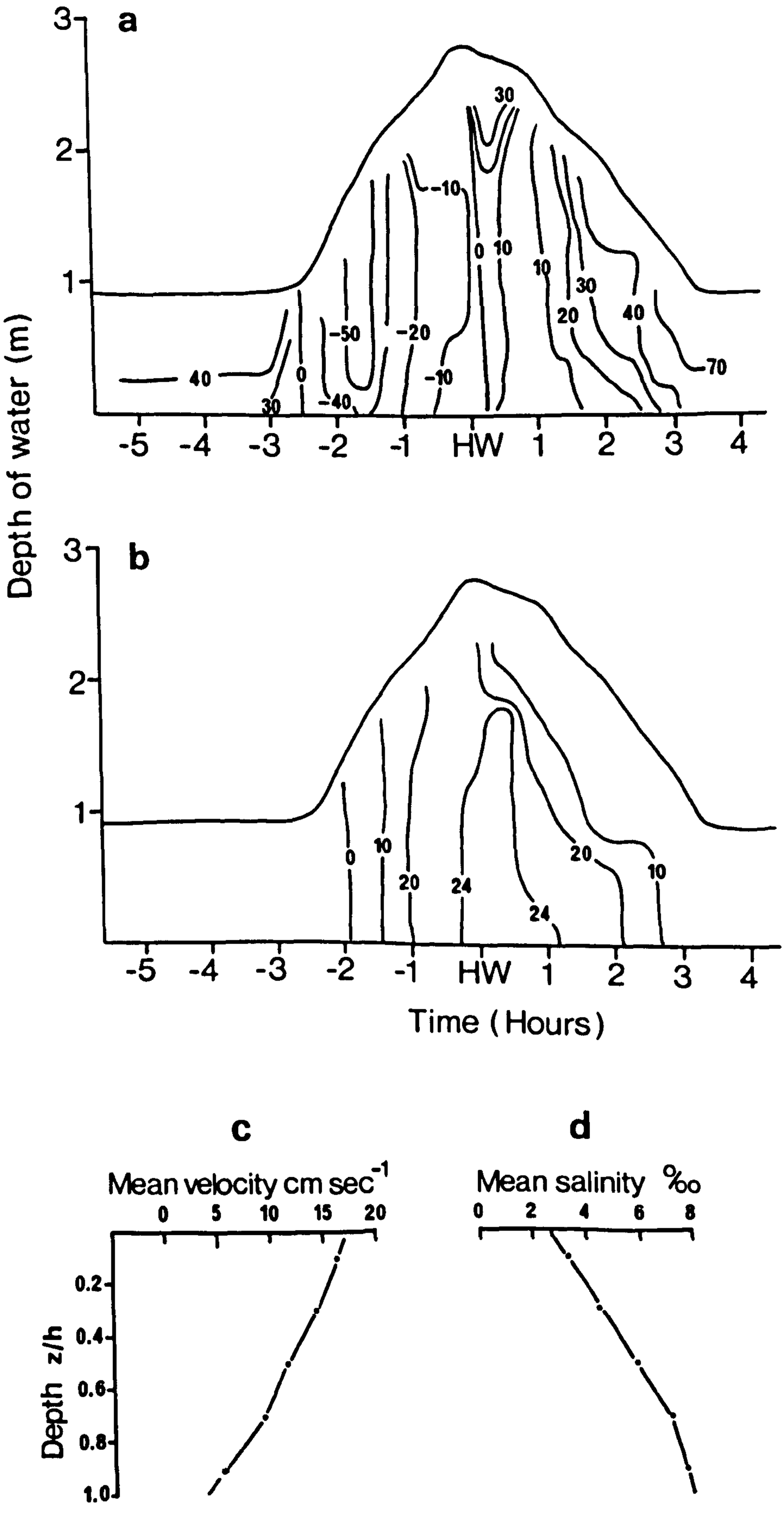

Fig. 2.26. Station 4: Guardbridge. Variation of: (a) velocity (cm sec^{-1}); (b) salinity ($^{o}/oo$); (c) tidal mean velocity, and (d) tidal mean salinity.

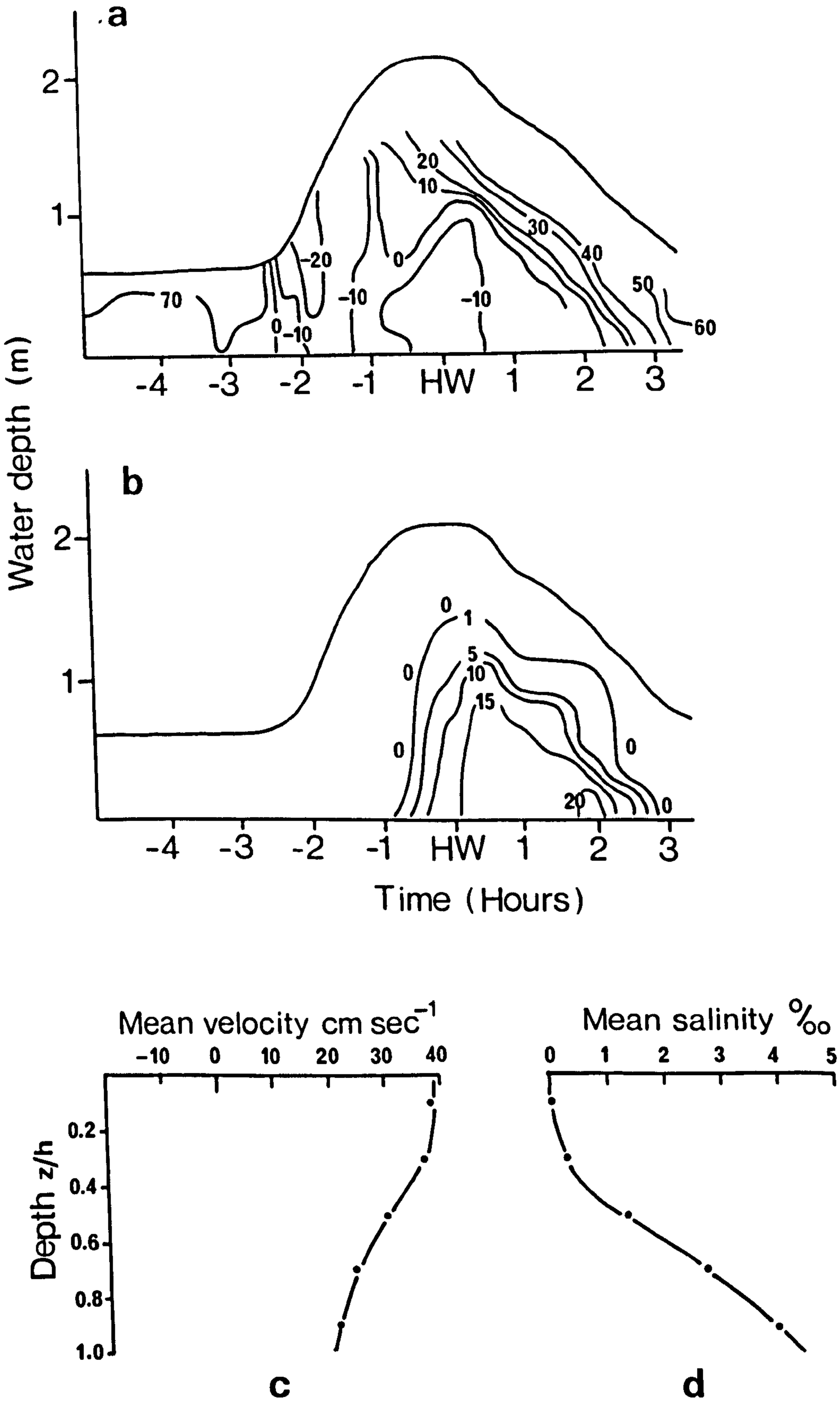

Fig. 2.27. Station 5: Upper estuary. Variation of: (a) velocity (cm sec^{-1}); (b) salinity (^{o}/oo); (c) tidal mean velocity, and (d) tidal mean salinity.

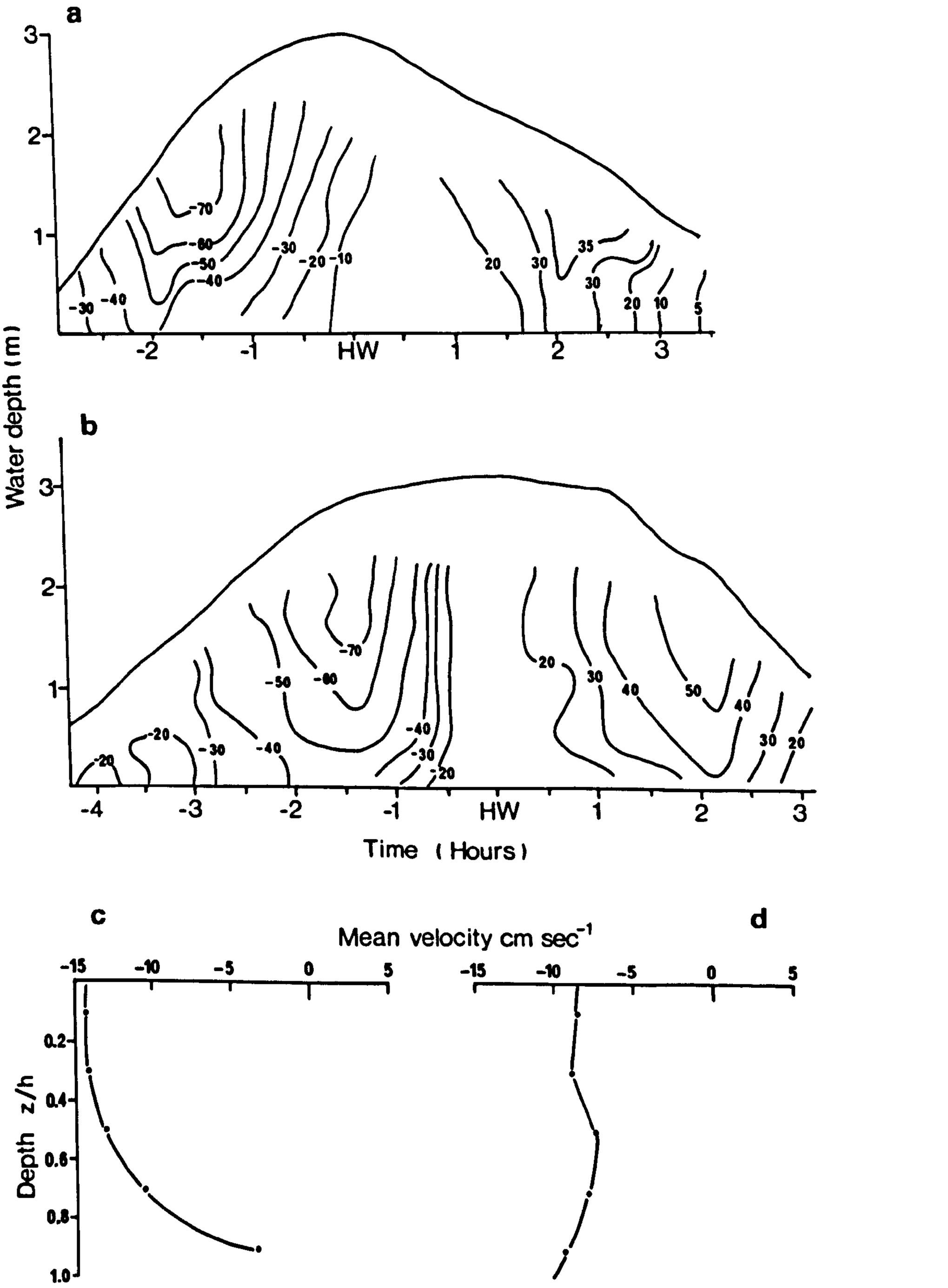

Fig. 2.28. Variation of: (a) velocity at Station 6 (cm sec^{-1}); (b) velocity at Station 7 (cm sec^{-1}); (c) and (d) tidal mean velocities for Stations 6 and 7 respectively.

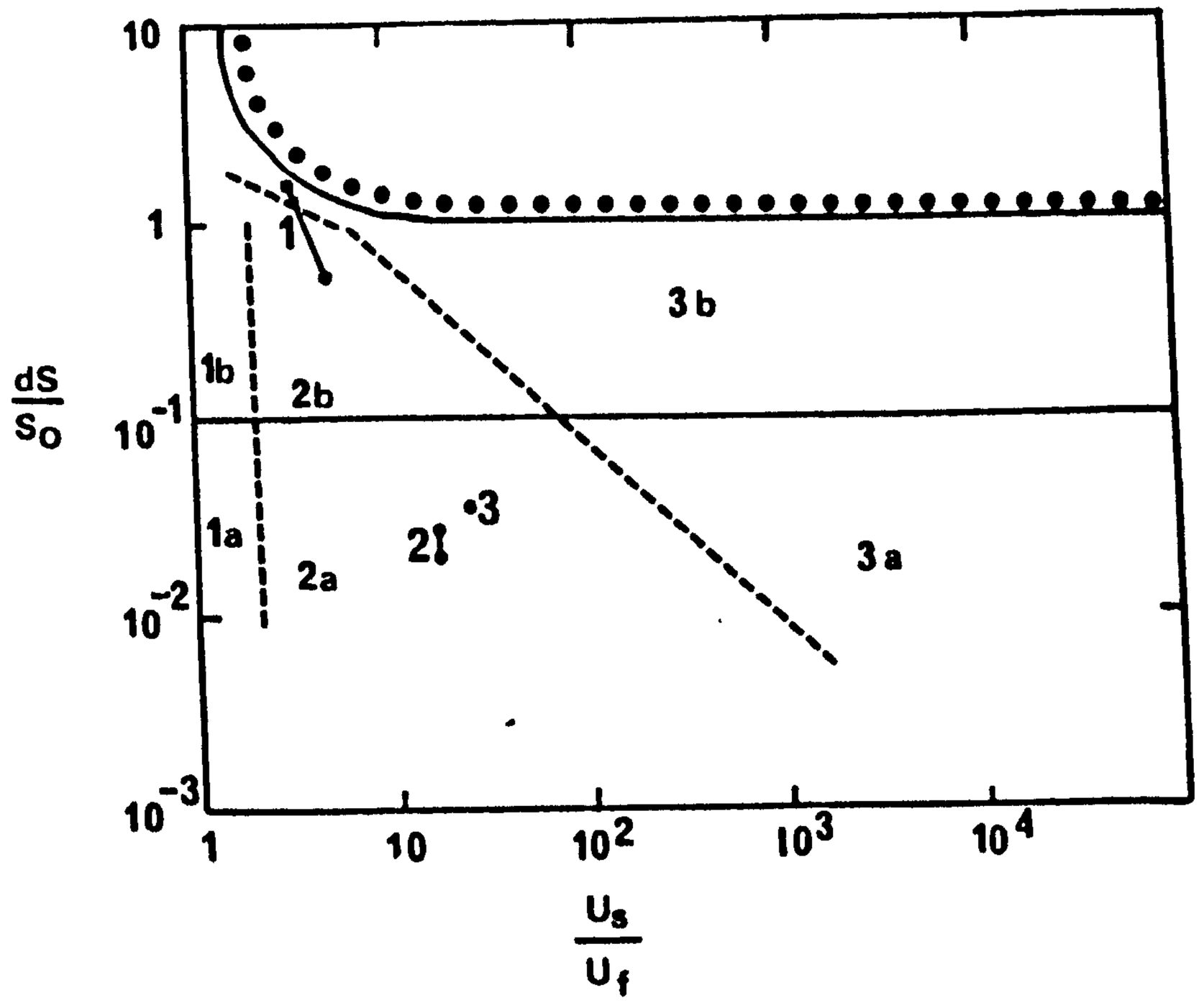

Fig. 2.29. The stratification-circulation diagram of Hansen & Rattray (1966) with the Eden estuary points plotted.

1. Upper Estuary
2. Middle Estuary
3. Lower Estuary.

Where, for a section of the estuary:-

dS = Top to bottom salinity difference

S_o = Sectional Mean Salinity

U_s = Net Surface Current

U_f = Mean Fresh Water Velocity.

Chapter 3 MAJOR TOPOGRAPHIC FEATURES OF THE ESTUARY, THEIR BEDFORMS AND INTERNAL STRUCTURES

I. INTRODUCTION

On the basis of air photography and field mapping, five major topographic divisions of the intertidal zone may be recognised:

1. The Eden channel,
2. Intertidal sand and mud flats,
3. A flood-tidal delta,
4. An ebb-tidal delta,
5. Beaches.

In situ measurements, trenching and box-coring provided the basic data on bedforms and internal sedimentary and biogenic structures.

Air Photographs

A series of controlled vertical air photographs of the whole estuary, taken in 1948, 1953, 1964 and 1973, showed the development of certain topographic features within the intertidal zone, whereas a number of oblique air photographs, taken in 1974 and 1975, provided a detailed record of the topography during the period of study.

Field Mapping

Field mapping of bedforms was carried out at all points on the same grid system as that used for sample collection (see Chapter 4, p. 90). The terms descriptive of bedforms and the indices necessary to quantify bedform geometry were taken from Allen (1968). A standardised data-collection sheet was completed at each locality (Appendix 2).

Sub-sea topographic profiles were obtained with a Ferrograph echo-sounder.

Box-Coring

Orientated box-cores taken either with a Senckenberg-type box-corer (Bouma, 1969) or with standard 4.5 litre oil cans with the bases removed were the main source of data on internal sedimentary and biogenic structures. Little information was directly obtainable by trenching in the fine sands of the lower estuary, and recourse was made to the preparation of large epoxy resin peels in the field.

Laboratory Treatment of Box-Cores

The internal sedimentary and biogenic structures of box-core samples (25 x 16 x 10cm) were revealed by x-ray radiography (Bouma, 1969; Krinitzsky, 1970; Hamblin, 1972) and the preparation of relief peels by surface impregnation (Bouma, 1969; Klein, 1972).

The initial preparation of the box-core was the same for both types of analysis and consisted of placing the core, maximum surface area downwards, on a perspex tray with sidewalls 1 or 2cm high, and then removing the bulk of the sample, retaining only a 1 or 2cm thick slice. The upper surface of the slice was made as smooth and even as possible to facilitate the production of the peel. Clay-rich samples were cut and smoothed with an electro-osmotic core-cutter (Chmelik, 1967).

1. Radiography

Radiography was used in the analysis of silty and clayey cores which were not amenable to study by epoxy resin peels. The samples were normally 1cm thick and occasionally up to 2cm. Slices less than 1cm thick are preferable, but even with the aid of the core-cutter, it is difficult to prepare very thin slices without distorting and fracturing the sample.

Radiographs were taken on a Phillips medical x-ray unit equipped

with a Mullard Guardian 125 tube. Standard medical x-ray film (Kodak PE 4006) was used. The radiographs were processed automatically on a Kodak RP X-Omat Processor Model 100. The optimum operational settings on this machine for sediment slices between 1 and 2cm thick were a kilovoltage of 55, a target-film distance of 76.2cm (30 inches) and an exposure of 180 milli-ampere seconds.

2. Relief Peels

Relief peels of sandy and silty sediments were prepared using liquid epoxy resins supplied by CIBA (Resins MY 750 and MY 740, Hardeners HY 850 and HY 830) and Synthetic Resins Ltd. (Kollercast Resin 607, Hardeners LD and ND).

The CIBA resins were used in the laboratory in the proportions five parts each of MY 750 and MY 740, three parts of hardener HY 850 and one part of hardener HY 830 (Burger, Klein and Sanders, 1969). After thorough mixing the epoxy was poured on the surface to be impregnated, and a thin layer was spread on a piece of hardboard which was then placed on the sample. The board and sample were then inverted and the resin was allowed to cure for 24 to 48 hours. Scraping-off of the excess sand and washing with a strong jet of water revealed the internal structures. Inversion of the sample and board resulted in the production of low-relief peels (1-3mm) in which delicate structures could be identified. A contrasting technique is to allow the resin to penetrate from the surface of the sample downwards, in which case high-relief peels are produced. This latter technique was used on some samples employing the low viscosity Koller-cast resins and peels of 1 to 3cm thickness were produced in fine sands with the retention of very good surface detail.

Large peels (1m x 0.25m) were taken in the field by the method of Barr, Dinkelman and Sandusky (1970). Kollercast resin 607 (2

(2parts) was added to one part of hardener ND. Hardener ND is especially useful outdoors, as it has the property of rapid cure under cold/wet conditions. The peels were sufficiently dry to be removed from the trenches after curing for 4–5 hours.

II. THE EDEN CHANNEL

Channel Plan

The Eden channel has a course approximately 10km in length through the intertidal zone between the Pouch and the West Sands of St. Andrews.

In the landward half of the estuary between the Pouch and Coble House Point the channel plan is in the form of two large sinuses of wavelength approximately 2.5km. The sinuosity of the channel (1.2) is too low to warrant the application of the term 'meandering'. In the section of 1.5km west of Guardbridge, where the river leaves the confines of the narrow valley cut through boulder clay and crosses a narrow area of intertidal flats, there occur well-developed mid-channel and point bars (Fig. 3.1, 3.2).

At Coble House Point the channel is abruptly turned southwards by the outcrop, just above river bed elevation, of compacted late-Glacial gravelly sands which lie stratigraphically below the peat at the base of the local Carse sequence.

In the area to the east of Coble Shore and south of Shelly Point the channel shows many bifurcations and often appears braided. The islands between the channels are composed of sediment stabilised and capped by mussel banks. Persistent diversion of flood and ebb tidal currents by these islands produces deep narrow channels between them, often floored by lag gravels of shell material.

East of a N-S line through Shelly Point the channel effectively meanders (sinuosity 1.5) through the intertidal flats. The course of the River Eden in the lower estuary is strongly affected by the spit-platform which has accumulated to the north and east of Out Head (Fig. 3.3). The channel eventually terminates on the stoss side of the ebb-tidal delta, and at low-water Spring Tide communication of the River Eden with the water of St. Andrews Bay is maintained only

by a shallow south-east trending distributary (Fig. 3.3). The rapid shoaling of the Eden channel to the east of the tidal inlet is shown on the echo-sounder profile of Figure 3.4.

Channel Cross-Sectional Profiles

The general cross-sectional shape of the channel is that of an asymmetric V. The shape varies considerably both in degree of asymmetry and width to depth ratio (Fig. 3.5). Profile 1 (Fig. 3.5) shows the channel profile at the tidal inlet to the near symmetrical with a high width to depth ratio of 24:1. The symmetry is distorted slightly by a ledge attached to the south bank with an elevation of approximately 1m above the channel bottom. The deepening of the channel adjacent to the north bank probably reflects the fact that both late ebb-stage and early flood-stage, high-velocity, tidal currents impinge on the north bank at this locality.

Profiles 2 and 3, from the limbs of meander loops, show higher width to depth ratios (50:1) and a slight asymmetry. Profile 3 also shows the easterly part of a flood channel (F), which is beginning to diverge from the trend of the main channel. The feature shoals to the south-west and appears as the broad, shallow depression (F1) on profile 4. The beginning of a flood-channel can also be seen at the base of the south bank of the main channel in profile 4. This flood-channel becomes more prominent in profile 5, but then shoals rapidly to the south-west.

Profile 7 from the middle estuary shows a very steep south bank which may be partially explained by the cohesive nature of the sediment in this area.

Channel Migration

The migration of the Eden channel as determined from Ordnance Survey maps and air photographs reveals that considerable movement

has occurred only to the east of a N-S line through Sanctuary Spit (Chapter 1, page 12). When viewed with a knowledge of the textural variation in the estuary sediments, there is a distinct relationship between channel stability and cohesive bank material (muds, clays, sandy-silts) and between channel mobility and non-cohesive bank material (>90% sand).

Fig. 3.1. The sinuous course of the River Eden in the upper estuary between the Pouch and Guardbridge.

Fig. 3.2. A well developed point bar which occurs immediately to the south of the road bridge at Guardbridge (A on Fig. 3.1). Note, on the convex side of the bar, the plane-bedded surface (P) which grades, downstream, into a zone of megaripples (M).

Fig. 3.3. The meandering course of the River Eden in the middle and lower estuary.

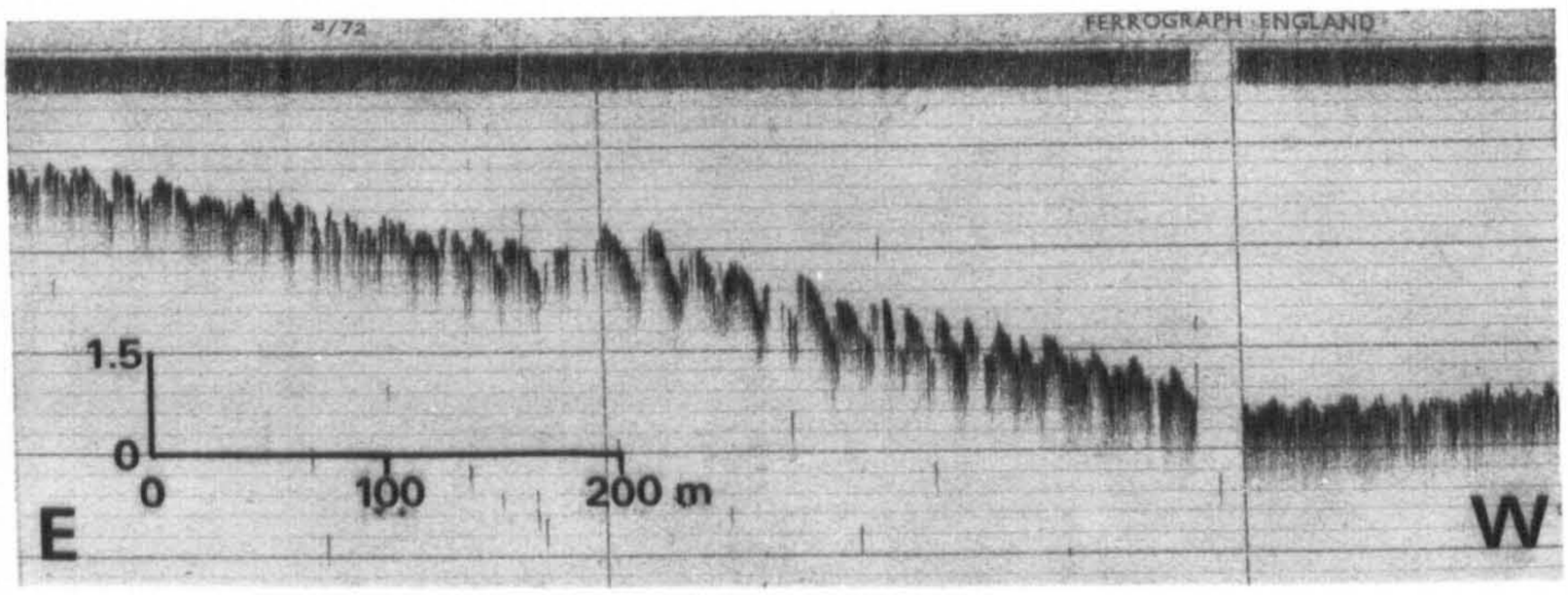

Fig. 3.4. Echo-sounder profile showing the rapid W-E shoaling of the Eden channel on the stoss-side of the ebb-tidal delta.

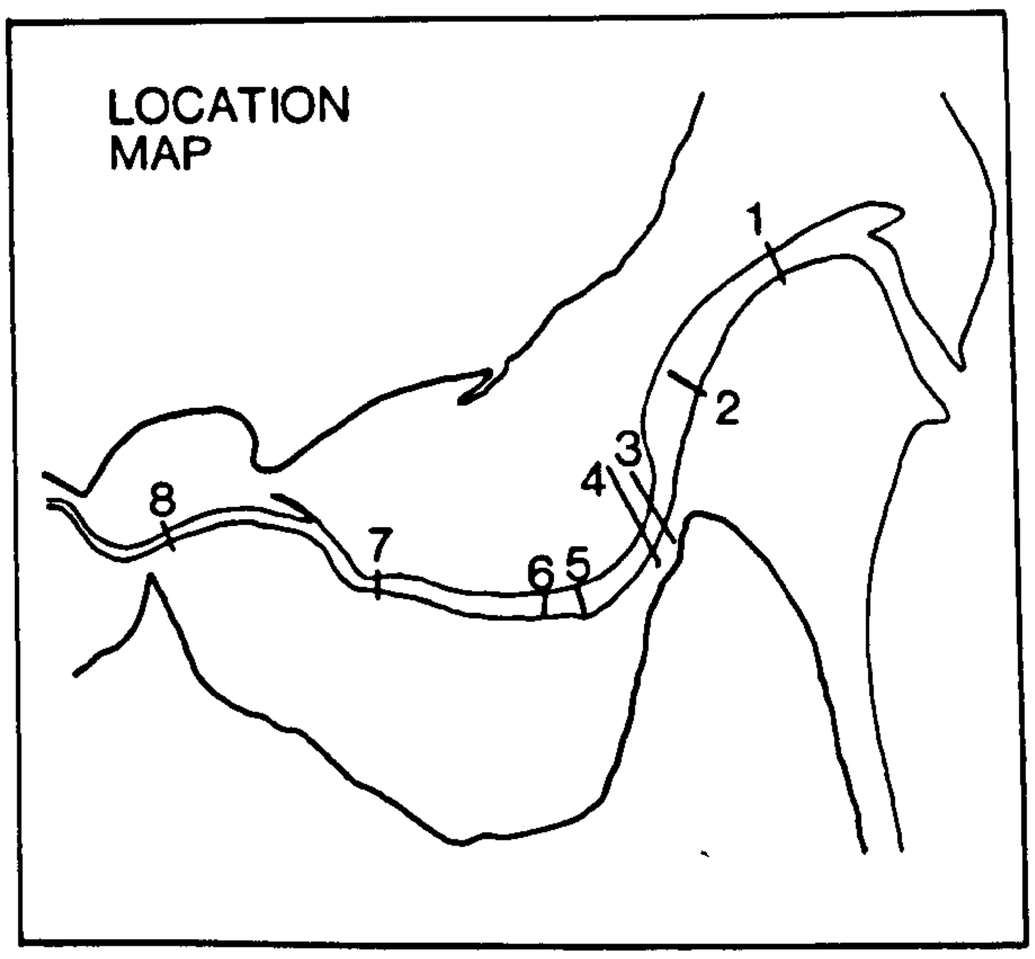

EDEN CHANNEL
ECHOSOUNDER PROFILES

Fig. 3.5. Channel-bottom profiles of the River Eden in the middle and lower estuary. Arrows indicate flood channels.

III. THE INTERTIDAL SAND AND MUD FLATS

Topography

The intertidal flats of the middle and upper estuary cover an area of 4.25km^2 and are the most extensive of the topographic sub-divisions of the estuary. The width of the individual flats, perpendicular to the Eden channel, varies from 0.1km at Guardbridge to 1km on Kincaple Flat.

Topographic features of the intertidal flats fall into three groups: (a) a dendritic system of drainage channels; (b) a zonal arrangement of mussel banks and algal colonies; and (c) minor occurrences of salt-marsh deposits.

The Dendritic Drainage System

The dendritic drainage system is very well developed on Kincaple Flat where four major channels are fed by numerous minor channels (Fig. 3.6). Near the southern margin of Kincaple Flat the minor channels have relatively straight courses and retain a constant angular relationship of 50°-60° with the shoreline. The regular spacing and orientation of the channels suggests that they may be related to undulations on the bed of very low amplitude and large chord (≈20m). Such bedforms were also noted on the north shore of the estuary between Sanctuary Spit and Shelly Point, in the middle estuary to the east of Coble Shore, and between Pilmour Links and the Eden channel to the south-west of Out Head. The origin of the undulations may be related to current flow parallel or nearly parallel to the estuary margins during the period around the time of high-water.

De-watering of the intertidal flat sediments produces sufficient contrast in their surface coloration to allow the drainage areas of individual channels to be recognised (Fig. 3.6).

Headward progression of very minor channels by a process of collapse during de-watering was observed on the marginal areas of Kincaple Flat.

On Edenside Flat the dendritic pattern is less well-developed and minor drainage channels only become important within 200m of the Eden channel. The drainage courses are straight and at right angles to the channel (Fig. 3.7). Edenside Flat is also drained by a channel which runs parallel to the western margin of Coble Shore.

A comparison of air photographs taken in October 1964 and August 1974 shows that the Kincaple Flat drainage system is very stable with virtually no discernible changes in the number or orientation of the channels (Fig. 3.8).

Mussel Banks

Mussel banks are present in areas which border the Eden channel and the major drainage channels on Kincaple Flat. They are restricted to the middle estuary in a zone which extends from a point some 600m west of Out Head to Coble House Point (Fig. 3.9).

A three-dimensional exposure of a mussel bank undergoing severe erosion showed that in cross-section (E-W) the structure was asymmetric with an easterly facing stoss-side of very low angle (3^{o}-4^{o}), a broad crestal area and a more steeply dipping (10^{o}) westerly facing lee-slope. The east-west dimension was approximately 35 metres (Fig. 3.10). In external appearance the structure bears the same relationship to flood-tidal currents as do the sand-waves of the flood-tidal delta.

A 1.13m vertical section of sediment was exposed on the south side of the bank (Fig. 3.11). The lower 63cm of the exposure consisted of two beds (40 and 23cm respectively) of fairly coarse-grained heterogenous sediments (means of 0.44 and 0.57 phi) with components including lithic fragments, quartz pebbles (up to 2.5cm),

whole and fragmented gastropod and bivalve shells, coal, wood and plant debris. Both beds showed a general fining upwards, and in the upper part of the higher bed there was poorly developed, ebb-orientated cross-stratification. Lying discordantly upon the coarse sands was a 43cm thick bed of black bioturbated mud which contained indistinct layers of shell fragments, plant remains and occasional whole Mytilus valves. Resting upon the convex surface of this bed was a 7cm thick agglutination of live specimens of Mytilus edulis.

In several aspects the mud layer 'draped' over the coarse sands is not unlike the longitudinal cross-bedded deposits described by Van Straaten (1954) and Reineck (1958, 1973). The uniform thickness of the bed, continuity of laminae within the bed, and the overall upward convexity of the bed would, however, seem to preclude the possibility of accumulation by lateral sedimentation. It is suggested that this deposit is the result of predominantly vertical sedimentation of both faecal material from the overlying mussel colony and silt and clay-size material which is trapped in the well protected depositional sites between individual mussels. Live mussels would naturally tend to move upwards at a rate commensurate with sedimentation in order to maintain their position in an environment which is covered twice daily by oxygenated, phytoplankton-rich water. Consequently the faecal and other materials are protected from extensive erosion, and the bank grows vertically.

Shell pavements are common in channels adjacent to mussel banks and are composed mainly of the valves of Mytilus edulis. Valves are commonly disarticulated and orientated with their long axes in the flow direction with the umbo facing in the upstream direction. The valves often lie with their convex side uppermost and imbricate structures are common (see Fig. 2.9, Chapter 2,III).

Algal Colonies

Colonies of brown and green algae cover large areas of the inter-tidal flats of the middle estuary (Fig. 3.12). The filamentous green alga *Chaetomorpha* sp. occurs as extensive 'algal mats', which are composed of interwoven filaments which have been compressed into a layer some 0.5 to 1cm thick. In the more marginal areas of the middle estuary *Chaetomorpha* occurs as isolated threads and algal scrolls.

Two colonies of brown fucoid seaweeds occur adjacent to the Eden channel. Both are areas of mussel bank development. The fucoid zones are less extensive than the *Chaetomorpha* zones and are completely enclosed by them.

Salt Marsh

Salt marsh occurs around the southern margins of Kincaple and Edenside Flats and occasionally on the northern margin of the estuary near Sanctuary Spit and between Shelly Point and Coble House Point. It is not areally extensive (Fig. 3.12).

The edge of the salt marsh zone is marked in some areas by a small cliff up to 25cm high and in others by a more rounded, abraded margin which is intersected by a number of digitating areas of inter-tidal flat sediments. Isolated mounds of salt marsh may be found seaward of the general salt marsh limit giving the impression that the zone is retreating.

The salt marsh surface is broken by a series of drainage channels and oval depressions in which accumulate materials such as bivalve and echinoderm tests brought into the area during Spring Tides. The oval depressions are also depositional sites for fine grained materials transported onto the marsh in suspension.

The internal structure of a salt marsh deposit consists of alternations of sand and silty-sand which show a landward (southerly)

dip of approximately 10^{0} (fig. 3.13). The sand layers are up to 1.5cm thick and contain shell debris, lithic fragments up to 3mm maximum diameter and occasionally whole mollusc valves.

Sediment Type

The zonal arrangement of exposed flats, Chaetomorpha flats, Fucus colonies and Mytilus banks, is reflected in the variations in sediment type over the intertidal flats. The distribution of sediment types, based on the nomenclature of Folk (1954) and derived from a ternary diagram with sand, silt and clay as end-members, is shown in Fig. 3.14.

In contrast with the sediments of the outer estuary, which are composed of over 90% of sand-sized material, those of the middle estuary are rather variable in texture. Silty-sand[1] is the most widespread sediment on both Edenside and Kincaple Flat. Less sandy sediments are present in an elongate zone adjacent to the Eden channel from Guardbridge to Coble Shore and again on the central areas of Kincaple Flat where sandy-silt[2] is the most abundant sediment type, followed by sub-equal amounts of muddy-sand[3] and mud[4]. On the south marginal areas of Kincaple Flat two areas of muddy-sand are present. A comparison of Figures 3.12 and 3.14 shows that there is a general areal relationship between exposed flats and muddy-sand; Chaetomorpha flats and silty-sand; and between areas of mussel banks and Fucus colonies and sandy-silts and muds.

The fine grained sediments on Edenside Flat are located in topographically low areas surrounding the silty-sand flats. The finest sediments are found on the sloping banks of the Eden channel in the transition zone between the intertidal flats and channel proper.

---

1. Silty-sand: sand 50-90%; silt:clay ratio 2:1.
2. Sandy-silt: silt 50-90%; silt:clay ratio 2:1.
3. Muddy-sand: sand 50-90%; silt:clay ratio approximately 1:1.
4. Mud - no member in excess of 50%; ratio approximately 1:1.

Bedforms

The distribution of algal mats and very fine grained sediment with cohesive properties limits the development of bedforms of ripple-type to a few scattered localities around the estuary margin (Fig. 3.15). Where bedforms do occur, small-scale asymmetrical ripples are predominant, and are well represented in drainage channels. Occasionally two ripple trains are superimposed, forming ladder-ripples. On south Kincaple Flat the dominant trend was 128°, the secondary trend 032°. The majority of ripples were in sinuous, out-of-phase trains with individual heights of 0.4cm and chords of 4cm.

Internal Sedimentary Structures

Box-core samples for analysis by x-ray radiography and epoxy resin peels were collected from three north-south traverses over Kincaple Flat and one over Edenside Flat. Several additional samples were collected from the eastern part of Kincaple Flat (Fig. 3.15).

A diagrammatic representation of the sedimentary and biogenic structures found in this study is presented in Figure 3.16.

Traverse 7

Each core shows essentially the same sequence of lithologies and consists of (a) a basal shell-bed composed predominantly of fragments of Cardium edule[1] but with whole valves towards the upper surface; (b) approximately 15cm of sand, which is virtually devoid of primary sedimentary structures. Relicts of bedding features are occasionally preserved, but the general appearance is of a totally bioturbated sediment with scattered bivalve shell fragments; (c) the upper 2-3cm of each core shows small-scale cross-stratification which is generally revealed only by x-ray radiography (Fig. 3.17).

The sequence may be complicated by additional shell-concentrates at any level, eg. Core 7V (Fig. 3.17).

1 Cardium edule syn. Cerastoderma edule

Traverse 10

These cores show similar features to those of traverse 7, but cross-lamination is not a major feature of their upper portions. Poorly developed cross-laminations were present in cores 10U, T and VA, but flat-lamination interrupted by bioturbate structures is more characteristic.

A shell-bed at a depth of approximately 20cm is present in most of the cores and its main features are shown to advantage in cores CC16 and CC18 (Fig. 3.18). These features are:

(a) up to 10cm of shell debris which shows a distinct increase in grain-size towards the upper surface,

(b) a gradational base and a fairly even upper surface,

(c) the major components are fragments of Cardium edule with subsidiary amounts of other bivalves and gastropods including Hydrobia. The upper layer often contains whole but disarticulated valves,

(d) the absence of a preferred orientation of the carbonate fragments,

(e) a poor degree of packing.

The textural attributes mentioned in (d) above cast some doubt on the assumption of an aqueous depositional medium for this deposit. In most cases where carbonate material is deposited in water the fragments assume a resting position with the maximum surface area parallel to the bed. Whole valves, for example, of Cardium, would also tend to rest with their convex side uppermost. Such features are illustrated by a beach deposited shell-bed (Fig. 3.19), which should be compared with Figure 3.18.

The deposit is strictly comparable to the 'Hydrobia Beds' described by Van Straaten (1954) in terms of the gradation in grain-size, absence of preferred orientations, depth of occurrence, and

association with bioturbated sediment. A similar origin is therefore postulated, whereby the shell debris and whole valves are concentrated by the activities of the lugworm Arenicola marina (Figs. 3.20 and 3.21) which is extremely abundant in these sediments. The composition of the bed is controlled by the nature of the detrital material deposited on the intertidal flat surface by waves and currents.

Traverse 16

The important feature of several cores of this traverse was the presence of a grey clay underlying the surficial silty-sands at a depth of 8-10cm. The depth of the clay surface increased in a northerly direction and passed beneath the range of penetration of the cores (25cm). Cores 16VA and 16U showed a grey clay with an irregular surface of burrows occupied by Mya arenaria or infilled with shell debris including large numbers of Hydrobia sp. (Fig. 3.22). Bedding in the clay was indicated on radiographs only by plant remains (Fig. 3.21, feature a).

Cores 16S and 16T consist of poorly defined alternations of sands and silty sands (Fig. 3.23). In 16RA flaser-bedding is poorly developed in the lower part, above which there was a 2-3cm thick layer of wood, twigs and leaves. The upper part of the core shows intense bioturbation and remnants of horizontal lamination. U-shaped and branched burrows are abundant near the surface.

Traverse 20

Three distinct lithologies, which, in ascending order, were reddish-brown laminated silts, a gravel of lithic fragments and shell debris, and a sandy-silt, characterised the southernmost core. The more northerly cores do not show the two lower lithologies and are composed entirely of bioturbated sands and silty-sands (Fig. 3.24).

The grey clay underlying the surficial deposits of the cores in traverse 16 is correlated with the grey silty-clay or Carse Clay of the north shore of the Eden estuary (Chisholm, 1971) on the basis of the stratigraphic sequence revealed by an auger-hole sited 100m east of core 16V. The sequence was:

Thickness (m)	
0.10m	silty-sand
0.15m	gravel and shell concentrate. Quartz pebbles and lithic fragments up to 4cm diameter
1.80m	light grey clay with abundant plant remains in upper 0.5m. becomes micaceous towards the base
0.25m	peat, dark brown with pieces of wood
0.15m+	medium sand with light green staining.

But for the light green staining of the sand below the peat, this sequence is identical to that given by Chisholm for the lower part of the post-Glacial sequence.

To the west of Coble Shore, however, an auger-hole revealed a different succession beneath the surficial sandy-silts and gravel layers. At least 5.1m of alternations of reddish-brown tenacious clay and red micaceous silty-sands were present. These may be correlated with the reddish-brown laminated clays at the base of the succession described by Chisholm. The Carse clay and sub-Carse peat were absent.

Further west the grey Carse clay again overlies the red clay, a fact which suggests that the area of Coble Shore may have stood as an island during the early part of the Flandrian transgression.

Conclusions

Surficial sediments of the middle estuary are dominated by structures of biogenic origin which have almost completely replaced sedimentary structures. Bioturbation has resulted in a homogenous appearance of many sediments even after epoxy-resin peel and x-ray

radiographic analysis.

Shell-concentrates are important, and on the eastern part of Kincaple Flat there is a widespread shell-bed at depths of 10 to 25cm. The origin of this feature is problematical, but on textural grounds a biogenic accumulative process is favoured.

In the vicinity of Coble Shore the surficial silty-sands and muddy-sands decrease in thickness and the underlying Carse deposits feature in the cores.

Fig. 3.6. The dendritic drainage pattern on Kincaple Flat.

Fig. 3.7. The drainage pattern on Edenside Flat. Note that the predominant trend is perpendicular to the Eden channel.

Kincaple Flat, October 1964. (Infra-red photograph)

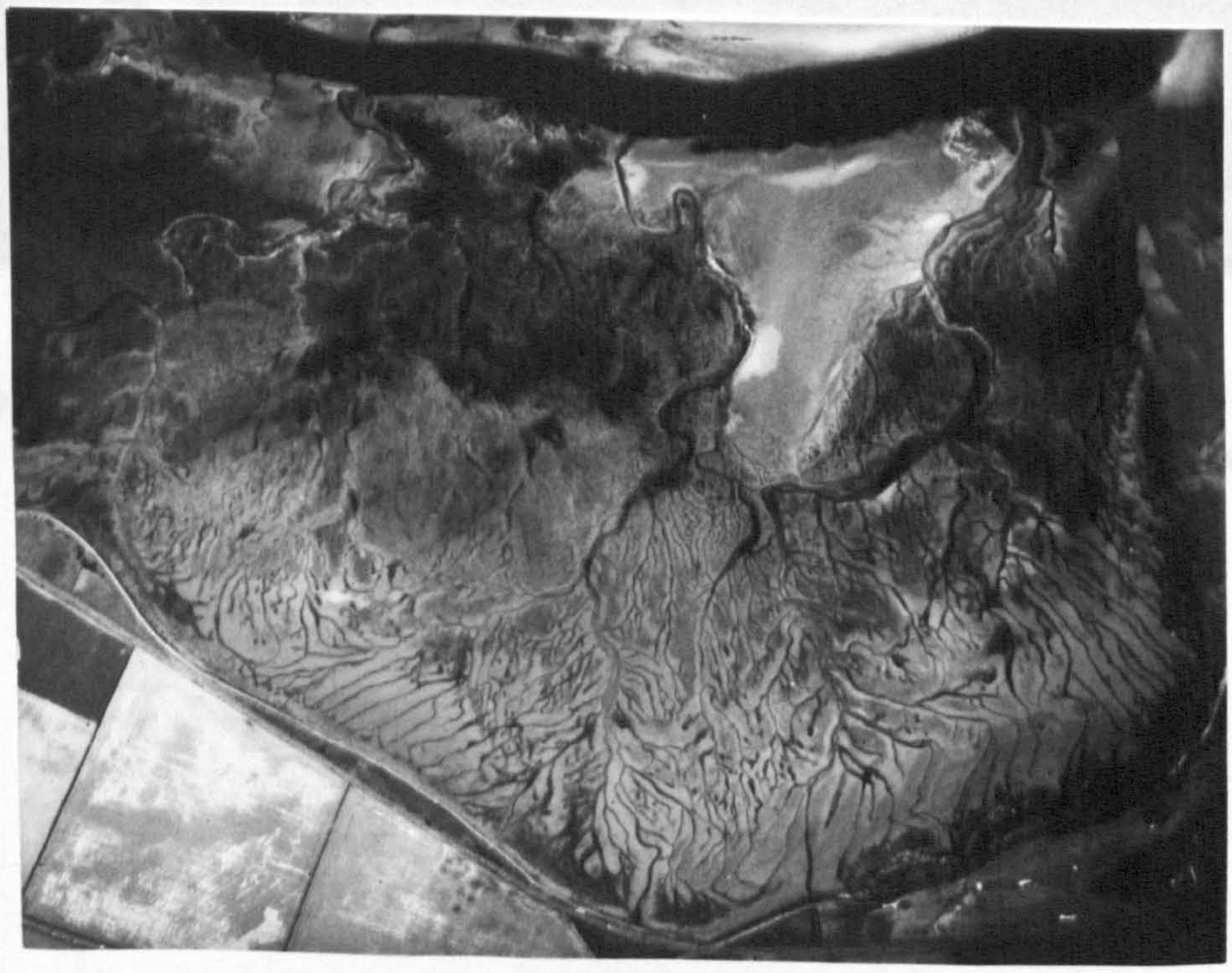

Kincaple Flat, August 1974.

Fig. 3.8. A comparison of the dendritic drainage patterns on Kincaple Flat, October 1964 and August 1974.

Fig. 3.9. The distribution of mussel banks in the Eden estuary (white areas). (Infra-red photograph, 1953). The distribution has remained stable.

Fig. 3.10. A lateral view of a mussel bank presently being eroded by tidal currents. View in the ebb direction (eastwards).

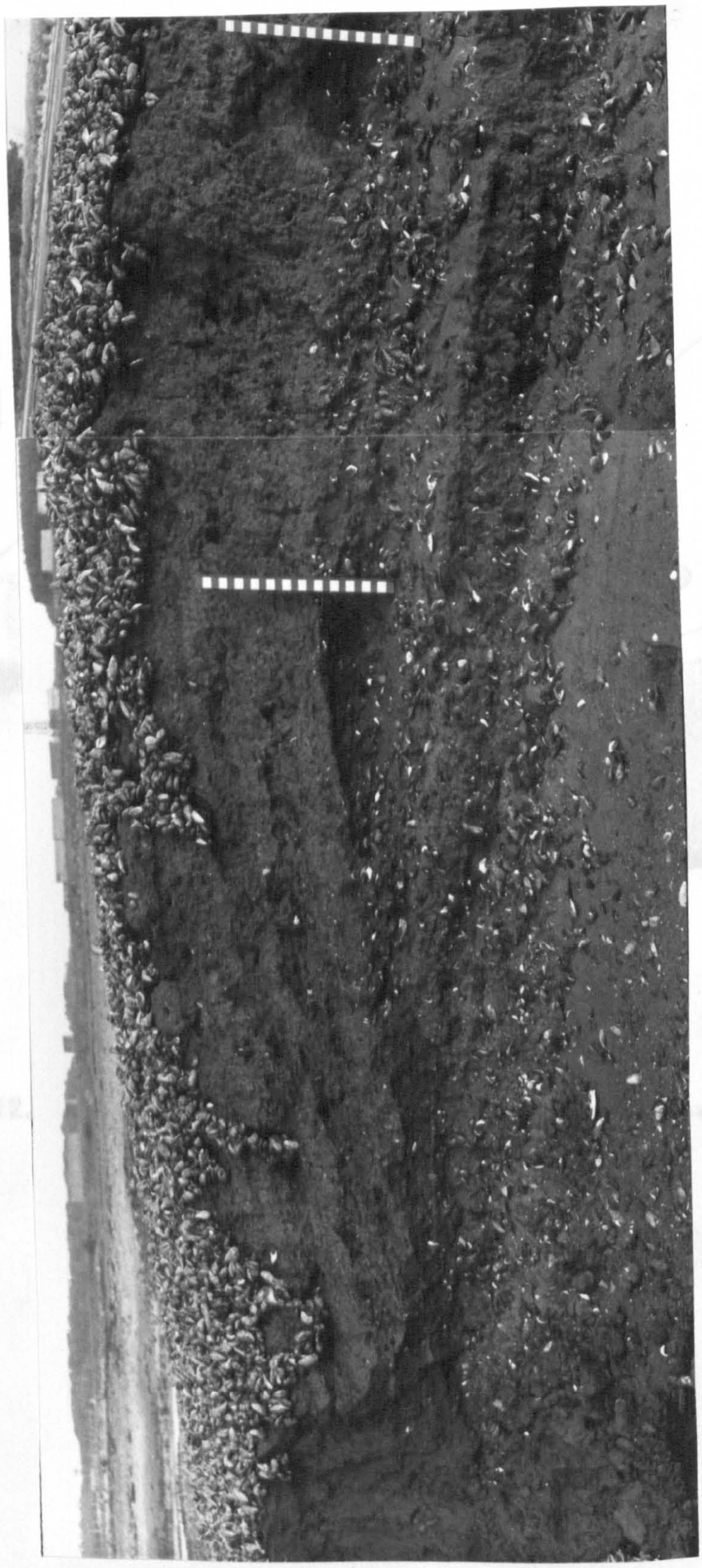

Fig. 3.11. The internal structure of a mussel bank. Note the disconformable bedding relationships. Scale-bar = 0.5m.

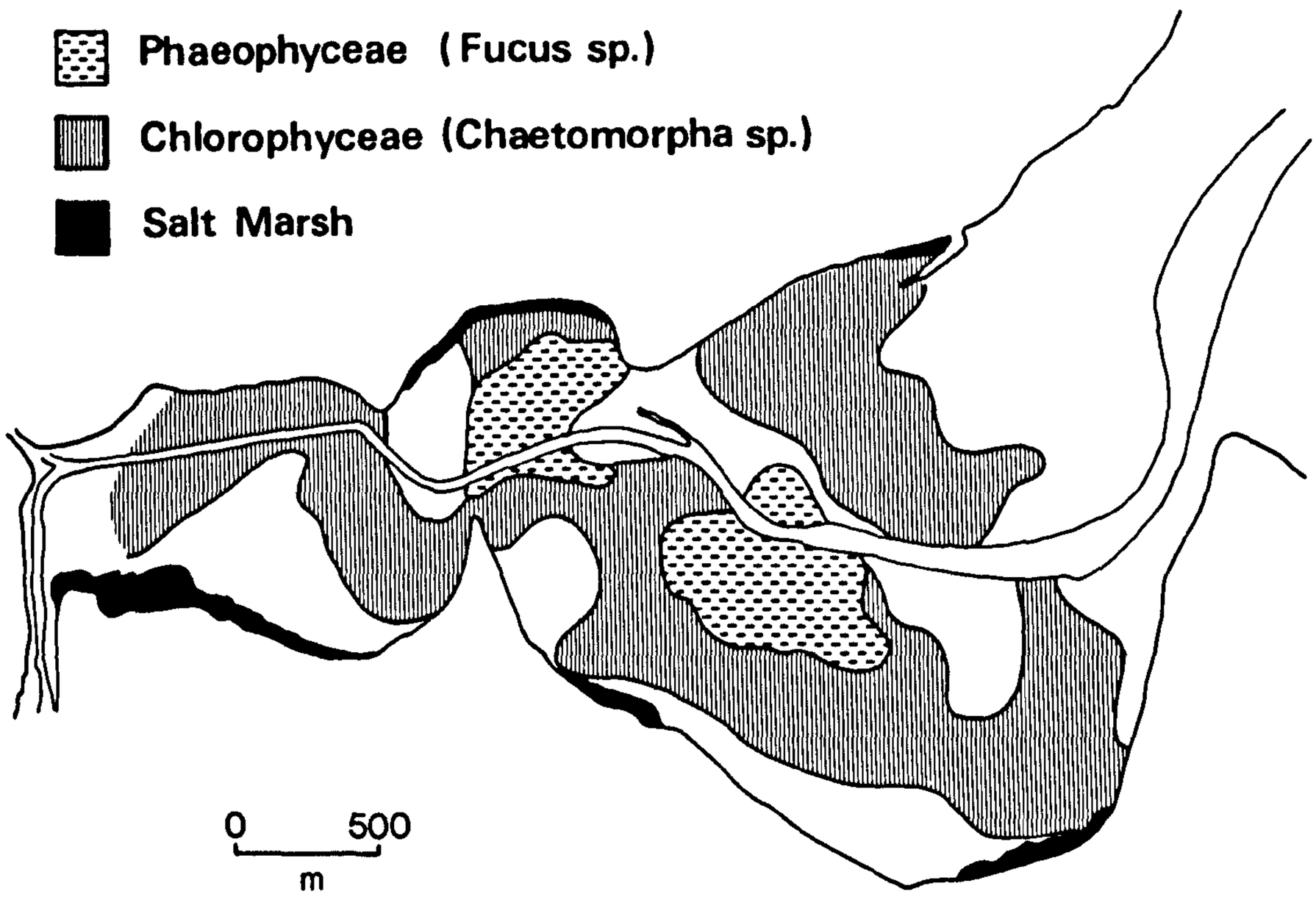

Fig. 3.12. The distribution of algal material and salt marsh deposits.

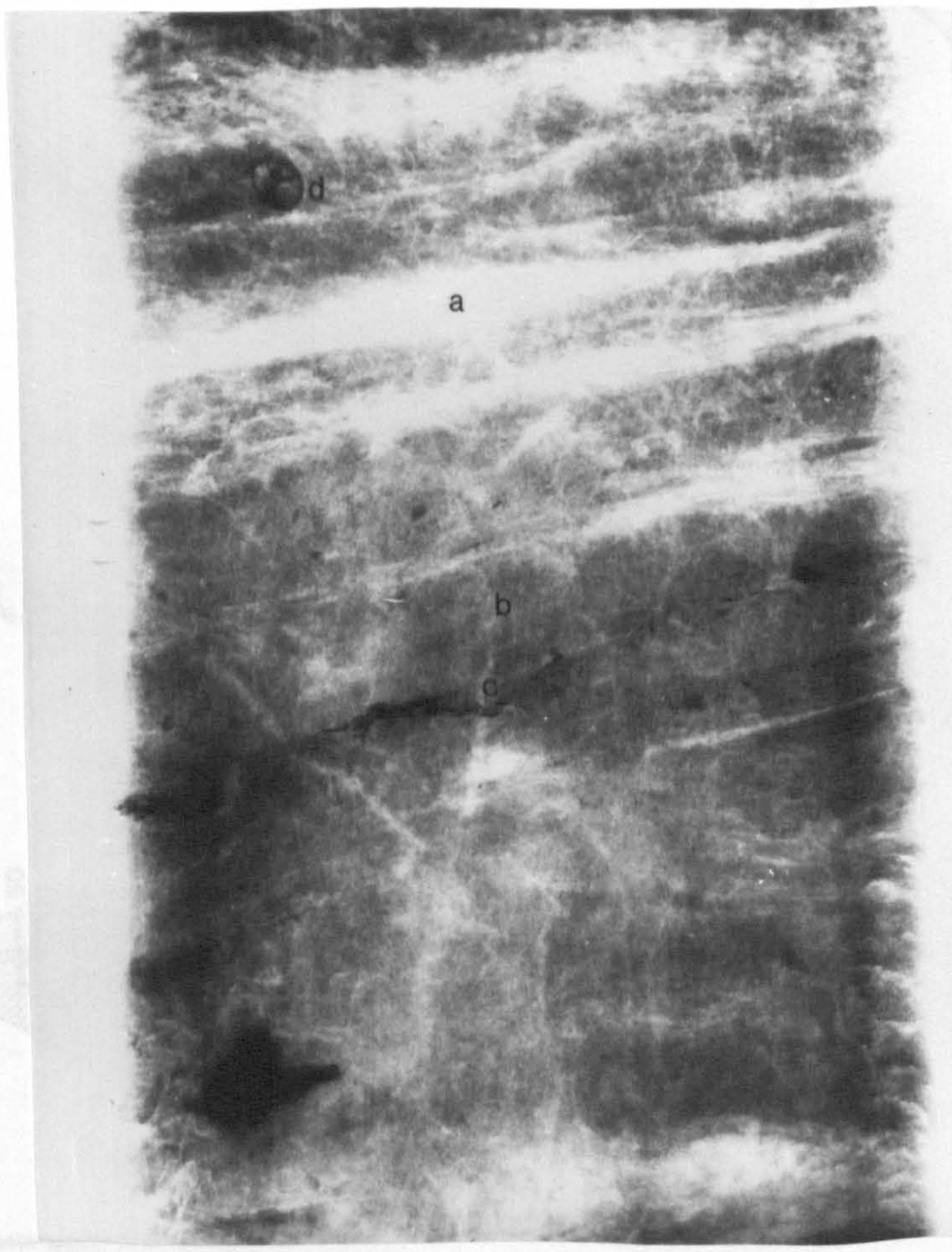

Fig. 3.13. The internal sedimentary structure of a salt marsh deposit.
Top: epoxy resin peel.
Bottom: x-ray radiograph (a) sand-rich layers, (b) silt and clay-rich layers, (c) shell fragments, (d) whole gastropod test.

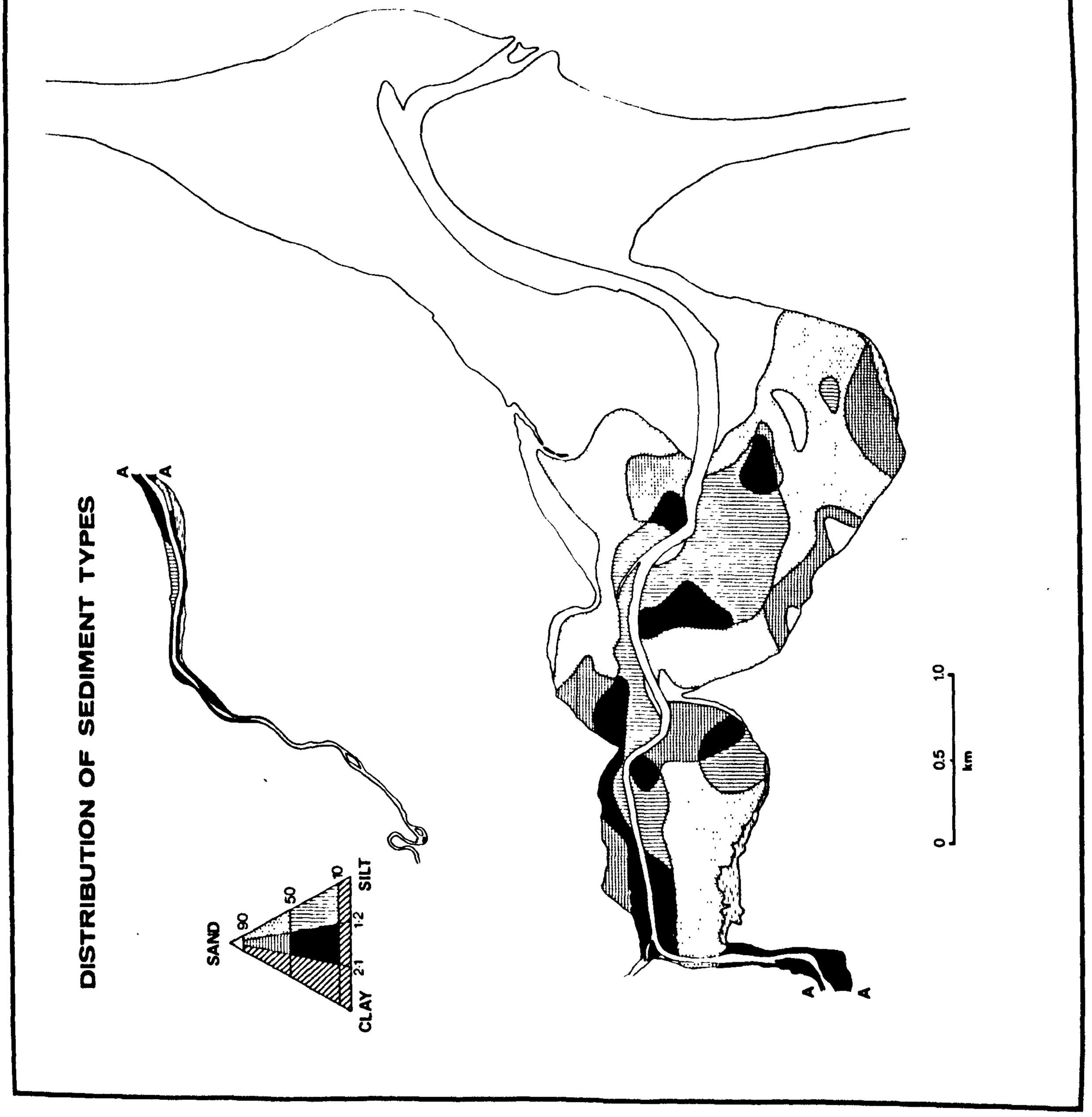

Fig. 3.14. The distribution of sediment types in the estuary based on Folk's (1968) classification.

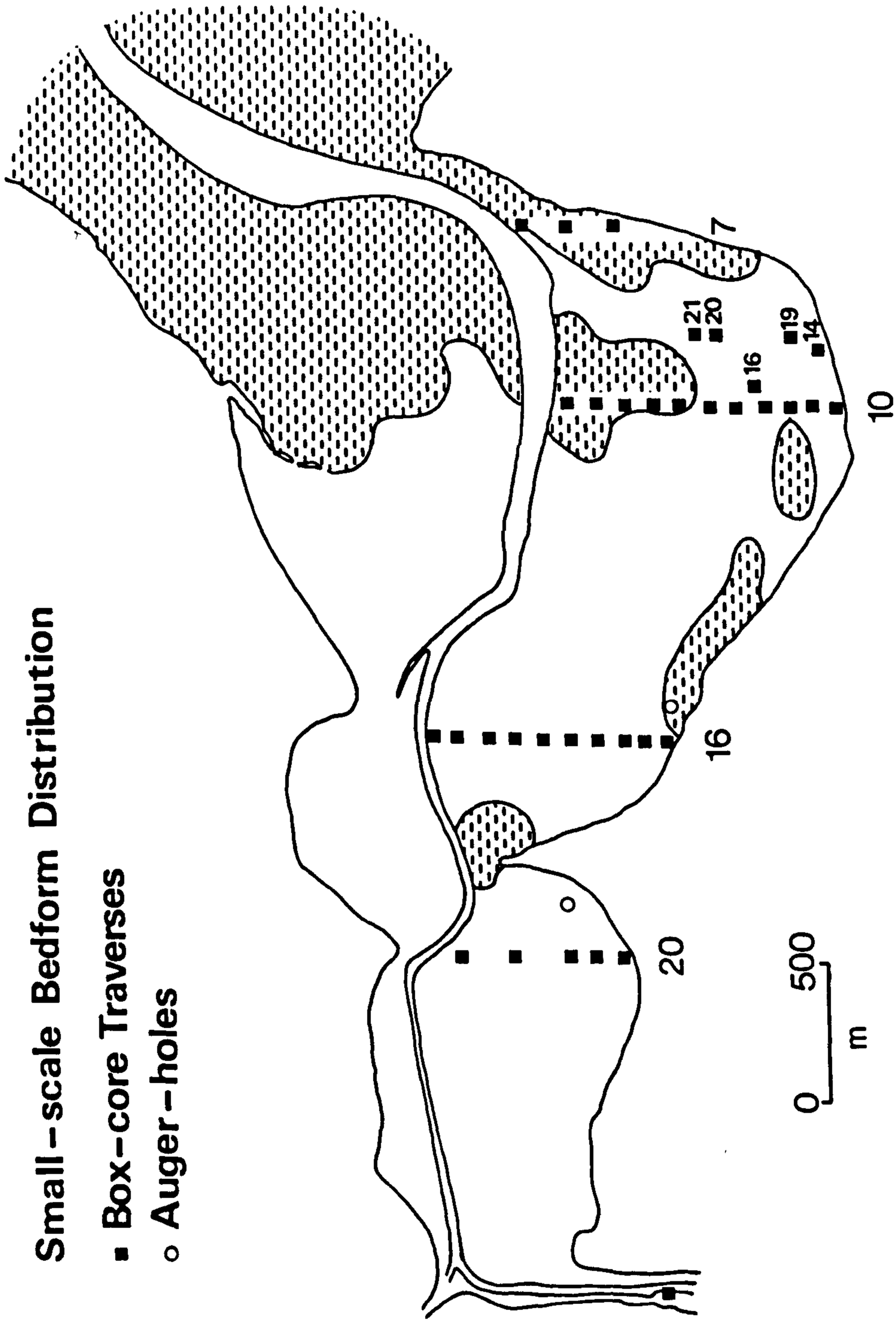

Fig. 3.15. The distribution of small-scale bedforms and the sites of box-cores and auger-holes. Shaded areas show the distribution of small-scale bedforms of ripple type.

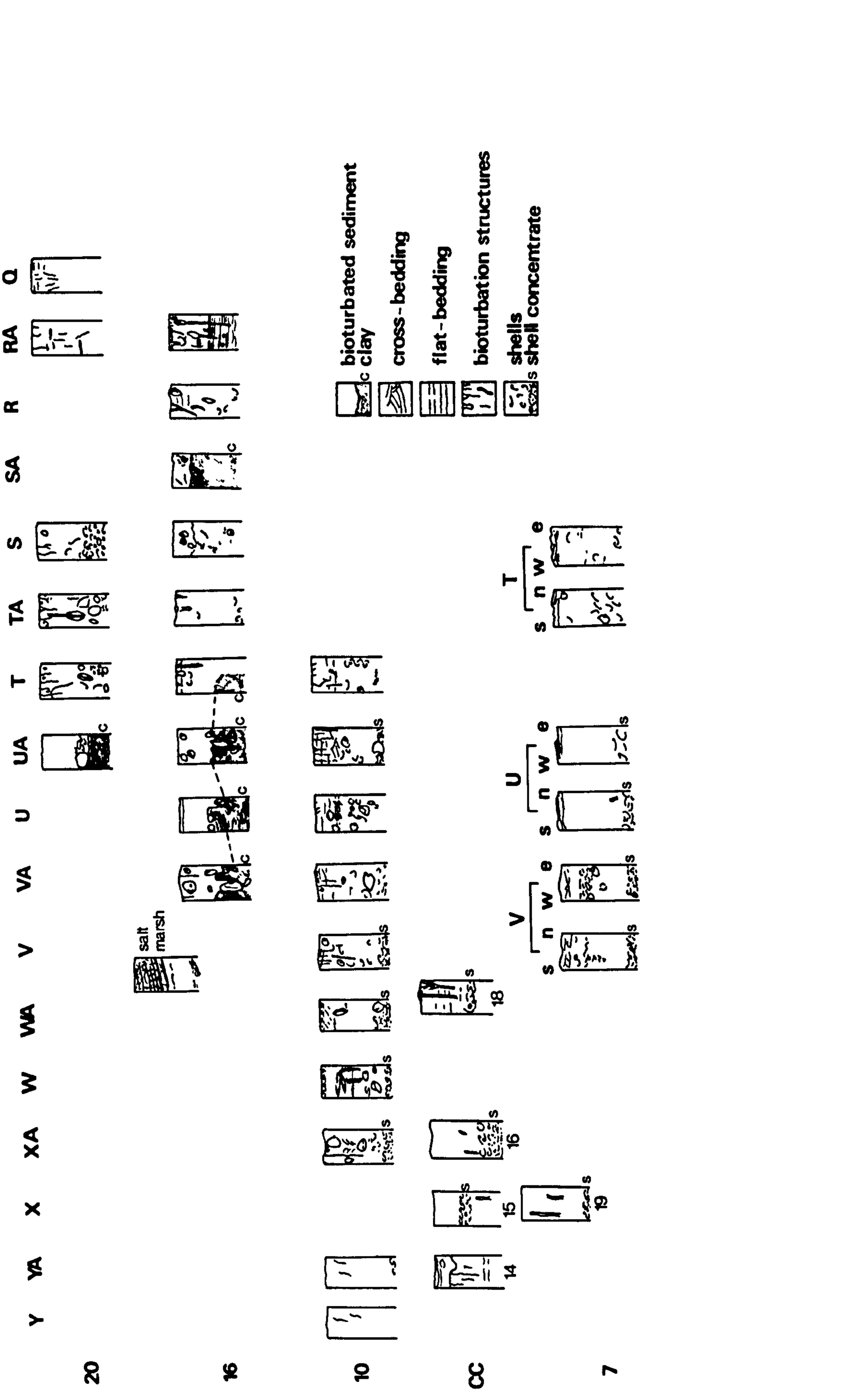

Fig. 3.16. A diagrammatic representation of the internal sedimentary and biogenic structures found in the box-cores. Each box-core measured 25 x 16cm.

Fig. 3.17. A box-core (7U) showing two shell beds (a and a') with a bioturbated zone between (b) and a small-scale, cross laminated zone above.

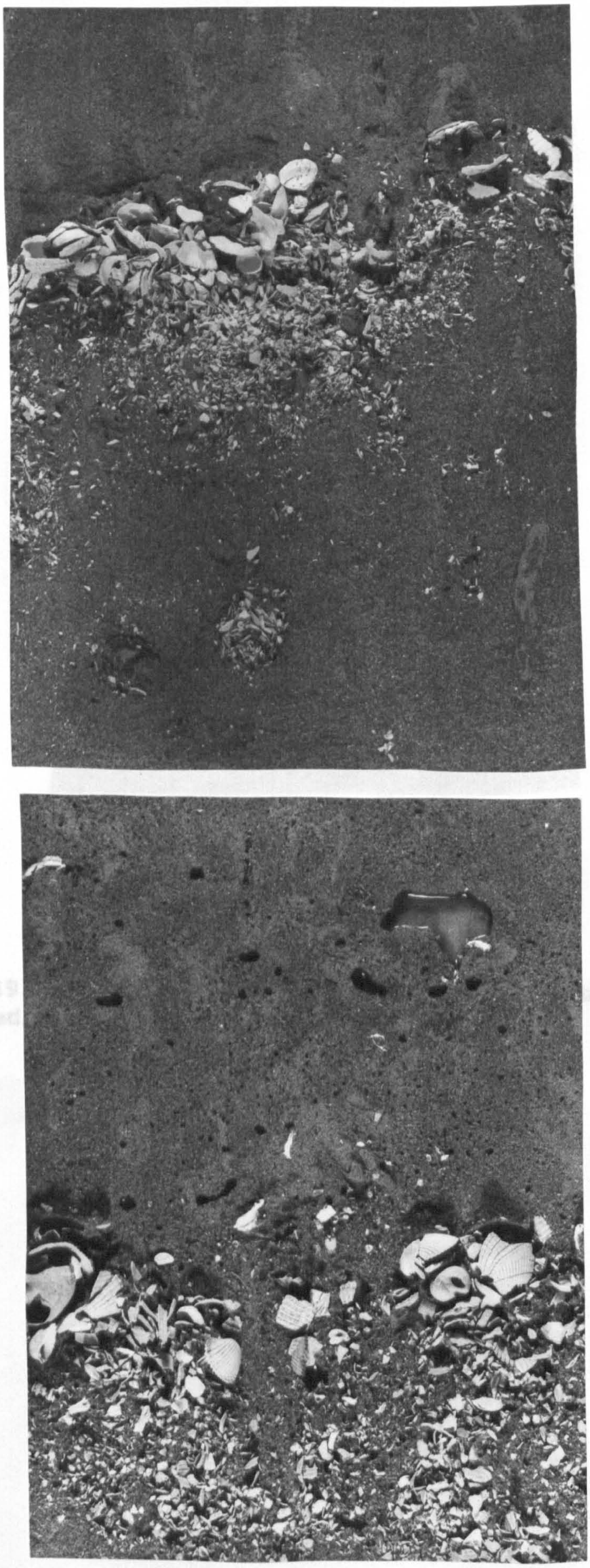

Core CC16

Core CC18

Fig. 3.18. The textural characteristics of a shell bed which is of widespread occurrence in the surficial sediments of Kincaple Flat.

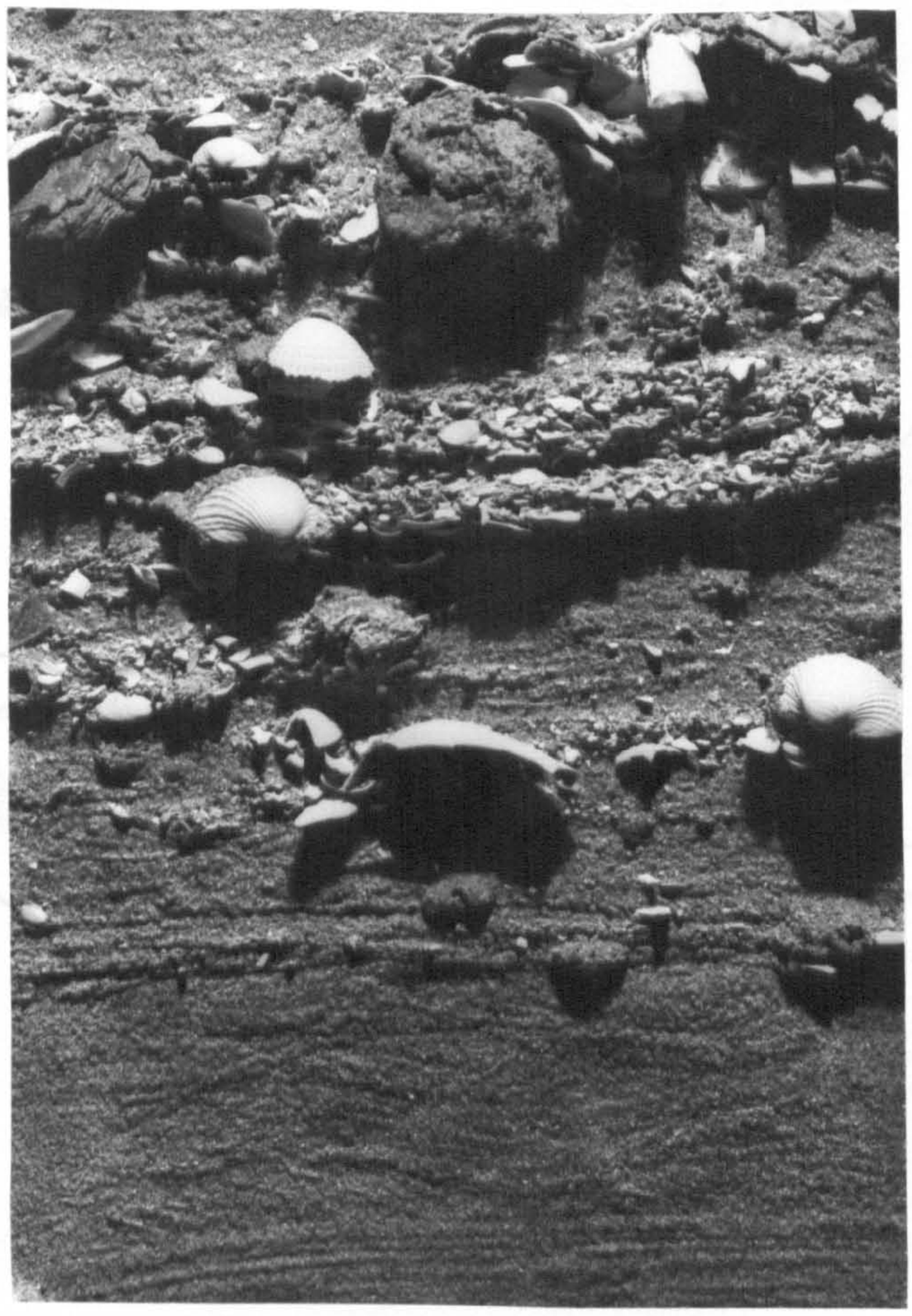

Fig. 3.19. Characteristic textural features of a beach-deposited shell bed. Compare with Fig. 3.18.

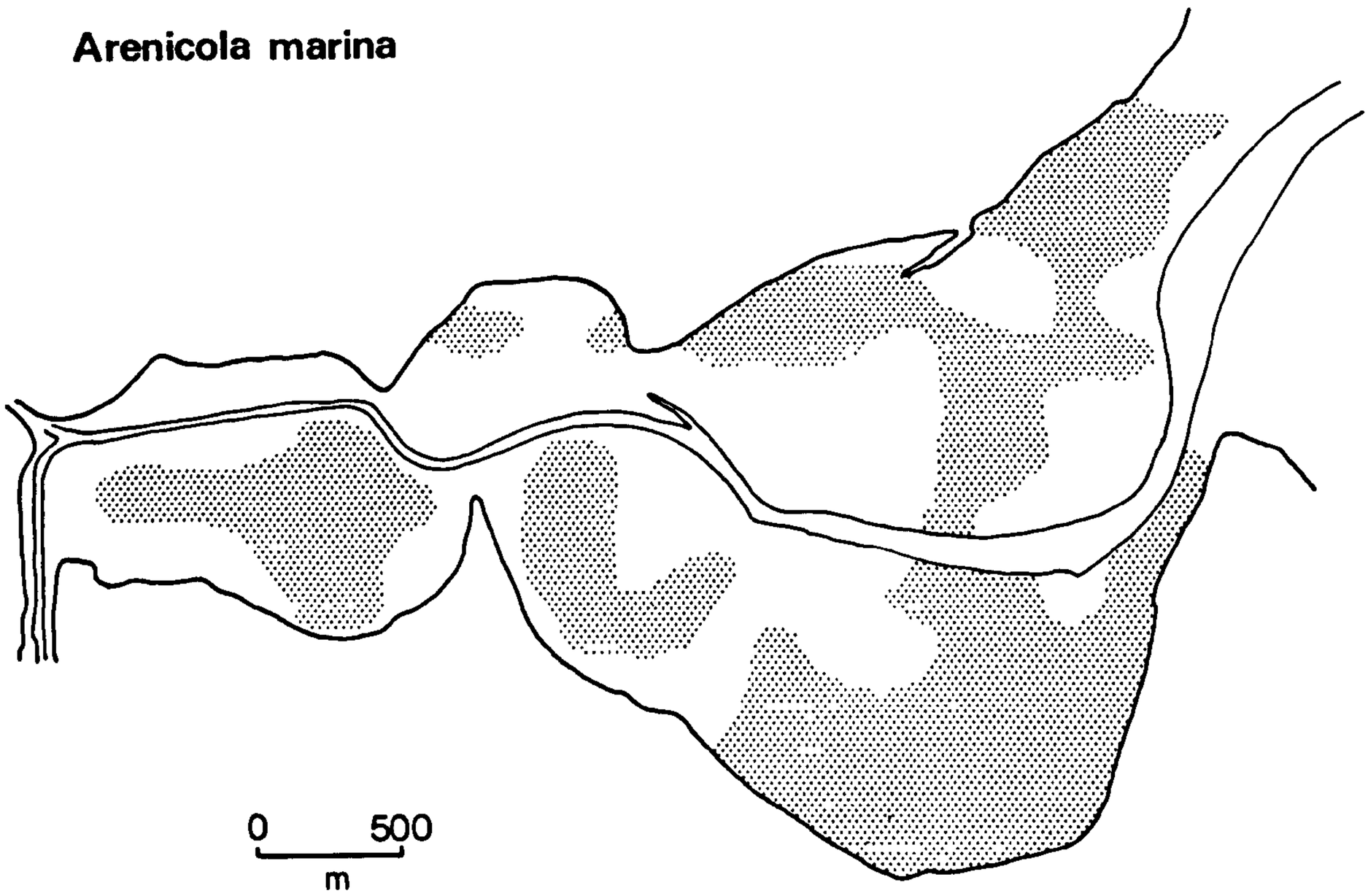

Fig. 3.20. The distribution of Arenicola marina. Map pertains to the period June to September 1973.

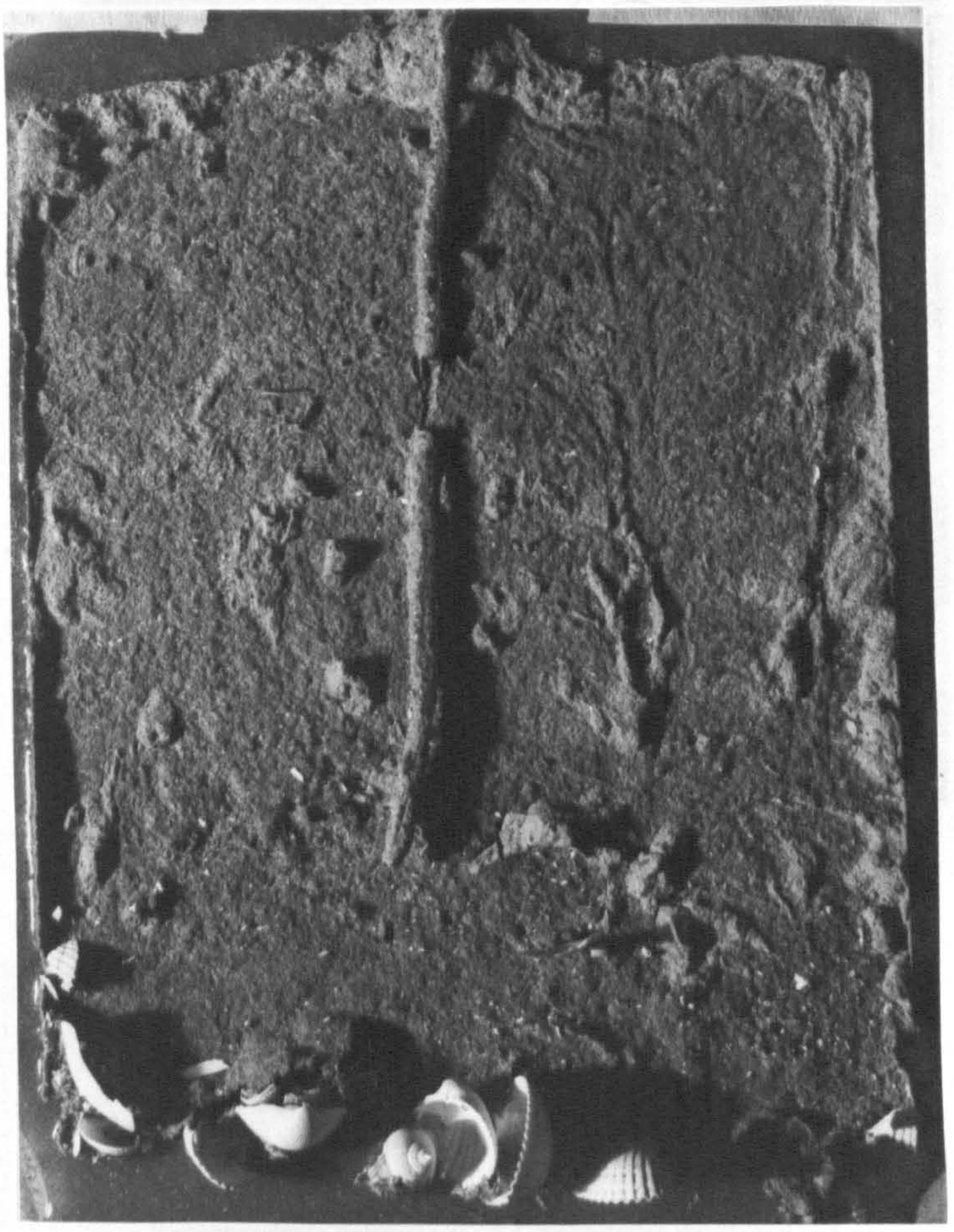

Fig. 3.21. Epoxy resin peel of the feeding structure of Arenicola marina. The outlet shaft is preserved and can be seen to bifurcate near the surface beneath the pile of expelled sediment. The intake shaft is not preserved, but its presence to the right of the outlet shaft might be inferred from the distorted bedding. Note the shell bed just beneath the bottom of the Arenicola burrow.

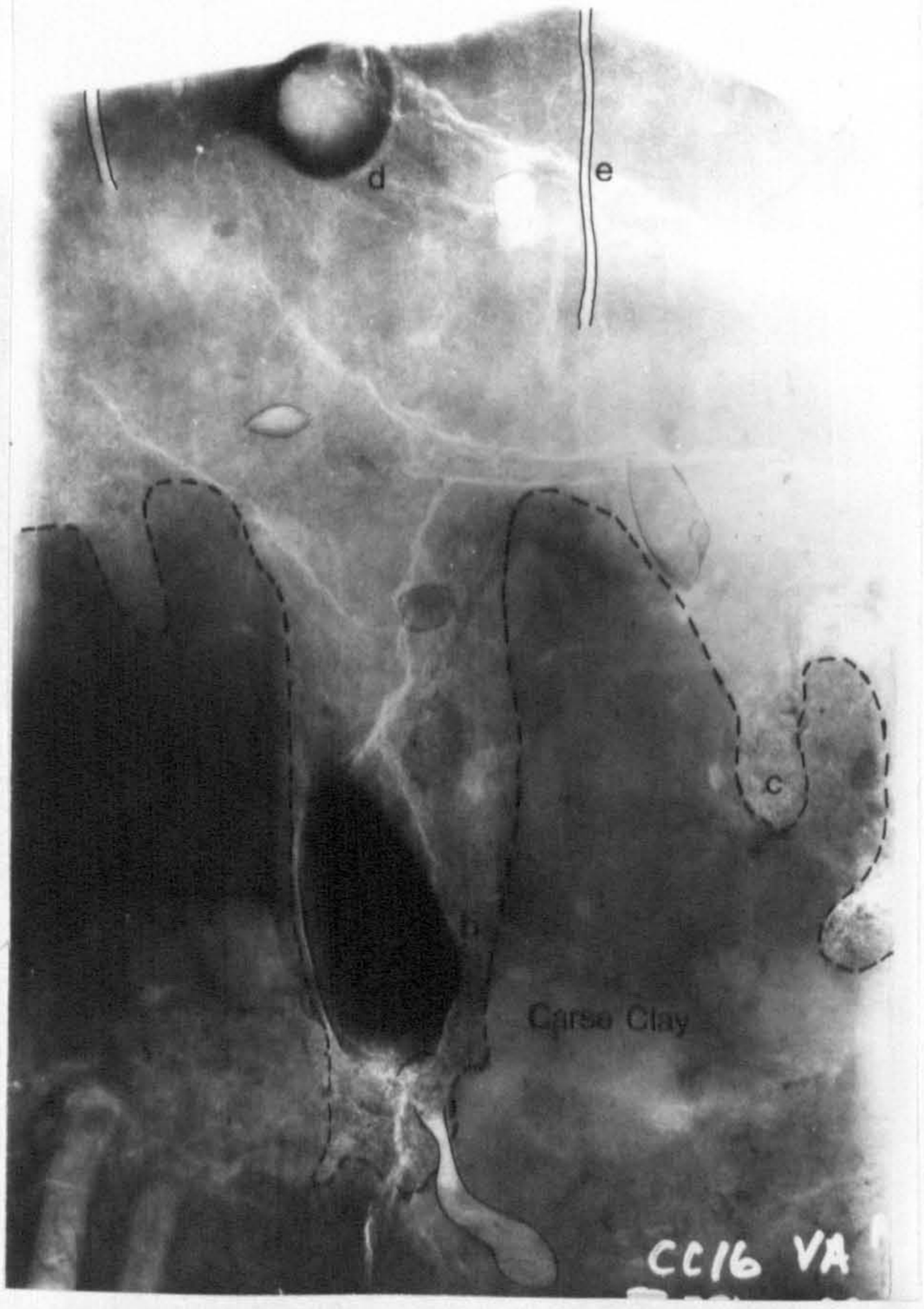

Fig. 3.22. Top: Box-core of sample CC16 VA. Silty sand, with Cardium in life position, lies on an irregular surface of Carse clay. Mya arenaria is present in life position in a burrow on the clay surface.

Bottom: X-ray radiograph of CC16 VA. (a) bedding in the clay marked by plant remains, (b) Mya arenaria with foot extended into the clay, (c) hollow on clay surface filled with Hydrobia debris, (d) Cardium edule in life position, (e) outlet shaft of Arenicola marina.

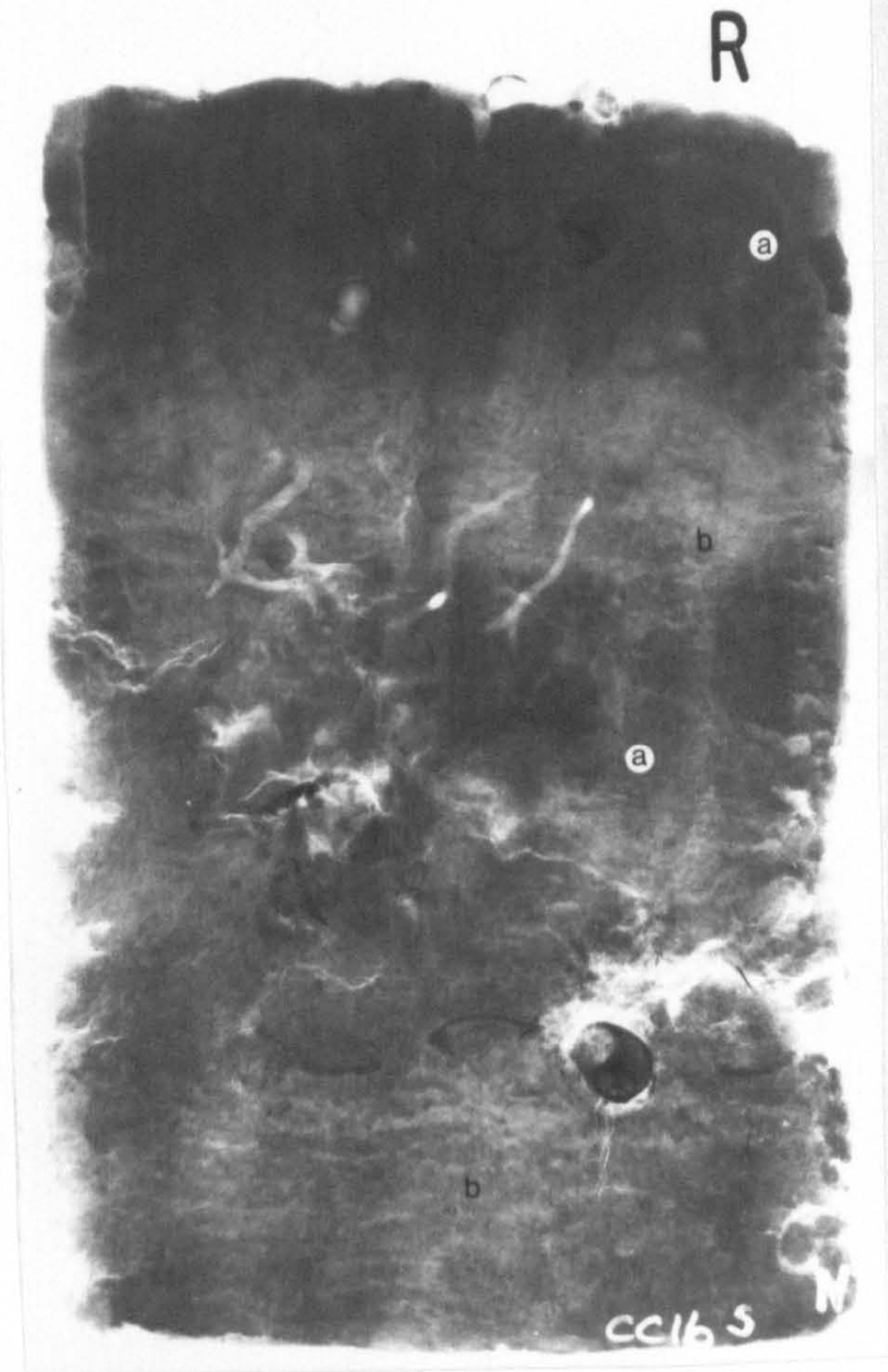

Core CC16S

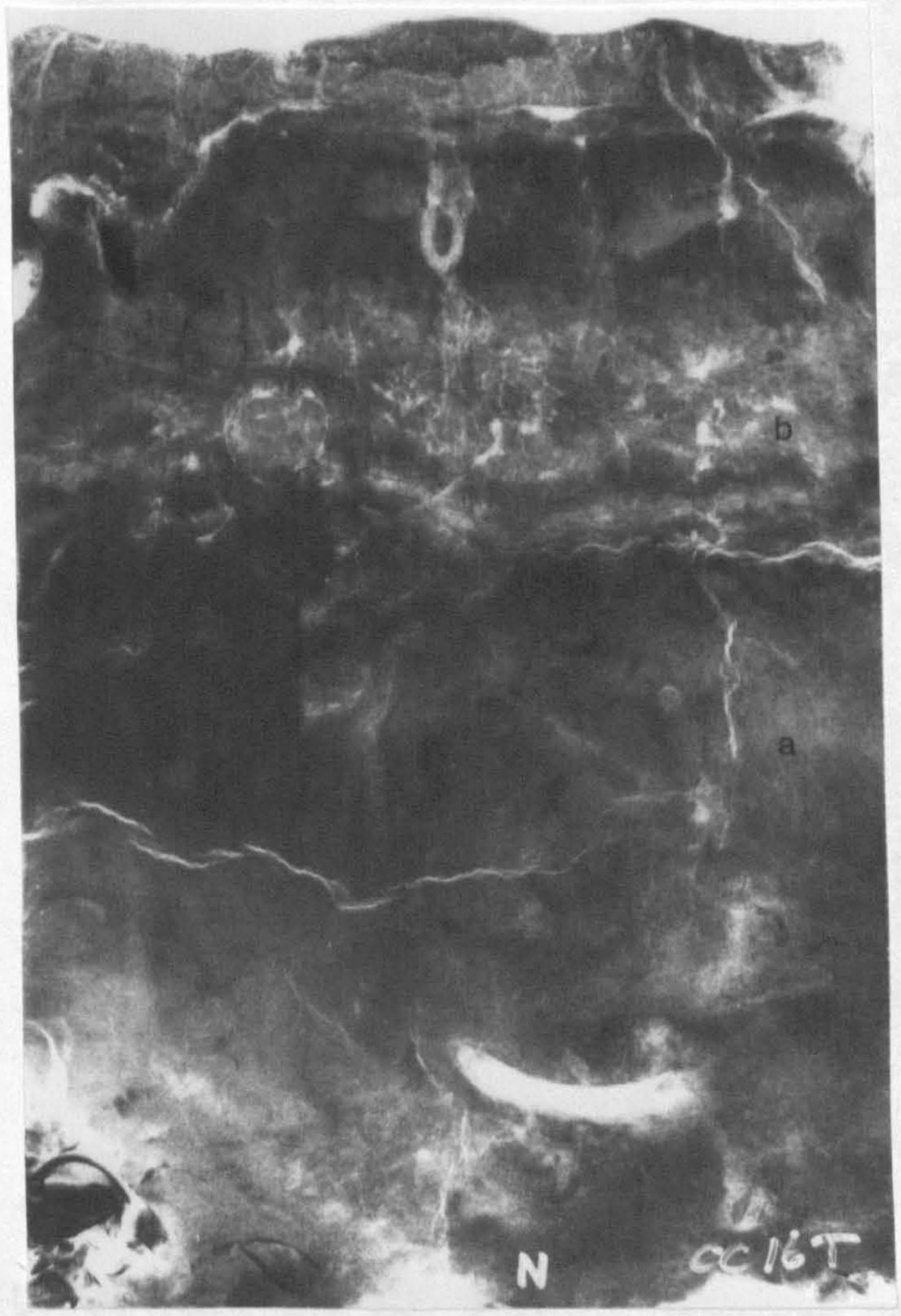

Core CC16T

Fig. 3.23. Alternations of clay-rich (a) and silty-sand-rich layers (b).

Core 20RA

Core 20Q

Fig. 3.24. Cores 20RA and 20Q showing numerous bioturbate structures. Little trace of primary bedding remains.

IV. THE FLOOD-TIDAL DELTA

Terminology

A flood-tidal delta is a sediment accumulation which occurs landward of a tidal inlet and is the result of deposition from waning flood-tidal currents (Coastal Research Group, 1969, cited in Schubel, 1971; Hartwell, 1970; Hayes, 1971).

Hayes (1971) stated that a flood-tidal delta usually has six major components:

1. a flood ramp
2. flood channels
3. a high area
4. ebb-shields
5. ebb-spits
6. spillover lobes.

The flood ramp is the area where the bed rises in a landward direction from its maximum depth at the inlet.

Flood channels are generally landward shallowing features dominated by flood-tidal currents.

The 'high area' is situated on the landward part of the delta and is normally colonised by bivalves.

An ebb-shield is a topographically high rim around a sand-body which protects portions of the sand-body from extensive modification or destruction by ebb-currents.

An ebb-spit is a sediment accumulation commonly attached to the borders of a flood-tidal delta and formed by ebb-tidal currents.

A spillover lobe is a lobate ridge of sediment formed by unidirectional currents and is often found where ebb-currents have cut through ebb-shielded areas.

Topography

The flood-tidal delta of the Eden estuary is a sand-body of area $0.7k^{-2}$ which occurs on the north side of the Eden channel in the lower estuary (Fig. 3.25).

The eastern part of the delta consists of a digitating system of flood- and ebb-channels (Van Straaten, 1952; Robinson, 1960), between which are curved, convex-southward sand-ridges which serve as ebb-shields (Fig.3.25,B,E).The ebb-shields also extend around the western ends of the flood-channels. The western part of the delta consists of a 'high area' colonised by mussel banks and fucoid sea-weeds (Fig. 3.25, H).

The two flood-channels (Fig. 3.25, A, D) are landward shoaling branches of the main Eden channel. Air photographs (Fairey Surveys Ltd., 1973) indicate that the northern channel (A) originates immediately to the west of the tidal inlet, whereas the southern channel (D) forms to the north of Out Head. Channel D is shown on echo-sounder profiles in Figure 3.5 (profiles 3 and 4, features F and F1).

The two ebb-channels (C and C1, Fig. 3.25) both receive drainage water from around the northern margin of the high area. During the later stages of ebb-flow water in ebb-channel C drains into the eastern part of flood-channel D and eventually joins the Eden channel. At the junction a small delta has formed (Fig. 3.25, F). Ebb-channel C has developed since 1964. Before this time the area was occupied by a single flood-channel. Up to 1964 the area now covered by the southern flood-channel had the form of a lobate sand-body with a slightly concave surface surrounded by a sand-ridge.

Features termed 'ebb-shields' curve around the western parts of the two flood-channels (Fig. 3.25, B, E). The northern ebb-shield (B) consists of the western part of Sanctuary Spit and its southward

extension as a sand accumulation (spit-platform) with a level above that of the surrounding flats. The ebb-shield serves to direct water draining from the northern part of the middle estuary in a southerly direction around the northern flood-channel and into the ebb-channel (C). The western extremity of Sanctuary Spit consists of a north-south trending accumulation of sand and shell debris. The northern part of this feature, which consists almost entirely of single valves of Cardium edule, has been moulded into an ebb-orientated bedform with the dimensions of a sand-wave (Fig. 3.26).
The southern ebb-shield (E) has an acute western closure and its southern limb forms the north bank of the Eden channel.

To the west of the flood-ebb channel system is a 'high area' which is colonised by Mytilus edulis and Fucus sp. (Fig. 3.25, H). The area is roughly triangular in plan and presents a straight and elevated western margin to ebb-tidal currents. The whole area is sufficiently elevated to be the last area in the middle estuary to be submerged during the flood-tide.

Bedforms

The major topographic features of the flood-tidal delta have smaller bedforms superimposed upon them, the most important of which are asymmetrical, large-scale ripples. The term 'large-scale' is used to denote those bedforms of chord greater than 60cm and height of more than 4cm (Allen, 1968).

Bedform Orientation

On the 25th. and 27th. June 1974 chord lengths and lee-slope orientations of well-formed, large-scale bedforms were measured. The distribution of lee-slope azimuths was distinctly bimodal (Fig. 3.27,a). Eighty-four readings plotted in the range 150° to 270° (flood orientation) and 80 in the range 000° to 090° (ebb orientation). The ebb-

orientated features showed less diversity in lee-slope direction because of their generation on inter-channel high areas which are affected by a uniform flow direction during the early stages of the ebb-tide. The modal orientations were almost diametrically opposed with a flood mode between 210° and 240° and an ebb mode between 000° and 030°. There would, therefore, appear to be a slight net clockwise sediment dispersal pattern over the flood-tidal delta.

c. Chord Length

The frequency distribution of chord lengths of flood-tidal delta bedforms was bimodal and asymmetrical (Fig. 3.27,b). The majority of bedforms had chords between 2.5 and 5.6 m and only one example occurred in the chord range 0.5 to 2.5m. A secondary mode occurred at a chord length of 11m. In view of the bimodal distribution, it would seem in order to classify the observed bedforms into two groups with a division between the two at a value of 6.0m. Following American usage (Hayes, 1971) large-scale bedforms of chord less than 6.0m are termed 'megaripples' and those of chord greater than 6.0m 'sand-waves'.

Figure 3.27,c shows a notable relationship between chord length and bedform orientation: flood orientated bedforms are, with very few exceptions, sand-waves, whereas ebb-orientated bedforms are megaripples.

Bedform chord lengths for the individual flood-channels and the interchannel areas are given in Table 3.1.

Table 3.1. Chord Lengths in Metres: Flood-Tidal Delta 25.6.74 and 27.6.74.

	Mean	S.Dvn.	Min.	Max.	Mode
North Flood Zone	10.87	4.67	2.90	20.90	5.24+9.91
South Flood Zone	12.11	2.29	6.50	17.00	10.70
North Ebb Shield	3.95	1.07	1.14	9.00	3.75
Ebb Channel	5.11	2.25	3.80	13.00	4.18
South Ebb Shield	9.06	2.22	6.00	11.50	10.81

1. Northern Flood Zone (Fig. 3.25,A)

Bedforms in the northern flood zone are dominantly sand-waves with chords up to 20.9m and heights of up to 50cm (Fig. 3.27,c). Bedform size decreases westwards as the channel shoals. Sand-waves on the edge of the channel are gently curved in plan with a slight convexity to the west, whereas, in the deeper parts of the channel, crest-lines become more sinuous. The gently curved bedforms tend to be in-phase, whereas the sinuous forms become out-of-phase.

2. North Ebb Shield (Fig. 3.25,B)

Bedforms of the northern interchannel-ebb-shield are megaripples with chords between 1.1 and 9m (Fig. 3.27,c). Chord lengths are relatively constant at 3 to 5m throughout the zone, and high values occur only at the seaward end. The area is topographically high and supports sinuous megaripples with well developed spurs attached to their lee-sides (Fig. 3.28). Within the troughs between spurs ripple-fans are developed. These structures show a variety of ripple-marks, and Figure 3.29 shows the concentric arrangement of arcuate ripples which increase in chord length away from the trough and eventually become linguoid in plan as the bed rises in the flow direction.

3. The Ebb Channel (Fig. 3.25,C)

Ebb-channel bedforms are generally of greater chord length than those of the adjacent but topographically higher interchannel-ebb-shield; values range from 3.8 to 13.0m.

4. South Flood Channel (Fig. 3.25,D)

Bedforms of the south flood channel are of similar chord length

to those in the northern flood zone, but there is a total absence of megaripples. The minimum recorded chord length is 6.5m.

5. South Ebb Shield (Fig. 3.25,E)

This ridge forms the northern bank of the Eden channel. Under intermediate and neap-tide conditions the ridge is covered by small-scale ripples, but under Spring Tide conditions the crest of the ridge takes the form of a sand-wave with an E-W trend, associated with which are megaripples with north-easterly orientated lee-slopes (Fig. 3.30).

Sand-Wave Modification

Flood-orientated large-scale bedforms are modified by ebb-currents but not sufficiently to alter their asymmetry. Ebb-modification of a flood-orientated sand-wave from the northern flood-zone is illustrated in Figure 3.31. Ebb-tidal currents are of sufficient strength to remould the crest of the sand-wave into an ebb-orientated megaripple with a chord of 1.5m and a height of 15cm. The stoss-sides of both the megaripple and sand-wave bear small-scale linguoid ripples with ebb-orientation. Figure 3.32 shows the development of large scours, covered by ebb-orientated small-scale ripples, on the stoss-side of a sand-wave in the north flood zone. The crestal area and intertrough areas have been completely planed off by the ebb-flow.

Run-Off Structures

Further modification of the sand-waves occurs during late-stage run-off when water is confined to the troughs between individual bedforms. Lee-sides of sand-waves often exhibit two structures generated by the combined effects of flow in the trough parallel to the sand-wave crest, and falling water level. The restricted flow generates

small-scale asymmetrical ripples which trend perpendicular to the sand-wave crest and occur on the sand-wave lee-slope and in the trough (Fig. 3.33). Falling water level engraves parallel marks of the lee-slope. Fissuring and slumping in the water-laden sediment on the lower part of the lee-slope also occurs (Fig. 3.33).

Troughs between bedforms often act as depositories for material being carried by the residual currents. Situations arise where changes in bed elevation are rapid and currents may encounter deep still water. In such cases conditions are suitable for the growth of microdeltas. Figures 3.33 a and b show two examples of sediment deposition in arcuate troughs at the base of lee-slopes of sand-waves. In the first case a wide shallow flow from the left has produced a sediment accumulation with a roughly planar lee-slope. In the second case residual ebb-currents have cut a narrow channel through a broad low spur and the resulting delta is lobate in plan. A ripple-fan has also been formed around the delta. In both cases an abundance of detrital carbonate is present on the foreset beds of the microdeltas.

Internal Sedimentary Structures

Internal sedimentary structures of sand-waves and megaripples from the flood-tidal delta were studied in order to determine their relationship to the surface expression of the bedform and to aid the interpretation of the depositional conditions under which the bedform was generated.

Internal Structures of Sand-Waves

1. Physical Features

A sand-wave from the northern flood-channel of the flood-tidal delta is considered representative of all sand-waves in the area. The internal structure of such a sand-wave is complex and consists of a number of tabular cosets of cross-laminae which dip at low angles

in the flood-direction and a wedge-shaped coset which thickens in the ebb-direction (Fig. 3.34). Structures generated within each coset create a discordance between the internal structure and the surface expression of the bedform.

With only slight variation, each of the flood-orientated cosets consists of the same sequence of three sets of laminae which total approximately 10cm in thickness. The three sets in each coset in ascending order are:

3. 0-4cm small-scale trough cross laminae
2. 4-8cm foreset laminae
1. 2cm very low angle cross laminae.

Sets 1 and 2 are the product of progradational depositional episodes related to flow in the flood-direction. Set 3 is more complex and could be interpreted as a separate coset in which two or more depositional and erosional events may be recognised.

Set 1 is less than 2cm thick with individual laminae of 2-3mm thickness. The lower bounding surface of this set has a slightly irregular topography in the form of small-scale ripples and shallow depressions, and displays a dip of 8^{o} to the west. Lensing laminae occur in the troughs between ripples (A) and over planar areas laminae are almost parallel to the depositional surface (B). In local depressions in the depositional surface laminae overlap in the flood-direction and attain maximum dips of $10-11^{o}$ (C). Micro-cross-lamination with foreset dips of 20^{o} and angular bases are developed occasionally within this unit (D). Perpendicular to the dominant flow direction the laminae retain their planar character and are traceable for over 50cm, until they eventually terminate against small-scale bedforms (Fig. 3.35,E).

Set 2 consists of up to 8cm vertical thickness of foreset laminae with moderate angles of repose (20^{o}) and tangential contacts with the

underlying set. In the majority of cases the foreset laminae are thinner than the laminae of Set 1 and are not as well defined. Perpendicular to flow the foreset laminae dip at 8^{o} (south) and hence have a very slight angular contact with Set 1 (Fig. 3.35,F).

Set 3 consists of 2 or 3 units of ebb-orientated laminae with a total thickness of up to 4cm. The lower bounding surface of the set is an irregular, sharply defined erosion surface which truncates the upper parts of the foreset laminae of Set 2 (Fig. 3.34,G). The lower unit of Set 3 consists of small-scale, low-angle cross-laminae and micro-delta cross-laminae which infill the scours on the surface of Set 2 (Fig. 3.34,H). The cross-laminations are invariably of ebb-orientation. Within Set 3 of coset 2, in the sand-wave illustrated (Fig. 3.34) occurred a single heavy-mineral-rich lamina of 2mm thickness which truncated both the lower unit of Set 3 and the foresets of Set 2 (J). Above this lamina occur ebb-orientated, small-scale ripples (K).

The flood-orientated cosets are terminated upwards by an easterly dipping (5^{o}) well defined, irregular, erosion surface (Fig. 3.34,K). Depressions or scours in the surface are filled by the foreset laminae of flood-orientated small-scale cross-laminae (L). The upper surfaces of the flood features are planed off and overlain by ebb-orientated small-scale bedforms (M). The major part of the superimposed wedge-shaped coset consists of up to 10cm of ebb-orientated foreset laminae which dip at 31^{o} and have tangential bases (N). The upper surface of the foresets is eroded and the bedform is capped by a form-set of ebb-orientated, small-scale, linguoid ripples (P).

2. Interpretation and Significance

The sequence and degree of development of the sedimentary structures in each coset suggests that essentially similar depositional

conditions are repeated through time. The frequency of occurence of conditions suitable for the generation of a coset of cross-laminae is not determinable from the preserved structures. It is obvious however from a consideration of the orientation of cross-laminae that sets 1 and 2 are the product of deposition from flood-tidal currents and set 3 from ebb-tidal currents. Whether the two sets of currents were of the same tidal cycle is unknown, as is the period between the deposition of cosets. It is known that the rate of migration of these bedforms is related to the lunar controlled spring-neap tidal cycle when migration is at a maximum during the occurence of spring tides. Migration distances of up to 41cm per tide have been recorded (page 82), and it was observed that a coset could be deposited during one tidal cycle.

Set 1: Depositional conditions associated with set 1 are such that (a) bedforms on the lower bounding surface are not always destroyed, and (b) planar laminae and micro-cross-laminae can form.

Trenching (Fig. 3.36) indicated that the dip angle of the bounding surfaces of each flood-orientated coset is approximately the same or slightly longer than that of the lee-slope at the free-surface of the bedform. In so far as set 1 is flood-orientated and overlies ebb-orientated small-scale bedforms, it is considered to have formed actually on the lee-slope of an existing sand-wave under the influence of flood-tidal currents. Two depositional processes are suggested: (1) under the combined influence of rising water-level and the 'lapping' of wind-generated waves on the lee-side of the sand-wave, the equilibrium of the dry sand is disturbed, and the sediment may be redistributed by grain-flow down the lee-slope. Grain-flow in laterally extensive, very thin sheets of sand could produce grain segregation and laminations. Micro-delta cross-laminae might form wherever a shallow depression appears on the lee-slope; (2) some laminae may be

the product of deposition of material which has avalanched down the foresets of the succeeding set (set 2) to concentrate on the sand-wave lee-slope, eventually to be overridden by set 2.

Set 2: The foresets of set 2 are associated with the phase of megaripple progradation down the lee-slope of the sand-wave. This phase probably coincides with the period of maximum tidal current velocities some 2 to 1.5 hours before the time of High Water (Fig. 2.23, Chapter 2, IV).

The foresets have moderate dip angles (20^{o} to the depositional surface) which may be indicative of the high current velocities, and the importance of deposition from suspension is indicated by the tangential foreset contacts with set 1 (Jopling, 1965).

When compared with the laminae of sets 1 and 3, the foreset laminae of set 2 are less distinct, and there appears to be little textural variation between laminae.

Set 3: After the phase of megaripple progradation flood-tidal currents decrease in velocity and small-scale ripples may be generated on the stoss-side and crestal areas of the sand-waves. With the turn of the tide and increasing ebb-current velocity the crestal area of the sand-wave undergoes erosion which truncates the tops of the foreset laminae of set 2. The migration of small-scale bedforms on the erosion surface produces the observed ebb-orientated, cross-laminae and micro-delta cross-laminae of set 3.

Ebb-coset: Concurrent with sediment erosion from the crest and upper lee-slope of the sand-wave during the ebb-flow, deposition takes place on the upper part of the stoss-side of the sand-wave. Sand accumulates in the form of a megaripple with tangential foresets and well-developed toesets. The foreset dip angle with the surface of deposition (25^{o}) is greater than that of the flood-orientated foresets

of set 2, which implies lower flow velocities. Measured velocities over the sand-wave field during the ebb tide were only of the order of 50% of those during the flood tide. Small-scale linguoid ripples often develop over the whole surface of the sand-wave during the later stages of ebb-tidal flow, and their migration leads to the truncation of the upper part of the ebb-orientated megaripple with the formation of topset cross-laminae.

A diagrammatic representation of the development of sand-wave internal structures is given in Figure 3.37.

The erosion surfaces which occur as slightly convex upward features parallel to the eroded lee-slope of the sand-wave have been described from fluvial deposits by Collinson (1970) and from intertidal zone sediments by Klein (1970). Collinson (1970) gave the name 're-activation surface' to the discontinuities which occurred at regular distances from the slip-face. In the sand-waves of the Tana River one set of foresets was succeeded by another usually with no sedimentary unit between the two. This attribute may be characteristic of sedi-ments formed by unidirectional currents, and Banks (1973) showed that such structures could be generated by the migration of ripples over a wavy bed which was wavy on a scale larger than that of the ripples.

In the intertidal zone reversal of tidal currents produces re-activation surfaces, and, additionally, ebb-orientated bedforms. In the Eden estuary sand-waves at least two reactivation surfaces are present in each coset: one between sets 2 and 3, and one below set 1. Klein (1970) stated that a unimodal orientation of bedforms and cross-strata resulted from dunes and sand-waves being subjected to a combined constructional/destructional history. His conclusions are substantially supported by the Eden estuary sand-waves, as, in the preserved portion of the bedform (that below the ebb-orientated megaripple), there is but little evidence of current-reversal in the form of herring-bone cross-

stratification. Ebb-orientated cross-laminae are of minor occurrence, and the herring-bone structure occurs only where set 3 is superimposed on set 2.

Should the sediments of the flood-channel of the flood-tidal delta be preserved, the overall structure would be one resembling PI cross-stratification (Allen, 1963) cut through by multiple reactivation surfaces.

Megaripple Internal Structures

1. Physical Features

Megaripples characterise the topographically high ebb shield areas of the flood-tidal delta. The internal structures illustrated in Figure 3.38 are from the crestal area of a megaripple on the northern ebb shield where mean bedform chord length was 3.95m and the range from 1.14 to 9.00m. Five major sedimentation units are recognised: the lowermost is cavernous sand and the remainder are cross-laminated. They are numbered 1-5 in ascending order. Unit 5 is of course a megaripple in its own right, though it forms only a part of the whole megaripple structure.

Unit 1 consists of 2-9cm of cavernous sand (syn. bubble sand, vesicular sand) which dips to the west at approximately 7^{0}. In the upper part of the bed the air bubbles are well preserved, even though overlain by up to 25cm of sediment. In cross section the bubbles are oval with a maximum short axis length of 2mm. In the lower left part of the peel the bubbles become more elongate and are arranged with their long axes parallel to the foresets of the flood-orientated cross-laminae.

It is generally accepted that cavernous sand forms in areas (a) subjected to rapid submergence, which prevents air from escaping completely from the sediment, the barrier being the wet surface layer,

or (b) where rapid deposition under moderately turbulent conditions allows air to be entrapped in the deposit (Emery, 1945; Van Straaten, 1954; Hoyt and Vernon, 1964; Reineck and Singh, 1973). Hoyt and Vernon (1964) stressed the importance of sediment dryness prior to immersion in the formation of bubbles and suggested that topographically high areas such as the crests of bars would be favourable sites for cavernous sand development. This example comes from just such a situation, an elevated ridge between two channels which is exposed early in the ebb part of the tidal cycle and becomes well drained. It is also subject to rapidly rising water level with the ensuing entrapment of air within the bed.

Cross-lamination characterises the sediments of cosets 2-5 and small bubbles (0.5mm diameter) occur parallel to the bedding in cosets 2 and 3.

Coset 2 shows evidence of extensive reworking of the sediments and several sets of cross-laminae are superimposed. The total thickness is between 5 and 12.5cm. Several tidal cycles are represented as shown by the development of multiple erosion surfaces and herringbone cross-stratification. The majority of structures presented in the set, however, have flood orientation.

The lower bounding surface of coset 3 is essentially planar and erosional in origin; the upper parts of flood- and ebb-orientated ripples have been truncated. The erosion surface is overlain by parallel thin laminae which overlap in the flood direction. These laminae are toeset deposits of climbing ripples of ripple-drift type (Jopling and Walker, 1968) with an angle of climb of approximately 10^{o}. The lower parts of foresets associated with the toesets can be seen in several cases (Fig. 3.38,A). Whether the ripples were of large or small-scale is not determinable. The individual laminae are 2-3mm thick and up to 25cm in length. The fact that the ripples were climbing

rather than simply migrating in the flow direction suggests that an abundant supply of sediment was available. It is also noticeable that the entrapment of air bubbles is restricted to the toeset laminae.

Coset 4 consists of several sets of small-scale cross-laminae with ebb-orientation. Total thickness is between 0 and 2.5cm. The lower bounding surface is non-parallel with the laminae of set 3 and is an erosional surface.

Coset 5, which is a megaripple in its own right, rests on the planed surface of coset 4 and consists of a wedge-shaped accumulation of foreset laminae which have tangential contact with well developed bottomset laminae. Foreset dip is approximately 34^{o}. The upper surface of the foresets is eroded and the last depositional structures are cross-laminae of linguoid small-scale ripples.

2. Significance

The important feature of this deposit is that although the area is covered by ebb-orientated megaripples at low-water, the majority of internal sedimentary structures within each megaripple have a flood orientation. The fact that only the last coset (5) has an ebb orientation (it is almost identical to the last coset of the flood sand-wave previously discussed) suggests that the bedforms within the interchannel areas, or ebb shields, change their orientation with each phase of the tide. At high-tide it seems likely that the flood-tidal delta is covered solely by flood-orientated structures, sand-waves in the channels and megaripples on the interchannel ridges or 'ebb shields'. During the ebb-tide the megaripples on the ebb shields are completely reversed in orientation, whereas in the channels the sand-waves are modified by the development of an ebb-megaripple, but not to such an extent that their flood-orientation is destroyed. The preservation of the sand-waves is due to the protection from ebb-currents offered by

the ebb shields. These topographically high features deflect ebb-currents around the flood-channels, thereby reducing the opportunity for extensive reworking of sediment. As previously stated, maximum ebb-current velocities in flood-channels are only half the magnitude of those of the flood-tide.

Bedform Migration

Introduction

The sand-waves of the northern flood-channel of the flood-tidal delta (Fig. 3.39) have been observed to migrate in a landward direction. In order to determine the rates of advance of these bed-forms and to obtain an estimate of the net amount of sediment deposit-ion in the flood sand-wave field, the movement of several sand-waves was monitored for periods of up to three months.

Method

Stakes were places at the base of the slip-faces of three sand-waves situated approximately 80m apart in the NE-SW direction. Sand-wave advance was recorded by measuring the distance from the stake to the base of the slip-face at time intervals which averaged seven days. Several other bedforms in a N-S traverse across the flood-tidal delta were monitored in a similar way.

Results

Sand-waves on the northern margin of the flood-channel migrated in a south-westerly direction over distances of 12.9 to 15.7m during the period 20 June 1974 to 5 September 1974 (Table 3.2). The total migration distance of individual bedforms within the zone decreased in the south-westerly direction, that is, in the direction of waning flood-tidal currents. If complicating factors, such as erosion by ebb-tidal currents and late-stage run-off, were neglected, the sand-waves might reasonably by expected to override each other in the south-

westerly direction. However, at the base of the lee-slope of each sand-wave is a shallow ephemeral drainage channel which serves to carry late-stage run-off in a direction parallel to the crest-line of the bedform. The bed over which the sand-wave eventually migrates is subject to considerable modification by the run-off which normally produces a decrease in the angle of inclination of the stoss-side of the adjacent downstream bedform.

The rate of bedform migration was found to vary with the lunar tidal cycle (Fig. 3.40). Significant migration occurred only during the periods of spring tides when the predicted tide heights at Leith were over 5m. Under such conditions sand-waves migrated over distances which averaged 0.20 to 0.34m per tidal cycle. During periods of neap and intermediate tides the rate of advance was only 0.01 to 0.06m per tidal cycle.

In the period up to 1 November 1974 the most easterly sand-wave migrated a distance of 24.0m, and the most westerly sand-wave a distance of 19.2m. To compensate for sediment being transported westwards, additional sediment must be introduced into the system from the Eden channel. The most important fact to emerge from this series of measurements was that there is a net deposition of sediment in a landward direction both in and on the margin of the northern flood-channel. The sand-wave field is intermittently migrating over intertidal sand-flats which are colonised by Arenicola marina. A stratigraphic sequence should develop in which fine sands with bioturbation structures (the Arenicola sand-flat) are overlain by several cosets of cross-laminae (the characteristic sand-wave internal structure). Between the two sand units may be an erosion surface produced by the run-off channel which invariably exists at the foot of the lee-slope of all sand-waves in the zone.

A migration of 19.2m by a sand-wave of height 0.30m and span 75m

Table 3.2. The record of bedform migration for three sand-waves showing the total migration distance, the amount of migration between successive sampling dates and the calculated rate of advance in metres per tidal cycle.

	Date	Total Distance m.	Increment m.	Rate m/tide
Red East	20. 6.74	-	-	-
	9. 7.74	2.29	2.29	0.06
	18. 7.74	3.29	1.00	0.06
	25. 7.74	8.00	4.71	0.34
	1. 8.74	8.30	0.30	0.02
	8. 8.74	9.14	0.84	0.06
	16. 8.74	12.00	2.86	0.18
	23. 8.74	13.90	1.90	0.14
	2. 9.74	14.10	0.20	0.01
	5. 9.74	15.70	1.60	0.27
	4.10.74	20.30	4.60	
	1.11.74	24.00	3.70	
No. 6	18. 7.74	-	-	-
	25. 7.74	5.80	5.80	0.41
	1. 8.74	5.90	0.10	0.01
	8. 8.74	6.40	0.50	0.04
	16. 8.74	7.00	0.60	0.04
	23. 8.74	11.50	4.50	0.32
	2. 9.74	12.70	1.20	0.06
	5. 9.74	14.10	1.40	0.23
	11. 9.74	14.80	0.70	0.03
Red West	20. 6.74	-	-	-
	9. 7.74	1.60	1.60	0.04
	18. 7.74	2.15	0.55	0.03
	25. 7.74	6.40	4.25	0.30
	1. 8.74	7.10	0.70	0.05
	8. 8.74	7.32	0.22	0.02
	16. 8.74	7.90	0.58	0.04
	23. 8.74	11.30	3.40	0.24
	2. 9.74	12.10	0.80	0.04
	5. 9.74	12.90	0.80	0.13
	11. 9.74	13.00	0.10	0.01
	4.10.74	16.70	3.70	
	1.11.74	19.20	2.50	

represents the deposition of approximately 580 tonnes of sediment. At the maximum rate of bedform advance (.41m/tide) some 316 kg/m of sediment are redeposited during each tide.

Conclusions on Bedforms and Sedimentary Structures of the Flood-Tidal Delta

1. There are two groups of large-scale bedforms:

   (a) megaripples of chord 1.1 to 6.0m,

   (b) sand-waves of chord 6.0 to 20.9m.

2. The lee-slope azimuths of large-scale bedforms show an almost diametrically opposed (bipolar) bimodal distribution. The general ebb-flow direction is slightly divergent from and to the north of the channel-controlled flood-flow direction.

3. There is a marked relationship between bedform orientation and chord length, whereby 87% of flood-orientated, large-scale bedforms are sand-waves and 89% of ebb-orientated, large-scale bedforms are megaripples.

4. The internal structure of sand-waves consists of a sequence of cosets each of three sets of strata. Each coset is bounded by a 'reactivation surface'. The sand-waves occur in trains which may be in- or out-of-phase. The overall structure resembles large-scale PI cross-stratification with numerous reactivation surfaces. The majority of preserved cross-sets have a flood orientation.

5. Megaripple internal structure is dominated by small-scale cross-stratification with flood orientation.

6. In the flood-tidal delta as a whole the preserved internal structures show a predominant flood orientation. This is at variance with the surface expression of the bedforms which

exhibit sub-equal numbers of flood- and ebb-orientated features. The internal structures illustrate the importance of flood-tidal currents in the formation of this sand-body and the secondary nature of the ebb-tidal currents which serve only to modify the surface features.

7. In the channels dominated by flood-tidal currents, sand-waves are migrating landwards, and an estimated 580 tonnes of sediment accumulated in the northern flood-channel between June and November 1974.

H

C1

E

C

D

B

A

F

Fig. 3.25a. The flood-tidal delta at the entrance to the Eden estuary.

Fig. 3.25a. The flood-tidal delta at the entrance to the Eden estuary.

A

F

A

Cl

B

C

D

E

H

Fig. 3.25b. Detail of vertical air photograph of the flood-tidal delta.

Fig. 3.25b. Detail of vertical air photograph of the flood-tidal delta.

(a)

(b)

Fig. 3.26a. The re-curved portion of Sanctuary Spit.
b. The composition of the re-curved portion of Sanctuary Spit: disarticulated valves of Cardium edule.

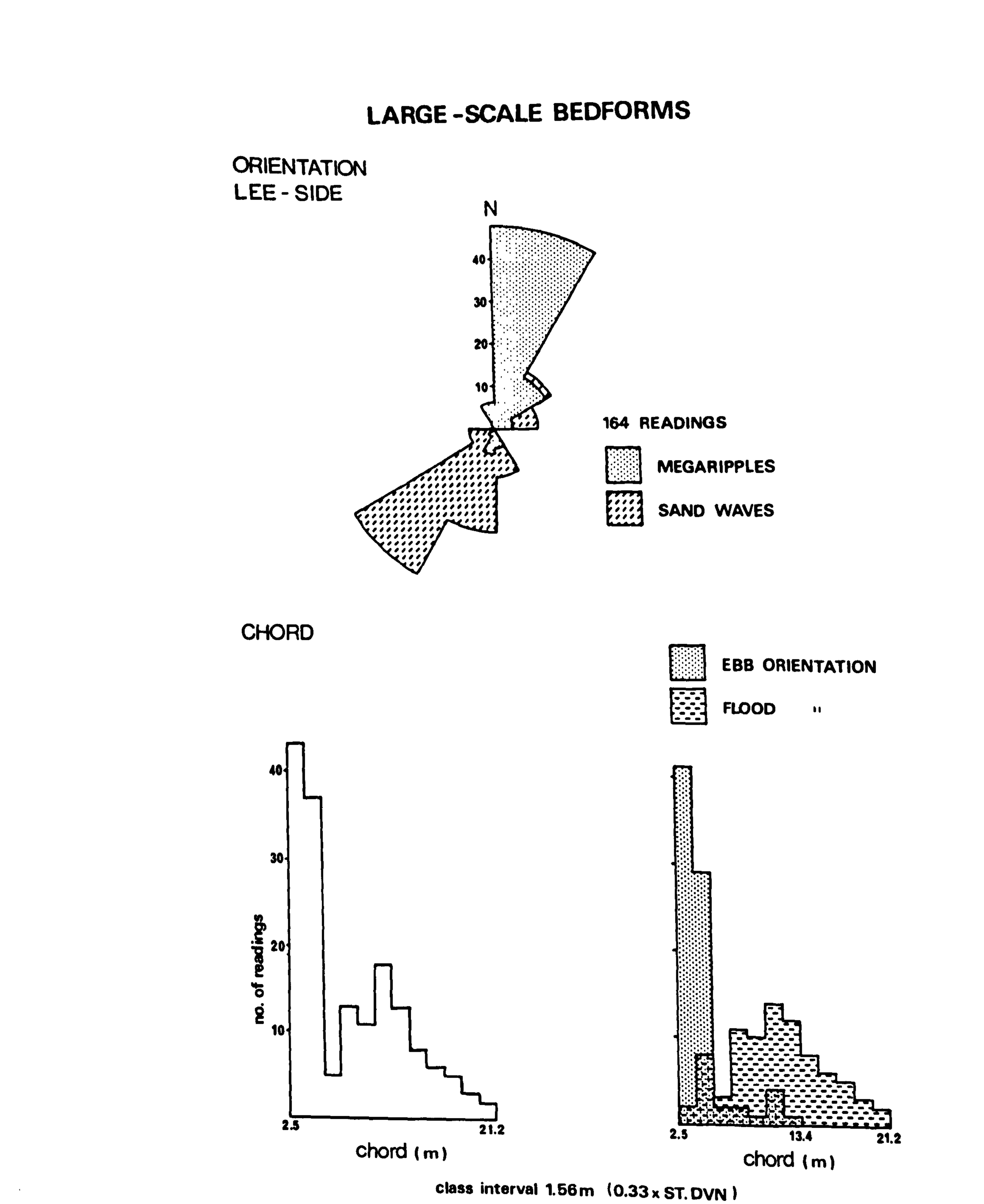

Fig. 3.27. Bedform chord and orientation data: Flood-tidal Delta.

Fig. 3.28. Flood-tidal delta: spurs and ripple fans associated with the lee-side of megaripples. Flow to left. Scale pen = 13cm.

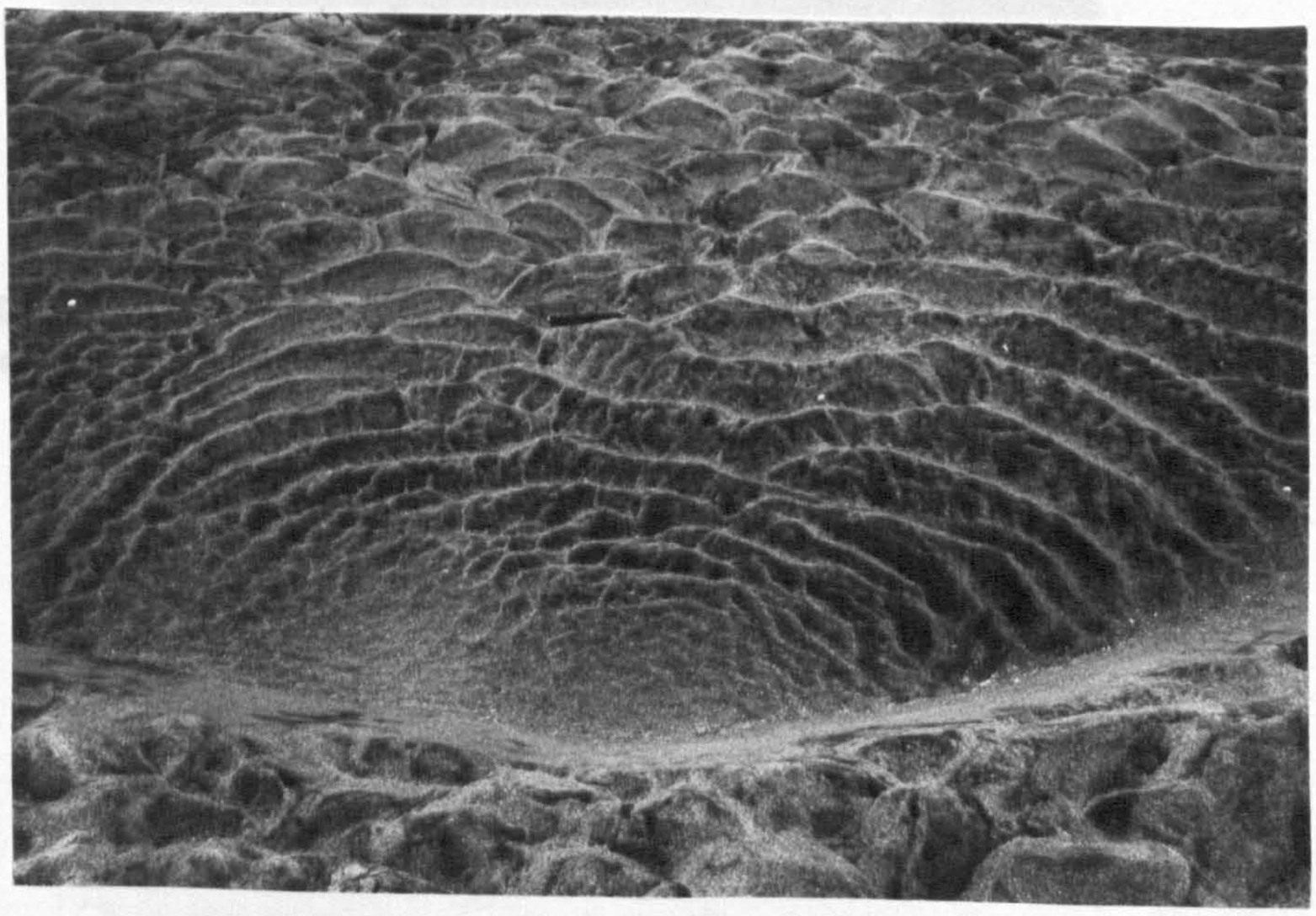

Fig. 3.29. Flood-tidal delta: symmetric ripple fan. Note the increase in chord length and the development of linguoid ripples in the flow direction. Flow to top of page. Scale pen = 13cm.

Fig. 3.30. The sand-wave on the crest of the South Ebb Shield with its associated megaripples.

Fig. 3.31. The ebb modification of a flood-orientated sand-wave in zone A (Fig. 3.25a). Flood flow direction to right. Note the ebb-orientated megaripple on the crest of the sand-wave and falling water-level marks on the lee-slope (bottom right).

Fig. 3.32. Extensive ebb-modification of a flood-orientated sand-wave. Large 'scours' with minor ripple fans develop in the lee of the ebb-megaripple. The scours are probably interspur troughs. Ebb-flow to left.

Fig. 3.33. An ebb-orientated sand-wave which illustrates several features produced by late-stage flow: (a) small-scale ripples on the lee-slope of the sand-wave which strike perpendicular to the crest of the sand-wave, (b) falling water-level impressions on the lee-slope of the sand-wave. Scale-bar: 0.5m.

Fig. 3.33a. A micro-delta prograding to the right and in-filling an interspur trough in the lee of a megaripple (zone C, Fig. 3.25a).

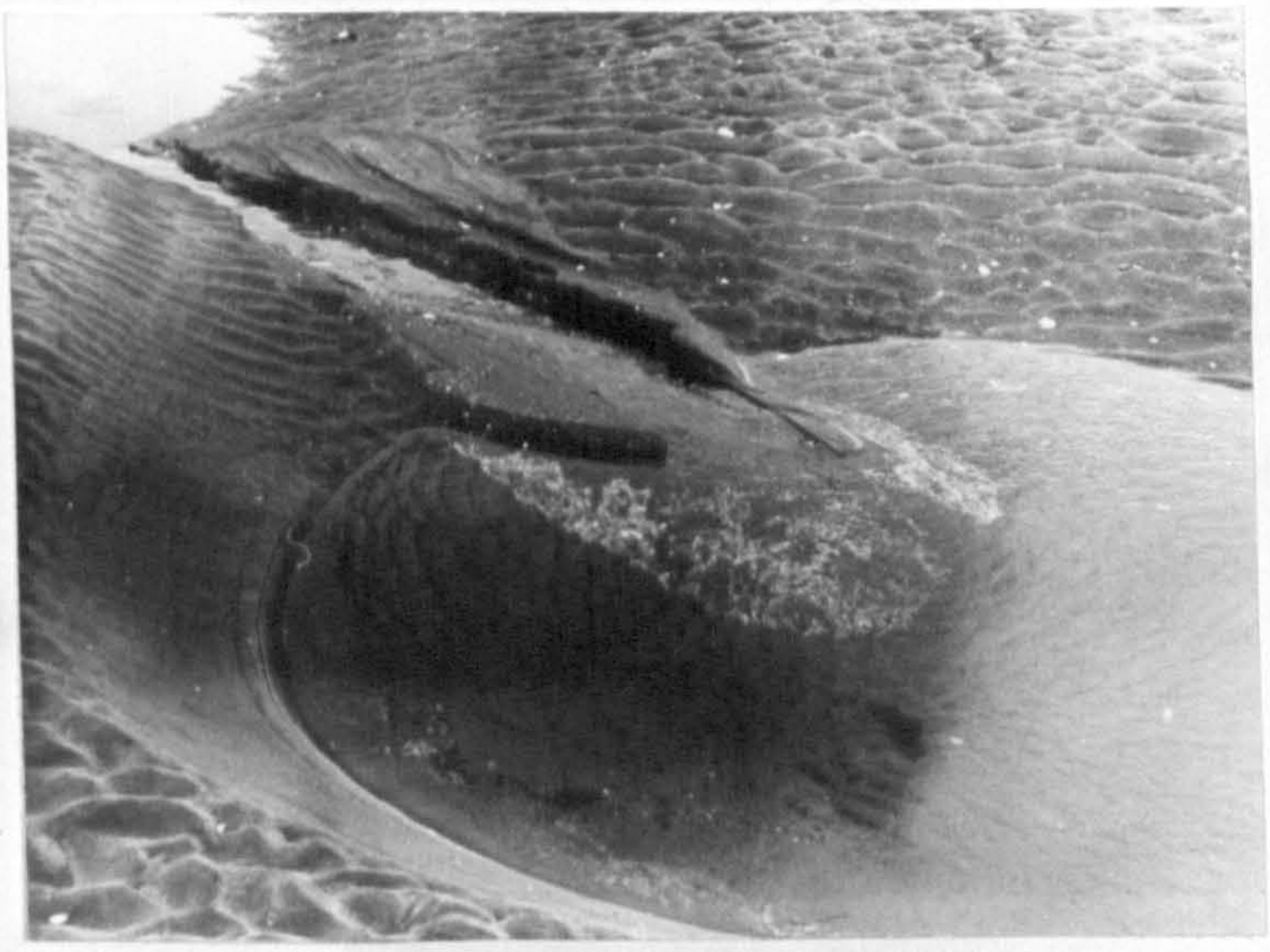

Fig. 3.33b. A lobate micro-delta prograding to the right. Note the presence of levees on the delta top and detrital carbonate on the slip face. Two ripple fans are superimposed in the trough, one due to ebb-tidal currents passing over the sand-wave and the second due to flow over the micro-delta.

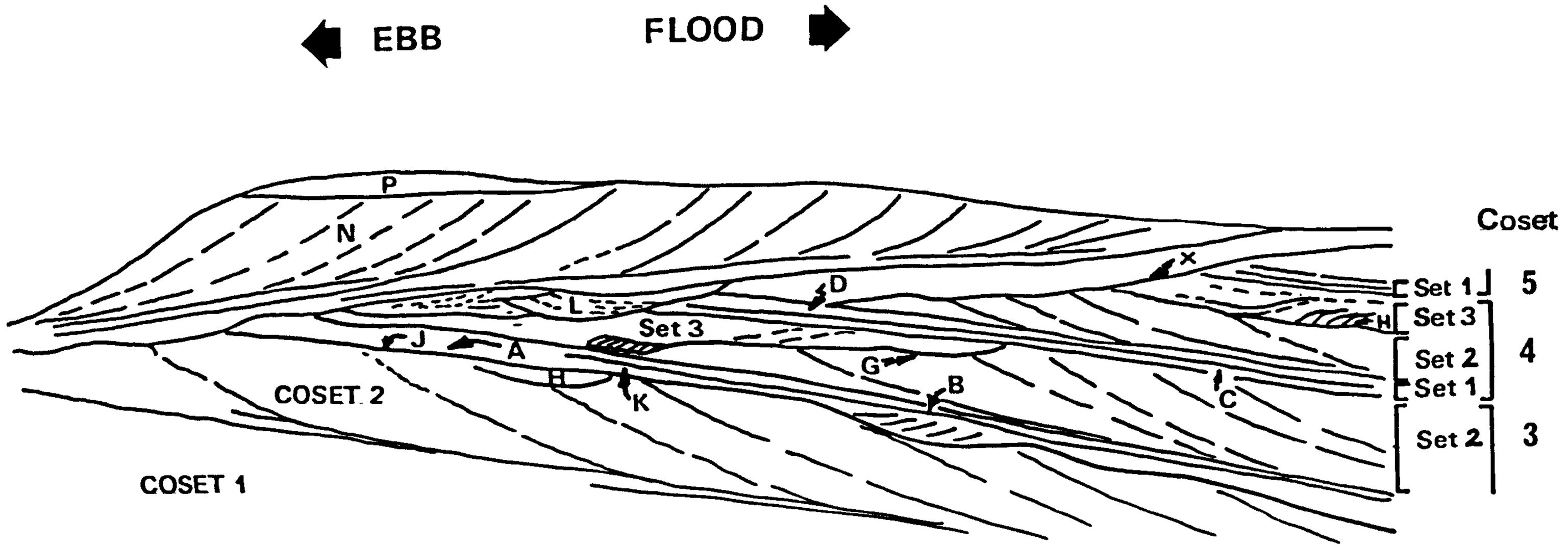
EBB
FLOOD
P
N
L
D
X
J
A
Set 3
H
G
B
K
C
COSET 2
COSET 1
Coset
Set 1
5
Set 3
Set 2
4
Set 1
Set 2
3

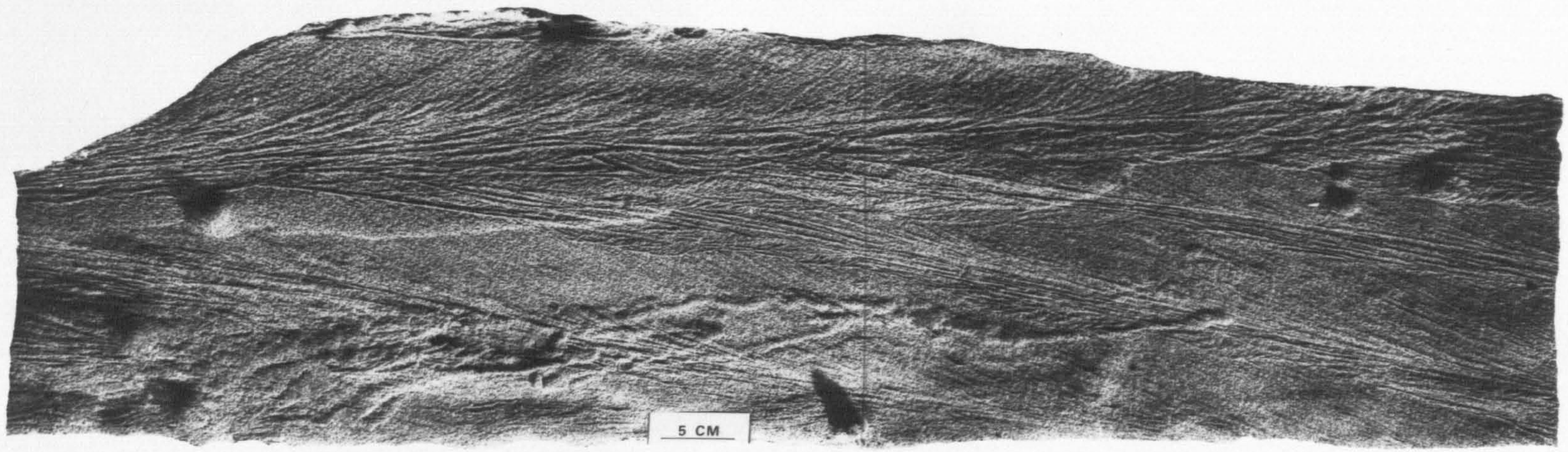

Fig. 3.34. Epoxy resin peel of the internal sedimentary structures of the crestal region of a sand-wave from the northern flood zone of the flood-tidal delta. The peel was orientated parallel to the flow direction.

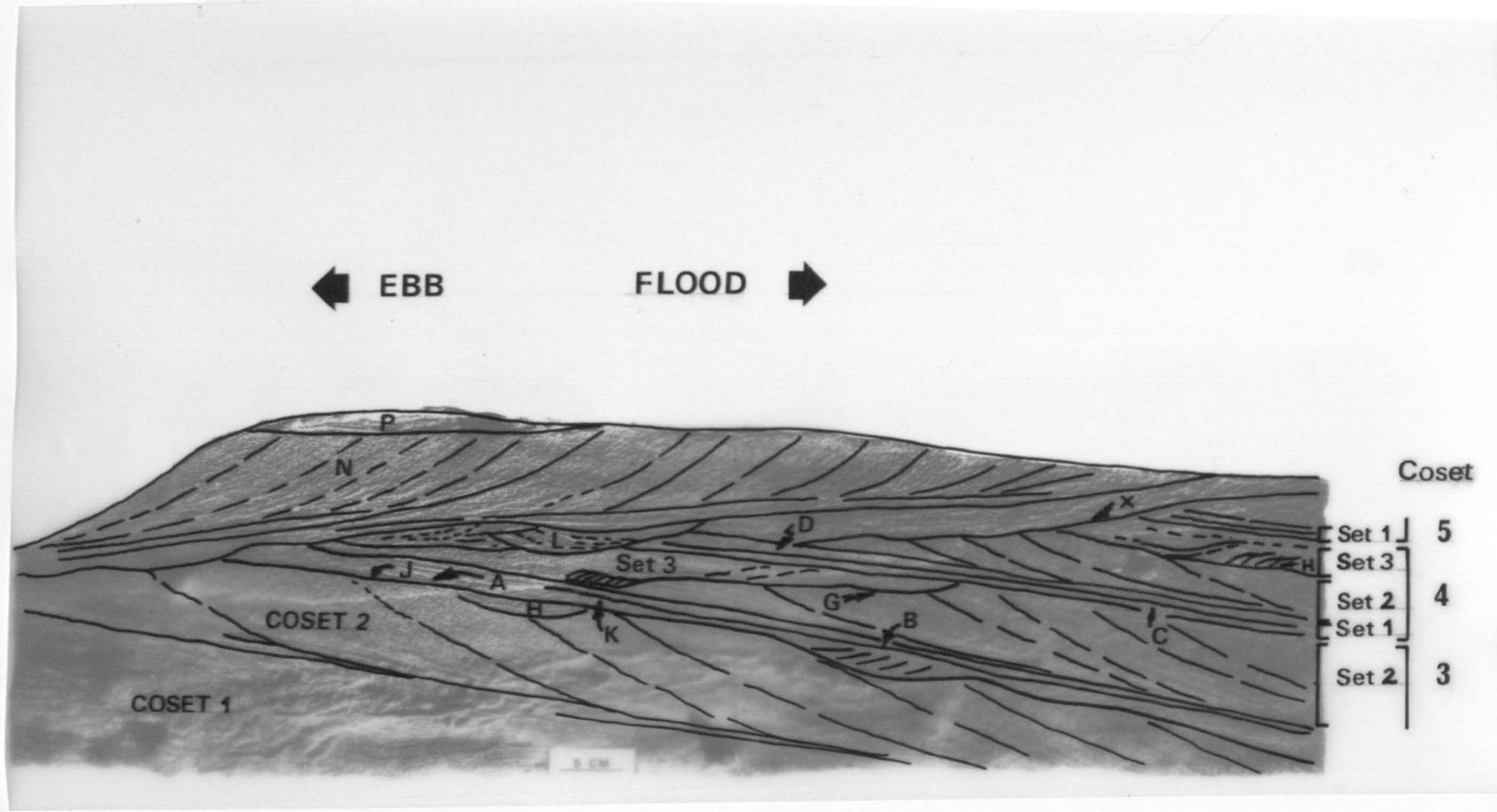

Fig. 3.34. Epoxy resin peel of the internal sedimentary structures of the crestal region of a sand-wave from the northern flood zone of the flood-tidal delta. The peel was orientated parallel to the flow direction.

S

N

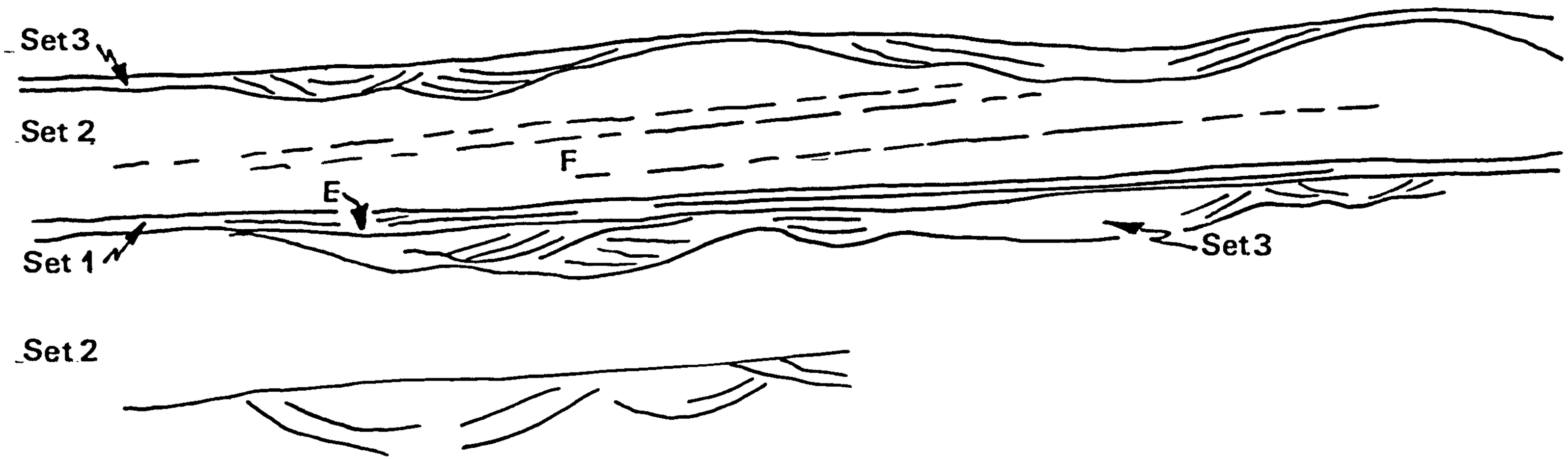

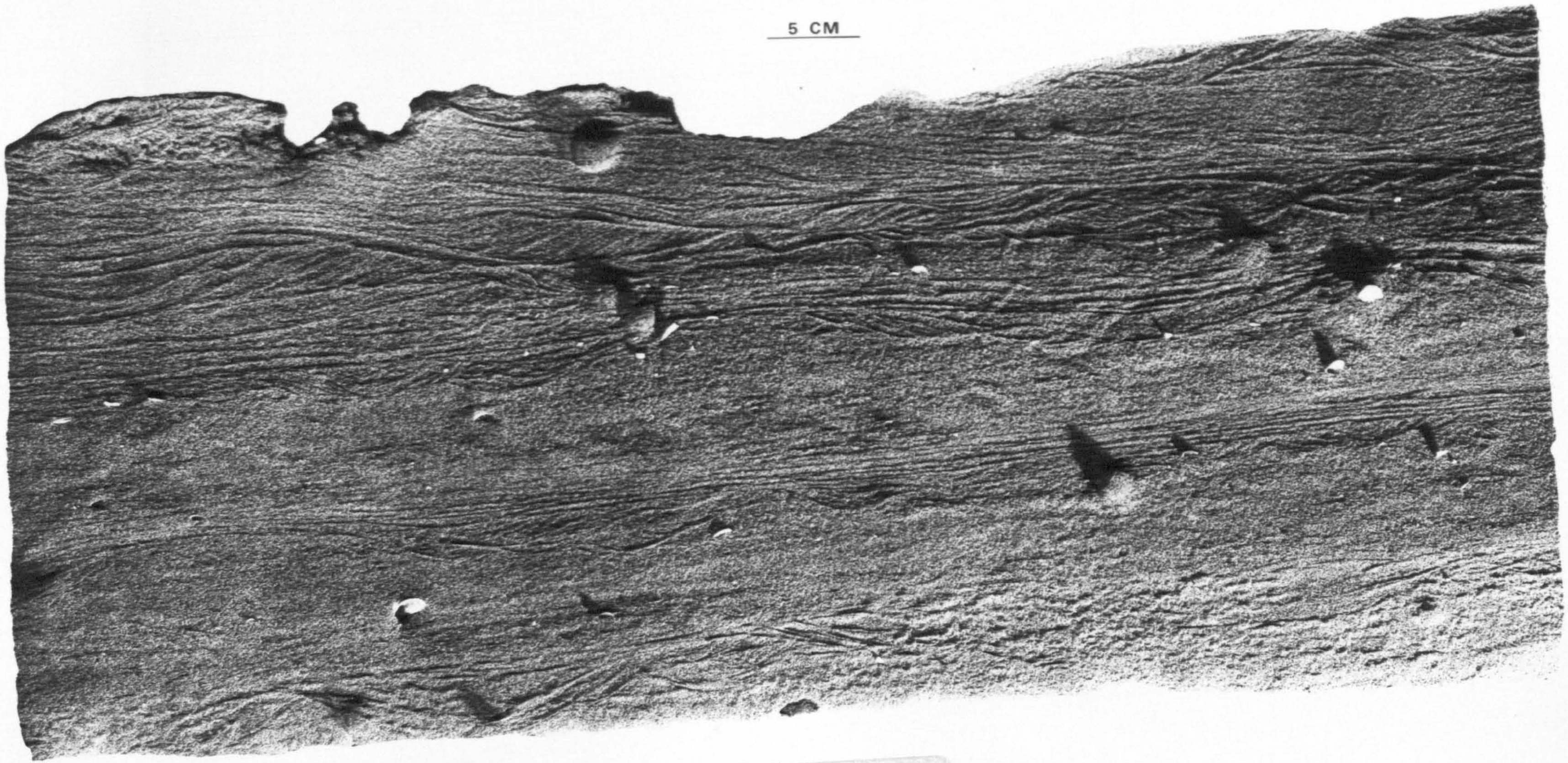

Fig. 3.35. Epoxy resin peel, perpendicular to flow direction, of structures in the same sand-wave as in Fig. 3.34.

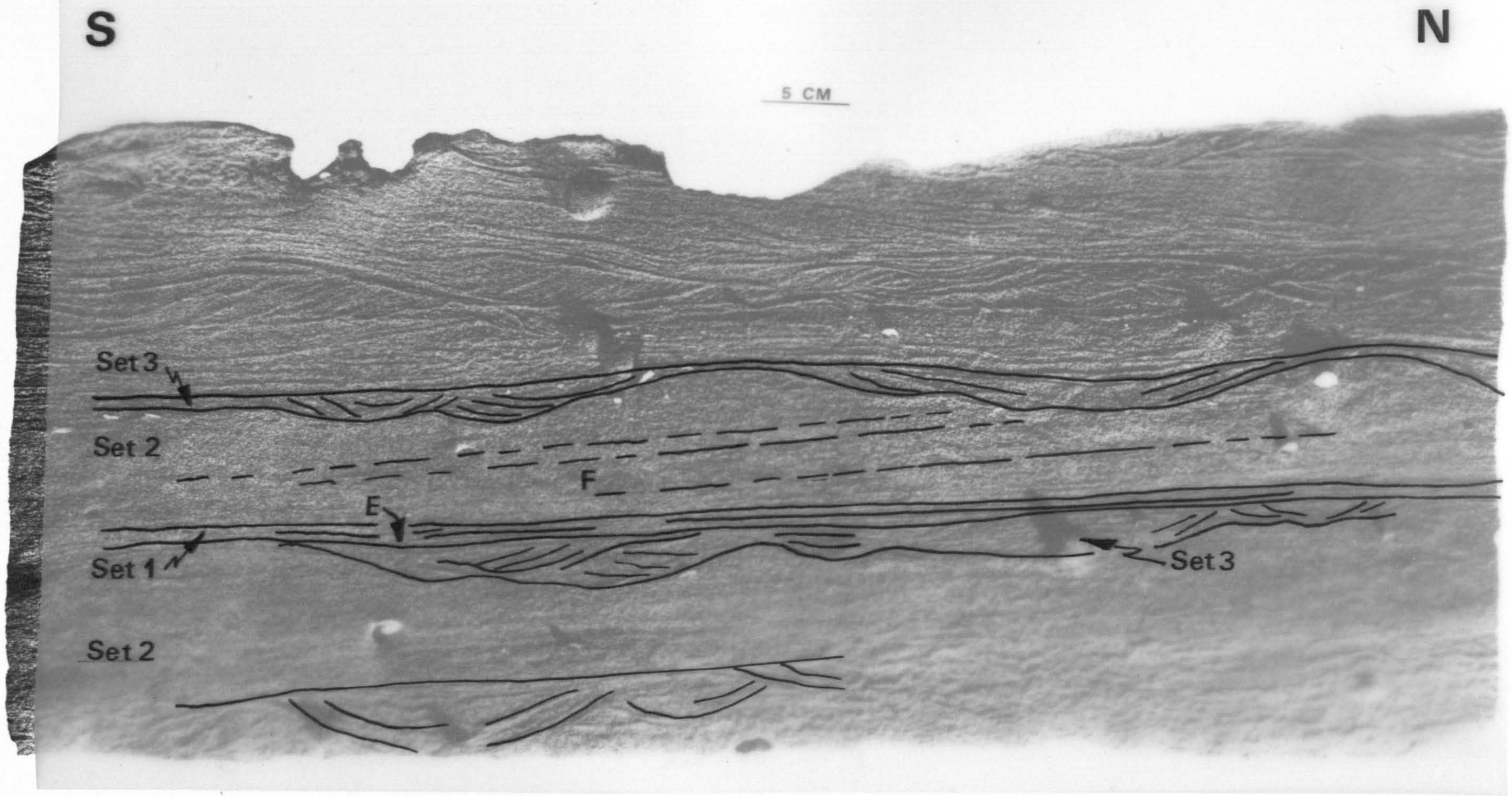

Fig. 3.35. Epoxy resin peel, perpendicular to flow direction, of structures in the same sand-wave as in Fig. 3.34.

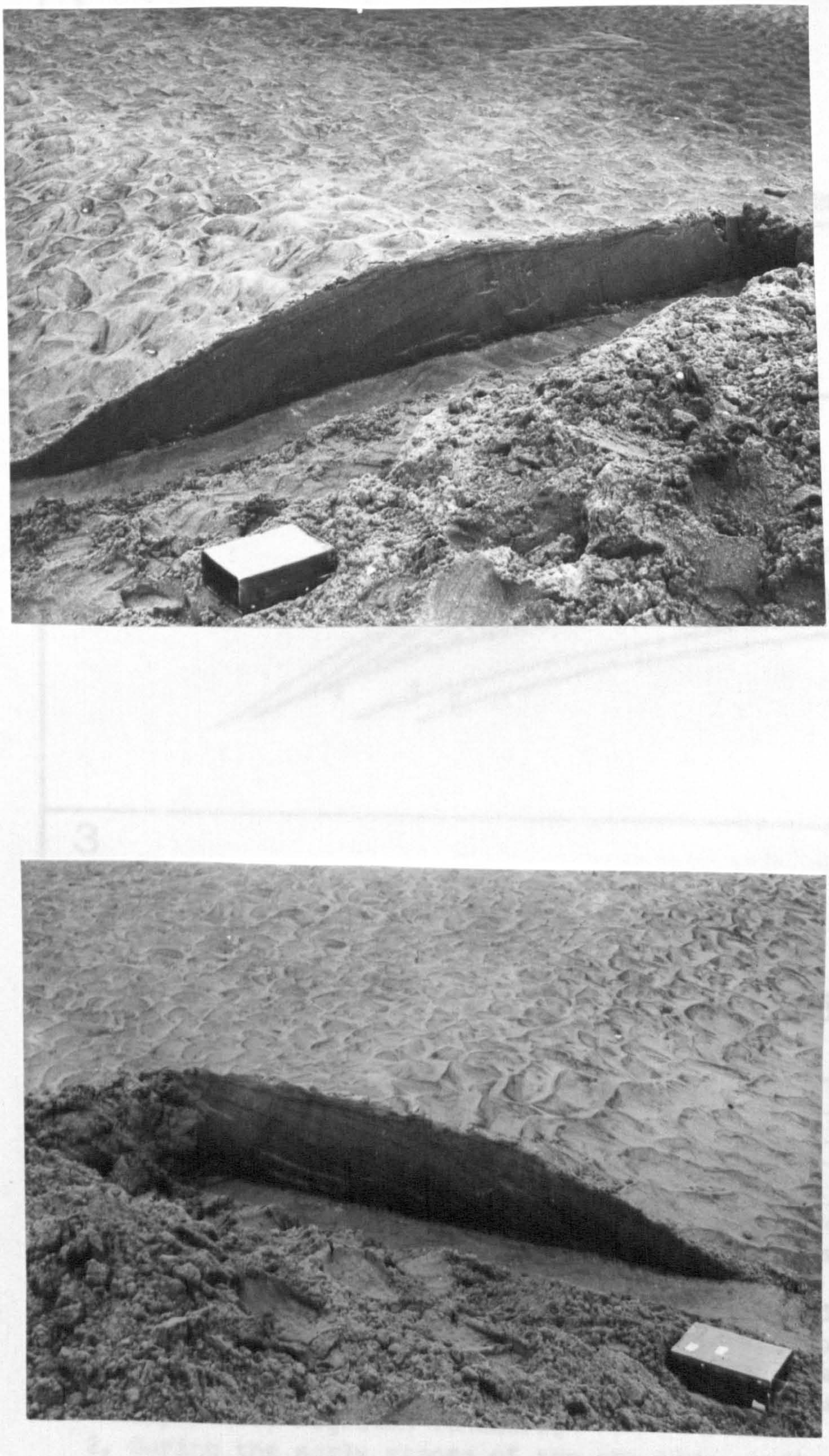

Fig. 3.36. Trenches in the crestal regions of sand-waves showing the parallelism of the free surface and the internal reactivation surfaces.

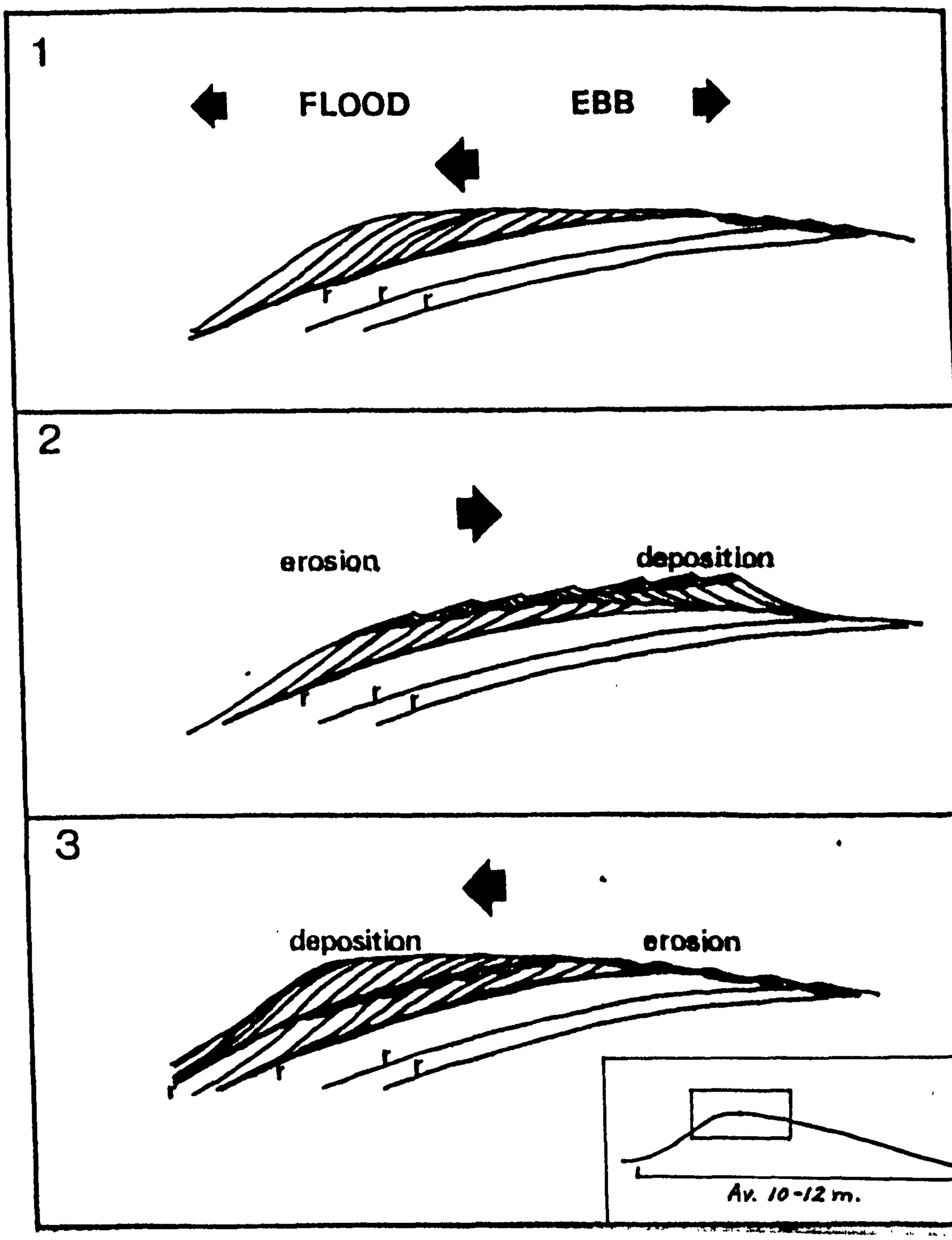

Fig. 3.37. A schematic representation of the formation of sand-wave internal sedimentary structures. Crestal area only, see insert.

1. During the flood tide a megaripple forms on the crestal region of the sand-wave. The whole sand-wave structure apparently migrates landward.
2. During the early stages of the ebb tide, sediment is eroded from the upper part of the flood-orientated megaripple and redeposited, in the form of an ebb-orientated megaripple, seaward of the crest of the sand-wave. The erosion on the upper stoss-slope creates a 'reactivation surface' semi-parallel to previous ones (r).
3. A subsequent flood tide removes the ebb megaripple and deposits a new flood-orientated megaripple.

Sediment deposited during the flood phase exceeds that eroded during the ebb.

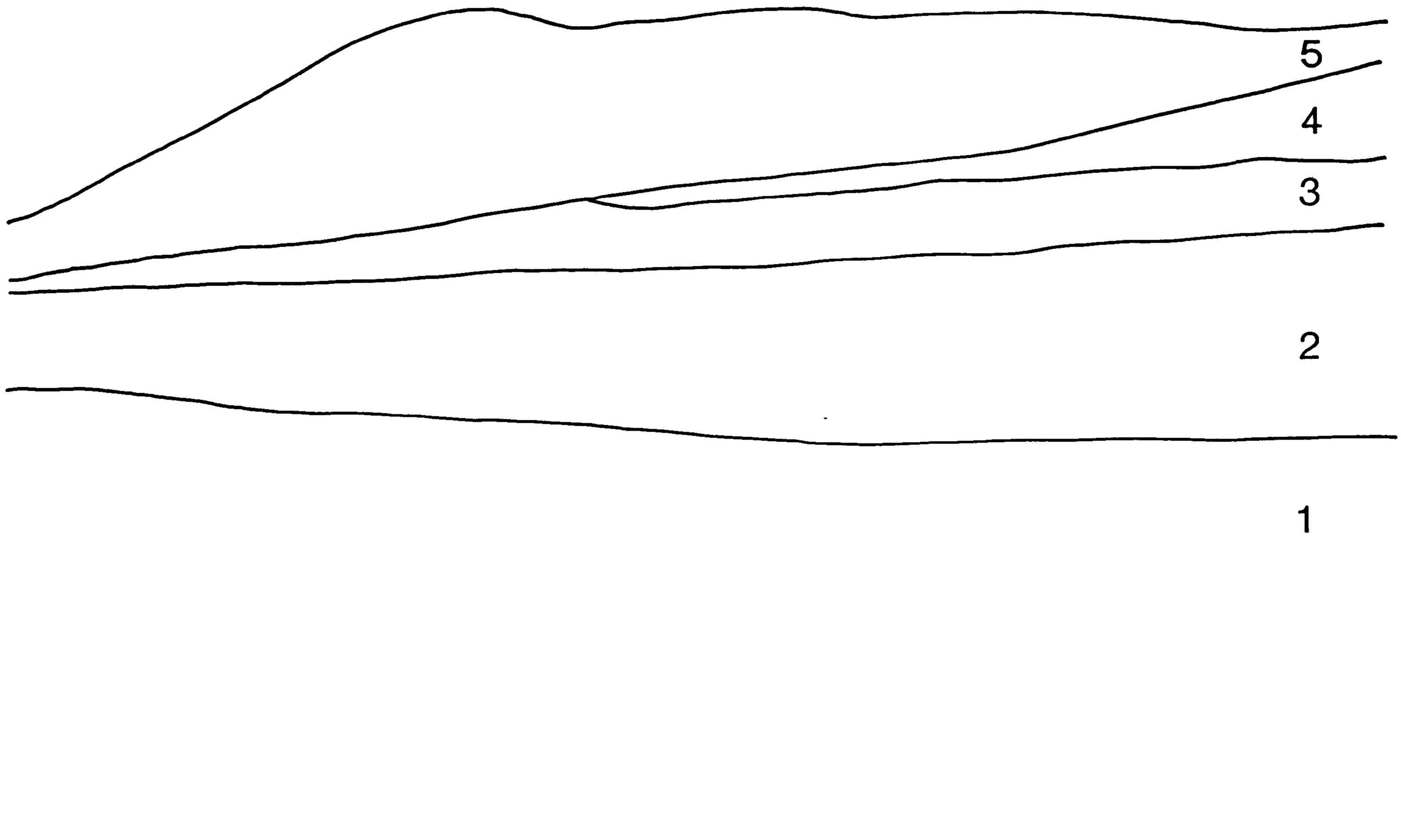
5
4
3
2
1

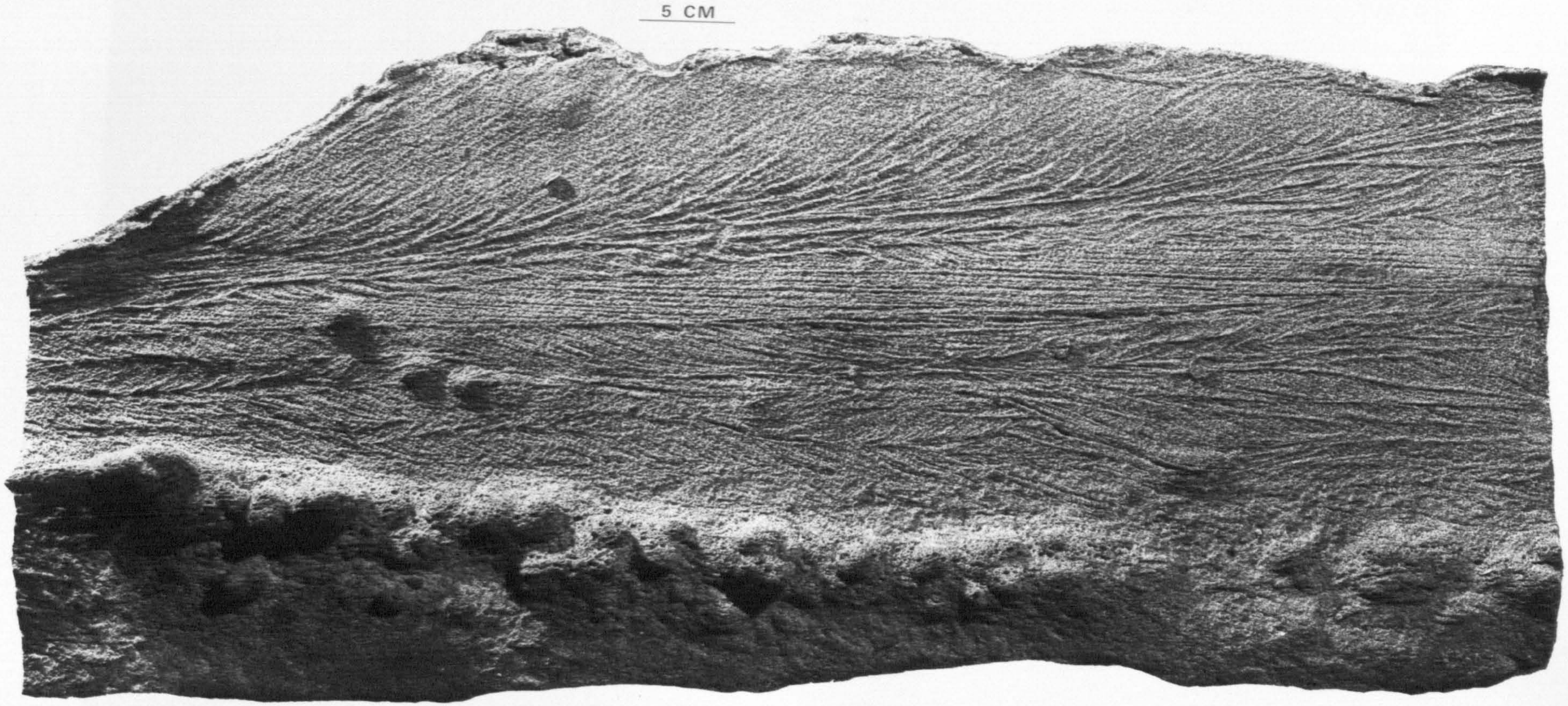

Fig. 3.38. Epoxy resin peel of internal sedimentary structures associated with the ebb-orientated megaripples of the northern ebb-shield. Ebb flow to left.

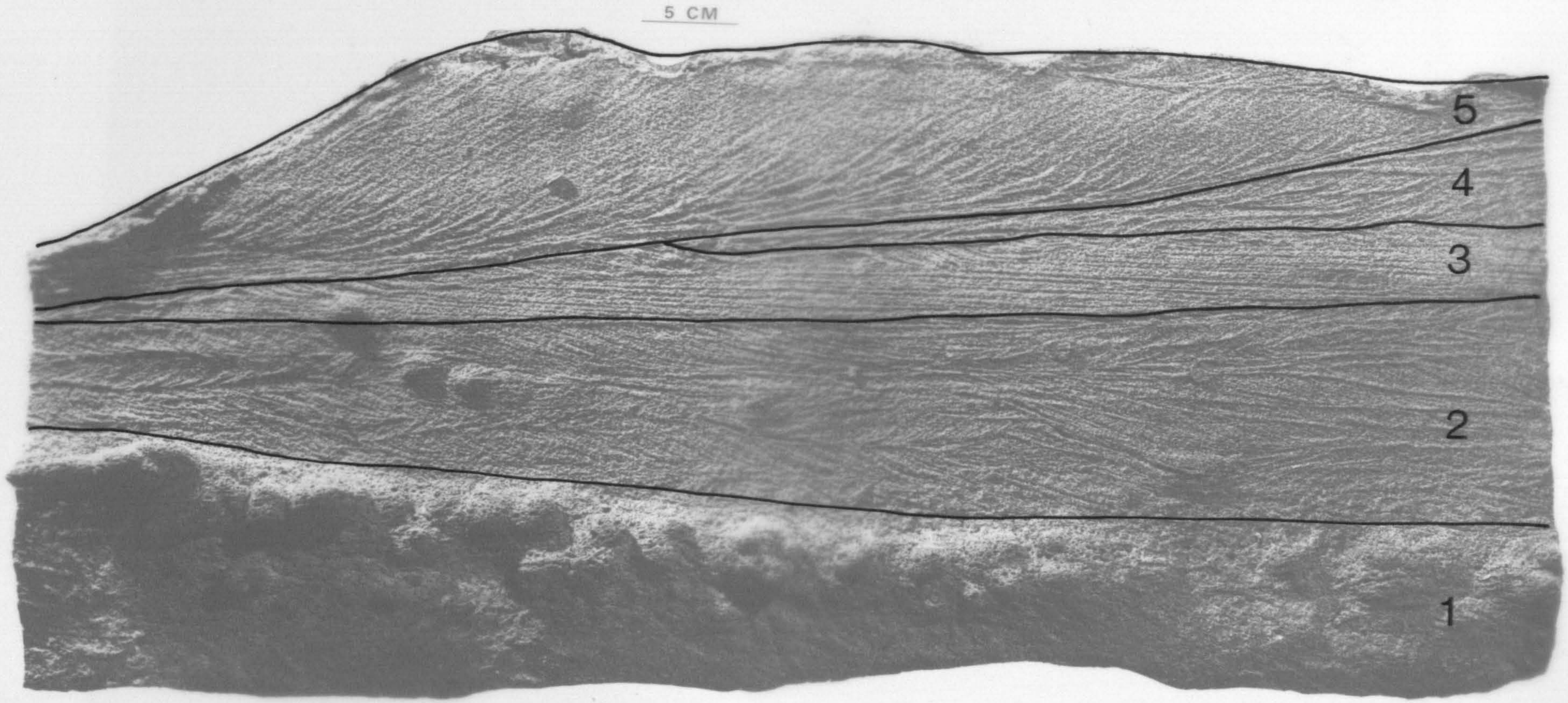

Fig. 3.38. Epoxy resin peel of internal sedimentary structures associated with the ebb-orientated megaripples of the northern ebb-shield. Ebb flow to left.

Fig. 3.39. Locations of the three sand-waves used for bed-form migration studies.
1. Red East
2. Number 6
3. Red West.

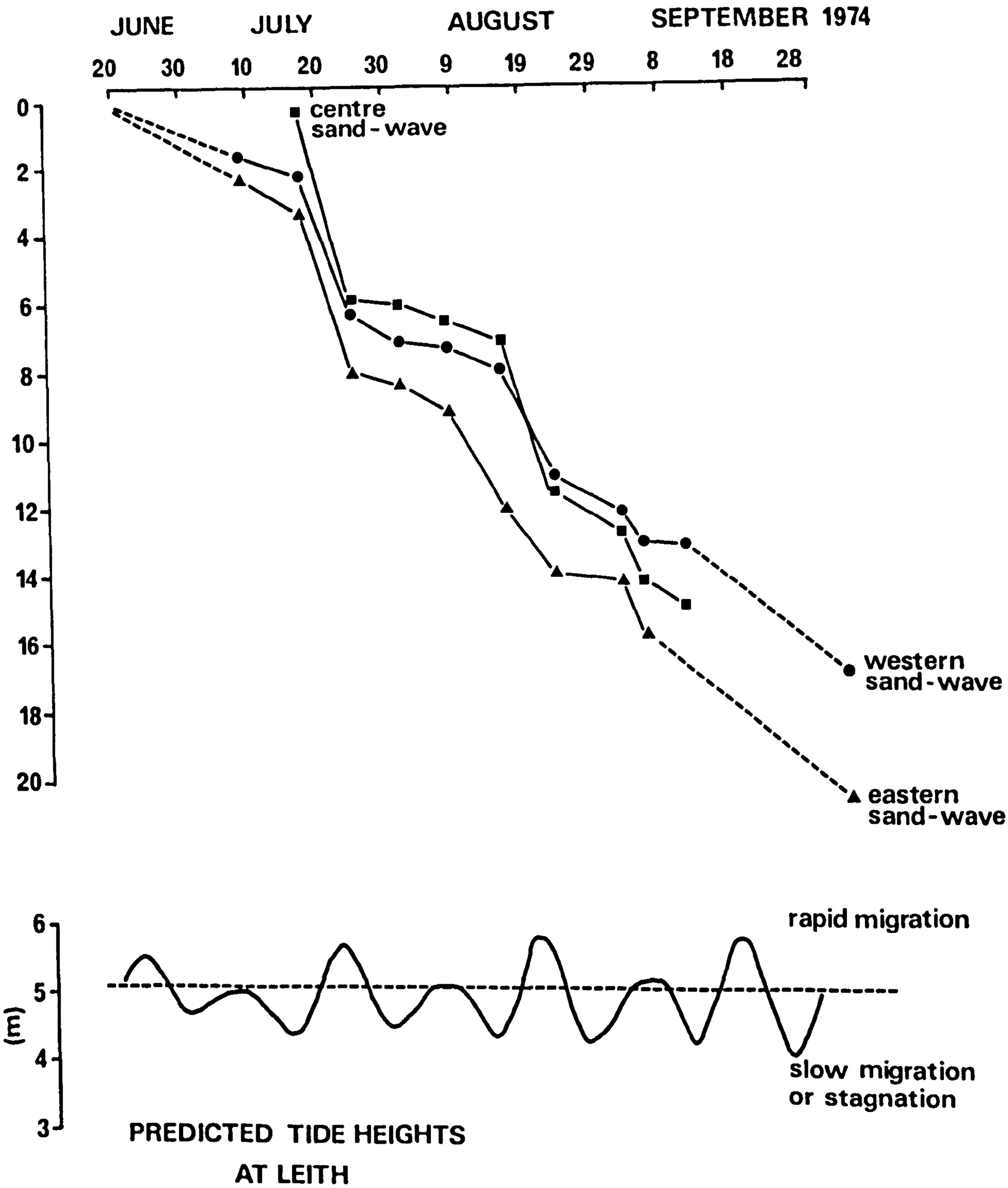

Fig. 3.40. The nett migration distances of sand-waves with respect to time. Note the correlation between periods of rapid advance and the occurrence of spring tides in a predicted tide height of more than 5m at Leith.

V. THE EBB-TIDAL DELTA

Sediment deposition seaward of the tidal inlet at the mouth of the River Eden has resulted in the accumulation of a large sand-body which is exposed periodically under spring-tidal conditions (Fig. 3.41).

Terminology

The structure has been termed an 'ebb-tidal delta' rather than a 'river mouth bar', because ebb-tidal flow is the dominant formative process and the discharge of the River Eden is probably insignificant in its formation. The delta does, however, block the path of the Eden channel at low-water, and a subsidiary channel or distributary carries late-stage ebb-flow in a south-easterly direction into St. Andrews Bay.

Hayes et al. (1971) proposed that ebb-tidal deltas consist of five major components:

1. a major ebb channel,
2. channel margin linear bars,
3. a terminal lobe,
4. marginal flood-channels,
5. swash bars.

Channel margin linear bars are the result of interaction between ebb-currents and waves; swash bars are wave produced; the ebb channel and terminal lobe are maintained by ebb-currents and the marginal flood-channels by flood currents. Several of these features are recognisable in the structure at the mouth of the River Eden (Fig. 3.41).

Sand-Body Geometry

In plan the ebb-tidal delta has a convex easterly facing base with a N-S dimension of approximately 1.5km. Marginal flood- and ebb-channels, which converge westwards, form the north and south boundaries

of the structure. The westerly limit is considered to be at the tidal inlet between the topographically high features of the spit-platform and the beach bar some 1.1km west of the crest-line of the terminal lobe. The northward extension of the delta has an acute termination whereas to the south the crest-line curves gradually to the south and west.

In profile the delta shape appears to vary with the lunar tidal cycle. During the periods of neap tides the delta consists of a landward portion which rises gradually eastwards from the tidal inlet, a broad, flat crestal platform and a seaward portion which dips more steeply than the landward one. Under spring tidal conditions the structure may become strongly asymmetrical with a very well defined crest-line.

Historical Development

Air photographs taken in April 1948 show that the ebb-tidal delta had a rather different configuration than at present, especially with respect to the position of the Eden channel (Fig. 3.42). The Eden channel shoaled as the delta was approached, but contact with the water of St. Andrews Bay was maintained by a very narrow channel cut through the crest of the delta. The narrow channel was gently arcuate in plan and skewed to the south-east. It also shoaled to both landward and seaward. The turning of the channel to the south-east, which may have been a function of the interaction of ebb-tidal currents from the inlet, and waves approaching from the NE, resulted in a seaward offset of the shoreface to the north of the channel.

Bedforms

The landward or stoss-side of the delta, with respect to ebb currents, bears a series of large-scale, ebb-orientated bedforms (Figs. 3.43, a and b). Chord lengths and orientations measured in two traverses

across the delta on 21 August 1974 are shown in Figure 3.44.

All bedforms had chords greater than 4m, and the maximum measured chord was 24m. Air photographs show that bedforms with chords of up to 50m were present on the northern margin of the Eden channel (Fig. 3.45).

The bedforms occur in a lobate zone on the stoss-side of the delta around the terminal point of the channel. Three east-west zones are recognised, each of which is characterised by an association of bedforms.

The northern zone (N) (Fig. 3.45) contains bedforms which are straight to slightly sinuous in plan in the west and which become more sinuous to the east. Bedform chord also decreases in an easterly direction.

The central zone (C), in direct line with the Eden channel, contains numerous bedforms which are mainly sinuous to catenary in plan. The majority have chords of less than 10m. The echo-sounder trace (Fig. 3.4) shows the ebb-orientated bedforms on a longitudinal profile of the stoss-side of the delta.

The southern zone (S) shows bedforms which increase in chord to the east and at the same time develop more irregular and out-of-phase crest-lines.

The deposition of sediment and the orientation of bedforms on the stoss-side of the ebb-tidal delta are directly related to the divergence of flow which occurs when the ebb-tidal current leave the confines of the tidal inlet. The divergence of bedform orientation becomes noticeable as the crest-line of the delta is approached and measured lee—slope azimuths ranged from 030° to 120°. The majority were however centrally situated with orientations of 060° to 090°.

Geometrical relationships between inlet width and depth, distance from the inlet to the first bar, and flow divergence based on modified

jet theory (Bates, 1953) have been expressed by Price (1963) for a variety of natural tidal passageways including tidal inlets and estuary mouths. In the case of the entrance to the Eden estuary the tidal-inlet width to depth ratio is approximately 30:1, and at low-water at the time of an equinoxial spring tide the crest-line of the delta was 1400m east of the inlet - a distance equal to 9.3 inlet-widths. The angle of flow-divergence based on the distribution of bedforms was 33^{o}.

beach
bar

marginal flood
channel

terminal lobe

ebb channel

marginal flood channel

beach bars

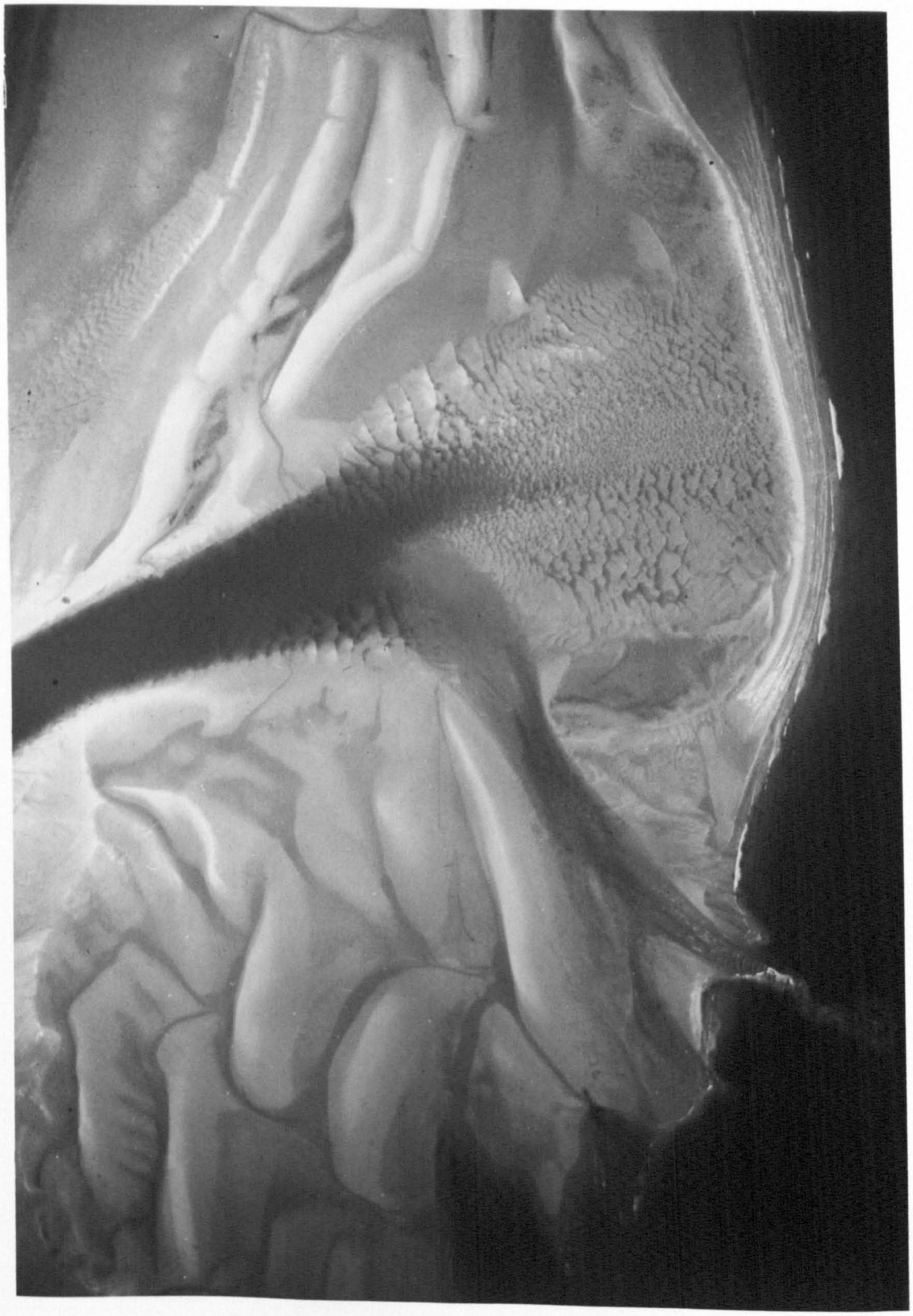

Fig. 3.41. The ebb-tidal delta (August 1974).

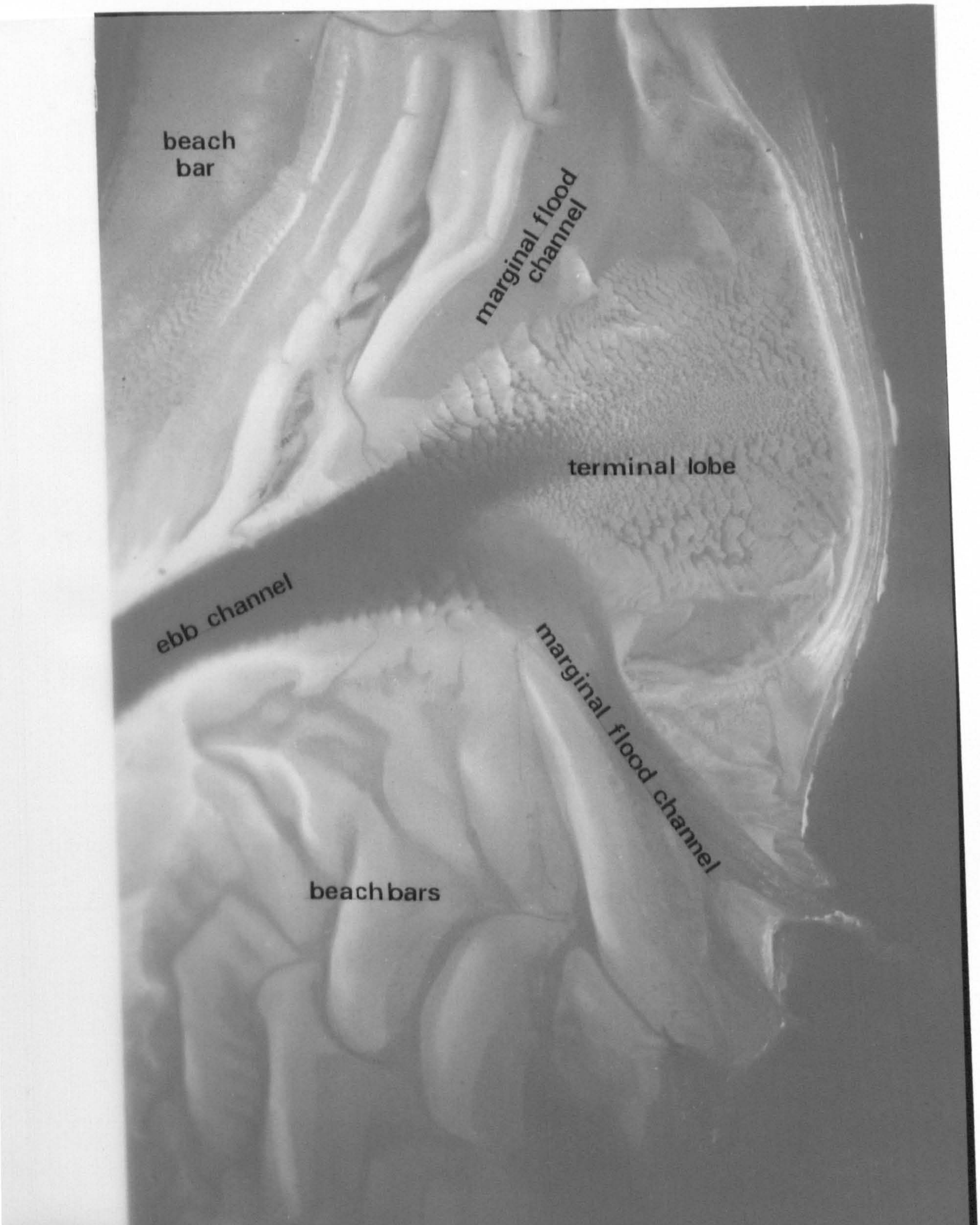

Fig. 3.41. The ebb-tidal delta (August 1974).

Fig. 3.42. The ebb-tidal delta, 1948.

(a)

(b)

Fig. 3.43. Ebb-orientated sand-waves from the stoss-side of the ebb-tidal delta.

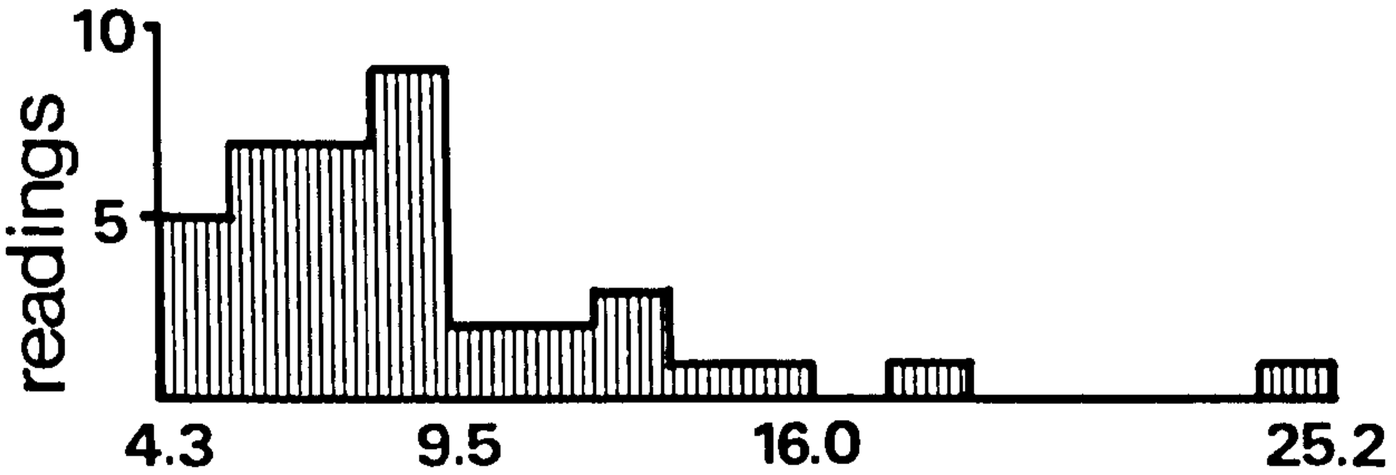

Mean 9.02 m
S.Dvn. 3.91 m

interval 1.3m (0.33 x S.Dvn)

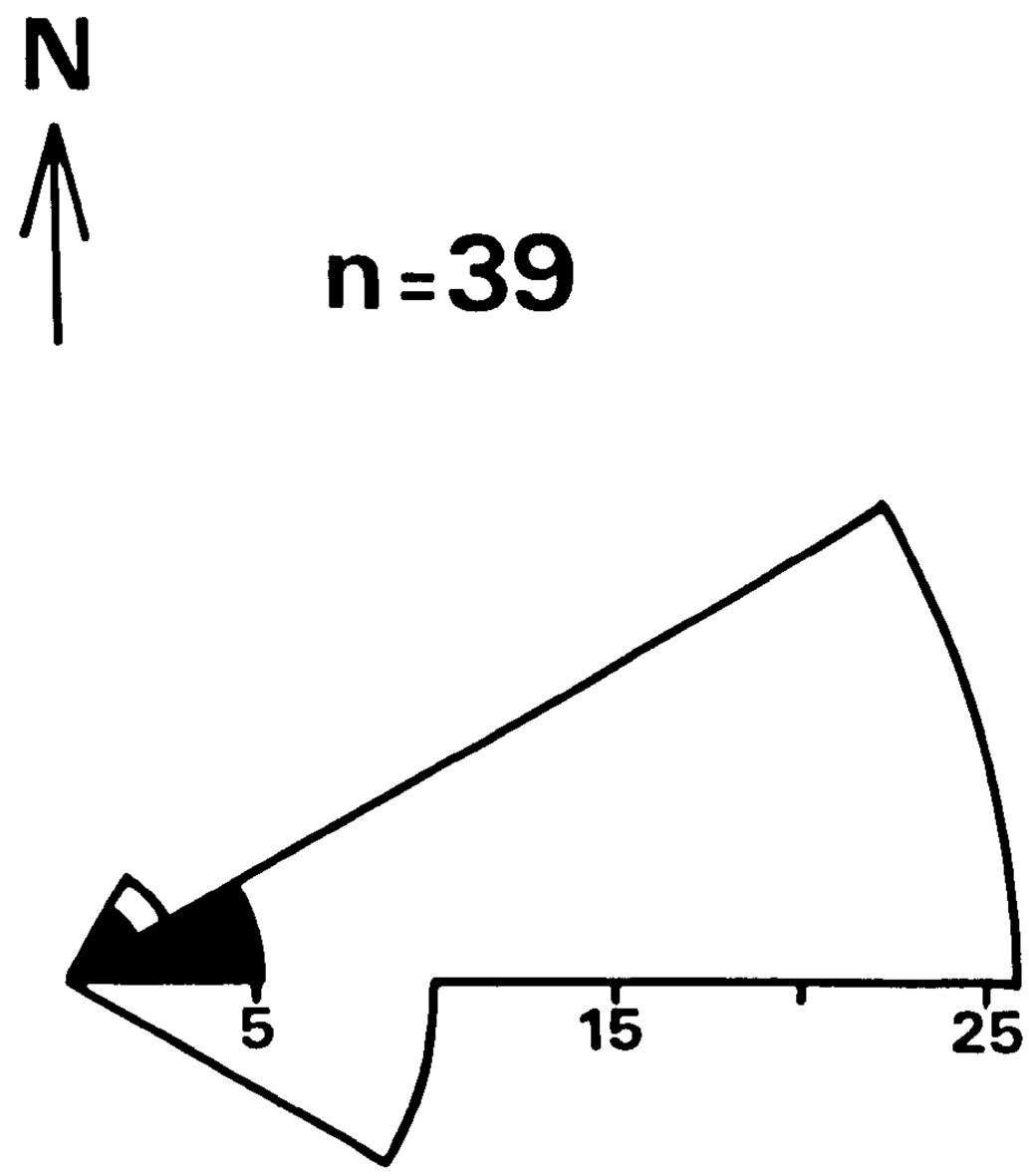

sand-waves

megaripples

Fig. 3.44. Bedform chord and orientation data - Ebb-tidal Delta.

Fig. 3.45. Bedform distribution on the stoss-side of the ebb-tidal delta. The arrow indicates ebb-orientated sand-waves of chord ±50m.

?N C,S - what?

V. BEACHES

The West Sands of St. Andrews and Tentsmuir Beach were considered to be out of the scope of this study. Attention was given only to those areas of the beaches which formed the tract of sand betueen Out Head and the flood-tidal delta in the west and the ebb-tidal delta in the east.

Tuo major topographic structures occur in this zone - a beach-bar and spit-platform which respectively lie to the north and south of the Eden channel (Fig. 3.46). The two structures were probably part of a single feature prior to 1948 (see Chapter 1,IV). The southern structure is a spit-platform (Meistrell, 1966) which is maintained and built up by wave and tidal current activity (see Chapter 2, page 35: Wave Induced Flou Patterns). During the period when sediment samples were collected on the West Sands, the eastern margin of the spit-platform was relatively abrupt and a change in bed elevation of 1.3m occurred over a horizontal distance of 5m. The northern structure is a broad N-S trending beach-bar which lies between two channels. The western channel is a relict of the 1919 Eden channel, and the eastern one an active channel used by flood-tidal currents. Flood-orientated large-scale bedforms are frequently generated on the eastern side of the beach-bar (Fig. 3.41).

The tract of sand to the south of the Eden channel between the spit-platform and the ebb-tidal delta supports large-scale beach-bars with flood asymmetry (Fig. 3.41). Measurements, from the air photograph, indicate that beach-bar chords may be up to 250m and spans 500m.

Fig. 3.46. Topographic features of the beaches at the entrance to the Eden estuary.
1. Spit platform
2. Beach-bar of South Tentsmuir
3. Beach-bars on the West Sands.

Chapter 4 THE SEDIMENTS

I. SAMPLE COLLECTION

One hundred and forty sediment samples were collected from the intertidal flats of the Eden estuary, seventeen from the channel of the River Eden and five from the sand-dunes at Out Head (Fig. 4.1). The sampling plan was based on the Ordnance Survey National Grid, and samples were collected at 400m intervals in N-S traverses with an E-W spacing of 200m. Twenty-eight of the 140 intertidal flat samples were off-grid from the areas of the flood- and ebb-tidal deltas.

At grid points where the bed was flat samples consisted of the uppermost one centimetre of sediment collected from an area of 625cm^2. In rippled areas the whole ripple, including the trough, was sampled. In megaripple and sand-wave zones a sample was scraped from the whole surface area of a section cut perpendicular to the crest-line of the bedform. Channel samples were collected at low-water by means of a van Veen grab and a Senckenberg-type box-corer (Bouma, 1969). Neither instrument was found to be very efficient, as fine-grained sediment was able to escape from the sample as it was raised to the surface.

At each sample location the sediment-type was identified and the bedforms described and measured with respect to the indices given by Allen (1968). Biogenic features were also noted.

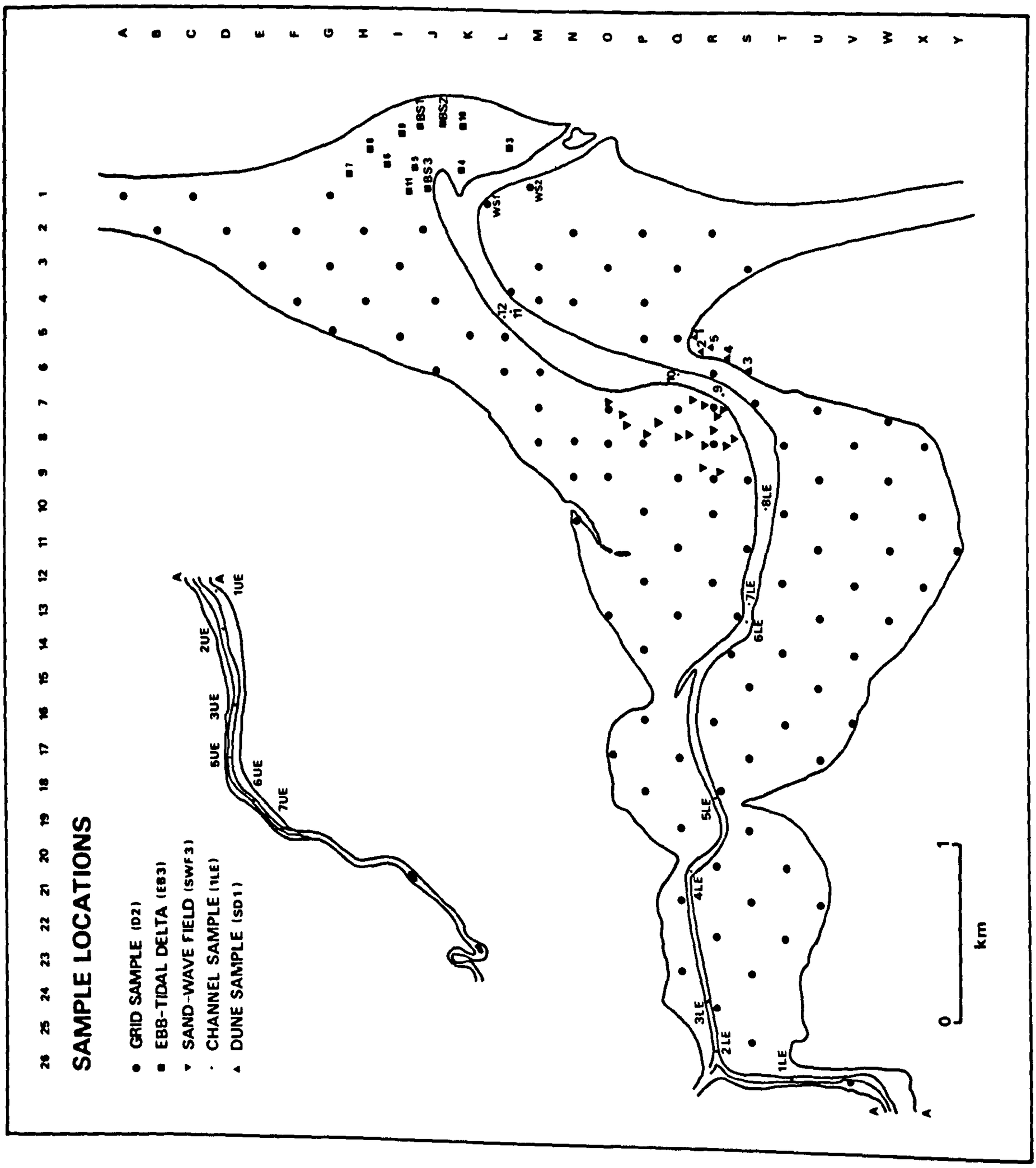

Fig. 4.1. Sediment sample locations in the Eden estuary.

II. LABORATORY TECHNIQUES

Particle-Size Measurement

Samples were air-dried under infra-red lamps at 30°C and then coned and quartered to reduce the amount for analysis to between 75 and 100gm for sands and approximately 50gm for silts and clays.

Organic matter was removed by the method of Jackson, Whitting and Pennington (1949), which utilises the oxidising properties of hydrogen peroxide. The removal of organic matter was regarded primarily as part of the pre-treatment of a sample prior to size analysis, but the actual organic content, on a weight-loss basis, was calculated for between-sample comparison (Appendix 3).

Water-soluble salts were removed by the dialysis method (Müller, 1967; Carver, 1971). Samples were placed in dialysis tubing and immersed in distilled water, which was renewed daily, for periods of up to seven days. The dialysis process was considered complete when no reaction was observed on testing the ambient distilled water for chloride with a 4% solution of silver nitrate.

The samples were then dispersed using sodium hexametaphosphate (calgon) as a deflocculant. As the clay content of the samples was unknown, ASTM specification D422-63 (cited in Carver, 1971) was followed, and 50ml of 10% calgon were added to each sample which was then allowed to stand overnight. The sample was then stirred for 5 minutes and washed through a B.S. 240 mesh (64 micron) sieve using distilled water. The silt and clay fraction which passed through the sieve was collected in a one litre flask in preparation for pipette analysis.

The sand fraction retained on the 64 micron sieve was dried at 30°C either under infra-red lamps or in a ventilated oven. It was then sieved through a set of B.S. sieves with a mesh spacing of 0.25 phi over the range -1 phi to 4 phi, using a Ro-tap sieve-shaker.

Sieving time was 10 minutes. Each sample was sieved in three sets of seven sieves; the maximum number which could be handled by the Ro-tap. Each 0.25 phi fraction was then weighed to two decimal places on a top-loading Mettler P12 precision balance.

The fines (<64 microns) which were collected during the sieving operation were added to the silt and clay size fraction which was then analysed by the pipette technique (Griffiths, 1967; Carver, 1971). Settling times used were those given in Carver (1971) based on Stokes Law of settling velocities. Pipette analysis permitted the calculation of the amount of material in 0.5 phi intervals between 4 phi and 7 phi and in 1 phi intervals from 7 to 9 phi. The quantities of sediment in each 0.25 phi interval was subsequently determined by interpolation.

In the process of sediment-size analysis problems were encountered concerning the silt and clay and detrital carbonate fractions of the samples:

1. The silt and clay fraction

It is recognised that the application of sieving and sedimentation techniques to the sand and silt plus clay fractions of a sample might produce anomalous results for the size intervals around the sand-silt boundary. In this investigation it was found that the total weight of silt plus clay in a sample, determined by the first withdrawal in the pipette analysis, was often less than that obtained by the subtraction of the weight of the sand fraction from the total sample weight. (Fig. 4.2).

Samples with fines in the range of concentration 3-27gm l^{-1} (less than 1% by volume) showed good agreement between pipette and direct weighing results (Irani and Callis, 1963), but the majority of samples showed fewer fines than expected. Best agreement occurred over the range of concentrations 8-16gm l^{-1}. Experimental error and the fact that particles between 50 and 64 microns do not necessarily obey

Stokes Law may account for some of the deviation. It was necessary to split the samples indicated by triangles on Figure 4.2 in order to reduce the initial concentration of fines to a level suitable for the application of pipette analysis. The splitting was done with the sample in the aqueous medium and the results show that an equal division was obviously not attained. In order to overcome this effect, the values determined by pipette analysis were multiplied by a correction factor equal to the weight obtained by direct weighing divided by the weight obtained by the first pipette withdrawal. This procedure only compensates for experimental error and does not affect the relative values obtained for each sedimentation-size interval.

2. The detrital carbonate fraction

Detrital carbonate in a sediment poses the problem of whether or not it should be included in the size analysis. The hydrodynamic (settling) behaviour of carbonate (shell) fragments is very different from that of quartz particles (Maiklem, 1968; Braithwaite, 1973), and it cannot be inferred that all carbonate present in a sediment was necessarily transported and deposited along with the lithic component.

Braithwaite's experimental data on the settling behaviour of skeletal particles suggests that bivalve shell fragments and quartz grains with intermediate diameters of less that 0.6mm (0.73 phi) are relatively uniform in their fall velocities (Fig. 4.2a). If, on this basis, it may be assumed that small quartz particles and shell fragments respond in a like manner to a given set of hydrodynamic conditions, it may then be permissible to include carbonate of sieve-diameter less than 500 microns in grain-size frequency distributions which are to be a basis for the hydrodynamic interpretation of a sediment.

Bivalve shell fragments and quartz particles of intermediate diameter greater than 0.6mm diverge in their fall velocities because of the influence of the shape factor. Relative to quartz the bivalve

fragments have a much slower settling velocity and hydraulic equivalence may not be assumed. The carbonate fragments would have a fall velocity equal to a quartz particle of a smaller intermediate diameter. This is also the case for carbonate graded by sieving as being coarser than the coarsest lithic fragment.

In the literature there has been no agreed method for dealing with the detrital carbonate fraction of a sediment. Some researchers retain all carbonate, others remove it. In this study the carbonate finer than the coarsest lithic fragment was retained on the assumption that it was in hydrodynamic equilibrium with its associated lithic particles. This is valid because lithic fragments in the vast majority of intertidal flat sediments did not exceed 0.5mm in intermediate diameter (based on sieving). Detrital carbonate coarser than the coarsest lithic fragment was excluded from the size analysis. This procedure was advocated by Frank and Friedman (1973) although they presented no factual support for the adoption of such a measure.

Sand Fraction Analysis

Light-Mineral Identification

The light-mineral composition of the fine-sand fraction (2-3 phi) of seventeen estuary samples was analysed in terms of quartz, orthoclase, plagioclase and lithic fragments. Five samples were from the intertidal sand and mud flats of the middle estuary and six each from the Eden channel and the beach environment.

Determination of the minerals was aided by the etching and staining technique of Gross and Moran (1970), whereby the grains are mounted in a black tar medium, etched with hydrofluoric acid fumes, and stained with solutions of 5% calcium chloride, saturated sodium cobaltinitrite, 5% barium chloride and 1% amaranth red. Orthoclase is stained a bright yellow, plagioclase red, and quartz remains clear.

Grain counts were made using an equal area method (Carver, 1971) whereby a 2mm square grid was placed over the grain mount and all grains in alternate squares identified. The total number of grains identified varied from sample to sample but in no case was it less than 300 which should result in the percentages quoted being accurate to $\pm$1.5 percent (Table 4.1).

The fact that quartz is unaffected by the staining may result in an overestimation of its abundance in a sediment which contains a high proportion of grains of quartzite or orthoquartzite. Grain counts made on thin sections of these sediments showed that the counting after staining technique may have attributed up to 6 per-cent of lithic fragments to the quartz category.

Table 4.1. Percentage of individual light minerals and lithic fragments versus number of grains counted.

Grains	Qu.	Or.	Pl.	LF.
100	66.0	11.0	4.0	18.0
200	65.5	16.0	4.0	13.5
300	66.0	13.7	4.3	15.3
430	66.4	14.5	5.4	13.3
560	66.7	16.0	5.9	11.4
680	66.3	15.3	5.5	12.8
809	66.0	14.7	5.3	14.0
S.Dvn for grain counts in excess of 300	0.3	0.9	0.6	1.4

Qu. = Quartz; Or. = Orthoclase; Pl. = Plagioclase; LF. = Lithic Fragments.

Heavy Mineral Content

A detailed analysis of heavy mineral species in the Eden estuary sediments was not undertaken as it was believed that it would provide very little information on sediment dispersal patterns.

The weight percentage of heavy minerals in the fine sand fraction

of 24 intertidal flat and 16 channel samples was determined however to show whether there was any significant variation in heavy mineral content in the two environments.

A 15 gramme split of the 2-3 phi fraction of each sample was separated into light and heavy fractions by centrifuging for 15 minutes (Gallenkamp instrument setting no. 6) with bromoform of specific gravity 2.89gm cm^{-3} as the separating medium. The heavy fraction was removed from the settling tube by freeze drying in liquid nitrogen (Scull, 1960).

Calcium Carbonate Content

Detrital carbonate in the form of shells and shell fragments is ubiquitous in the sand-fraction of the intertidal flat sediments. In order to establish the relationship between the grain-size frequency distributions of the carbonate and silicate fractions of these sediments, 72 samples were sieved into 1 phi size grades and the carbonate fraction in each grade determined by weight-loss on acidification with 10% HCl. Frequency distributions of each fraction were then plotted after recalculating the data on the basis of 100% carbonate and 100% silicate.

Quartz Grain-Surface Microtextures

Surface microtextures of quartz grains in the size range 250-1000 microns were analysed using a Cambridge 600 scanning electron microscope. The techniques of sample preparation are given by Krinsley and Margolis (in Carver, 1971).

Identification of the physical and chemical processes related to the observed microtextures was based on the associations of microtextures given in Table 4.2 (after Setlow and Karpovich, 1972).

Table 4.2. Physical and chemical processes related to microtextures. (After Setlow and Karpovich, 1972)

Process	Microtexture	Symbol
EOLIAN	meandering ridges	mr
	graded arcs	ga
	orientated fractures	of
	flat pitted surfaces	fps
GLACIAL	irregular small-scale indentations	issi
	striations	s
	chatter marks	cm
	large-scale conchoidal fractures	lscf
GLACIAL/SUB-AQUEOUS	high relief	hr
	semi-parallel steps	sps
	arc-shaped steps	ass
	imbricate breakage blocks	ibb
	small-scale conchoidal fractures	sscf
	small-scale breakage blocks	ssbb
SURF	straight and curved grooves	scg
	mechanical v-shaped indentations	mv
CHEMICAL	orientated triangles	ot
	chemical etching	ce
	diagenesis	d
	chemical deposition	cd
	recrystallisation	r

Clay Fraction Analysis

Air-dried samples (11) were treated with EDTA (ethylenedinitrilo-tetraacetic acid) in order to remove carbonates without altering the clay mineral assemblages (Glover, 1961; Bodine and Fernalld, 1973). Organic matter was removed by H_2O_2 oxidisation. Each sample was then dispersed with 50ml of 10% calgon and samples of the less than 2μm fraction obtained by standard sedimentation techniques.

For x-ray diffraction analysis the air-dried <2μm fractions were mounted on glass slides by a smear technique to give orientated mounts (Gibbs, 1968; Carver, 1971) and scanned from 3^o to 30^o 2θ at 0.5^o per minute with Copper Kα radiation. Diffractograms of three splits of each sample were obtained to facilitate interpretation of the clay mineralogy. Sample split 1 was an untreated sample; split 2 was heated to 550^oC for one hour; split 3 was treated with glycerol for a period of 24 hours.

Equipment and operational conditions:

Phillips PW1012/20 Diffractometer
Cu K_α radiation
18mA 36kV
Attenuation $1x10^3$
Time constant 8.

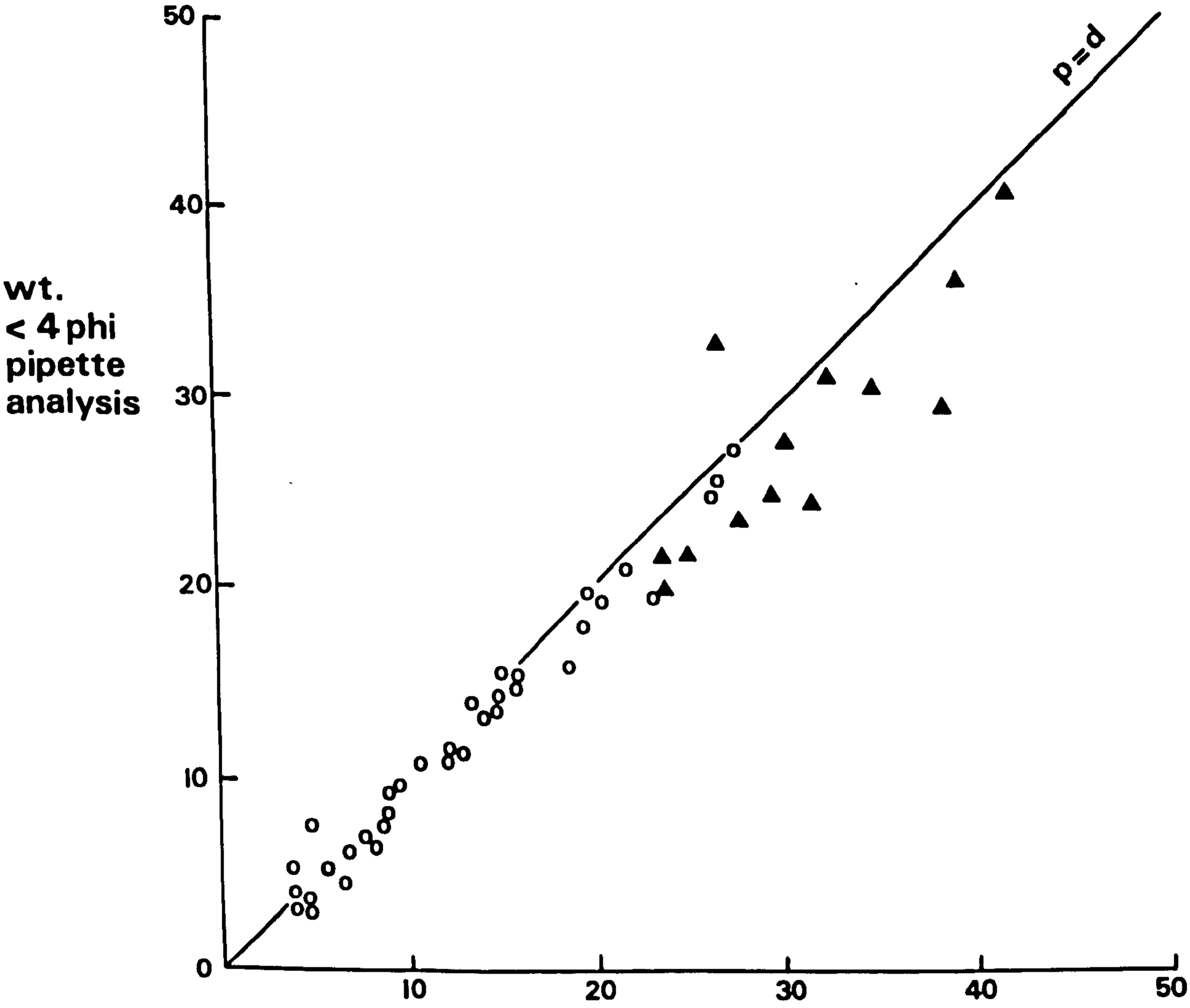

Fig. 4.2. The relationship between the weight of material in the size grades finer than 4.0 phi as determined by the direct weighing method and pipette analysis. Samples represented by triangles were sub-divided to reduce the concentration of sediment to a level acceptable for pipette analysis.

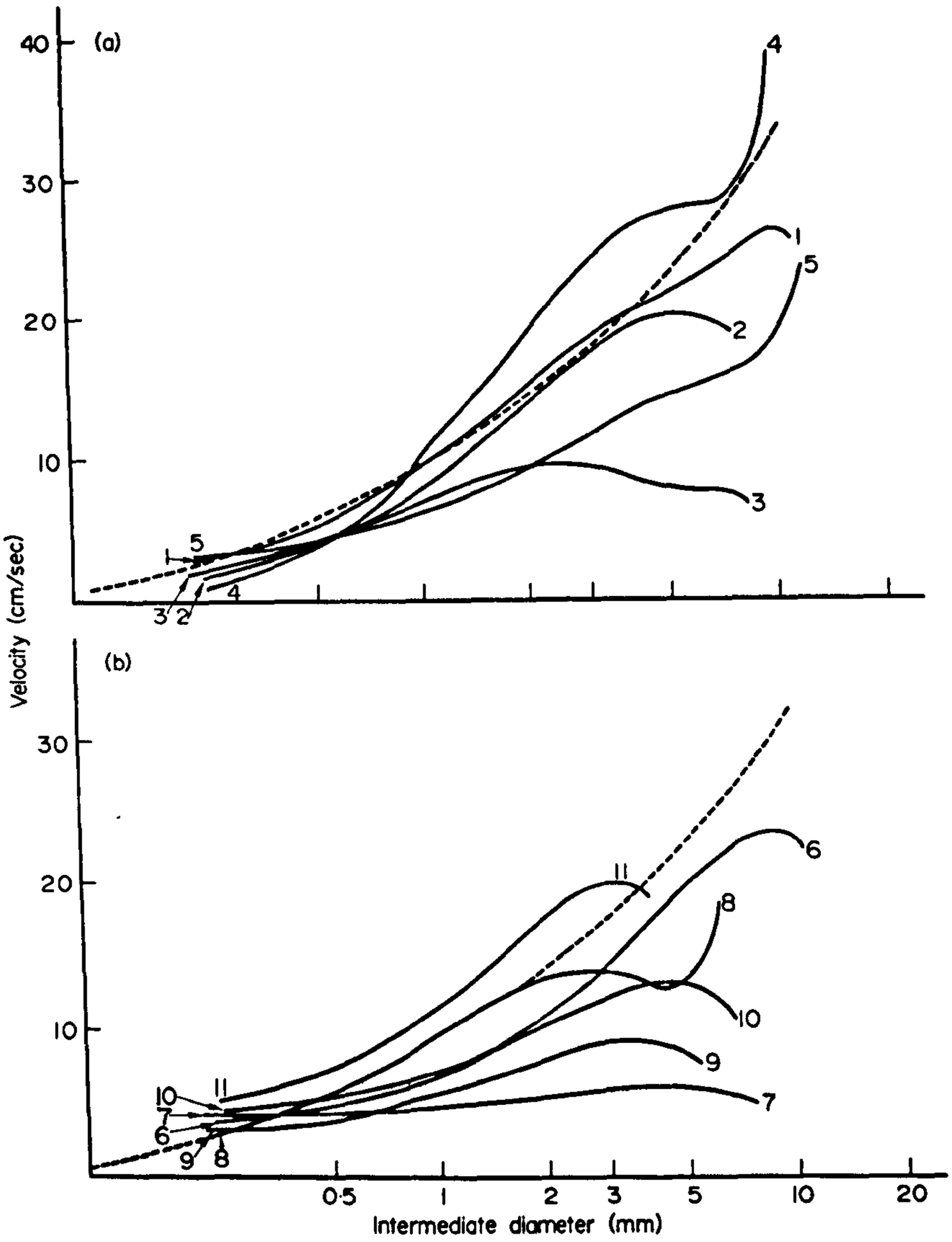

Computed best-fit curves for velocity plotted against intermediate grain diameter for different grain types. (a) 1, Coral fragments; 2, *Lithothamnion*-like algal fragments; 3, *Halimeda* segments; 4, quartz grains; 5, bivalve shell fragments; 6, microgastropods. (b) 7, *Marginopora* grains; 8, echinoderm fragments; 9, other foraminifera; 10, bryozoan fragments; 11, alcyonarian spicules.

Fig. 4.2a. A comparison of the fall velocities of quartz grains and various carbonate fragments (from Braithwaite, 1973).

III. SEDIMENT COMPOSITION

Sand Fraction

Light Minerals

As a group the estuary sands may be classified as SUBLITHARENITES (Pettijohn, Potter and Siever, 1972, after Dott, 1964). The average composition of the fine sand fraction shows that quartz is the major detrital component with feldspar and lithic fragments present in sub-equal amounts (Table 4.3). Within the feldspar group orthoclase is approximately three times more abundant than plagioclase.

Table 4.3. Composition of the Fine Sand Size-Fraction

Sample	Grains Counted	Qu. %	Or. %	Pl. %	LF. %	Class[n].
8bJE	932	75.21	12.98	3.97	7.83	SAA
7UE	344	59.01	15.12	3.49	22.38	SLA
2AUE	679	71.13	11.19	3.39	14.29	SA
V2S	476	66.39	18.07	9.03	6.51	AA
1LE	399	59.90	13.28	2.51	24.31	SLA
4LE	416	68.75	11.06	3.61	16.59	SLA
R3	500	63.00	14.60	1.40	21.00	SLA
R6	827	62.52	21.04	5.32	11.12	AA
R8	475	61.47	15.37	5.26	17.89	SA
R18	515	64.27	13.79	4.47	17.48	SA
R10	704	60.09	18.18	3.69	18.04	SA
C1	1042	58.16	13.53	5.57	22.74	SLA
E3	560	57.68	8.75	1.96	31.61	LA
K2	450	62.89	19.11	9.56	8.44	AA
L4	533	59.85	12.76	2.81	24.58	SLA
Q11	732	51.23	14.48	5.33	28.96	LA
S11	349	60.17	12.32	4.58	22.92	SLA
Average		62.45	14.45	4.47	18.63	SLA

SAA Subarkosic Arenite
SLA Sublitharenite
SA Subarkose
AA Arkosic Arenite
LA Lithic Arenite

Grouping of the sands according to environment (channel, beach, intertidal flat) does not reveal a relationship between sediment type and environment (Fig. 4.3).

Heavy Minerals (See Ch. 4, V, p. 135)

The variation in heavy mineral content of the fine sand fraction (Fig. 4.4) illustrates the concentration of heavy minerals in the sediments of the Eden channel and its immediate vicinity.

The fine sand fraction of the Eden channel contained approximately twice the amount of heavy minerals of the adjacent intertidal flats. The N-S traverse along grid line 11 showed constant values of 2%, except at the end points where to the north the value increased to 3.6% and to the south decreased to 1%. The N-S traverse from South Tentsmuir Beach towards Out Head showed a gradual increase in the proportion of heavy minerals as the Eden channel was approached.

Calcium Carbonate

The distribution of calcium carbonate (Fig. 4.5) shows that high concentrations (>3wt %) occur in areas around Out Head (up to 9.86%), and in a narrow zone which runs southwards from South Tentsmuir Beach to the Eden channel, then borders the north bank of the Eden, and eventually expands into a broad zone spanning the Eden channel in the west central part of Kincaple Flat. In the main area of carbonate concentration values of up to 16.8% were noted, and one sample containing whole Mytilus values had 44 wt % carbonate. The majority of samples outside of these two zones contain 1-3% of carbonate. Values of less than 1% were recorded from small areas on the estuary margins.

The high values of calcium carbonate are not associated with any particular sediment type. In the outer estuary the sediments with over 3% of carbonate are well-sorted fine sands with typically less

than 1% of silt and clay, whereas in the middle estuary muds and sandy-silts contain the high values. This situation is partially clarified by a study of the within-sample size-distribution of carbonate.

Replotting of the carbonate data on the basis of 100% carbonate showed that the size-distributions of the majority of outer estuary samples assumed similar shapes to the total sediment distribution, with the maximum carbonate weight percentage in the same size interval as the largest weight in the whole sample, eg. G3, J6, and N8 (Fig. 4.6) This may mean that the bulk of the detrital carbonate is in equilibrium with the sand fraction and is transported and deposited with it under wave and current action.

In other samples, however, especially those of the middle estuary, the carbonate fraction is coarser than the silicate fraction and is concentrated in the coarse and very coarse sand size-grades, eg. O17, P14, O13, R14, R22, S19, and T16. Sample A1 from South Tentsmuir is also of this type. Samples R22, S19 and T16 also carry high carbonate concentrations in the very fine sand range - the modal class of these samples. The coarse carbonate detritus is probably of local production, considering the areal coincidence between the high carbonate area of the middle estuary and the presence of mussel banks and Cardium concentrations. This is also supported by the fact that the carbonate fraction of the middle estuary sediments is almost exclusively of Mytilus and Cardium fragments, whereas, in the outer estuary carbonate, a large variety of molluscan genera is represented.

Quartz Grain-Surface Microtextures

The results of the SEM microtextural analysis (Table 4.4) indicate two main features of quartz grains from the estuarine environment:

1. a great variety in the overall shape of grains from euhedral to angular to well-rounded forms;

Table 4.4. Quartz Grain Microtextures. The number of grains upon which each microtexture was observed.

Sample (Grains Scanned):	C1(6)	N4(4)	Q13(5)	V12(2)	V16(2)	7UE(7)	5LE(3)
Microtexture							
mr	0	0	0	0	0	0	0
ga	1	1	0	0	0	1	0
of	0	2	0	0	0	2	0
fps	2	0	2	0	2	3	0
issi	0	2	1	0	0	1	1
s	0	0	0	0	0	0	0
cm	0	0	0	0	0	0	0
lscf	0	2	1	1	1	2	0
₊r	4	2	1	1	1	1	2
sos	3	3	2	1	1	2	3
ass	3	1	3	1	1	0	2
ibb	1	0	0	0	0	0	1
sscf	3	1	2	0	2	2	0
ssbb	1	0	2	0	0	3	1
scg	0	0	1	0	0	0	0
rv	0	0	0	0	0	4	0
ot	2	0	0	0	1	6	0
ce	1	1	3	0	2	0	1
d	0	0	0	0	0	0	0
cd	0	0	0	0	0	0	0
r	0	0	0	0	0	0	0

2. a similar variety in the surface microtextures which record a grain's environmental history.

Samples C1, D13, 5LE and V12 are dominated by features such as high relief, semi-parallel steps, arc-shaped steps, small-scale conchoidal fractures and imbricate and small-scale breakage blocks (Fig.4.7a,b). Many of these features were ascribed to a glacial origin by Krinsley and Donahue (1968), but Setlaw and Karpovich (1972) have indicated that the same features may form on moderate energy beaches. They do suggest, however, that glacial features are unmistakable by virtue of their great variety and intensity. In Figure 4.7a and b the features are well displayed and unmodified, and a glacial origin is inferred for the grains shown.

The effects of chemical weathering are well shown in several grains, and orientated v-shaped depressions and etched areas are common (Fig.4.8,4.9). Figure 4.8 (grain V16 (2)) shows orientated v-shaped depressions which are beginning to interlock. Figure 4.9 shows a more advanced weathering with the formation of sub-parallel ridges between areas where solution has taken place. Figures 4.10, 4.11, 4.12 illustrate the effects of solution on euhedral grains. The earliest stages of attack are seen in Figures 4.11c and 4.12c.

In several cases the overprinting of one set of textures by a second and even a third set may be recognised. Figure 4.13 illustrates a grain which originally had a surface texture dominated by large-scale conchoidal fractures and large-scale semi-parallel breakage blocks. The second stage in its history was the rounding of the surface and the development of an irregularly pitted surface. The final stage was chemical etching shown by an oval depression cutting across the semi-parallel breakage blocks. Figure 4.14 shows an angular grain, characterised by small-scale breakage blocks and high relief, which

is being corroded by chemical action. The orientated solution cavities are seen on the upper surface of the grain, and in Figure 4.14b.

Conclusions

On the basis of quartz grain microtextures it may be inferred that the Eden sediments have a mixed origin; no single physical or chemical environment could produce all the observed features.

Grains with features distinctively of glacial origin are present, as are glacial grains with an overprinting of aqueous origin - this would seem to be the dominant type. Chemical microtextures are also common. Very well-rounded grains with pitted surfaces are probably second or third cycle types. The euhedral grains apprear to be undergoing chemical attack rather than physical abrasion.

Clay Fraction

The major clay mineral groups were identified by their characteristic basal peaks. Material with diffraction peaks at 10Å, 5Å, and 3.3Å was identified as illite. Peaks at 3.5Å and 7Å were assigned to kaolinite + chlorite. Differentiation between kaolinite and chlorite was based on the resolution of the 004 reflection of chlorite (3.54Å) and the 002 reflection of kaolinite (3.58Å) by slow scanning at 0.5 degree per minute (Fig. 4.14c). Confirmation of chlorite was also attempted by heat treatment (550^{o}C for 1 hour), but in no case did the 001 reflection (14Å) become sharp and of increased intensity. On heating, the kaolinite became amorphous and the 3.5Å and 7Å peaks were lost. The 4.46Å peak of illite was enhanced on heating, whereas the 10Å peak was absent. No marked changes in the basal spacings of material with peaks at approximately 14Å were observed on treating the samples with glycol. Montmorillonite was therefore considered to be absent, or present in only very minor quantities.

The relative abundances of the four mineral groups, illite, kaolinite, chlorite and montmorillonite, were estimated using weighted peak areas following the semi-quantitative method of Biscaye (1964). The peaks and weighting factors used were: the 17Å glycolated peak area for montmorillonite; the 7Å glycolated peak area x2 for kaolinite and chlorite divided in proportion to the relative areas of the 3.58Å and 3.54Å peaks respectively; the 10Å glycolated peak area x4 for illite.

Average results for the six samples in which good kaolinite/chlorite separation was achieved show that illite is the dominant clay mineral (55.79%) with kaolinite and chlorite present in subordinate amounts of 22.32 and 18.58% respectively (Table 4.5). Montmorillonite is calculated to be present in very small amounts with an average of 3.30%.

Table 4.5. Relative Proportions of the Clay Mineral Groups

	Mont.	Illite	Kaolinite	Chlorite	Ka + Ch
U20	3.03	51.52	26.86	18.59	45.45
[illegible]13	1.64	43.72	28.96	25.68	54.64
* S23	1.32	28.95	42.54*	27.20	69.74
* 1LE	1.72	27.59	41.00*	29.69	70.69
[illegible]9	4.17	58.33	20.45	17.05	37.50
C2	4.35	69.57	13.00	13.00	26.00
Average (6)	2.71	46.61	28.80	21.87	50.69
Average (4)	3.30	55.79	22.32	18.58	40.90

* Samples with abnormally high kaolinite content.

The clay mineral proportions stated above are rendered suspect because of the influence of artificially introduced clay mineral species into the estuarine environment. The two samples S23 and 1LE contain abnormally high kaolinite values (40%+). Both samples are from the western part of Edenside Flat and the adjacent channel and are in close proximity to the paper mill at Guardbridge. It was

established that kaolinite (China clay) is used extensively in the paper making process at Guardbridge, and inevitably the mineral forms a part of the waste products discharged into the estuary. Clay mineral assemblages are therefore not further discussed.

Organic Matter

The percentage of organic matter per sample was determined during the pre-treatment of samples for size analysis. The technique used was weight-loss on low-temperature oxidisation by hydrogen peroxide (Jackson, Whitting and Pennington, 1949) which had the necessary advantage of not affecting the clay mineral assemblages present in many samples. The results are presented in Appendix 3.

The distribution of organic matter (Fig. 4.15) shows that the sediments of the lower estuary are virtually devoid of oxidisable material. In the middle estuary the organic content increases towards the central areas and a maximum of 12.6 wt% was recorded in Kincaple Flat.

Comparison of the distribution of organic matter with the distribution of sediment type (Fig. 3.14) shows that high organic content is related to sediments with less than 50% sand content, i.e. silty sands and muds. It is also in association with these sediments that mussel banks, Cardium colonies and algal concentrations are located.

Armoured Mud Balls

Armoured mud balls (Fig. 4.16) are a conspicuous feature of the surficial sediments in only one area of the Eden estuary, a zone which extends NE-SW parallel to the south bank of the Eden channel in the vicinity of Out Head (Fig. 4.17). The area is ebb-current dominated, and the beach slope is approximately 4^{o}. It is also an area in which man-made refuse (concrete, bricks and bottles) accumulates.

The zone was divided into three rectangular areas in the N-E to SW direction, and samples collected to determine whether any textural variation in the clay balls occurred in the flood or ebb direction. Sample distribution was uneven in terms of numbers: 42 in the western area, 7 in the central area, and 30 in the eastern area. Three clay balls were found in the swash zone to the east of Out Head.

Textural Characteristics

The lengths of the long (L), intermediate (I) and short (S) axes of each mud ball were measured to an accuracy of 0.1cm by vernier callipers. The three axes were mutually perpendicular.

The length of the long axis varied between 3.5 and 18.6cm with a mean of 7.35cm and a standard deviation of 3.0cm. Intermediate and short axes varied between 2 and 11cm with means of 5.24 and 3.94cm respectively. The results for all samples and the three areas are presented in Table 4.6 (page 108).

The mud balls from the central area were of the largest dimensions, and those from the western area are of larger size than those from the eastern area.

1. Shape

The shape of each mud ball was determined by plotting the data on the sphericity-form diagram of Sneed-Folk (1958) (Fig. 4.15). The ratios S/L and (L-I)/(L-S) are plotted on the triangular diagram. The sphericity Up is a value illustrating the departure from equi-dimensionality. The three end-points are (i) a sphere, also described as compact, (ii) an oblate spheroid (platey), and (iii) a prolate spheroid (elongate).

All samples but one plotted in the upper part of the diagram above an S/L ratio of 0.3. The majority of samples have S/L values between 0.3 and 0.7. A wide range of (L-I)/(L-S) values were recorded

Table 4.6. Size Statistics - Armoured Mud Balls

		Mean	Mode	S. Dvn.	Min.	Max.
I.	Long	7.35	5.00	3.00	3.50	18.60
	Inter.	5.24	3.74	2.07	2.70	11.40
	Short	3.94	2.36	1.53	2.10	11.00
II.	Long	7.33	4.87	2.74	3.50	14.00
	Inter.	5.20	3.24	2.07	2.90	11.30
	Short	4.05	4.16	1.59	2.30	11.00
III.	Long	10.29	6.45	4.52	5.70	18.60
	Inter.	6.04	3.72	2.54	3.30	10.00
	Short	4.97	3.41	1.87	3.10	7.90
IV.	Long	6.32	4.36	2.14	4.00	12.80
	Inter.	4.69	4.31	1.38	2.70	8.90
	Short	3.41	2.29	1.12	2.10	7.50

I = Statistics for 81 mud balls.
II = West Area 42 mud balls.
III = Central Area 7 mud balls.
IV = East Area 30 mud balls.

Table 4.7. The Percentage Distribution of the Various Shape Categories within each Area.

	West	East	Centre	Swash
C	11.90	13.30	0.0	0.0
CE	21.43	20.00	42.86	0.0
CB	21.43	30.00	0.0	0.0
CP	14.29	6.67	0.0	33.30
E	21.43	6.67	57.14	0.0
B	4.76	13.33	0.0	33.30
P	4.76	6.67	0.0	33.30
VE	0.0	0.0	0.0	0.0
VB	0.0	0.0	0.0	0.0
vp	0.0	3.33	0.0	0.0
Up	0.50-0.90	0.30-1.00	0.70-0.80	0.70

with values between 0.33 and 1.0 - a preference towards prolate rather than oblate shape. The percentage of each form in each section and the sphericity range are shown in Table 4.7. In the western area CE, CB and E forms were equally well developed. In the central area CB forms were absent and E forms best developed. In the eastern area CB forms dominate with CE and B less well developed. From west to east CB and B forms increase in numbers by 8.57% each, and CP decreased by 7.62% and E by 14.76%.

The three swash-zone samples showed special features. Each had two upper surfaces inclined and meeting at an oblique angle (Fig. 4.19). The facets had been developed by the reversal of flow in the swash-zone. The lower surface was irregular and buried in the sediment.

2. Armour

The nature of the armour was variable, but was composed mainly of lithic fragments, coal, brick and shell fragments. Several samples had granule and pebble-size fragments within the nucleus of the ball, but, in these cases, the composition of the ball was coarser than normal with more sand-sized material. The internal fragments were considered to be an integral part of the original deposit.

The thickness of the armour, which was generally one grain thick, varied from 0-1.5cm. The majority of samples had a cover of <5mm, but there is no obvious relationship between the size of the ball and the thickness of armour. In general, however, the large bladed ellipsoids had a larger number of grains up to 1cm. The distribution of the armour over the ball surface was also irregular, and this became more obvious as the forms became bladed or elongate, when pebbles were concentrated on the surfaces of largest area.

The Physical Properties of the Mud Balls

Of the 82 samples collected 81 were composed of a reddish-brown, tenacious sediment which appeared structureless in the hand-specimen. This sediment type is not exposed anywhere above low-water mark within the confines of the estuary. It does, however, occur at depths of over 15cm in parts of the estuary between Coble Shore and Guard-bridge, and also beneath a mobile cover of sand and gravel in the Eden channel to the west of Coble Shore. The remaining mud ball was of a sediment type exposed in several areas of the middle estuary, that is, the grey Carse clay.

The physical differences between the reddish brown and grey sediment may be expressed in terms of standard soils tests (Table 4.7).

Table 4.7. Soils Tests* on Mud Ball Material

	Reddish-brown	Grey
Moisture Content (%)	26.4	56.4
Plastic Limit (%)	20.6	30.1
Liquid Limit (%)	46.5	69.0
Plasticity Index	25.9	38.9
Vane Shear Strength (KN/m^2)	65.1	25.0
Remoulded V.S.S. (KN/m^2)	18.6	5.0
pH	8.7	8.0

* Soils Tests performed by A.R. Griffin, Dept. of Civil Engineering, University of Leeds.

Discussion

The main problems associated with the Eden estuary mud balls are the dominance of the reddish-brown clay and the restricted occurrence around Out Head.

The soils tests showed the basic physical differences between the red and grey clays with the red clay being better indurated and of far higher shear strength. The breakdown of the two clays may be controlled partly by the nature of the bedding. The red clay is

apparently homogenous, but in thin section it shows lenses and laminae of sand-sized particles (Fig. 4.20). In contrast the grey clay shows bedding marked by accumulations of plant debris which facilitate the splitting of the sediment into thin layers. Discoidal pellets of the grey clay less than 1cm maximum diameter were found in the Eden channel sediments to the east of Out Head, and it is apparent that of the two clays the grey one is more readily deformed and broken down.

There is no obvious source for the clay balls in the vicinity of Out Head. Mud balls are generally formed by a process of bank undercutting, collapse and local transportation regardless of environment, whether fluvial or intertidal (Stanley, 1969). In the Eden estuary, however, the red clay does not occur at the surface above low-water mark, and if the balls have been formed in a present-day erosional phase, they originated below low-water mark in the Eden channel. It is feasible that the Eden channel has cut down sufficiently to be eroding the red clay in parts of the middle and outer estuary: the evidence is, however, lacking as no red clay was recovered in grab-samples.

The most likely source-materials for the mud balls are the reddish-brown, gravelly, sandy clays which occur in the bed of the Eden channel to the west of Coble Shore. If this is the case, the mud balls have been transported at least 2.4km downstream and have been carried from the channel bed to the channel margin by ebb-currents at Out Head.

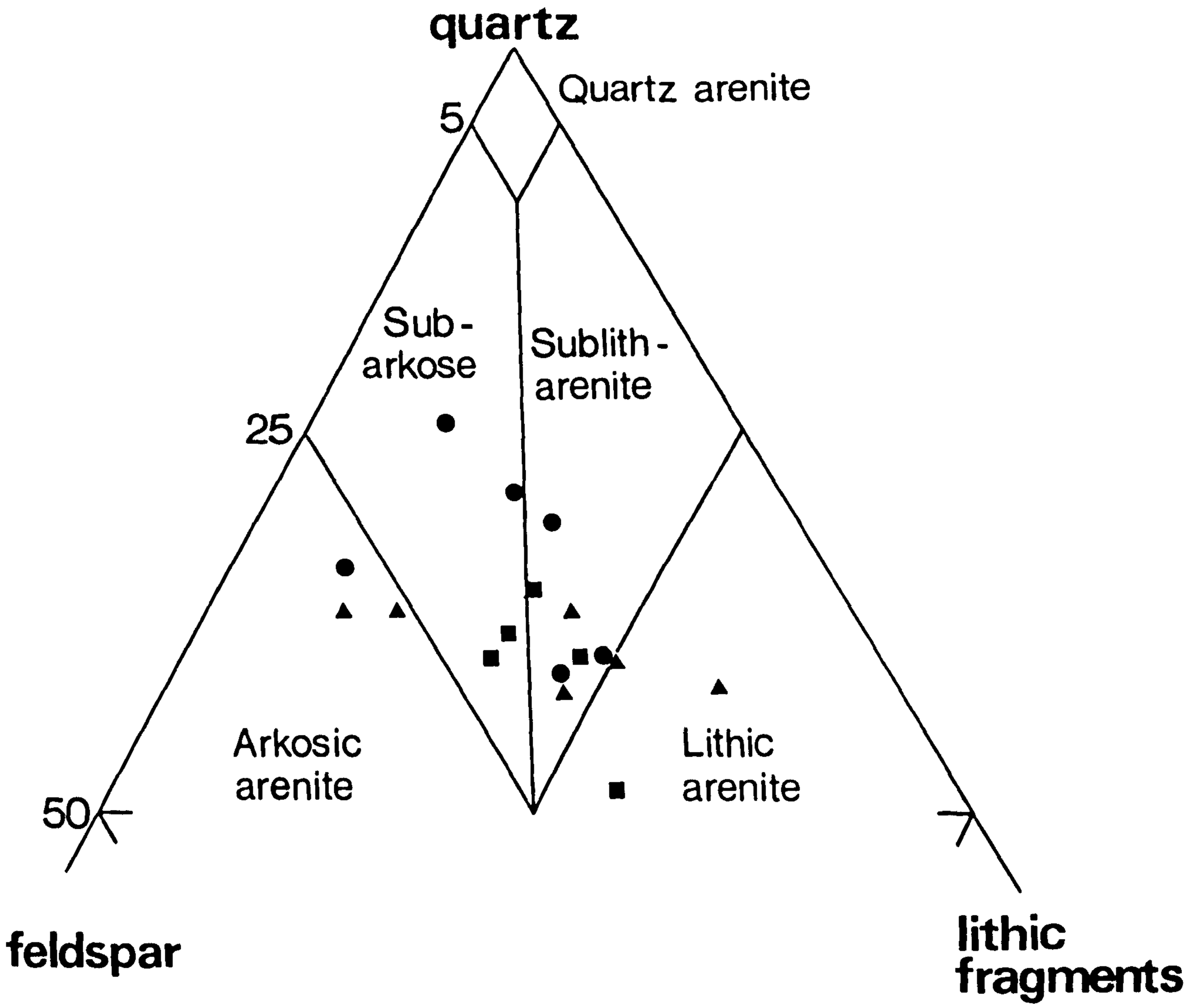

Fig. 4.3. Sand groupings according to environment.

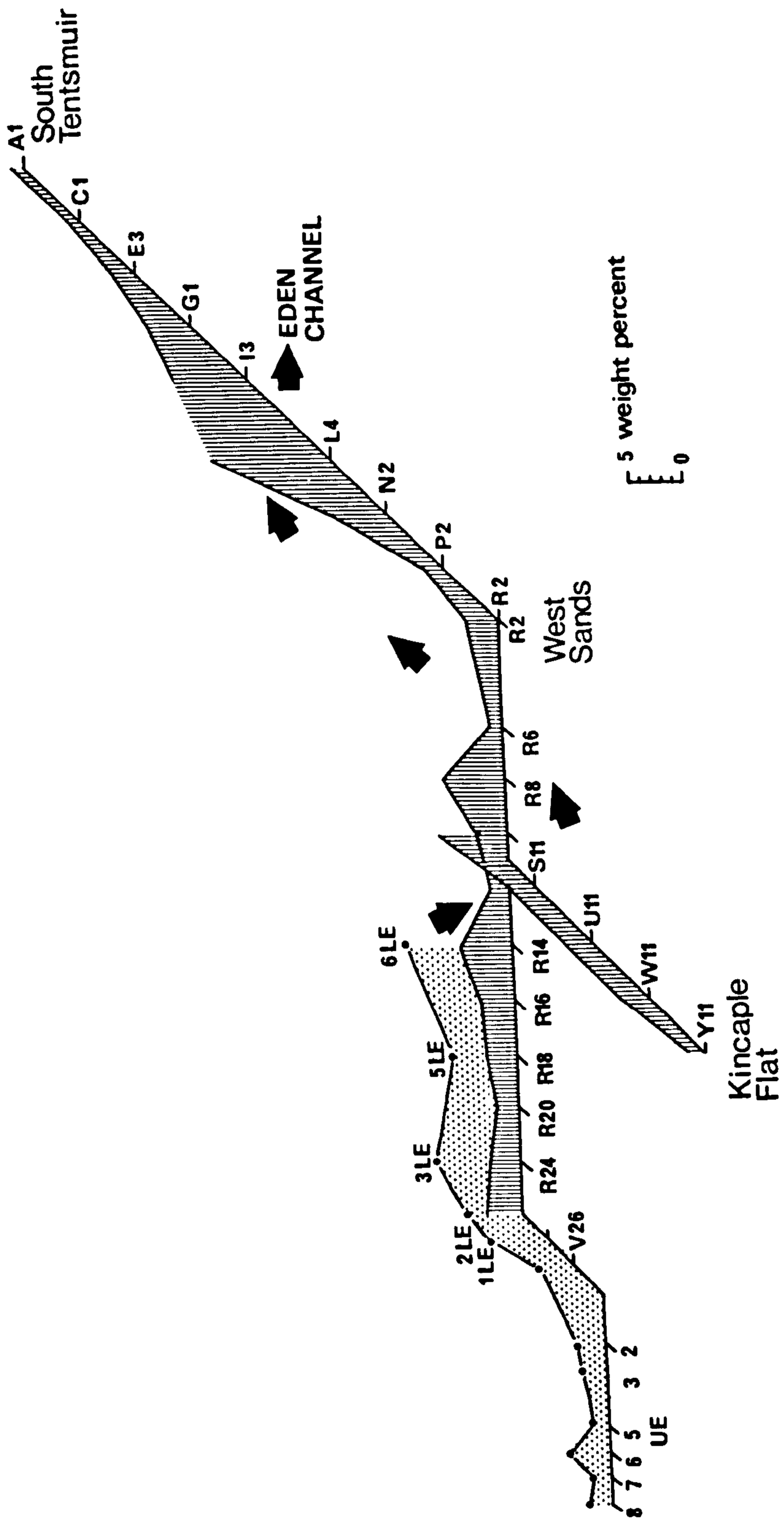

Fig. 4.4. The variation in heavy mineral content of the fine sand fraction in channel and intertidal flat sediments.

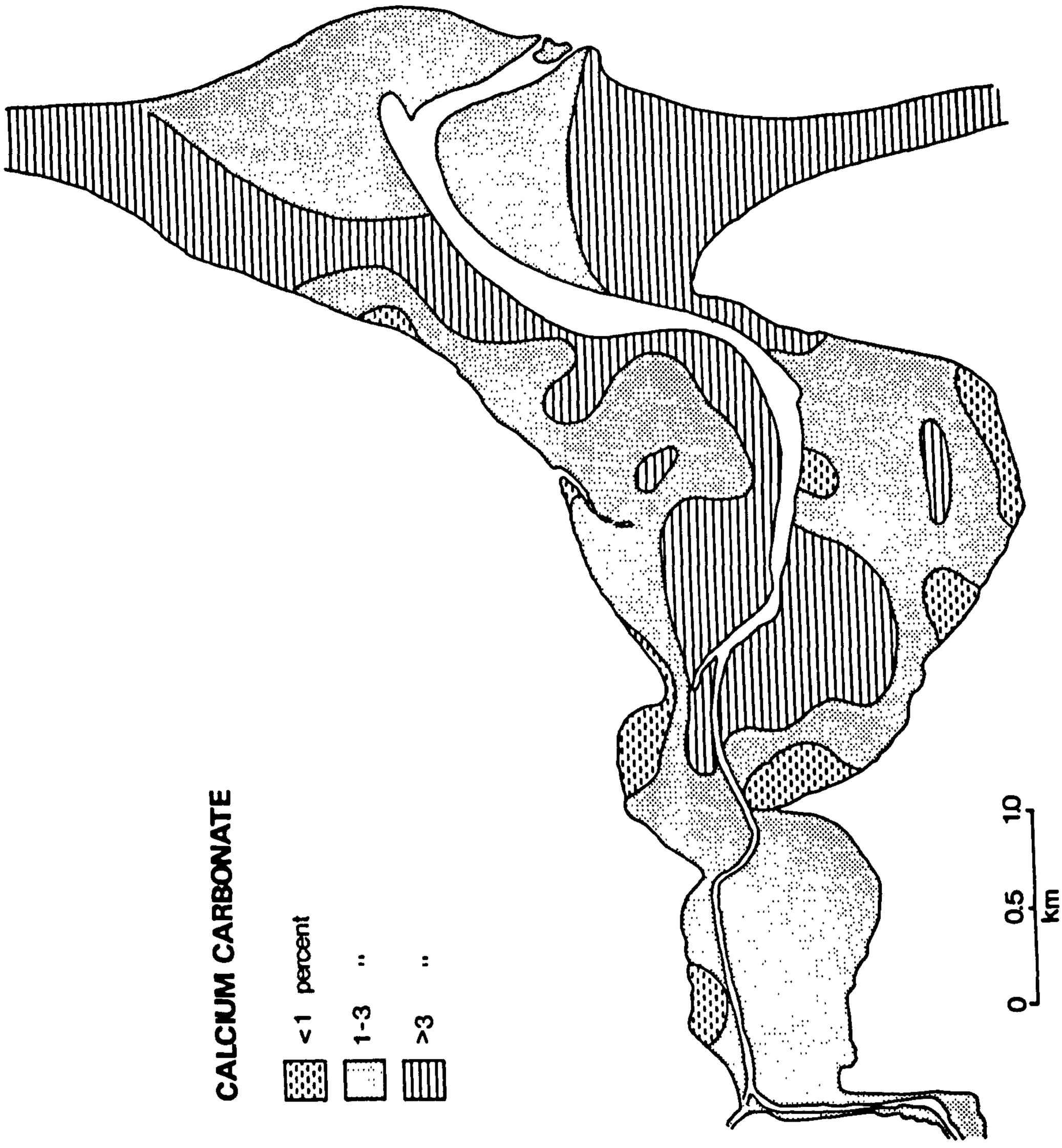

Fig. 4.5. The distribution of calcium carbonate in the sand fraction of Eden estuary sediments.

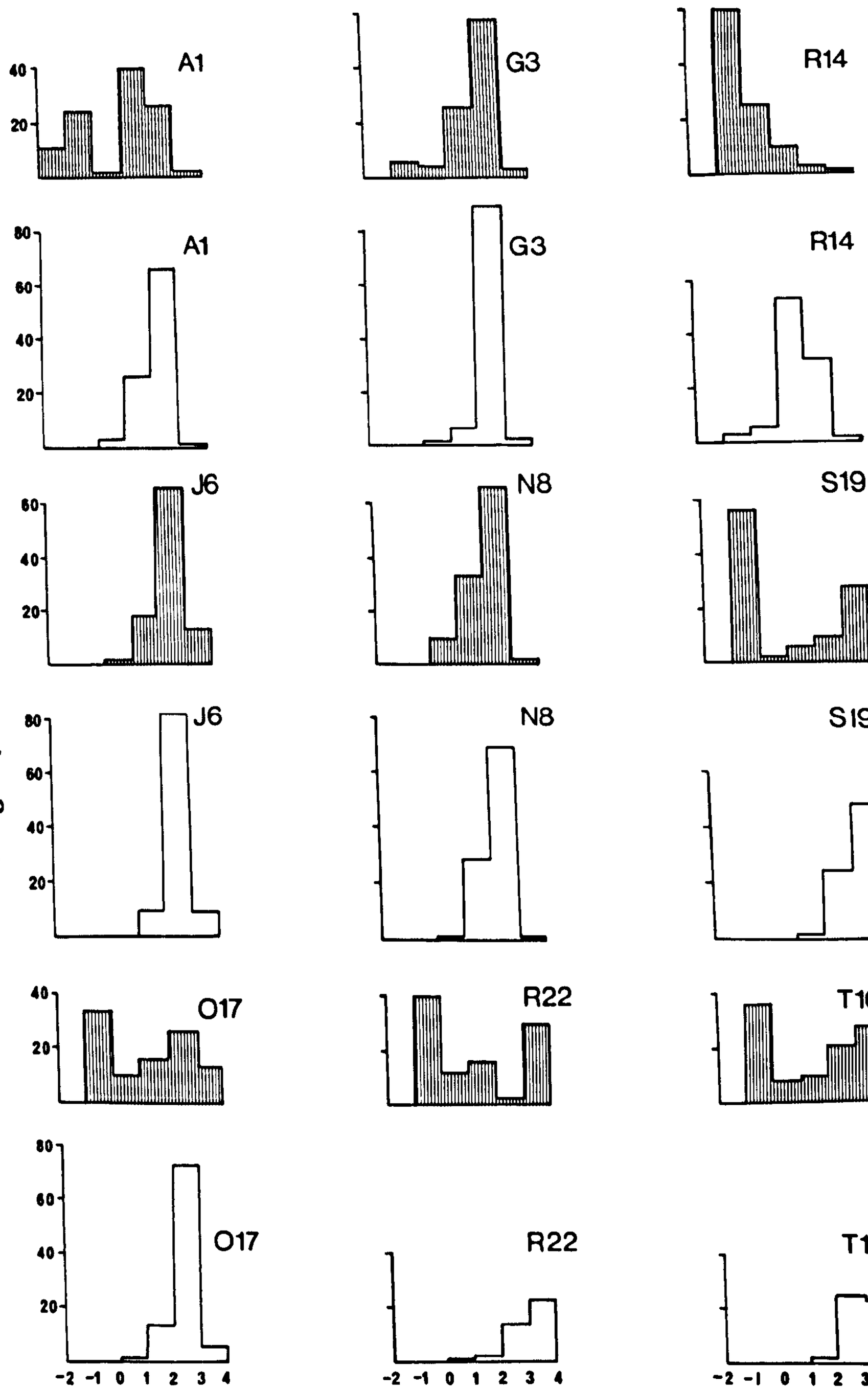

Fig. 4.6. Histograms of the grain-size distribution of carbonate material (shaded) and total sediment (unshaded) for selected lower and middle estuary samples.

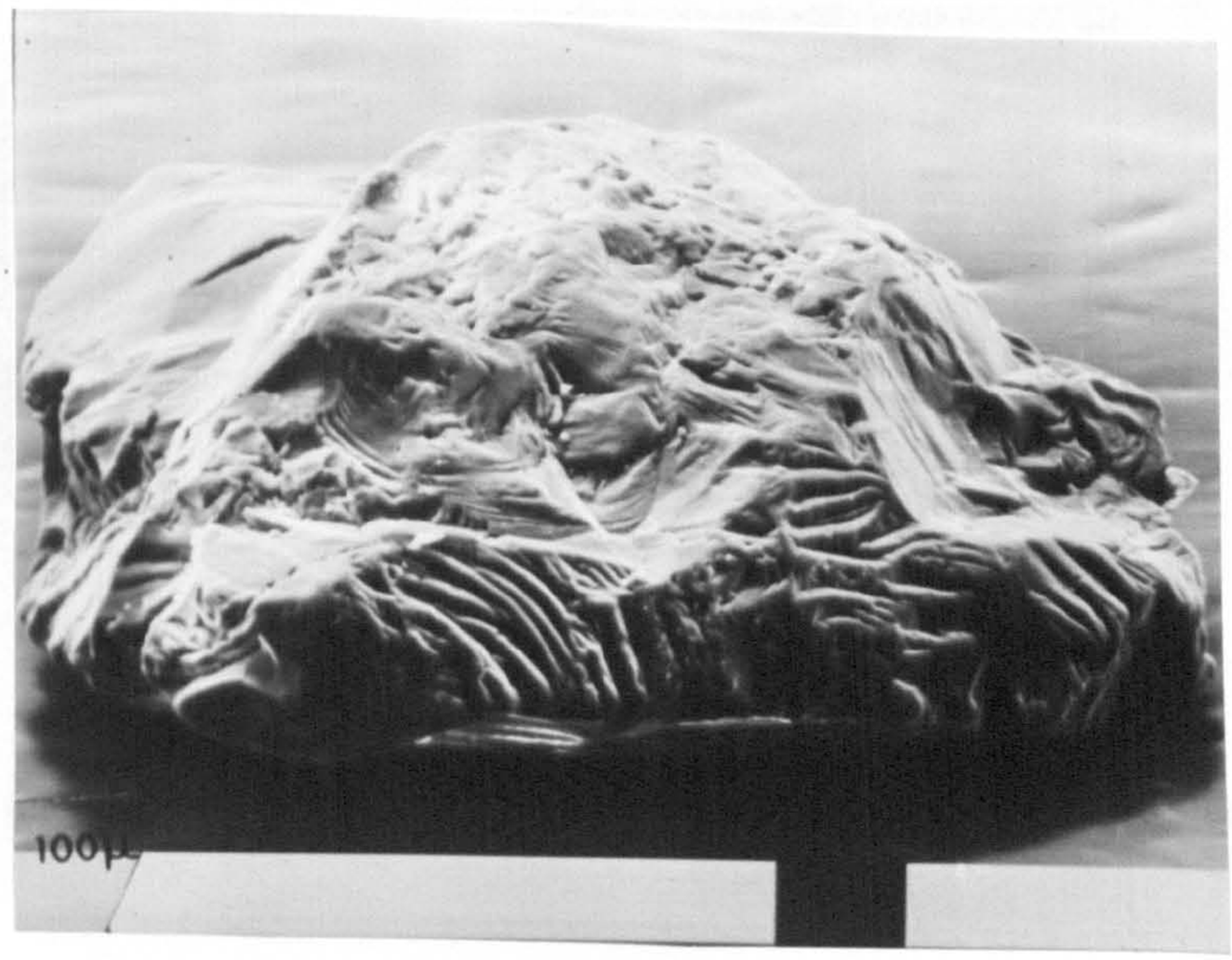

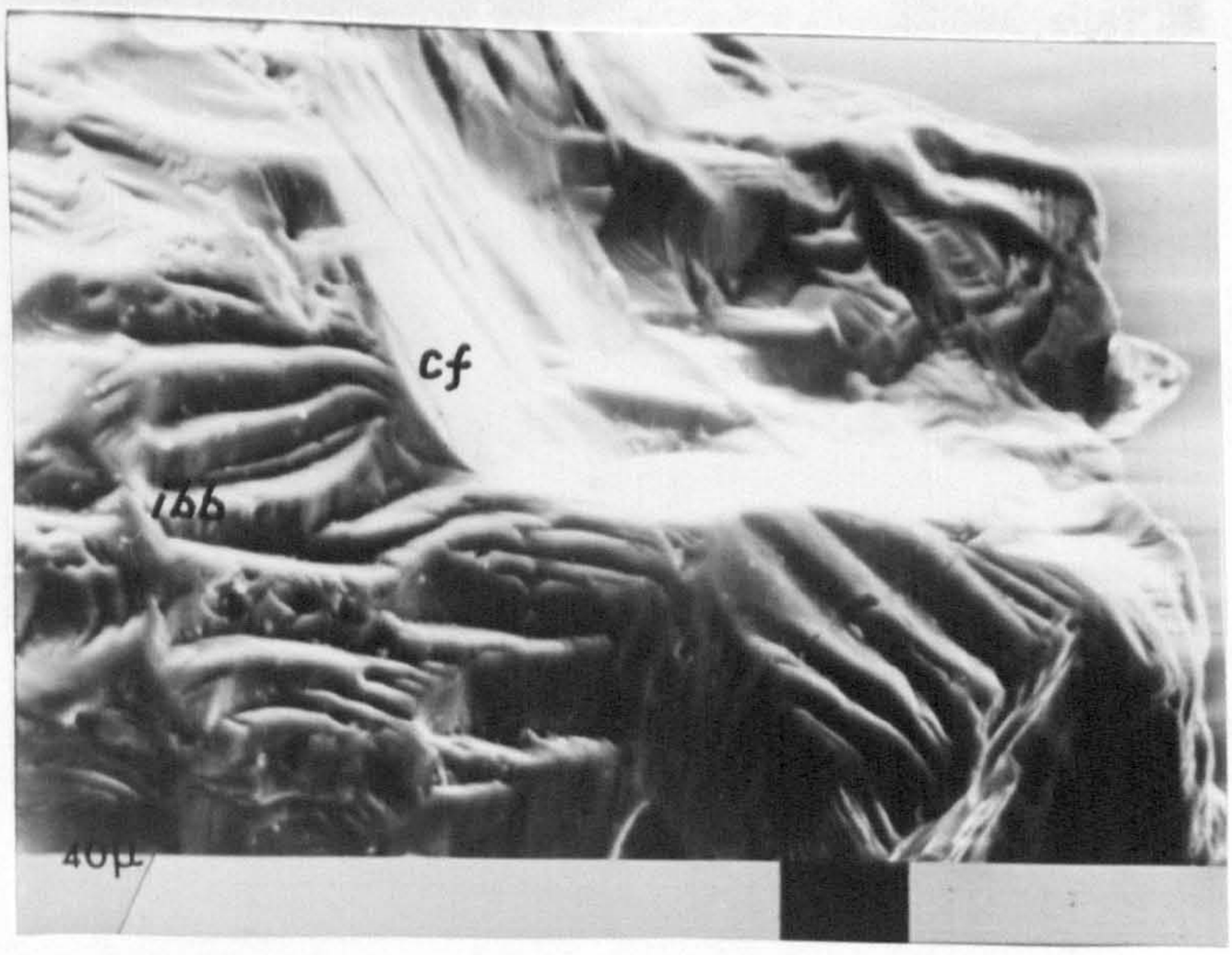

Fig. 4.7a. Sample C1, grain F.
The grain is characterised by high relief, conchoidal fractures (cf) and imbricate breakage blocks (ibb).

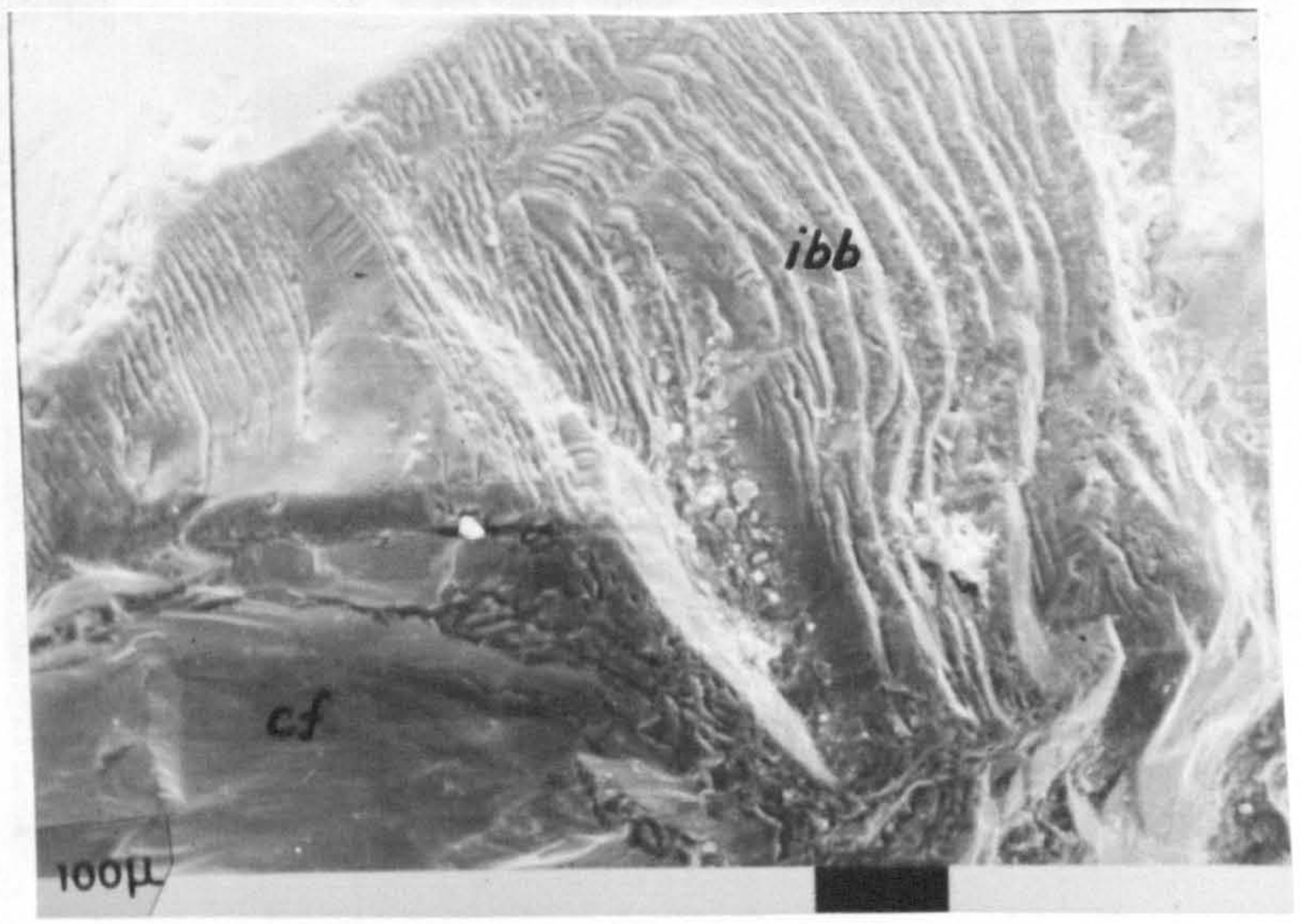

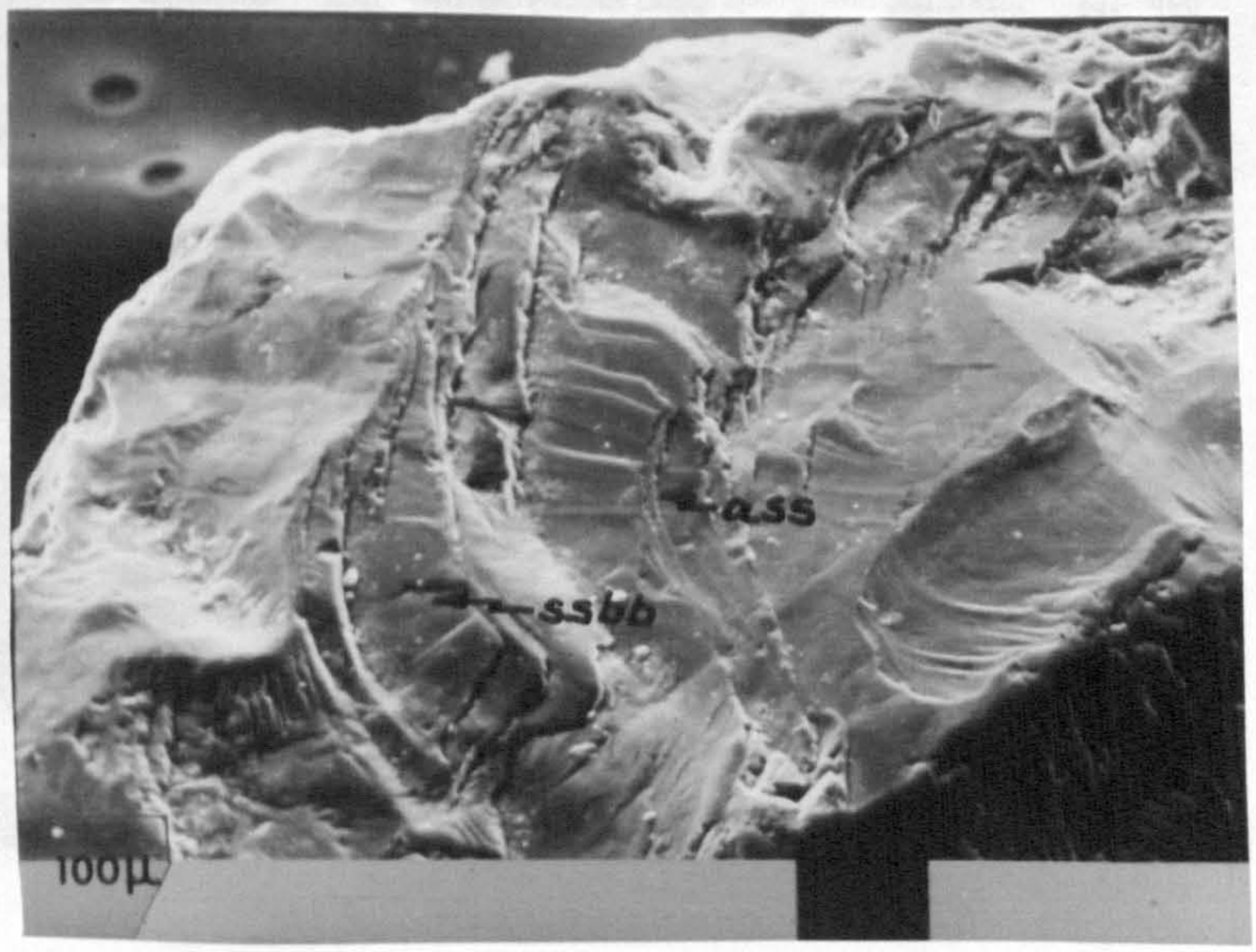

Fig. 4.7b. Sample 5LE, grain C.
Upper: conchoidal fractures (cf) and imbricate breakage blocks (ibb).
Lower: arc-shaped steps (ass) with small-scale breakage blocks (ssbb).

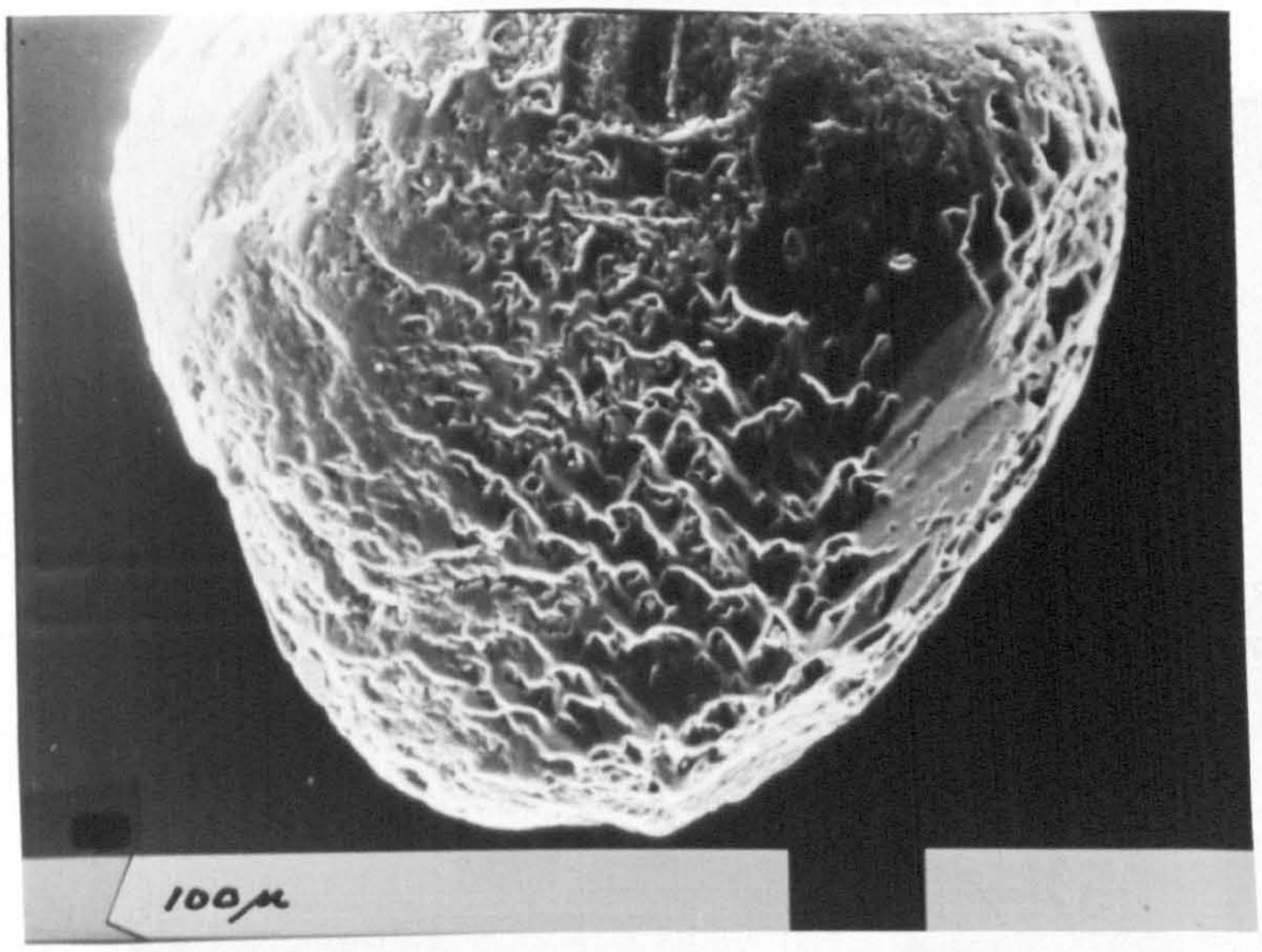

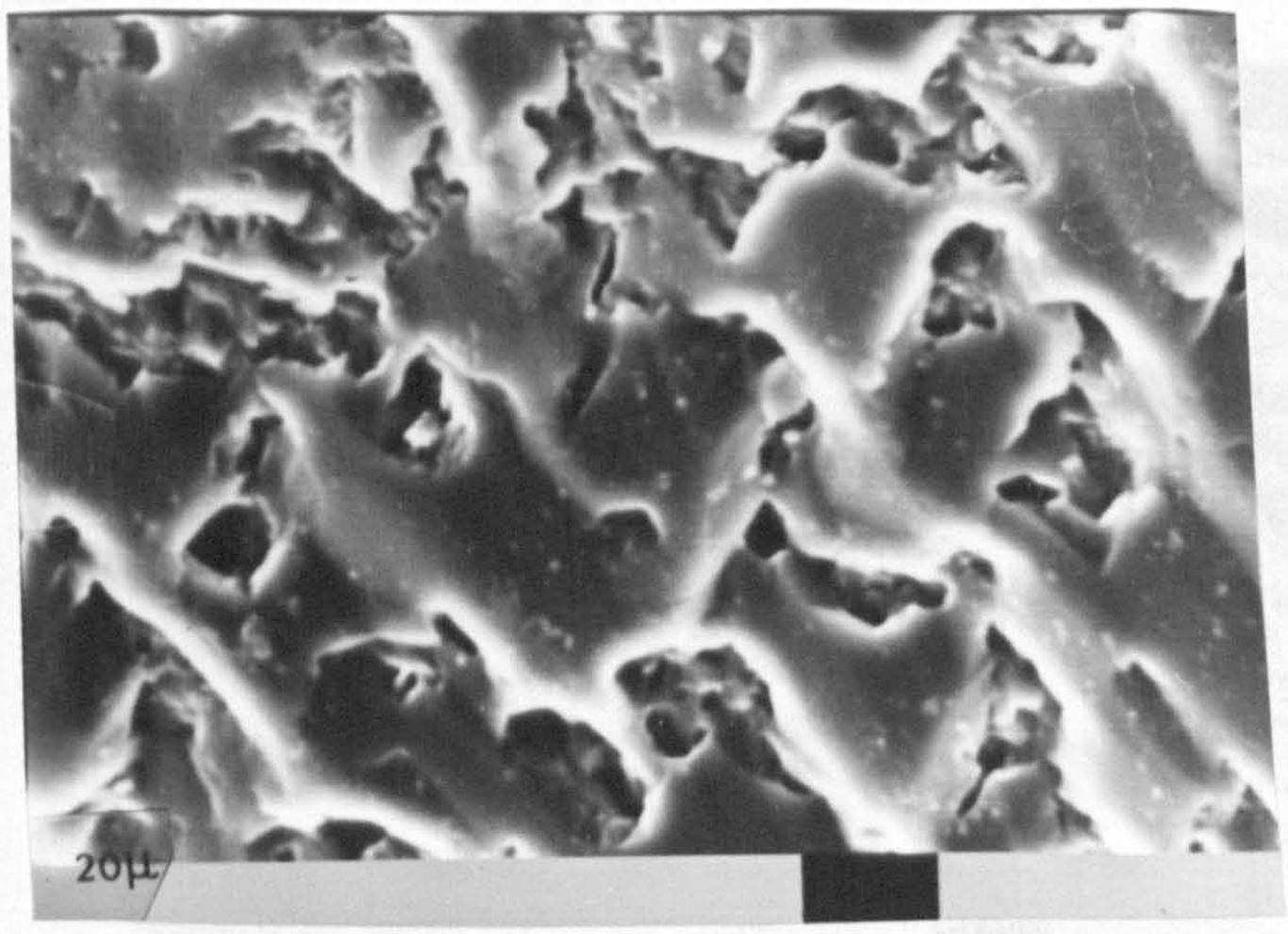

Fig. 4.8. Sample V16, grain 2.
Upper: V-shaped depressions or orientated triangles (ot) on a well rounded grain.
Lower: Detain of the solution triangles.

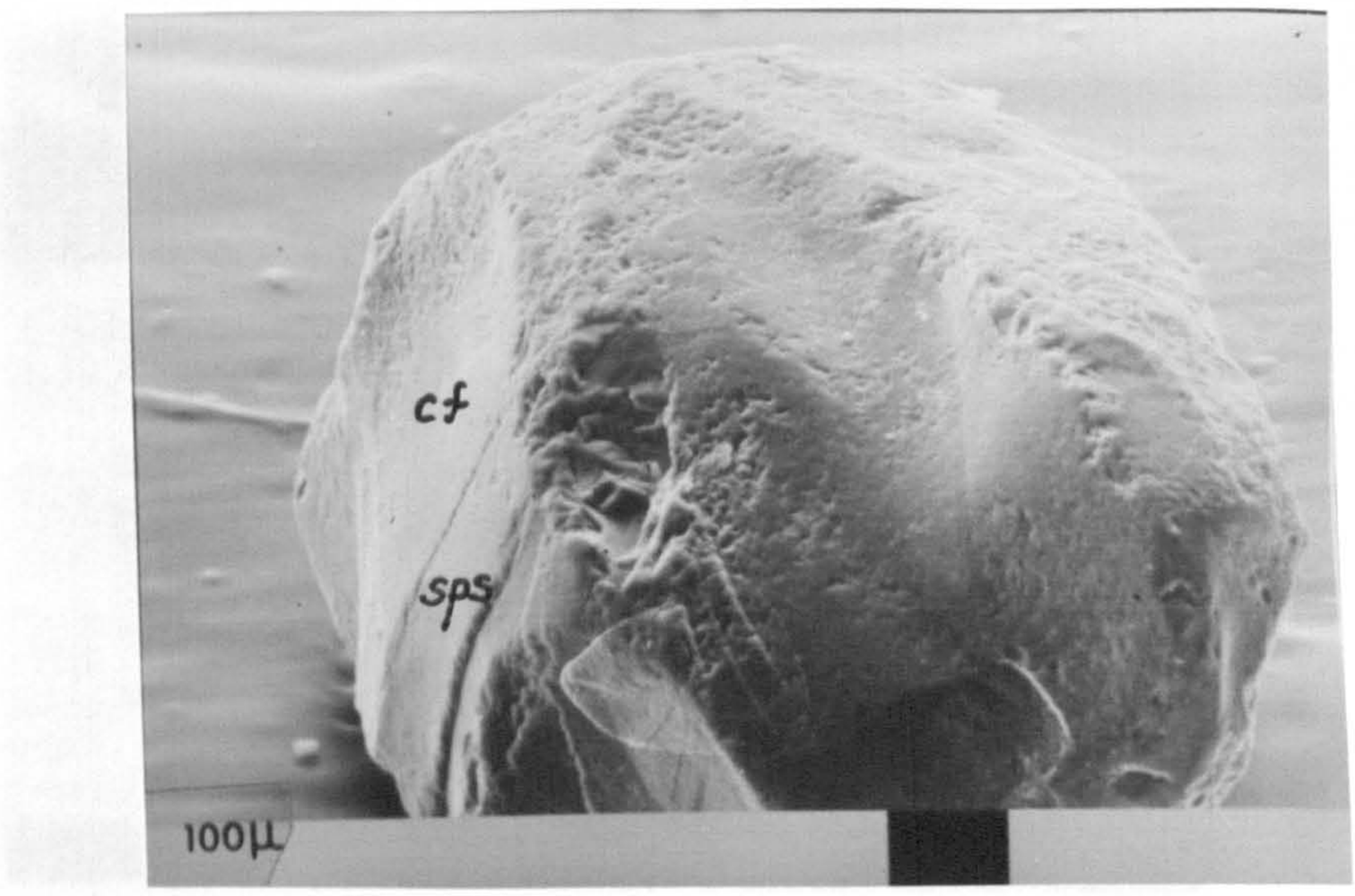

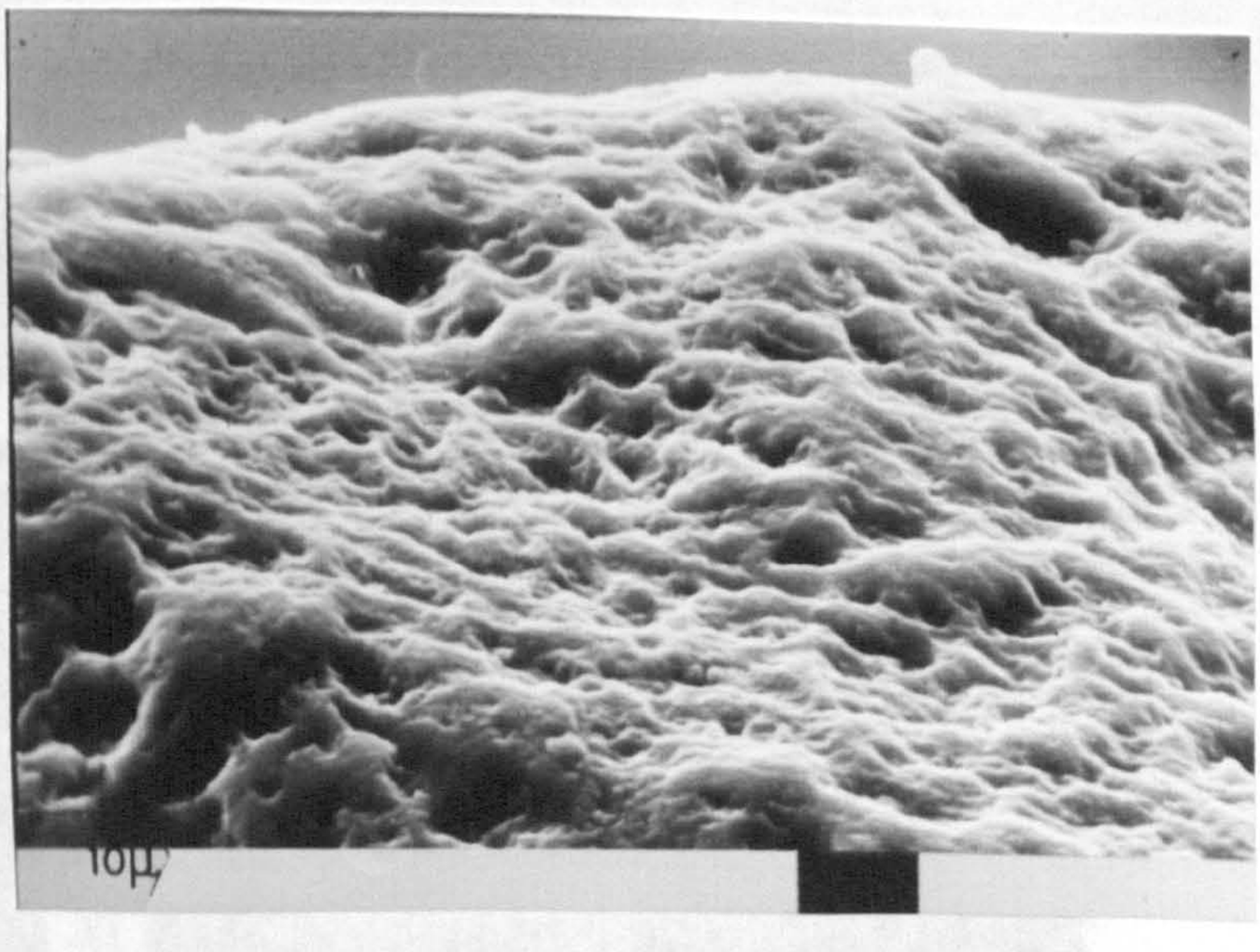

Fig. 4.9. Sample 7UE, grain A.
Upper: The overprinting of chemical solution on a grain showing large-scale conchoidal fractures (cf) and semi-parallel steps (sps).
Lower: Detail of the upper right surface of the above grain. Advanced chemical weathering has led to the formation of sub-parallel ridges between solution cavities.

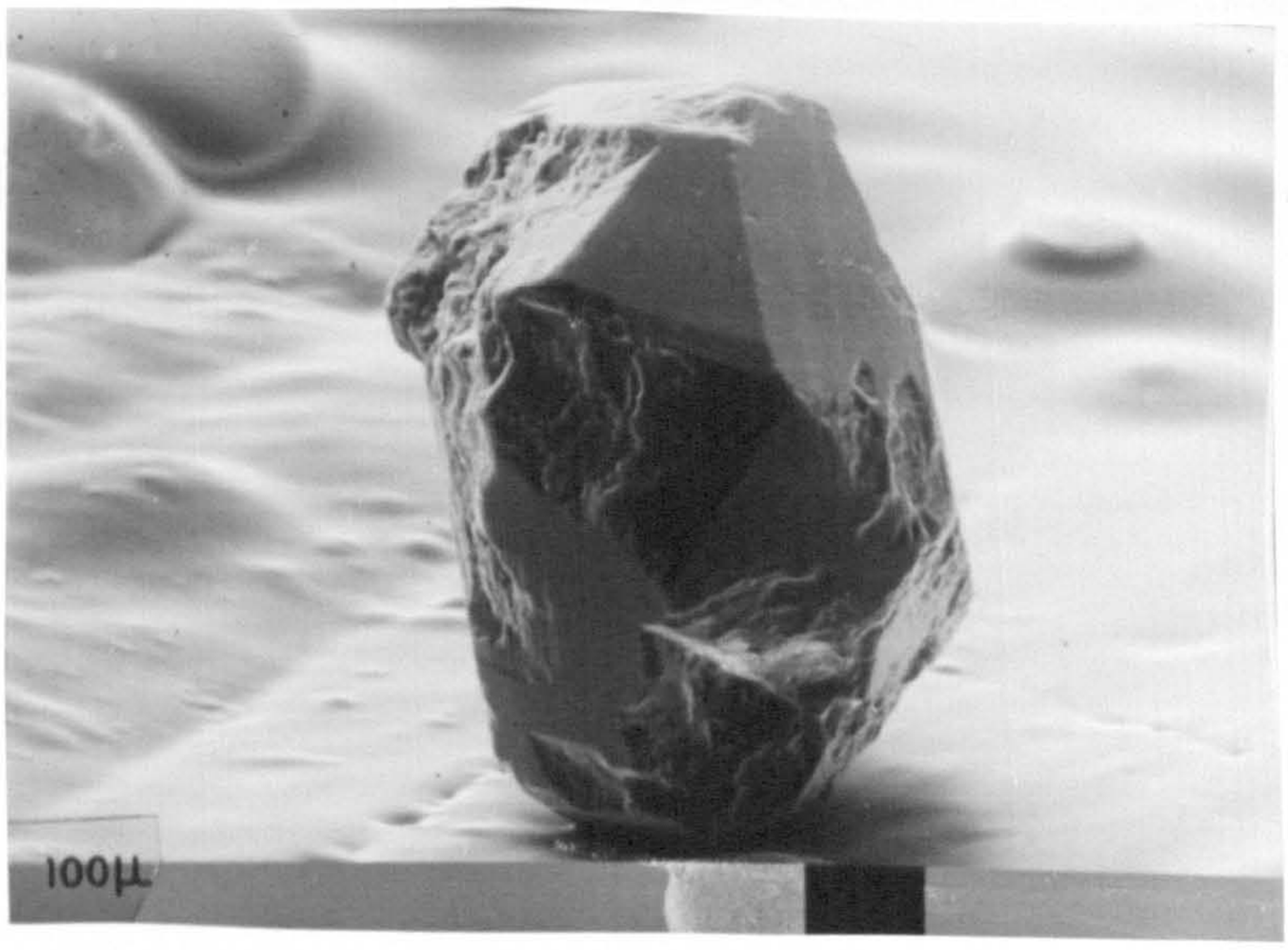

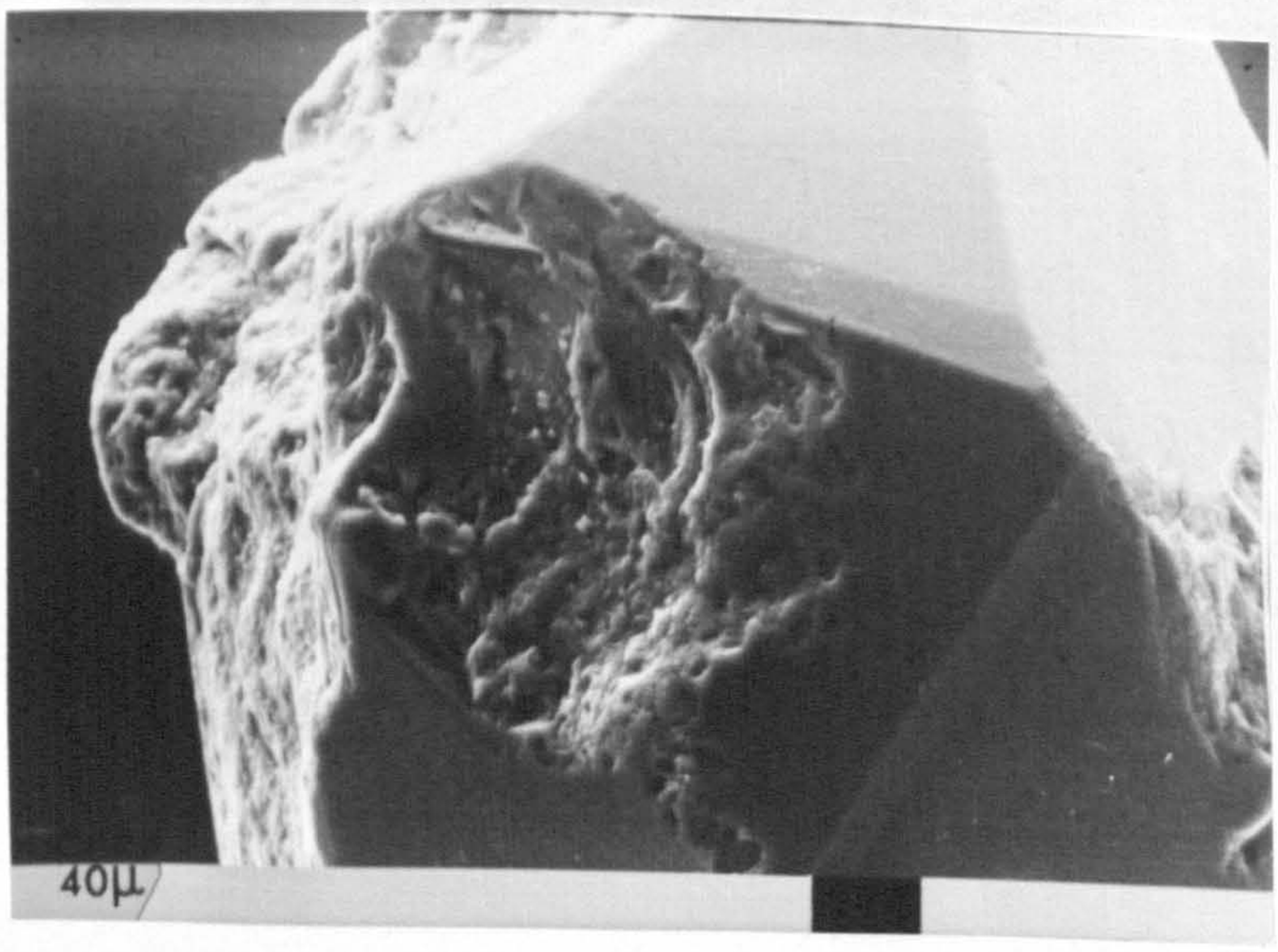

Fig. 4.10. Sample 7UE, grain A.
Euhedral grain undergoing chemical corrosion.

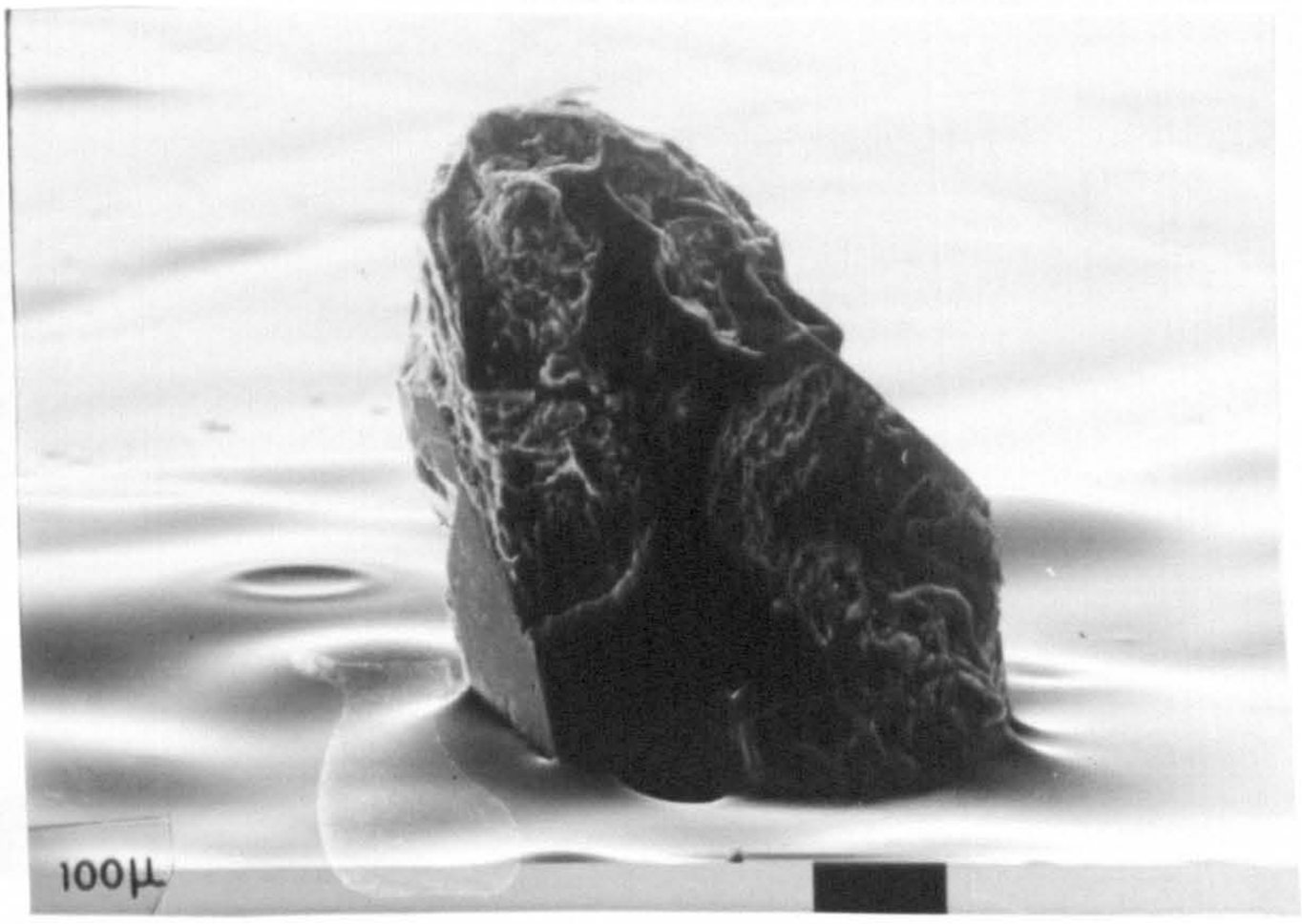

Fig. 4.11. Sample 7UE, grain C.
Chemical corrosion of a euhedral grain. Lower photograph illustrates etching along orientated lines of weakness and the advanced stage of corrosion.

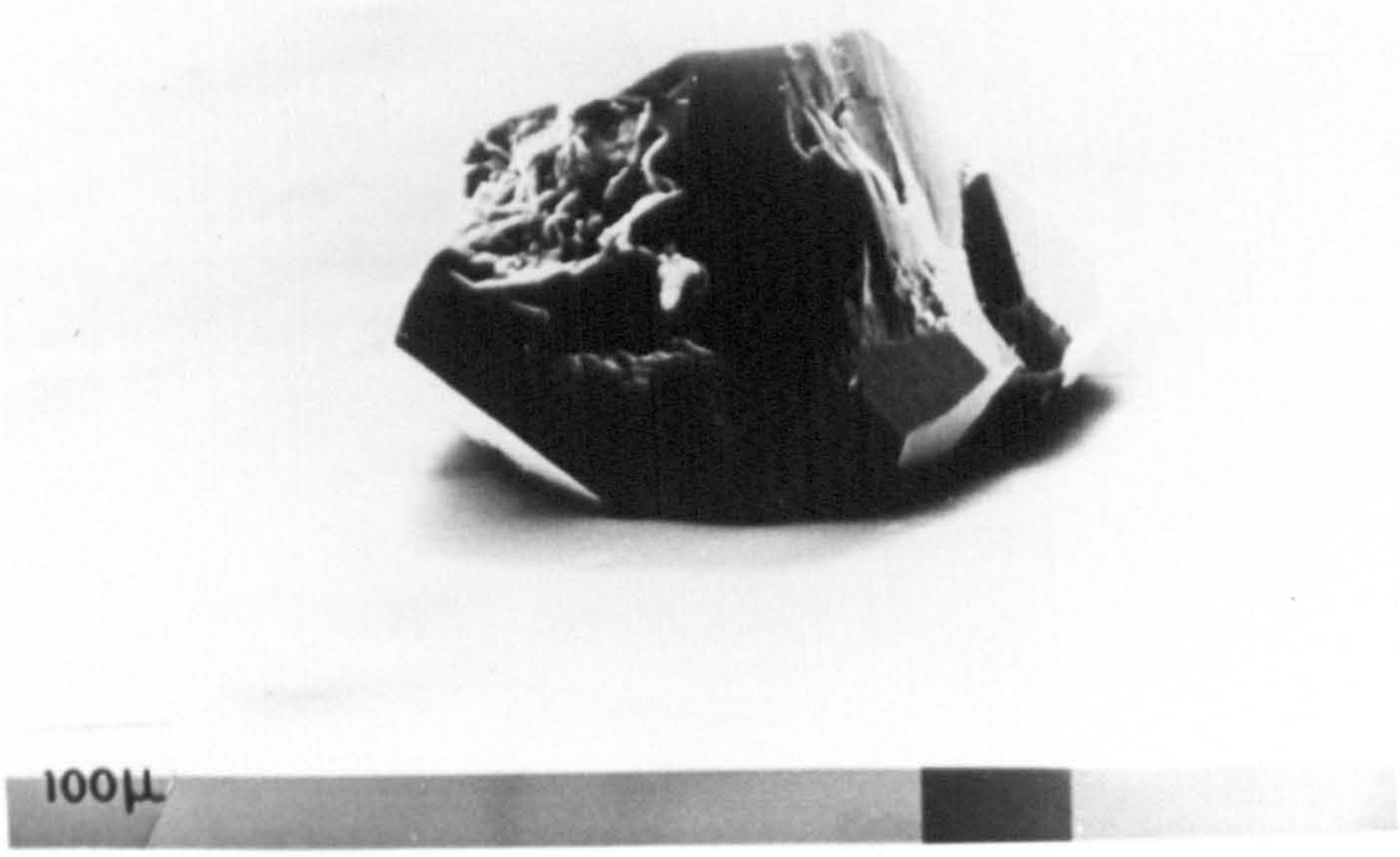

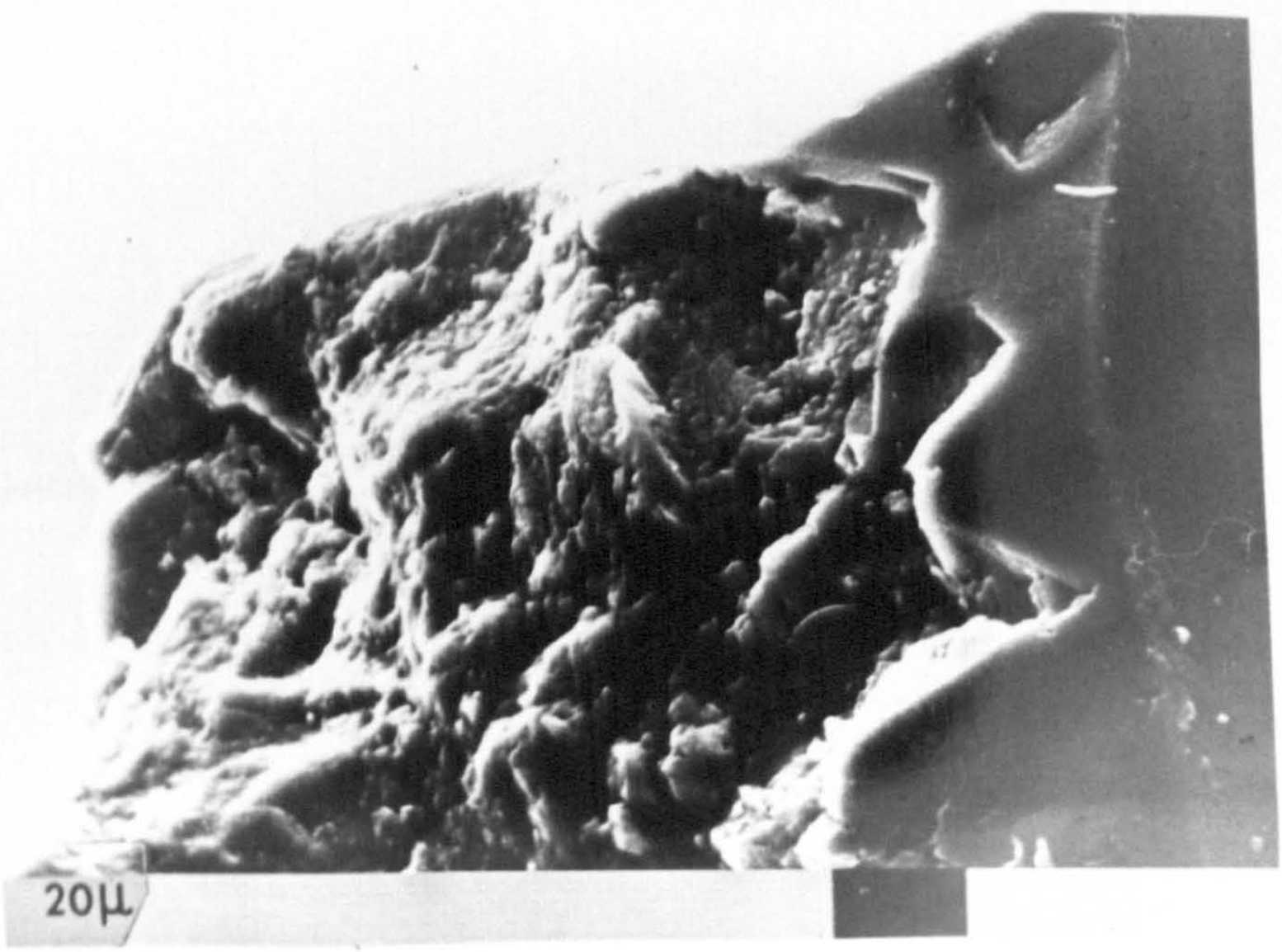

Fig. 4.12. Sample 7UE, grain D.
Chemical corrosion of a euhedral grain. Initial stages of corrosion include the formation of triangular shaped pits.

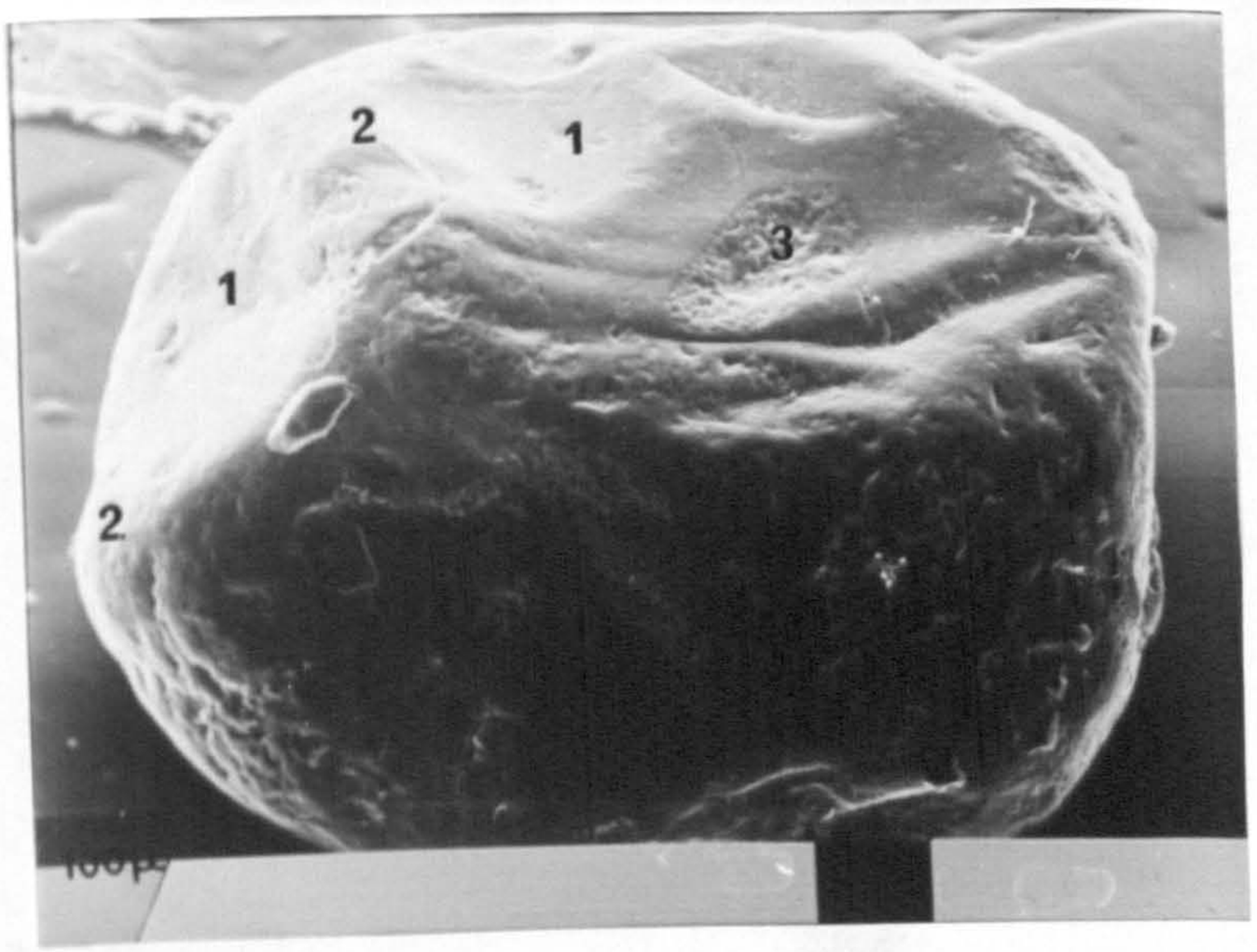

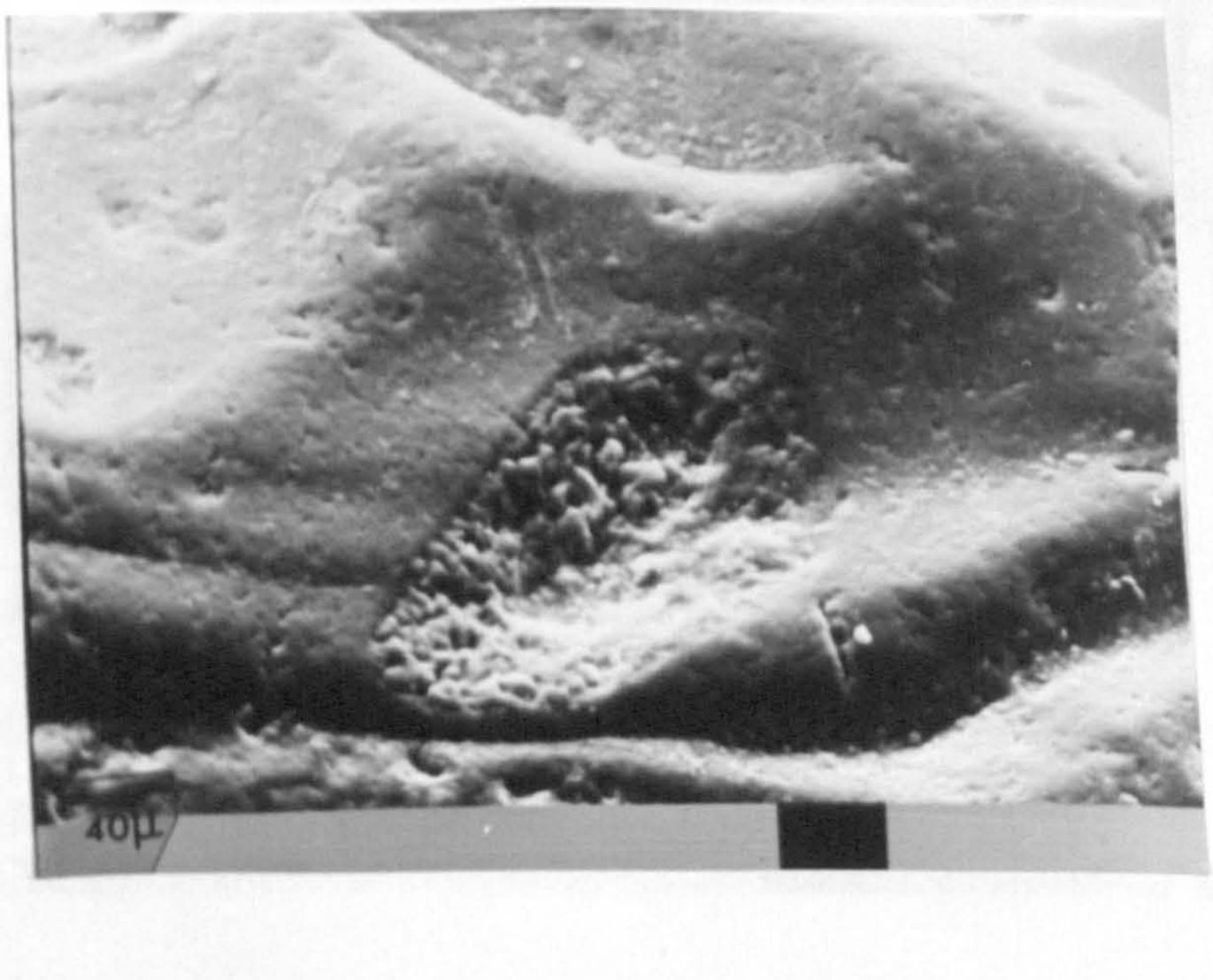

Fig. 4.13. Sample 7UE, grain D'.
Grain exhibiting three surface textures:
1. large-scale conchoidal fractures,
2. rounding and pitting,
3. chemical etching.
The lower photograph shows the chemically etched area in detail.

a

b

Fig. 4.14. Sample C1, grain 3.
Chemical etching (ce) overprinted on an angular grain of high relief with small-scale breakage blocks.
The lower photograph shows etching along orientated lines of weakness in the upper middle area of the upper photograph.

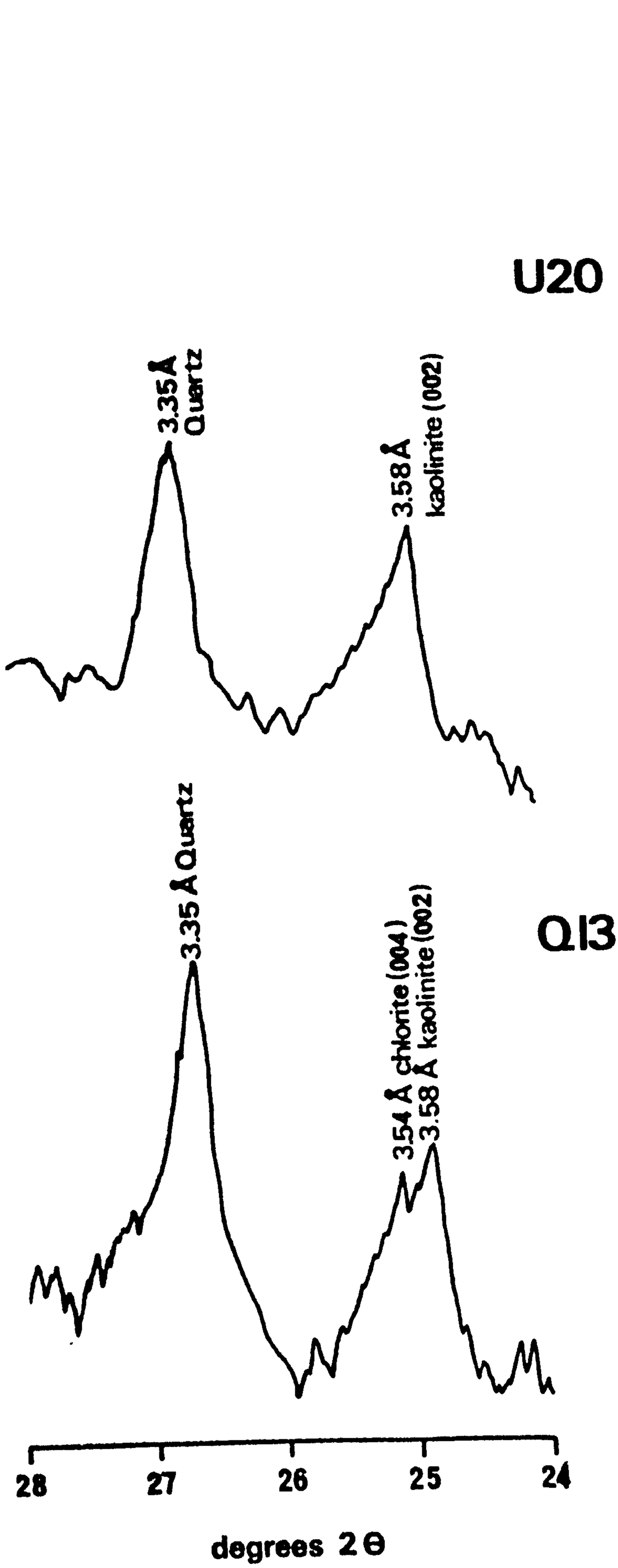

Fig. 4.14c. X-ray diffractograms of samples U20 and Q13.
Q13 shows the differentiation between chlorite and kaolinite.

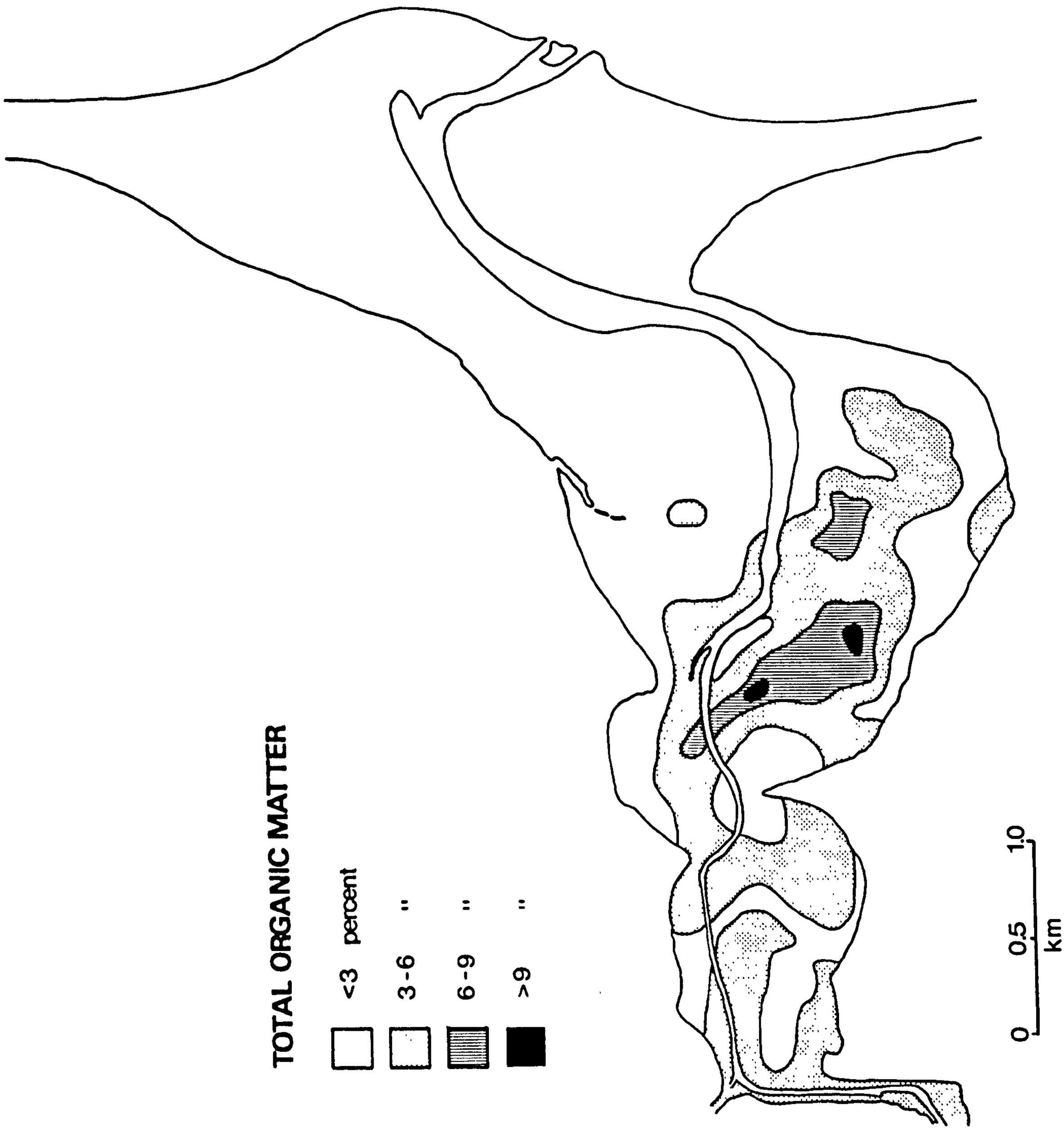

Fig. 4.15. The variation in total organic matter.

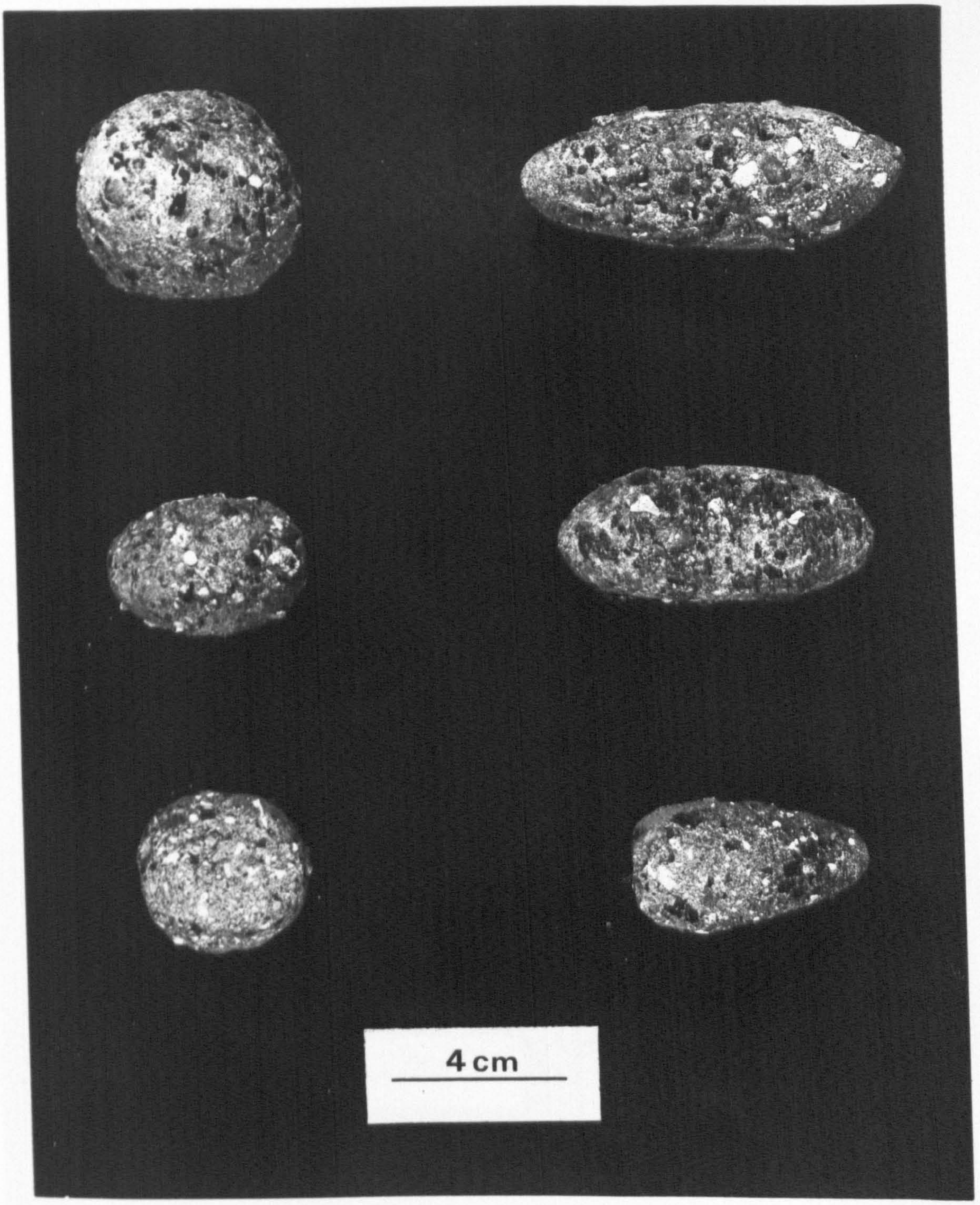

Fig. 4.16a. Armoured mudballs from the eastern area at Out Head.

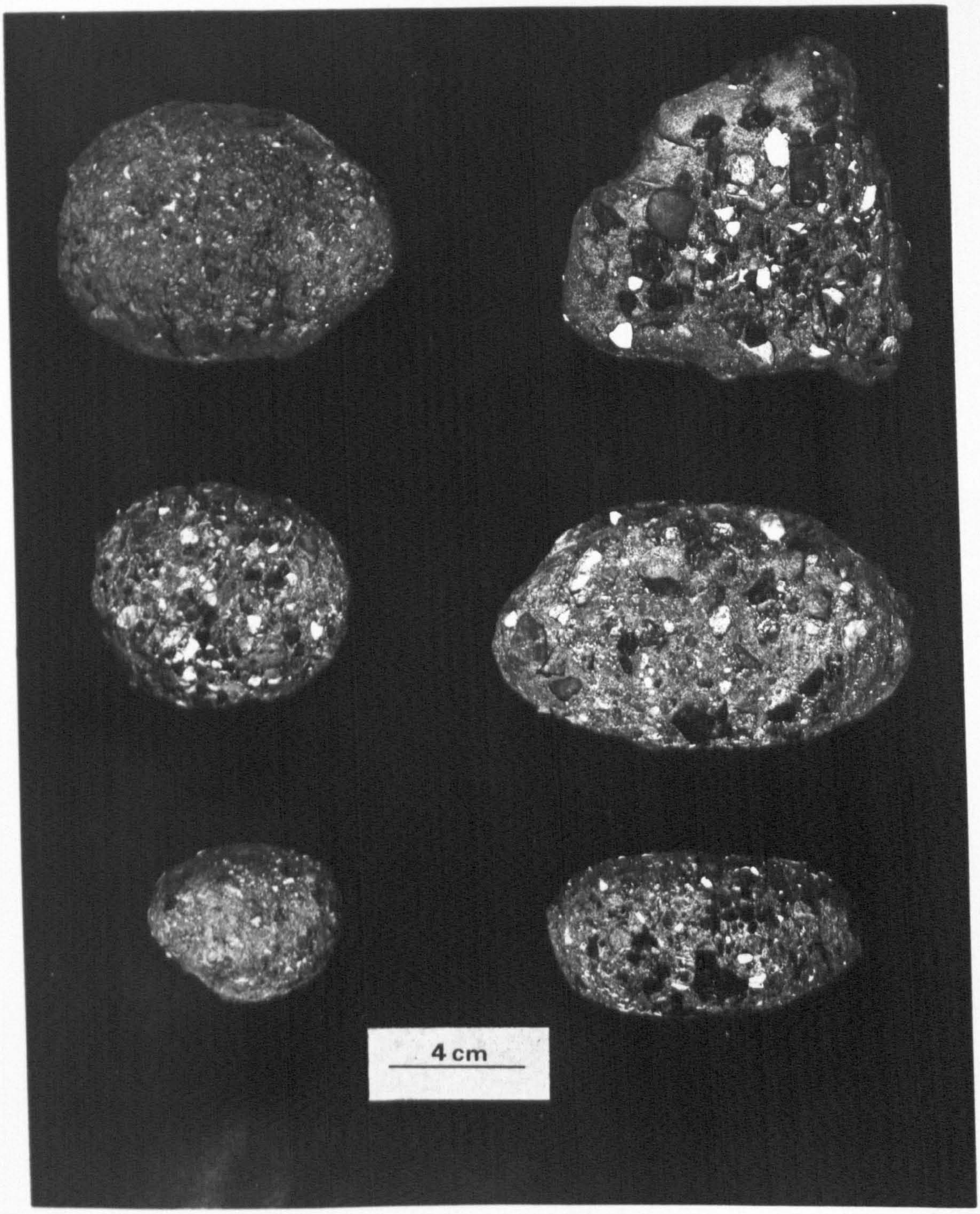

Fig. 4.16b. Armoured mudballs from the western area at Out Head.

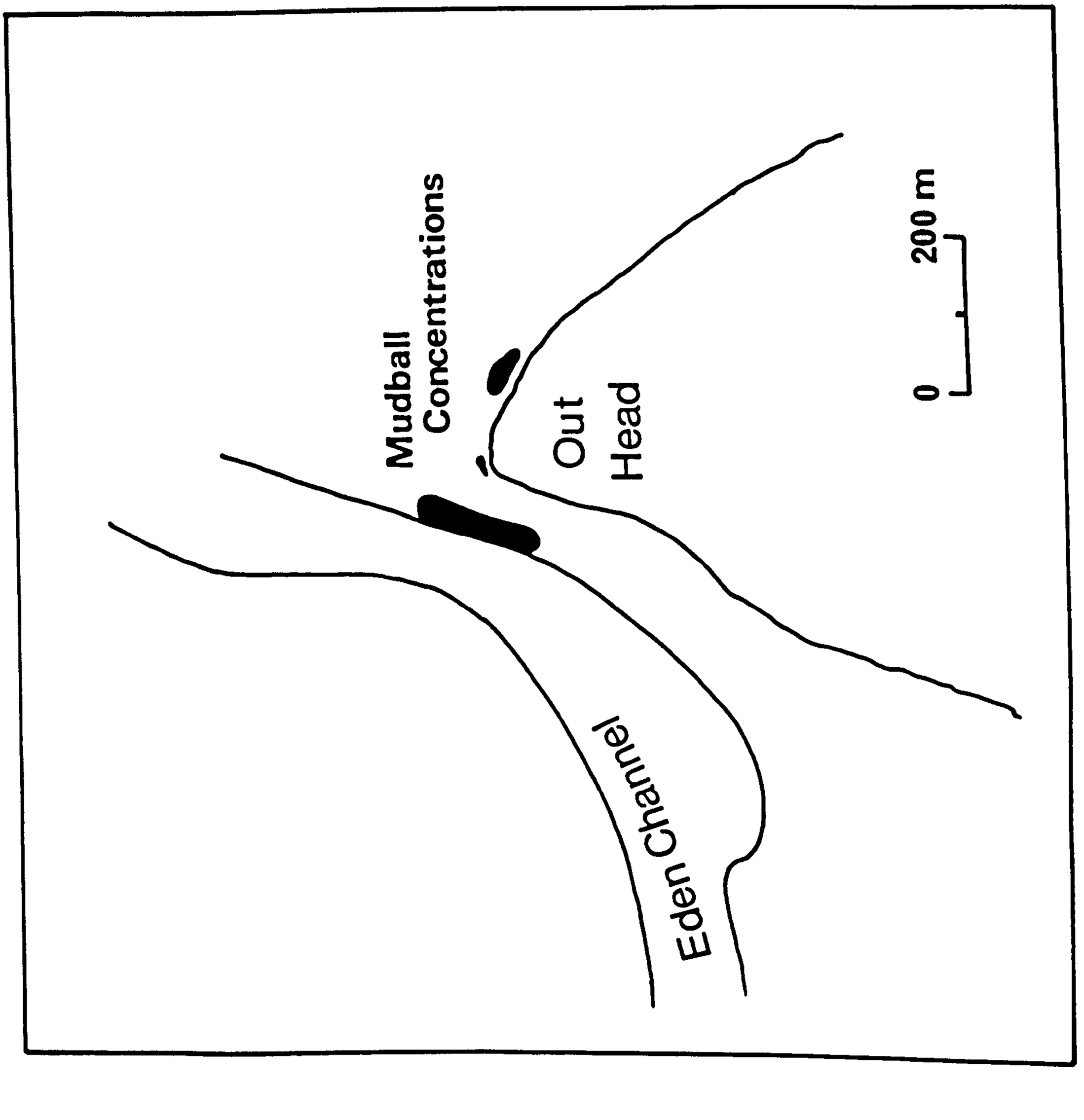

Fig. 4.17. Areas of mudball concentration.

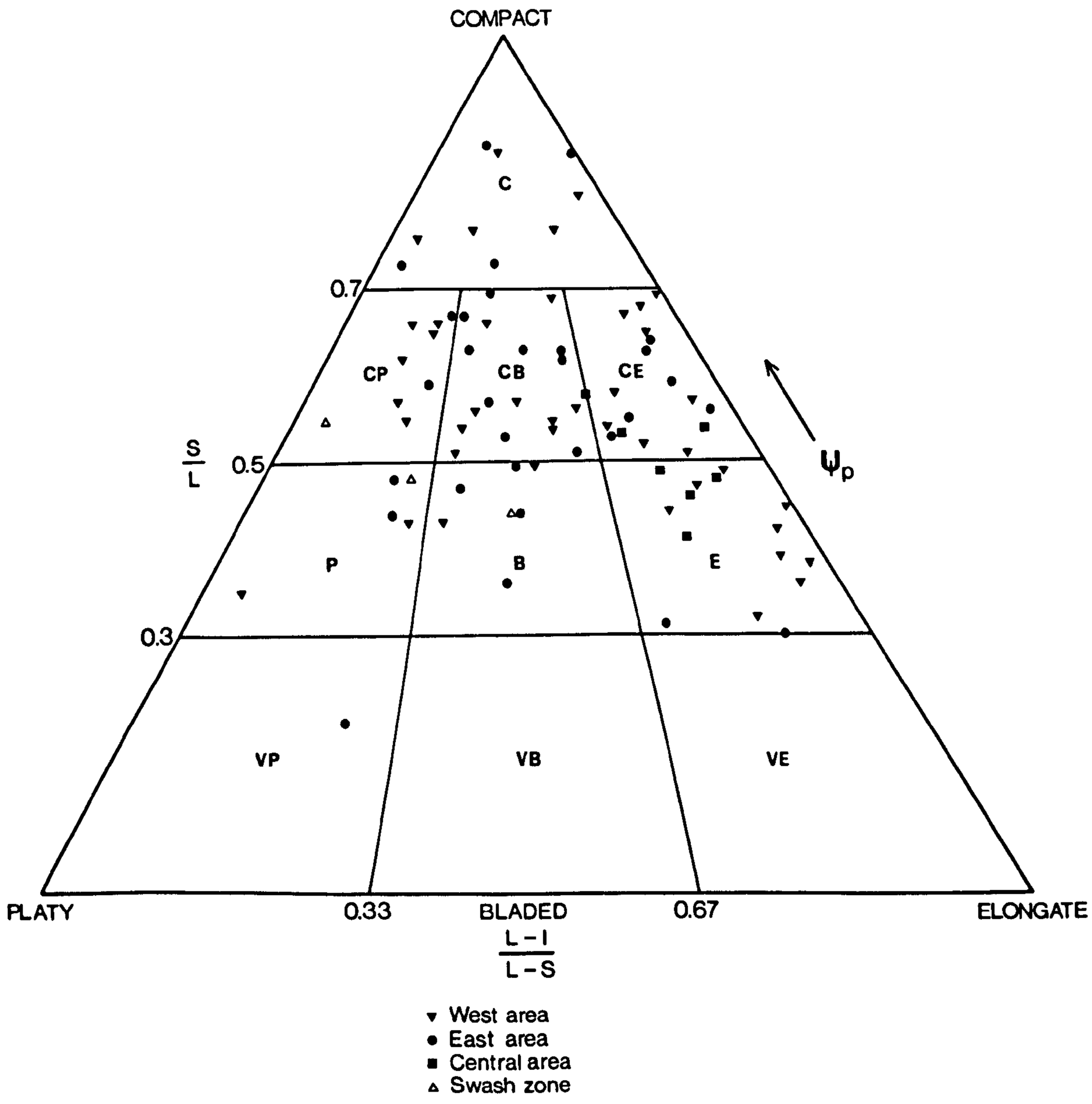

Fig. 4.18. Sphericity-form diagram for Eden estuary mudballs.

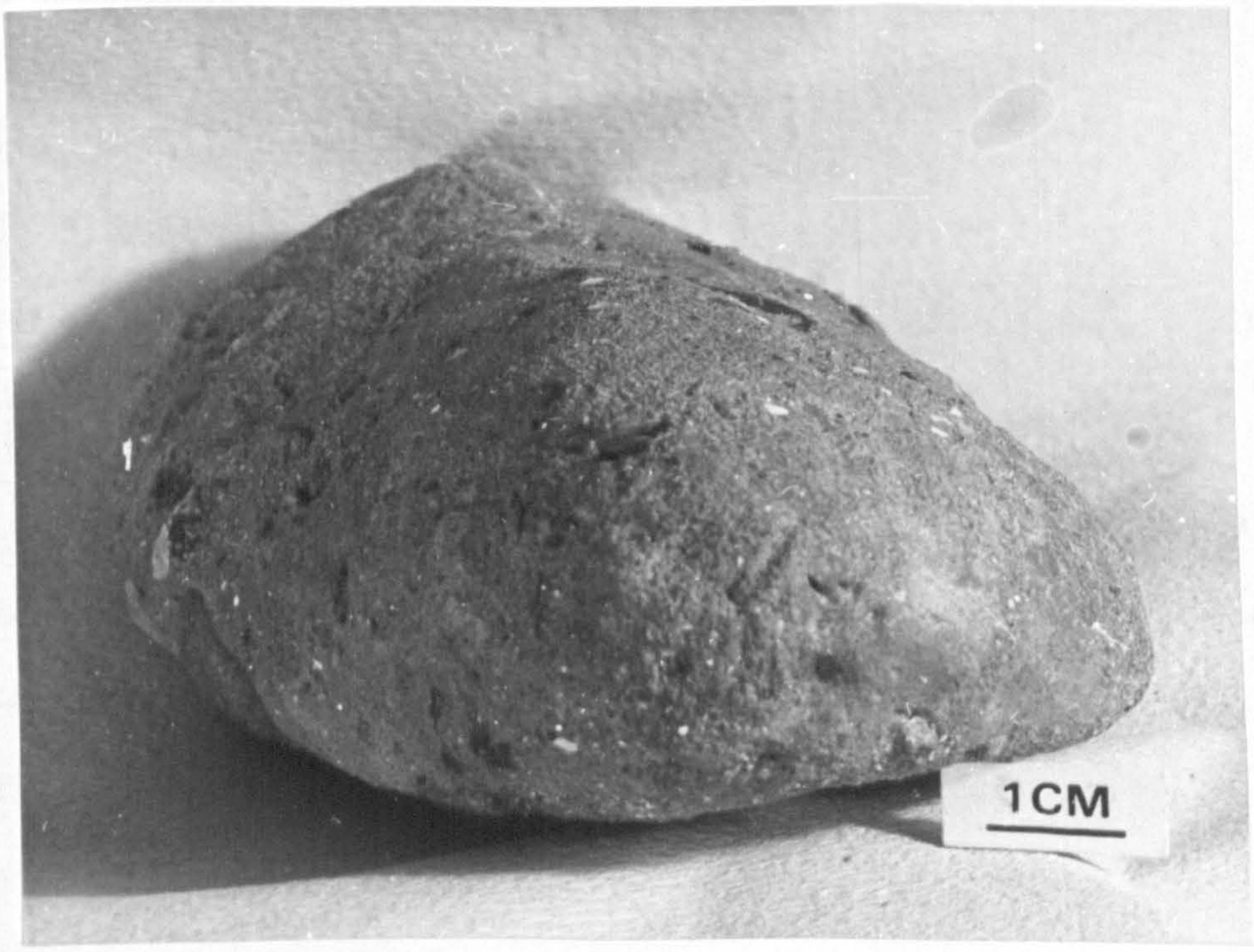

Fig. 4.19. A 'dreikanter' type mudball from the swash-zone.

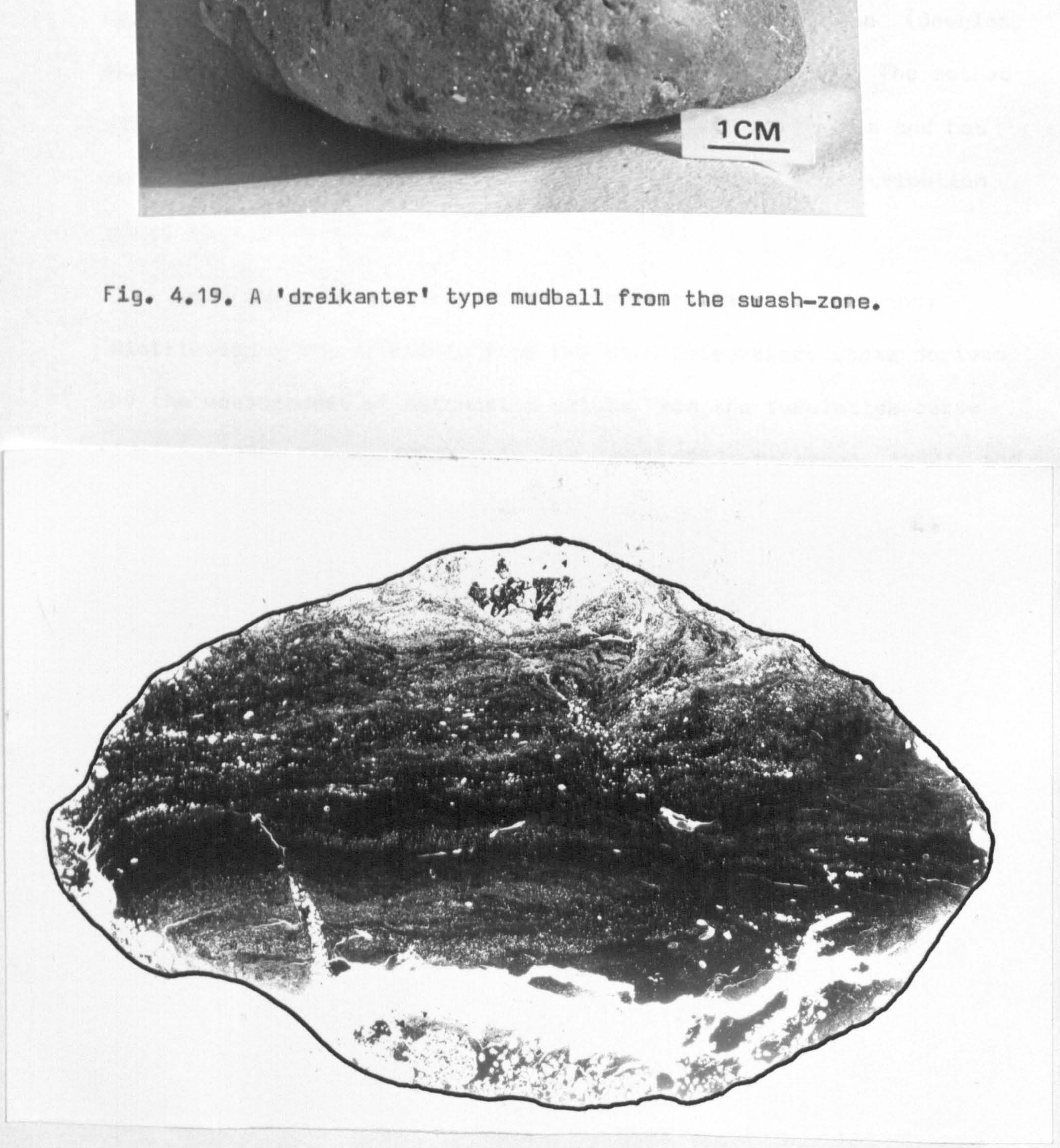

Fig. 4.20. Thin section of an armoured mudball (x5).

IV. TEXTURAL ANALYSIS

Graphical Methods and Summary Statistics

Weight frequency data may be summarised by graphical methods or descriptive statistics (Krumbein and Pettijohn, 1938; Folk, 1966; Griffiths, 1967).

Amongst the graphical methods of analysis the cumulative size frequency curve using phi-probablility scales is versatile (Doeglas, 1946, 1968; Moss, 1962, 1963, 1972; Visher, 1965, 1969). The method allows direct visual comparison of frequency distributions and has an in-built criterion for phi-normality: a phi-normal distribution plots as a straight line.

Descriptive or summary statistics of grain-size frequency distributions are divisible into two main categories: those derived by the measurement of percentile values from the cumulative curve (Trask, 1932; Inman, 1952; Folk and Ward, 1957; McCammon, 1962), and those calculated by the method of moments from the original weight-frequency data (Krumbein and Pettijohn, 1938; Griffiths, 1967).

Percentile techniques are influenced by (a) truncation of the data if distributions are more than 5% open-ended, (b) bias in the estimators introduced by skewness and kurtosis in the samples, and (c) the grouping process involved in sieve analysis (Jones, 1970; Hails, Seward-Thompson and Cummings, 1973).

Moment summary statistics are similarly affected by the grouping process and are not suitable for the description of distributions which are more than 1% open-ended (Jones, 1970).

In this study the distributions of 123 samples were open-ended by more than 1% due to the presence of material with an equivalent fall-diameter of less than 2 microns. To maintain uniformity, all grain-size parameters were therefore calculated from the Folk and

Ward (1957) formulae (Appendix 4, part 1). Samples which contained more than 5% of clay-sized material were treated by extrapolating from the last point determined by pipette analysis (9 phi) to 100% at 14 phi, assuming a phi-normal distribution with a mean of 11.5 phi (Folk, 1968).

The Folk and Ward measures of mean, standard deviation, skewness and kurtosis were calculated using an extensively modified version of Allen's (1970) computer program for granulometric analysis (Appendix 4, part II). The statistics for each sample are listed in Appendix 4, part III.

Mean Grain Size

Mean grain size decreases westwards from Out Head towards Coble Shore and from the north and south margins of the estuary towards the Eden channel (Fig. 4.21). The channel sediments are characteristically coarser than those of the intertidal flats. Grain-size ranges from -0.36 phi to 7.99 phi with an average value of 2.90 phi.

In the lower estuary east of Sanctuary Spit mean grain-size varies between 1.95 and 2.92 phi. North of the Eden channel means are coarser than 2.5 phi, and a zone characterised by mean grain-sizes of 1.95 to 2.25 phi runs southwards from South Tentsmuir beach and then turns to the south-west and trends parallel to the north bank of the channel; the zone eventually terminates in the flood-channel systems of the flood-tidal delta. To the south of the Eden channel, the West Sands and a south-west trending lobate zone to the west of Out Head are characterised by mean grain-sizes of 2.5 to 2.92 phi.

In the middle estuary means are more variable and range from 3.0 to 7.99 phi. Grain-size gradually decreases from the marginal areas of the intertidal flats towards the Eden channel. Minimum values occur in the sediments adjacent to the channel between Guardbridge and Coble House Point, and on Kincaple Flat to the south of the Eden channel.

The sediments of the Eden channel are the coarsest in the estuary with mean grain-sizes between -0.36 and 2.53 phi. Sediments from the channel in the middle and lower estuary are generally more coarsely grained than those from the channel of the upper estuary.

Standard Deviation

The distribution of Inclusive Graphic Standard Deviation is shown in Figure 4.22. Values range from 0.24 to 3.7 phi with an estuary average of 1.62 phi. Contouring at a one phi interval defined two main areas:

1. the lower estuary,

2. the middle and upper estuary.

The fine sands of the lower estuary have standard deviations of less than 0.5 phi, and on Folk's scale would be classed as 'well-sorted'. Three areas within the lower estuary are characterised by sorting indices of less than 0.35 phi, and hence are 'very well-sorted'. These are:

1. the West Sands (σ_I 0.24 to 0.36) which are subjected to the passage of the breaker zone four times a day. The best sorted sands occur on the lower foreshore in the area of low modal grain sizes (2.98ø). On the topographically high spit-platform which extends northwards from Out Head the sorting values are between 0.29 and 0.36 phi.

2. the counterpart of the spit-platform to the north of the Eden channel. Sorting values range from 0.28 to 0.33 phi.

3. the flood and ebb channels of the flood-tidal delta system.

In the middle estuary standard deviation increases from the marginal areas towards the channel. Values between 1 and 3 phi are general, with isolated areas of values greater than 3 phi occurring in the central parts of Kincaple Flat.

Skewness

The distribution of skewness values (Fig. 4.23) shows that the lower estuary samples have near-symmetrical or negatively skewed grain-size frequencies, whereas those of the middle and upper estuary are characterised by positive skewness.

Sediments of the lower estuary from South Tentsmuir beach and from south of the Eden channel are coarse skewed (Sk_I -0.1 to -0.29). A similar asymmetry is associated with the sediments around the terminal portion of the Eden channel on the stoss-side of the ebb-tidal delta. The majority of the remaining outer estuary samples have near-symmetrical distributions with Sk_I values between -0.1 and +0.1. Positive skewness (Sk_I +0.1 to +0.3) is developed in medium to fine sands in two restricted areas of the lower estuary, the crestal area of the ebb-tidal delta and the seaward parts of channels in the flood-tidal delta.

Strongly fine skewed sediments dominate the middle and upper estuary. There is a general trend towards increasing positive skewness to the south-west and maximum values ($Sk_I > +0.5$) occur on the marginal areas of Kincaple Flat and on Edenside Flat.

Kurtosis

The distribution of kurtosis, K_G, (Fig. 4.24) shows a two-fold division in the outer estuary and a zonal arrangement in the middle estuary.

The sediments of South Tentsmuir beach and the ebb- and flood-tidal deltas are mesokurtic (K_G 0.9 to 1.1) and are thus 'normal' with respect to kurtosis. Sediments of the West Sands and those immediately west of Pilmour Links are leptokurtic (K_G 1.1 to 1.5).

Middle estuary sediments grade from extremely leptokurtic ($K_G > 3.0$) examples on the south marginal area of Kincaple Flat to very platykurtic

(K_G < 0.67) examples in the zone adjacent to the Eden channel. Isolated samples with extreme kurtosis occur on Edenside Flat, to the south of Sanctuary Spit and to the west of Shelly Point.

Relationships between the Statistical Parameters

1. Standard Deviation versus Mean Grain-Size

The relationship between standard deviation and mean grain-size (Fig. 4.25a) conforms to the Folk and Ward (1957) model of a sinusoidal trend. The sediments with the minimum standard deviations have means in the fine sand range (2 to 3 phi). Sediments of coarser mean size, 2 to -1 phi, show increasing values of standard deviation (σ_I). Over the range of mean sizes from 3.0 to 6.5 phi there is a distinct trend towards larger standard deviations with a maximum recorded value of 3.59 phi. Mean values of 6.5 to 8.0 phi are accompanied by slightly decreasing values of standard deviation.

2. Skewness versus Mean Grain-Size

A sinusoidal trend is produced by variation in skewness with mean size (Fig. 4.25b). This again conforms to the Folk and Ward (1957) model. Negative skewness is associated with means between -1 and 2 phi. The majority of samples in the mean size range 2 to 3 phi have skewness values within the range -0.25 to +0.25, but there is an overall trend of increasing positive skewness with decreasing grain-size. Maximum skewness values are reached at mean size values between 3.5 and 4.0 phi and between 4 and 8 phi there is a trend towards decreasing positive skew.

3. Kurtosis versus Mean Grain-Size

The relationship between kurtosis and mean grain-size (Fig. 4.25c) shows that marked deviations from normality are associated with sediments of mean size 2.5 to 4 phi. Many sediments in the 2 to 3

phi range are, however, normal with K_G values of approximately one. Similar values are also shown by sediments with means of 4.5 to 5 phi.

4. Skewness versus Kurtosis

Variation of skewness with kurtosis (Fig.4.25d) shows two trends perpendicular to each other. Kurtosis values of less than 2 are associated with the whole range of skewness values from −0.5 to +0.8, whereas K_G values above 2 are always associated with positive skewness in the range 0.25 to 0.80.

The striking resemblance of the bivariate plots (Fig. 4.25, a – d) to those produced by Folk and Ward (1957) suggests that an interpretation of the textural variation of these sediments based on the thesis of the mixing of several modal populations may be valid. The various plots suggest that a well-sorted, fine sand with a near-symmetrical and mesokurtic grain-size distribution is modified by the addition of silt and clay and/or medium to coarse sand and gravel populations.

Grain-size Modes

Although the mean is a measure of the overall average size of a sediment, it is only of limited value in the interpretation of a sediment's geological history. The mean is only really significant for sediments which have normal grain-size distributions with low standard deviations. The measure does not adequately characterise the size of gravel/sand or sand/mud mixtures.

Curray (1960) and Brezina (1963) stressed the use of grain-size modes in the study of mixed sediments, and Kranck (1975) suggested that the modal size of a bottom sediment might be a better environmental indicator than the mean.

The distribution of modal grain-size in the Eden estuary (Fig. 4.25) shows a trend of decreasing diameters to the south-west. Modal grain-size is in the range of 2 to 3 phi over the whole of the intertidal area apart from a narrow zone adjacent to the Eden channel in the middle estuary. Each grain-size mode was taken as the mid-point of the 0.25ϕ size interval which contained the maximum weight percentage of sediment in a sample. The gradational nature of the distribution, from modes of 2.13 phi in the north-east to 2.38 in the south-west, suggests that the actual gradation is on a scale finer than that indicated by the above method of modal size derivation.

In the lower estuary the modal grain-size accurately reflects the mean grain-size, but this is to be expected as the distributions are near phi-normal. The dominant mode to the north of the Eden channel is 2.38 phi. Several high energy areas however are characterised by modes of 2.13 phi. To the south of the channel in the lower estuary 2.13 phi is the common modal size. The only exceptions were two samples from the lower foreshore of the West Sands which had modes of 2.88 phi.

The 2.63 phi modal size continues into the middle estuary and predominates in the marginal areas. However, in the central areas of Kincaple Flat and on Edenside Flat grain-size decreases and the modal size is 2.88 phi. These modal values bear no resemblance to the mean values. If the modal and mean grain-size data are integrated, it is evident that (a) the basic sediment population is fine sand which gradually decreases in grain-size to the south-west and (b) that silt and clay-size material has been added to, and mixed with this basic population in the middle estuary.

The channel sediments are somewhat coarser and have modes between 1.38 and 2.13 phi. The coarser modes tend to occur in the channel of the lower estuary.

Sediment Sub-Population Analysis

Introduction

An R-mode factor analysis (Harbaugh and Merriam, 1968; Allen, Castaing and Klingebiel, 1972; Mather, 1972; Klovan, 1975) was applied to the Eden estuary grain-size data in order to evaluate the relationships between the 53 variables measured on each sample. The result was that the variation in grain-size data could be accounted for by the changing proportions of eight groups of grain-size classes which are analogous to the sediment sub-populations of Moss (1962, 1963, 1972) and Visher (1965, 1969).

Input Data and Computer Program

The analysis was performed on the 53 variables measured on each of 156 samples. The variables were the weight percentages of sediment in each 0.25 phi size-interval between -3.75 phi and 9.0 phi and the weight percent of clay-size material of equivalent fall diameter less than 9.0 phi.

The computer program used was the Corfan-Fortran IV Factor Analysis with Varimax Rotation program of Ondrick and Srivastava (1970). From a raw-data matrix A_{nxm}, where n is the number of samples and m the number of variables, an m x m correlation matrix is computed utilising the Pearson product-moment correlation coefficient 'r'. From the correlation matrix eigenvalues and eigenvectors are extracted by principal components analysis. The eigenvectors are then converted into a form in which the vector length represents the magnitude of the eigenvalue, the result of which is a 'factor': a vector which is weighted proportionally to the amount of the total variance which it represents. The factor axes are then rotated by the Varimax procedure (Davis, 1973), so that they will be highly correlated with some of the original variables.

The Factor Model

The R-mode factor analysis technique seeks to reduce the number of variables required to describe a sample by the production of several new variables which are linear combinations of the original variables. The procedure should result in no significant loss of information. The new variables are termed 'factors'.

The factor model may be represented by the following equation (Rather, 1972):

$$Z_j = a_{j1}F_1 + a_{j2}F_2 + \cdots\cdots\cdots a_{jk}F_k + d_jU_j$$

where $j = 1,2,\ldots\ldots m$

This equation states that the original variable Z_j is represented by a linear combination of k common factors (F) plus a unique factor (U_j). Each of the k factors is assumed to be involved in the delineation of two or more variables, and hence is termed 'common'. The factor U_j is a factor unique to variable Z_j. The a's in the equation are factor loadings (a_{j1} is the loading of the jth variate on factor 1) and as such indicate the contribution of a factor to a variable. In terms of the factor model the total variance of a variable is made up of the sum of the squared a's (see Klovan, 1975). That portion of the total variance due to the common factors is termed the 'communality' (h_j^2); the remaining variance is attributed to the unique factor and may be due to specific and/or error variance. d_j is the loading of the unique factor.

Results

1. The Efficiency of the Method

R-mode factor analysis with varimax rotation produced eight orthogonal factors, which together explained 92.45% of the total variance in the data correlation matrix. This represents a reduction in the number of original variables by 85% with only a 7.55% loss in

information. The cumulative variance curve (Fig. 4.27) shows that the first three factors account for 70.29% of the variance, and that there is a marked decrease in the variance explained by the five succeeding factors. At the grossest level, therefore, three factors satisfactorily account for the variation in the grain-size frequency data.

2. Identification of the Factors

By definition 'factors' are linear combinations of the original variables, and as such are groups of grain-size classes. The rotated matrix of factor loadings (Table 4.8) shows the relationships between the eight factors and the 53 variables. The factor loadings in each row show the degree to which each factor contributes to a specified variable. Normally one factor is dominant over the others: for example, factor 7 is the main contributor to variable 1 and factor 6 to variable 2. The columns show that, although each factor contributes to each variable, certain groups of variables are associated with specific factors by virtue of numerically high factor loadings. Factor 1, for example, loads heavily on variables 33 to 53 and factor 2 on variables 3 to 15.

On the basis of the numerical values of the factor loadings listed under each factor in the rotated matrix groups of grain-size classes were isolated and termed 'sediment sub-populations'. The grain-size limits of each sub-population were determined by selecting a cut-off value for factor loadings below which the associated factor was not considered to contribute significantly to the variable. The cut-off value was set at 0.5 (Harbaugh and Merriam, 1968), and a sub-population was defined as a group of grain-size classes, each of which had a factor loading greater than +0.5 or algebraically less than -0.5. The loading profiles of six of the eight factors are diagrammatically summarised in Figures 4.28a, 4.28b. Factors 7 and 8 have

Table 4.8. The rotated matrix of factor loadings.

Variable	F 1	F 2	F 3	F4
1	-0.02346	-0.38915	0.00451	0.01781
2	-0.01738	-0.14498	0.05236	0.00346
3	-0.02686	-0.60644	0.18828	0.02167
4 -3Ø	-0.02920	-0.63294	0.14349	0.01110
5	-0.02835	-0.92058	0.15285	0.00725
6	-0.03473	-0.87543	0.17680	0.00116
7	-0.04306	-0.91202	0.29649	0.01270
8 -2Ø	-0.03251	-0.86242	0.40905	0.00396
9	-0.03957	-0.86631	0.39216	0.00514
10	-0.03259	-0.90901	0.37433	0.00308
11	-0.03427	-0.88329	0.42835	0.00424
12 -1Ø	-0.03607	-0.83023	0.49735	0.00822
13	-0.02442	-0.38766	0.63959	0.02033
14	-0.04489	-0.63031	0.71656	0.01467
15	-0.04401	-0.55631	0.79060	0.01076
16 0Ø	-0.04681	-0.46518	0.86258	0.00831
17	-0.04927	-0.36645	0.91501	0.00994
18	-0.05649	-0.31157	0.93608	0.01781
19	-0.06183	-0.28141	0.93793	0.02332
20 1Ø	-0.08033	-0.20959	0.95745	0.03450
21	-0.09292	-0.20026	0.93686	0.05542
22	-0.10244	-0.10298	0.92811	0.07382
23	-0.17841	-0.07450	0.80662	0.17411
24 2Ø	-0.28164	-0.01759	0.44509	0.39102
25	-0.40842	0.08040	0.08186	0.62784
26	-0.49410	0.10791	-0.18631	0.73786
27	-0.56658	0.17174	-0.31506	0.56005
28 3Ø	-0.51755	0.17501	-0.34066	-0.35765
29	-0.19760	0.10567	-0.23174	-0.88906
30	0.01722	0.06911	-0.18053	-0.84149
31	0.28229	0.03955	-0.09572	-0.45345
32 4Ø	0.46985	0.02835	-0.05062	-0.22219
33	0.63732	0.03012	-0.04327	-0.10177
34	0.60742	0.04346	-0.06085	-0.07758
35	0.70607	0.04432	-0.05989	-0.04687
36 5Ø	0.84109	0.04549	-0.06426	-0.04212
37	0.87803	0.04359	-0.05552	-0.04659
38	0.93700	0.03946	-0.06825	-0.06162
39	0.94437	0.03731	-0.06202	-0.05751
40 6Ø	0.94938	0.03767	-0.06025	-0.03395
41	0.93903	0.03765	-0.05619	-0.03383
42	0.95812	0.03312	-0.05052	-0.03354
43	0.97103	0.03209	-0.05131	-0.03168
44 7Ø	0.97421	0.03055	-0.05217	-0.03102
45	0.95252	0.02846	-0.05315	-0.01466
46	0.94523	0.03329	-0.03480	-0.01628
47	0.94727	0.02425	-0.04558	-0.03550
48 8Ø	0.95210	0.02494	-0.05609	-0.03466
49	0.95970	0.02393	-0.06351	-0.03869
50	0.93361	0.02543	-0.05767	-0.01358
51	0.91964	0.02867	-0.06517	-0.01897
52 9Ø	0.94853	0.02466	-0.05867	-0.02446
53 S+C	0.89806	-0.05102	-0.00677	-0.09984
SUM SQ	18.56900	8.78350	9.90143	3.38022
VAREXP	35.03584	16.57263	18.68193	6.37778
CUMPER	35.03584	51.60847	70.29041	76.66818

Table 4.8. The rotated matrix of factor loadings (continued).

Variable	F 5	F 6	F 7	F 8
1	0.00924	-0.17496	0.87012	-0.01956
2	0.01187	-0.94962	0.03321	-0.04740
3	0.00799	-0.68941	0.07072	0.05274
4 -3Ø	0.01533	-0.72862	0.18704	-0.01904
5	0.01523	-0.00787	0.32216	-0.01451
6	0.01423	0.12869	0.23847	-0.06209
7	0.01922	-0.08871	0.12170	-0.06329
8 -2Ø	0.02109	-0.24196	-0.08637	0.02795
9	0.02371	-0.21394	0.16704	-0.02223
10	0.01875	-0.07984	-0.11864	-0.00171
11	0.02077	-0.10808	-0.08540	0.00076
12 -1Ø	0.01983	-0.12834	-0.07499	0.02822
13	-0.08240	-0.03497	-0.01512	0.11633
14	0.02256	-0.07988	-0.16706	0.02820
15	0.01222	-0.04351	-0.17512	0.05565
16 0Ø	0.01903	-0.04225	-0.10519	0.05706
17	0.01351	-0.01193	-0.05320	0.04704
18	0.02045	-0.02270	-0.01984	0.02107
19	0.02722	-0.03015	0.03309	-0.00588
20 1Ø	0.03770	-0.02458	0.04832	-0.07154
21	0.05821	-0.03164	0.10928	-0.14694
22	0.06614	-0.04318	0.11473	-0.22391
23	0.09505	-0.06569	0.10817	-0.44081
24 2Ø	0.11625	-0.05169	0.03968	-0.69785
25	0.15556	0.02090	-0.04866	-0.57045
26	0.19852	0.05346	-0.07863	-0.09679
27	0.27614	0.07420	-0.04808	0.24757
28 3Ø	0.35232	0.06502	-0.02107	0.45887
29	0.03665	0.03895	-0.03697	0.17312
30	-0.39334	0.03044	-0.05287	0.01663
31	-0.74084	0.02160	-0.02912	-0.00983
32 4Ø	-0.80193	0.01038	-0.00559	0.00035
33	-0.71702	0.00729	0.00284	0.02571
34	-0.73086	0.00820	0.00947	0.07964
35	-0.63082	0.00929	0.01150	0.09540
36 5Ø	-0.36882	0.00987	0.01090	0.09377
37	-0.34198	0.01001	0.00930	0.08932
38	-0.22470	0.01078	-0.00068	0.05333
39	-0.21807	0.01011	-0.00067	0.04645
40 6Ø	-0.17701	0.01210	-0.00343	0.05389
41	-0.14006	0.01050	0.00154	0.05765
42	-0.08274	0.01066	-0.00576	0.02286
43	-0.07855	0.01032	-0.00454	0.03014
44 7Ø	-0.04672	0.01086	-0.00865	0.01464
45	-0.03260	0.00883	-0.00490	0.01529
46	-0.10006	0.01273	-0.00903	0.03212
47	0.02538	0.01134	-0.01946	-0.02544
48 8Ø	-0.03470	0.01096	-0.01612	-0.01125
49	0.00968	0.01021	-0.01746	-0.02072
50	-0.05002	0.01195	-0.01528	0.00622
51	-0.09043	0.01169	-0.01298	0.01460
52 9Ø	-0.05036	0.01059	-0.01556	-0.00385
53 S+C	-0.09610	-0.05758	0.03864	-0.02758
SUM SQ	3.55523	2.14674	1.17102	1.48367
VAREXP	6.70797	4.05046	2.20947	2.79937
CUMPER	83.37614	87.42661	89.63606	92.43542

significant loadings on only one and two variables respectively (Table 4.8, p. 122).

Factor 1 shows positive loadings in excess of 0.5 on the range of size intervals between 4.0 and 9.0 phi and on the variable representing the clay content (Fig. 4.28a). The maximum loading of 0.97 is associated with the 6.5 to 7.0 phi interval. Sub-population 1 is therefore defined as the combined silt and clay component of a sediment. This sub-population is the most important contributor to textural variation within the estuary accounting for 35.04% of the total grain-size variance.

Factor 2 shows high negative loadings on the grain-size classes between -1.0 and -3.0 phi (Fig. 4.28a) and sub-population 2 is therefore composed of granules and very small pebbles (size terminology of Griffiths, 1966, table 5.2, after Wentworth, 1922). This sub-population introduces 16.57% of the total grain-size variance.

Factor 3 loads heavily on the grain-size classes between -1.0 and 2.0 phi (Fig. 4.28a). The maximum loading occurs on the 0.75 to 1.0 phi interval and loadings in excess of 0.9 are associated with the 0.25 to 1.5 phi range of sizes. This very coarse-, coarse-, and medium-sand population accounts for 18.68% of the total grain-size variation.

Factor 4 shows high factor loadings on the range of grain-sizes between 2.25 and 3.50 phi (Fig. 4.28b). The corresponding sub-population (4) therefore consists of fine and very fine sand. The loading profile shows that there are two distinct sub-groups within the above size range. Size intervals between 2.25 and 3.0 phi have positive loadings with a maximum of 0.74 at 2.5 phi, whereas those between 3.0 and 3.5 phi have negative loadings with a maximum of -0.89 at 3.25 phi. That both groups have factor loadings greater than the cut-

off value, but of opposite sign, indicates that an inverse relationship exists between the two, that is, as the amount of very fine sand in a sample increases, there should be an equal decrease in the content of fine sand. In terms of the variance explained, the sub-population is relatively minor and accounts for only 6.38%.

Factor 5 loads heavily on the grain-size classes between 3.5 and 4.75 phi with a maximum loading of -0.80 at 4.0 phi (Fig. 4.28b). Sub-population 5 is therefore composed of very fine sand and very coarse silt. Both grades have been incorporated in previous sub-populations (4 and 1 respectively), but their combination in sub-population 5 may indicate that in certain areas and under certain conditions the two grades may behave as a separate grain-size unity. The sub-population accounts for only 6.71% of the total variance.

Factor 6 has high loadings on the size range -3.0 to -3.5 phi (Fig. 4.28b) and defines a small-pebble sub-population (6). 4.05% of the total variance is explained by this population.

Factor 7 has a loading greater than 0.5 on only one variable, and the sub-population (7) consists of the medium-sized pebbles found in only one sample. Consequently the variance accounted for is very low: 2.2%.

Factor 8 has negative loadings algebraically less than -0.5 on size intervals 2.0 to 2.5 phi and the sub-population (8) is composed of fine sand. Fine sand contributes very little to grain-size variation: 2.8%.

Although fine sand (2.0 to 3.0 phi) is only of very minor importance in terms of grain-size variation, it is the most abundant size-grade in the estuarine sediments (Appendix 5). Fine sand must be regarded as the basic sub-population with which all other sub-populations are mixed in varying proportions to produce the observed

textural variations.

3. Distribution of the Sub-Populations

The textural nature of a sediment is a function of the grain-sizes available for redistribution and the environmental conditions prevailing at the depositional site. Within the estuarine sediments as a whole eight sediment sub-populations are important in defining textural variations. Each sub-population does not, however, occur in each sediment sample, and in certain areas of the estuary one or more sub-populations are preferentially concentrated. Such concentrations are inferred to be controlled by local environmental conditions with a major role being played by the hydrodynamic factors of tidal current and wave action and the biological factors of sediment agglutination and sediment trapping.

The silt and clay sub-population of the intertidal flat sediments varies from less than 1% in the sediments of the lower estuary to over 90% in those in the vicinity of Coble House Point (Fig. 4.29). The general distribution is one of increasing silt and clay content to the west and south-west with a secondary trend of increasing values from the estuary margins towards the Eden channel. Maximum concentrations occur in a narrow zone adjacent to the Eden channel between Guard-bridge and Coble House Point and on Kincaple Flat to the south of the Eden channel.

Fine-grained sediment is transported into the estuary by the River Eden and the flood-tidal currents, but no quantitative data on suspended-sediment loads are available. Silt and clay-size material is also derived locally from the erosion of sedimentary deposits within the estuary. These include: the Carse clay, which is exposed in parts of the Eden channel and on Kincaple Flat; mussel banks which border the Eden channel; and the silty-sand and mud-flats of the middle

estuary.

The form in which the silt and clay were transported cannot be determined from a conventional analysis of bottom sediments, as the analytical procedure involves the dispersal of the sediment into individual mineral grains. Whether the grains were transported in a flocculated state, or whether flocculation played an important role in sediment deposition is indeterminable.

The environmental factors which are believed to influence the concentration of fine-grained sediment in the middle estuary include a decrease in the competency of waning flood-tidal currents, tidal effects of settling-lag and scour-lag (Van Straaten and Keunen, 1958), sediment agglutination by the mussel Mytilus edulis, and sediment trapping by the extensive algal colonies.

The granule and very small pebble sub-population occurs only in the Eden channel where it comprises between 1.11 and 33.42% of individual samples (Fig. 4.30). No component of this sub-population was found in the deposits of the flood- or ebb-tidal deltas, and it would appear that there should be a concentration of granules and very small pebbles in the lower reaches of the Eden channel. The high value of 33.4% recorded for a sediment off Out Head might indicate that this area is a null-point where a balance between flood- and ebb-tidal current transport of this size-grade is maintained. The values obtained for the grade are a function of sample position within the channel as shown by the figures of 8.78 and 0% at the tidal inlet (Fig. 4.30). The coarsest grains were to be found on the northern side of the channel where both flood and ebb-tidal currents concentrate.

The very-coarse-, coarse-, and medium sand sub-population is of major importance in the channel sediments and in the sediments of the lower estuary to the north of the Eden channel (Fig. 4.31). The channel sediments contain up to 58 wt% of medium sand and decreasing

amounts of coarse-sand (<24 wt%) and very-coarse sand (<15 wt%). The intertidal flat sediments contain up to 65 wt% of this sub-population, but are totally devoid of the very-coarse sand fraction and characteristically contain less than 1% of the coarse sand fraction. In this context sub-population 3 may conveniently be equated with medium sand alone.

In the area of medium sand concentration in the lower estuary there is a marked zonal arrangement in which concentrations in excess of 20 wt% border the north bank of the Eden channel and are flanked by a zone of concentrations between 10 and 20 wt%. A second area of high concentration (>20 wt%) occurs on the crest of the ebb-tidal delta.

The concentrations of medium sand coincide with areas which are strongly influenced by tidal currents and wave action. Flood-tidal currents dominate the northern margin of the Eden channel as witnessed by the development of large-scale, flood-orientated bedforms, and ebb-tidal currents similarly affect the stoss-side of the ebb-tidal delta. South Tentsmuir Beach and the crestal area of the ebb-tidal delta are subject to both tidal-currents and wave action at different stages of the tide. This combination favours the accumulation of medium- and, to a very limited extent, coarse sand.

<u>The very-fine sand sub-population</u> occurs in excess of 10 wt% in the sediments of the middle and upper estuary and the West Sands (Fig. 4.32). Maximum concentrations of 30-50 wt% occur in a narrow E-W trending zone on Edenside Flat. The similarity of the geographic distributions of this sub-population and the silt and clay sub-population in the middle estuary may be indicative of similar concentrating processes.

Sediments of the West Sands, however, are devoid of silt and clay,

but do contain up to 13 wt% of very-fine sand. Depositional conditions are markedly different from those in the middle estuary, and the upper few centimetres of sediment are constantly reworked by the passage of the breaker zone four times a day. Breaking waves and the associated swash and backward effects generate upper flow regime conditions (Clifton et al., 1971) under which fine grained sediments (<0.25mm) will be transported in the rheologic state and/or put into suspension (Moss, 1972). Moss's(1972) flume data suggest that during the rheologic stage fine sediment may be driven into the bed by dispersive pressure, so preventing its removal from the local system. It is interesting to note that the very-fine sand only accumulates in the lee of Out Head and Pilmour Links where the sediment is unaffected by ebb-tidal currents.

The very-fine sand/very-coarse silt sub-population shows a similar distribution to that of the silt and clay sub-population with a zone of high concentration (10-20 wt%) trending NW-SE across the middle estuary (Fig. 4.33).

The small-pebble sub-population occurred in only four samples, from the Eden channel between Guardbridge and Coble Shore. The pebbles may have been derived from boulder clays which border parts of the upper estuary or from the gravel at the base of the local carse sequence.

The fine-sand sub-population is ubiquitous and its distribution shows antipathetic relationships with the other sub-populations (Fig. 4.34). In the lower estuary the fine-sand content is generally in excess of 60 wt%. There is a general decrease westwards, and values also decrease from the estuary margins toward the central areas.

Conclusions

1. Eight sediment sub-populations contribute to textural variation

in the Eden estuary. These are:

1. Silt and clay
2. Granules and very-small pebbles
3. Very-coarse-, coarse-, medium sand
4. Very-fine sand
5. Very-fine sand and very-coarse silt
6. Small pebbles
7. Medium pebbles
8. Fine sand.

2. Fine sand is the most abundant and widespread of the sub-populations and accounts for very little textural variation. It is the basic sub-population with which the remaining seven sub-populations are mixed in varying proportions to produce the observed textures.

3. Sub-populations 1, 2 and 3 explain 70.29% of the total variation in the data, and the simplest expression of textural variation would be in terms of the mixing of gravel, medium to coarse sand, and silt and clay with fine sand.

4. By virtue of the fact that sub-populations 2, 6 and 7 are restricted to the Eden channel, intertidal flat textural variation is controlled mainly by sub-populations 1 and 3 (silt and clay, and medium sand) and to a lesser extent by sub-populations 4 and 5 (very-fine sand and very-coarse silt).

5. The concentration of specific sub-populations in certain areas of the estuary may be relatable to local environmental conditions which include hydrodynamic and biological factors.

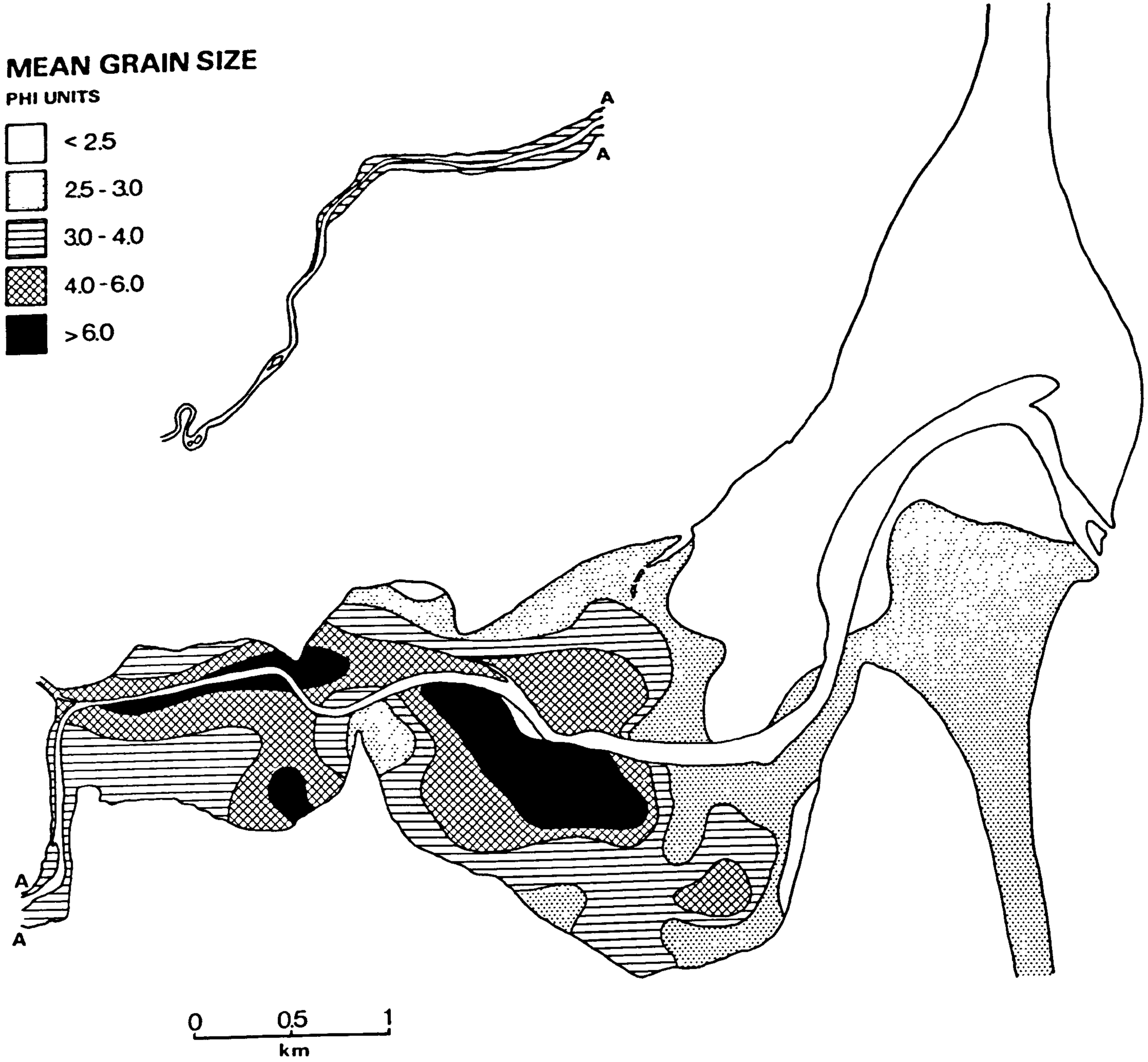

Fig. 4.21. The distribution of Mean Grain Size.

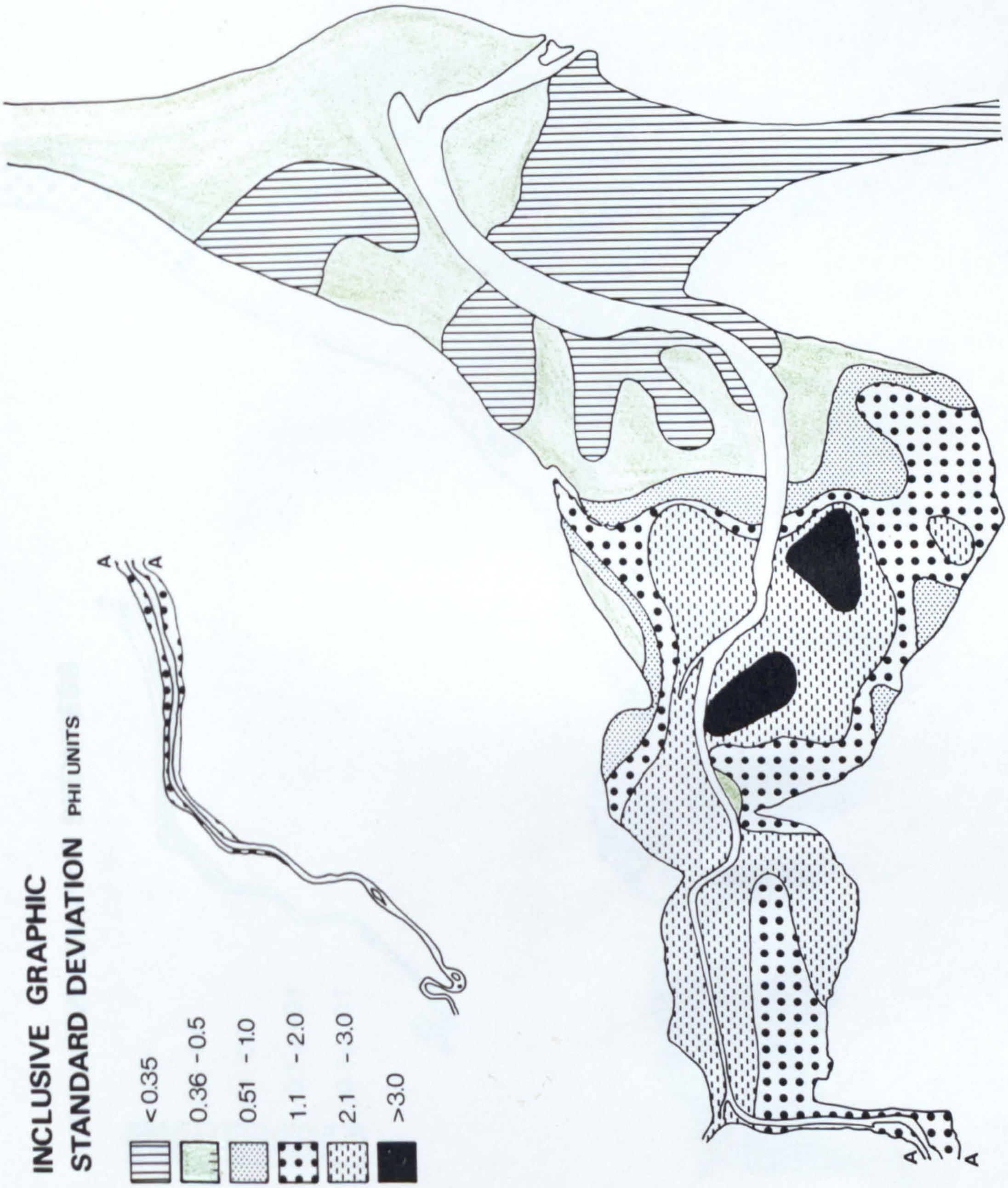

Fig. 4.22. The distribution of Inclusive Graphic Standard Deviation.

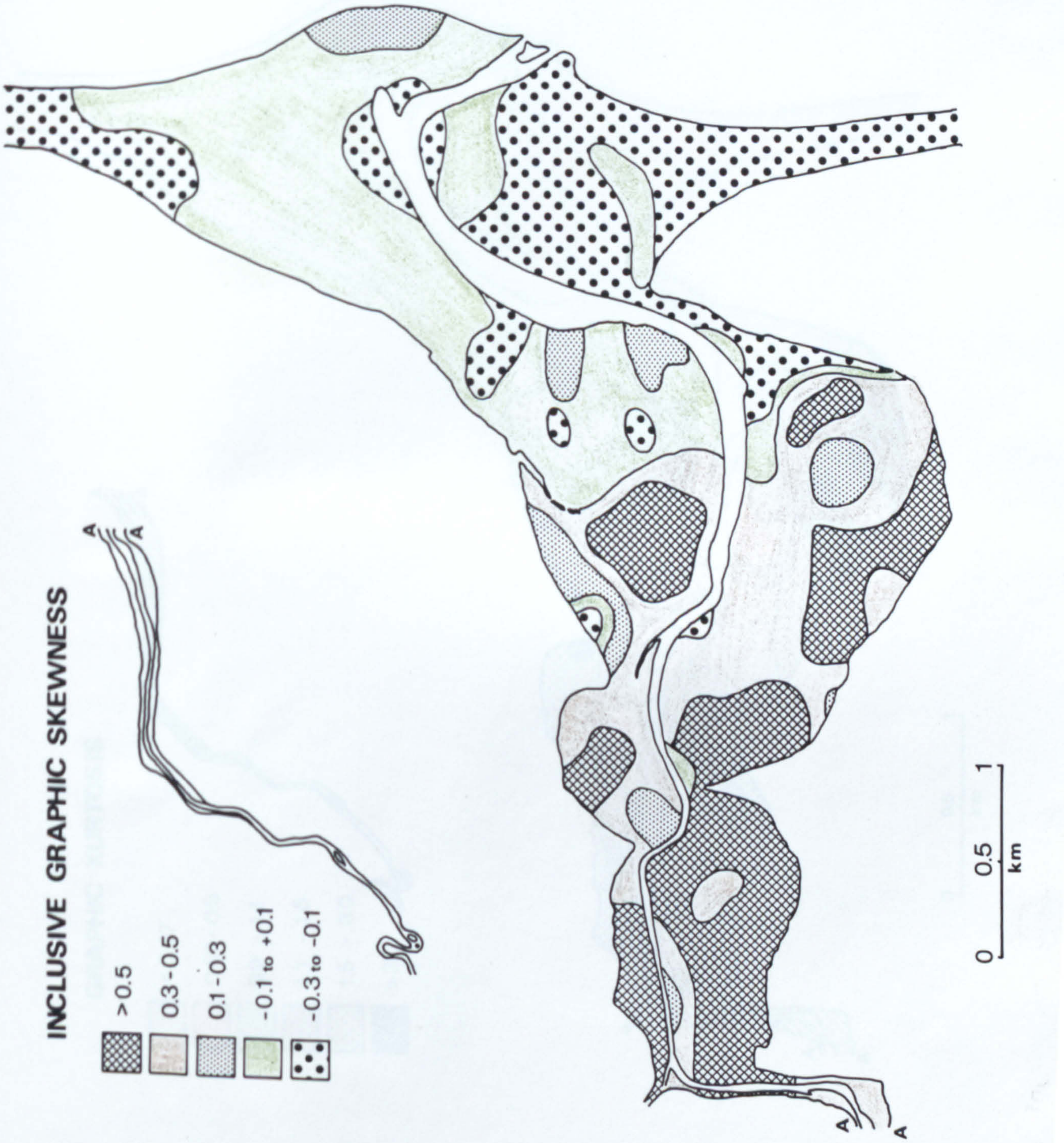

Fig. 4.23. The distribution of Inclusive Graphic Skewness.

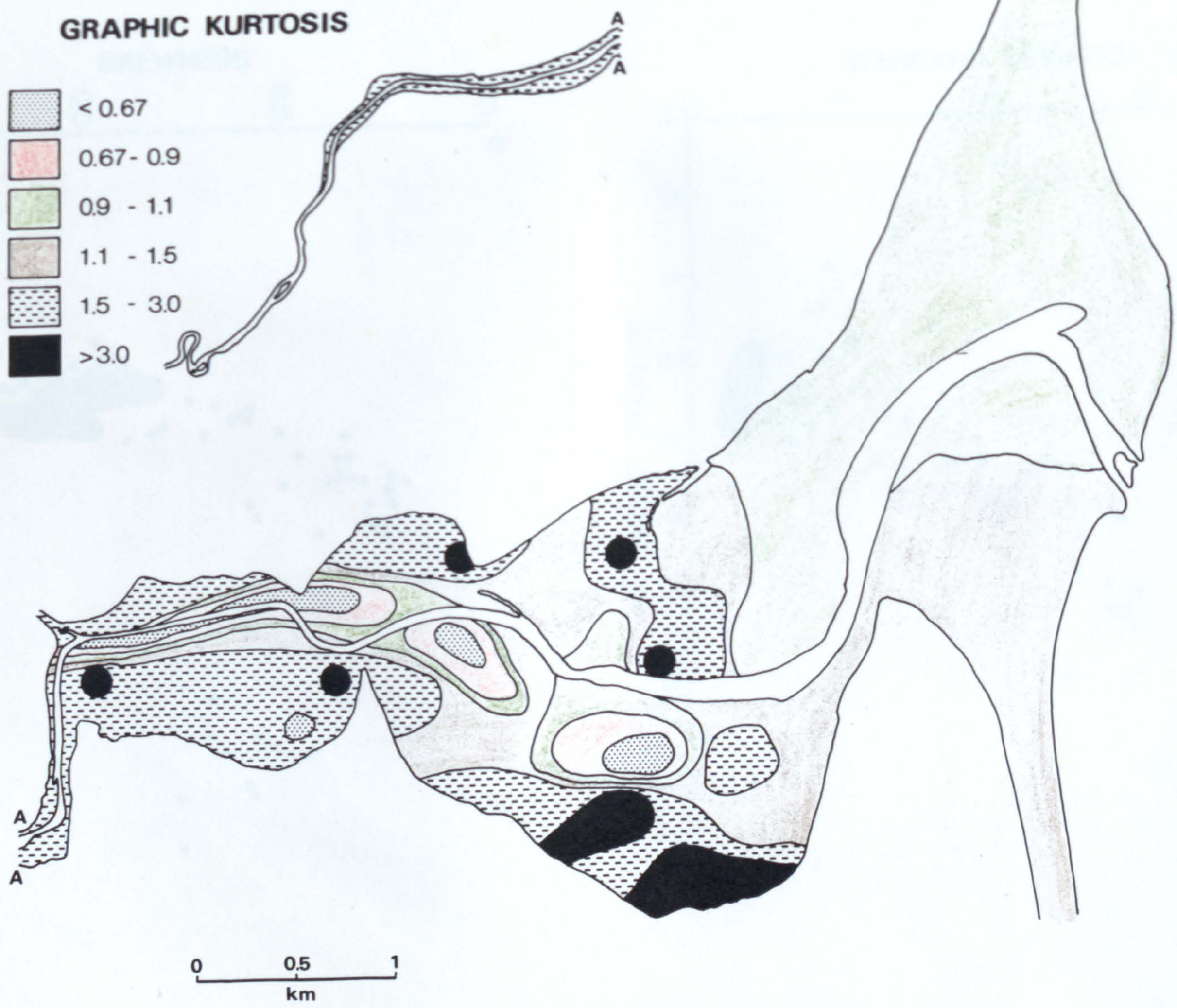

Fig. 4.24. The distribution of Graphic Kurtosis.

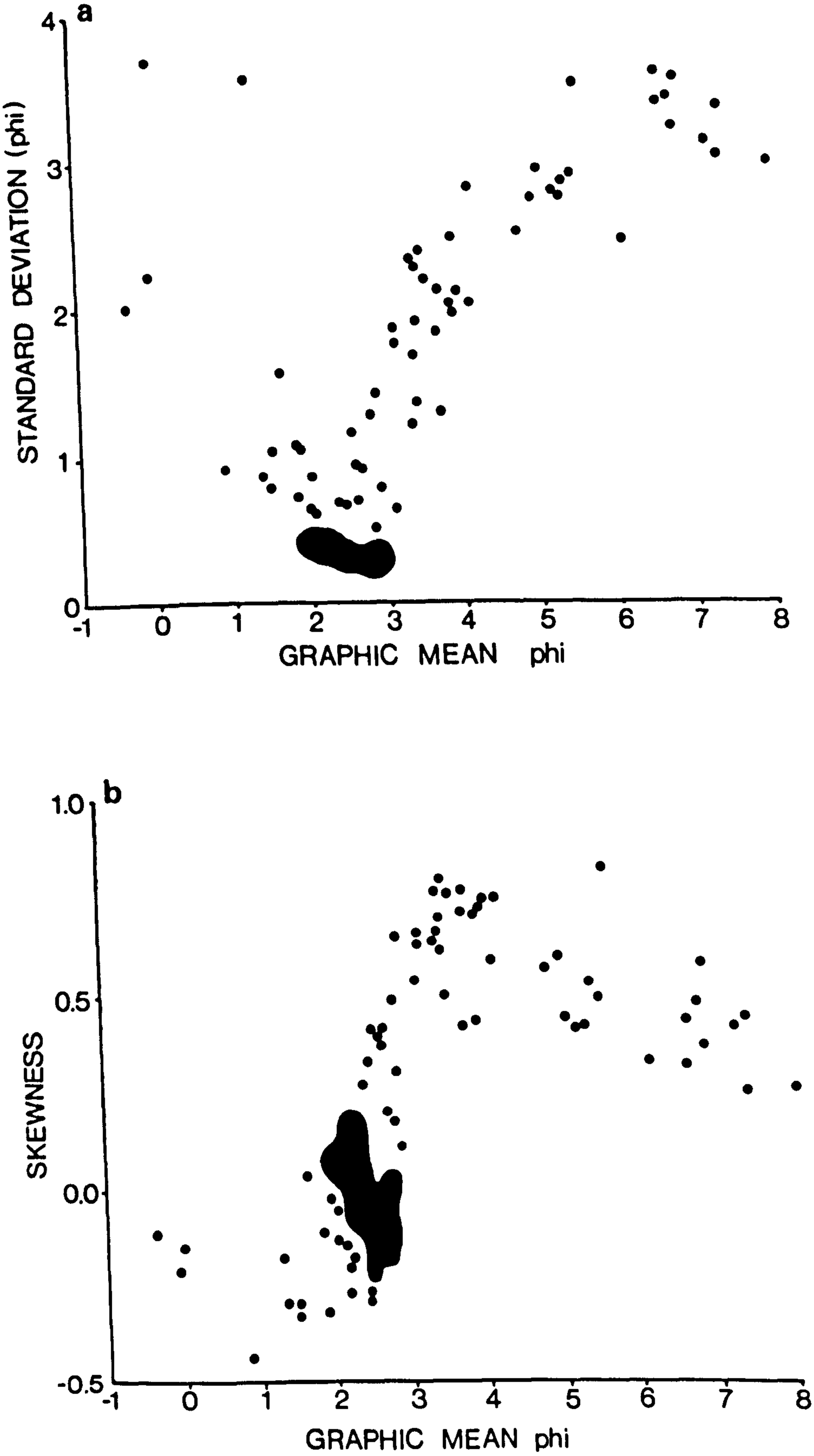

Fig. 4.25a. The variation in Standard Deviation with Mean Grain Size. Shaded area encloses 93 sample points.
b. The variation in Skewness with Mean Grain Size. Shaded area encloses 86 sample points.

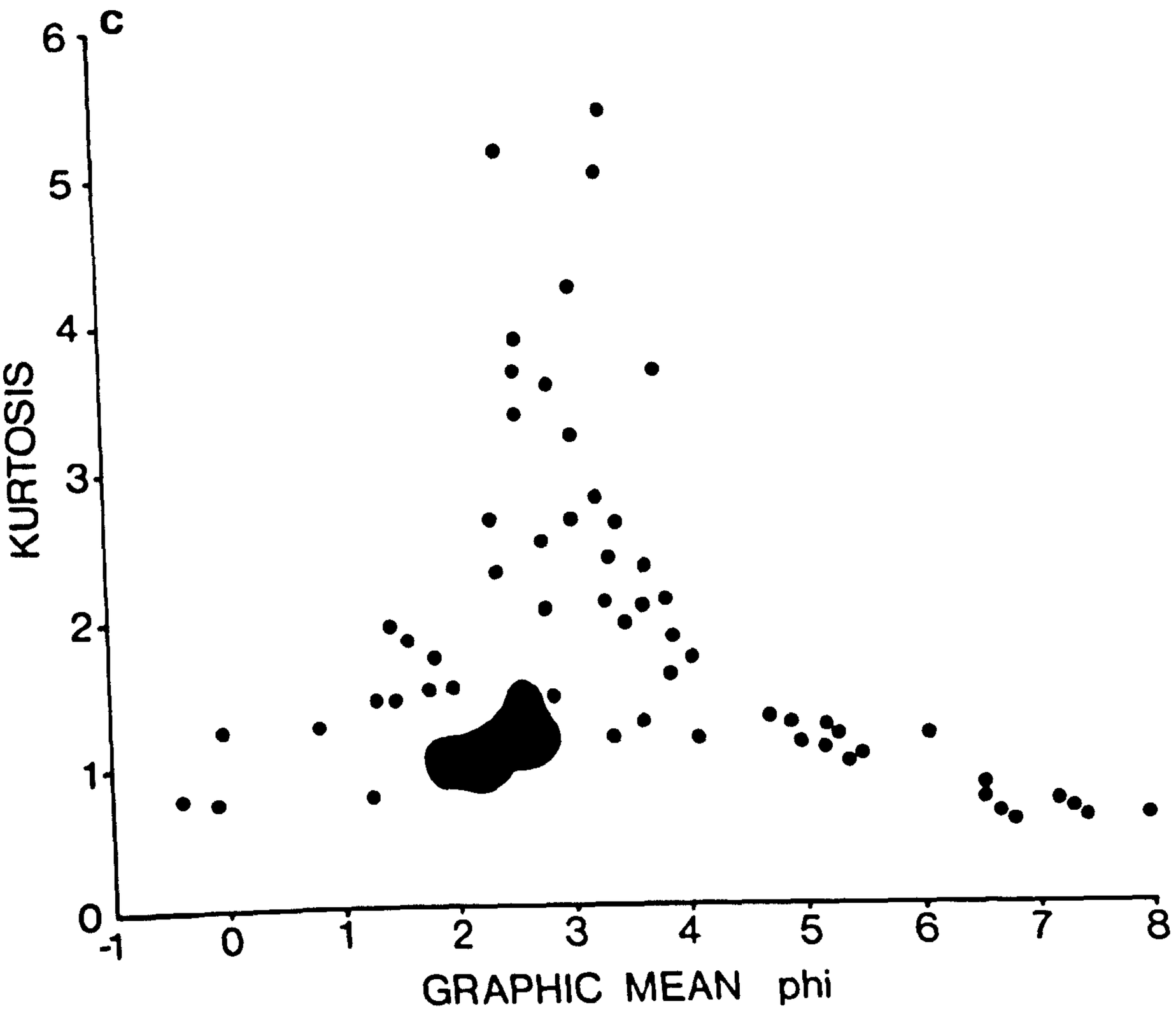

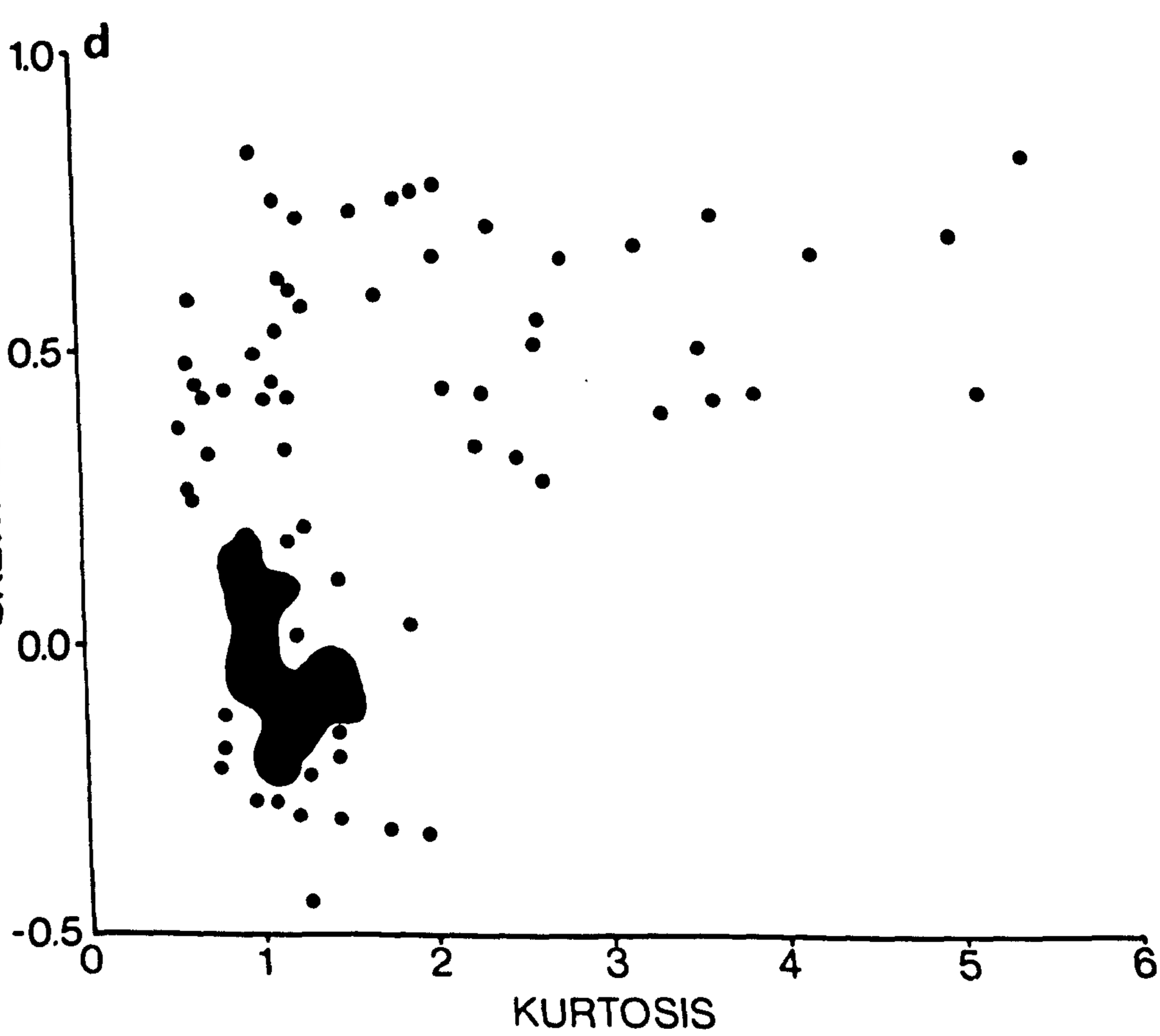

Fig. 4.25c. The variation in Kurtosis with Mean Grain Size. Shaded area encloses 95 sample points.

d. The relationship of Skewness to Kurtosis. Shaded area encloses 92 sample points.

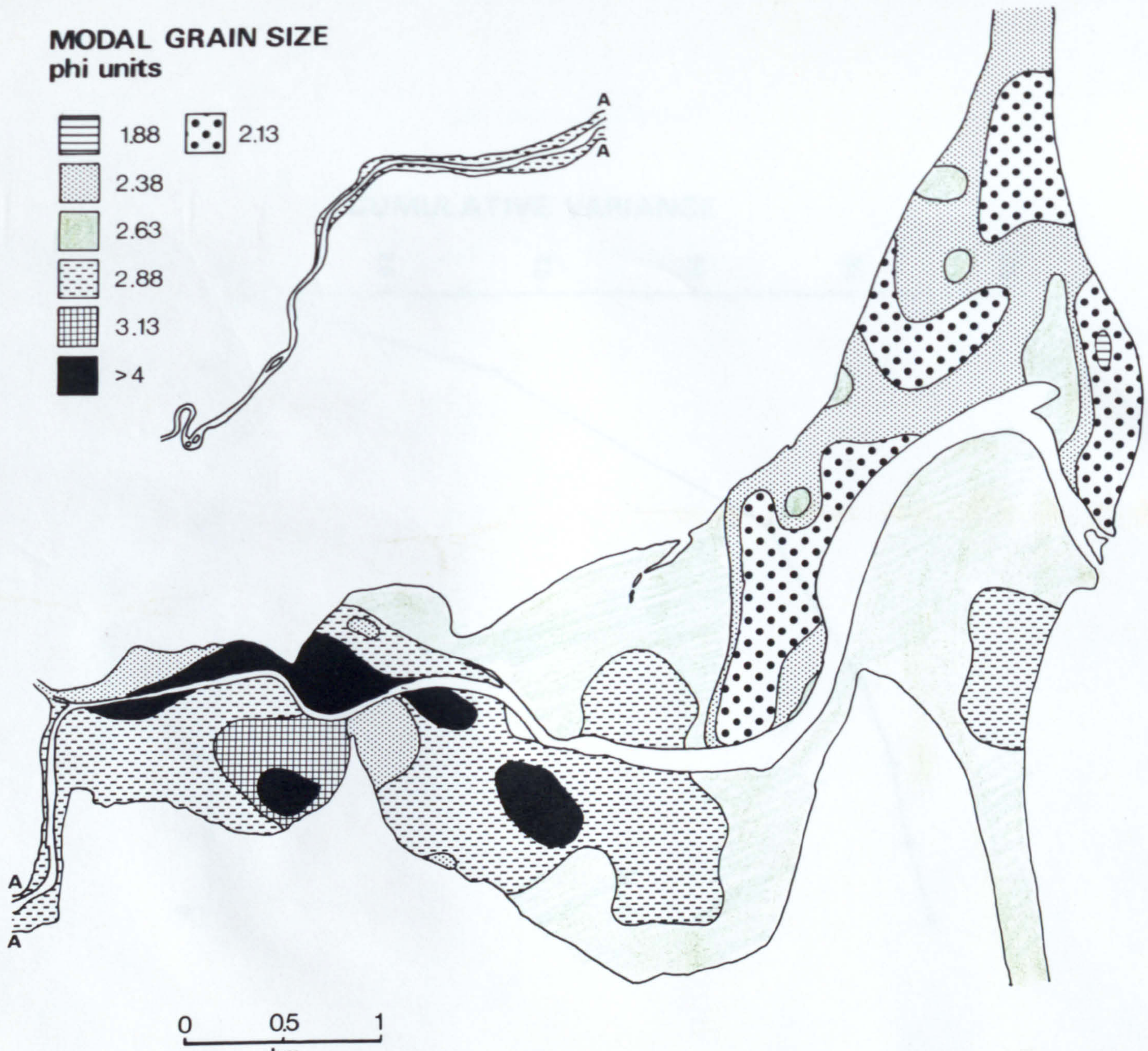

Fig. 4.26. The distribution of Modal Grain Size.

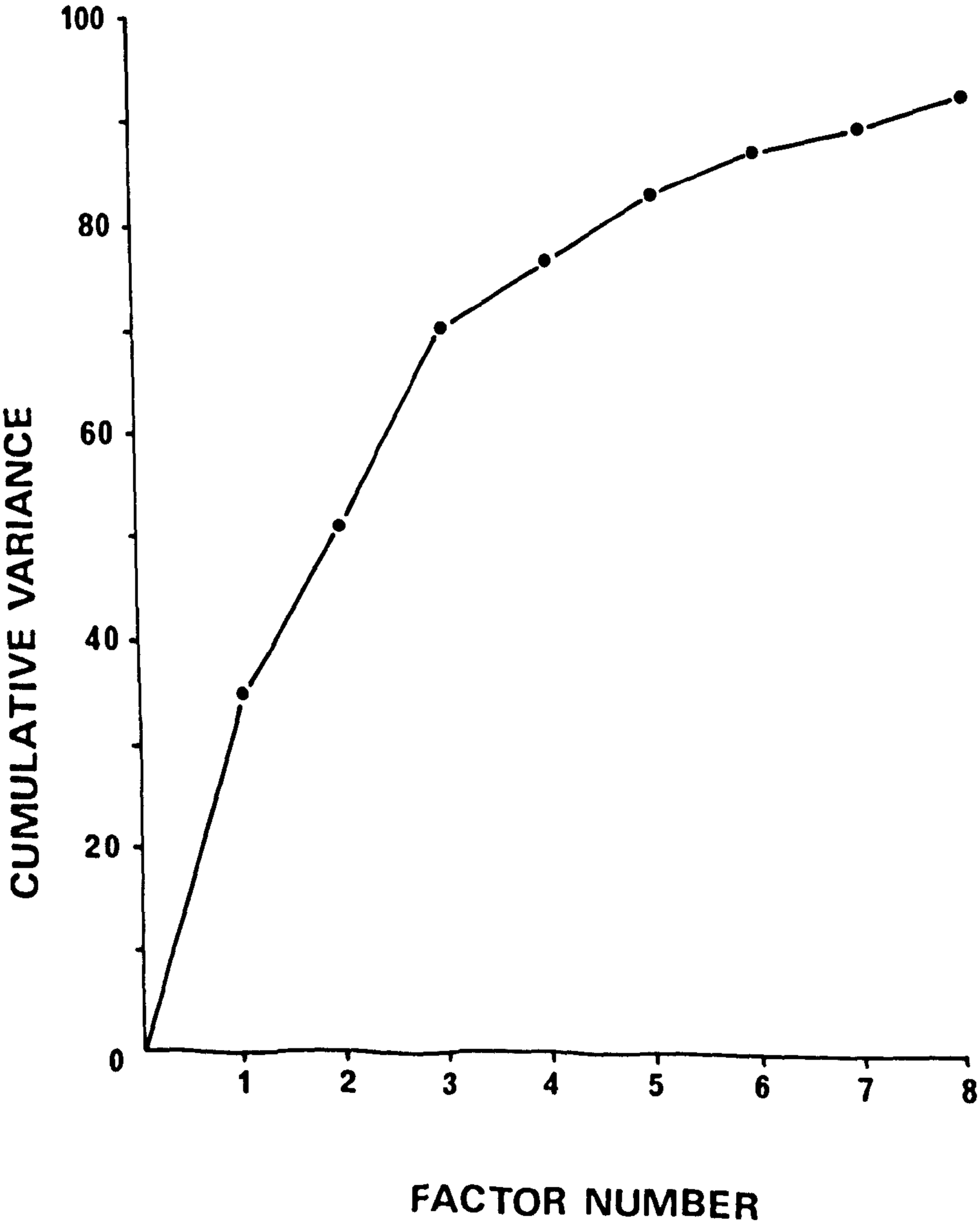

Fig. 4.27. R-mode factor analysis: cumulative variance curve.

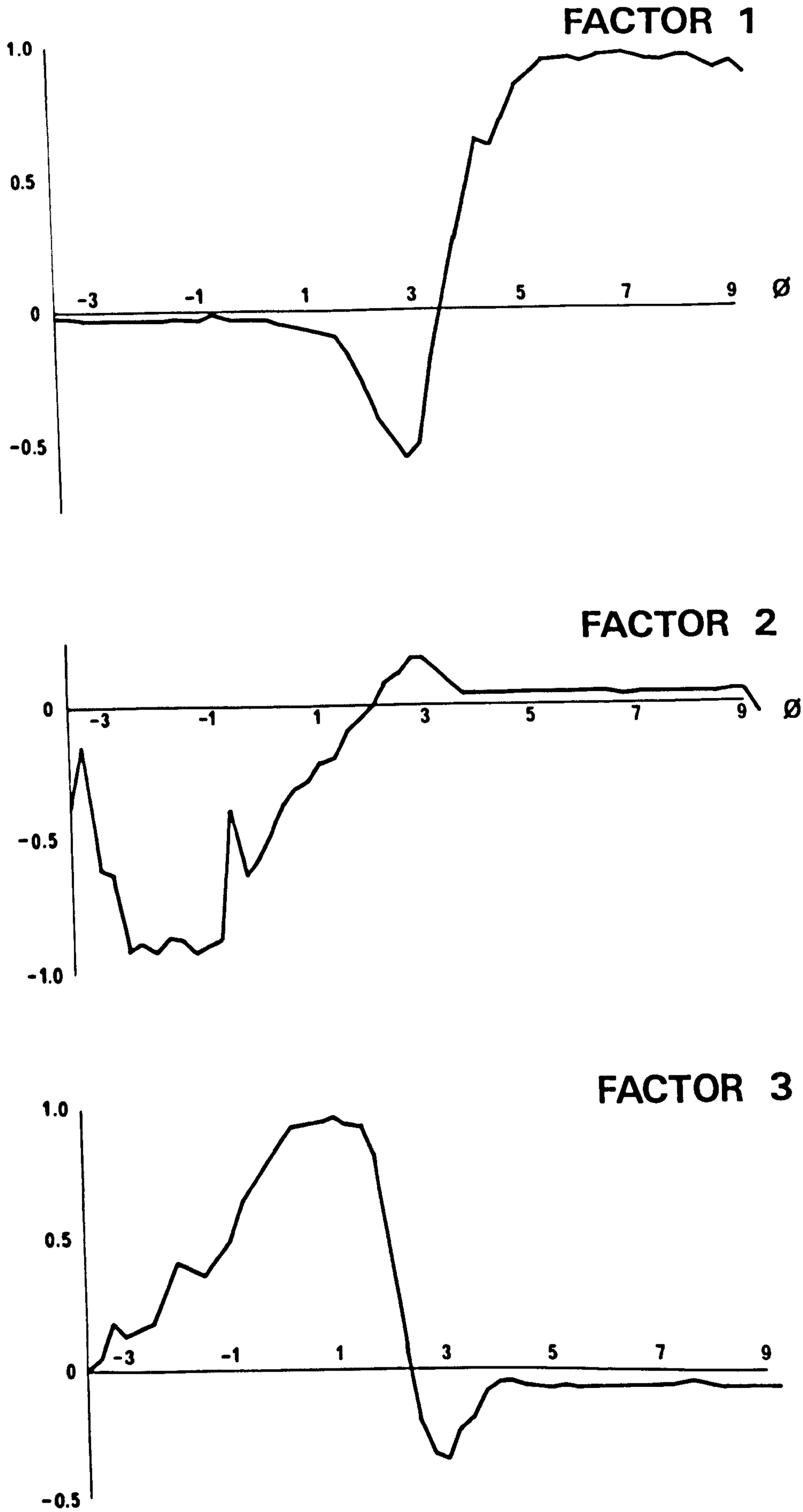

Fig. 4.28a. The loading profiles of Factors 1, 2 and 3 which define sediment sub-populations 1, 2 and 3.

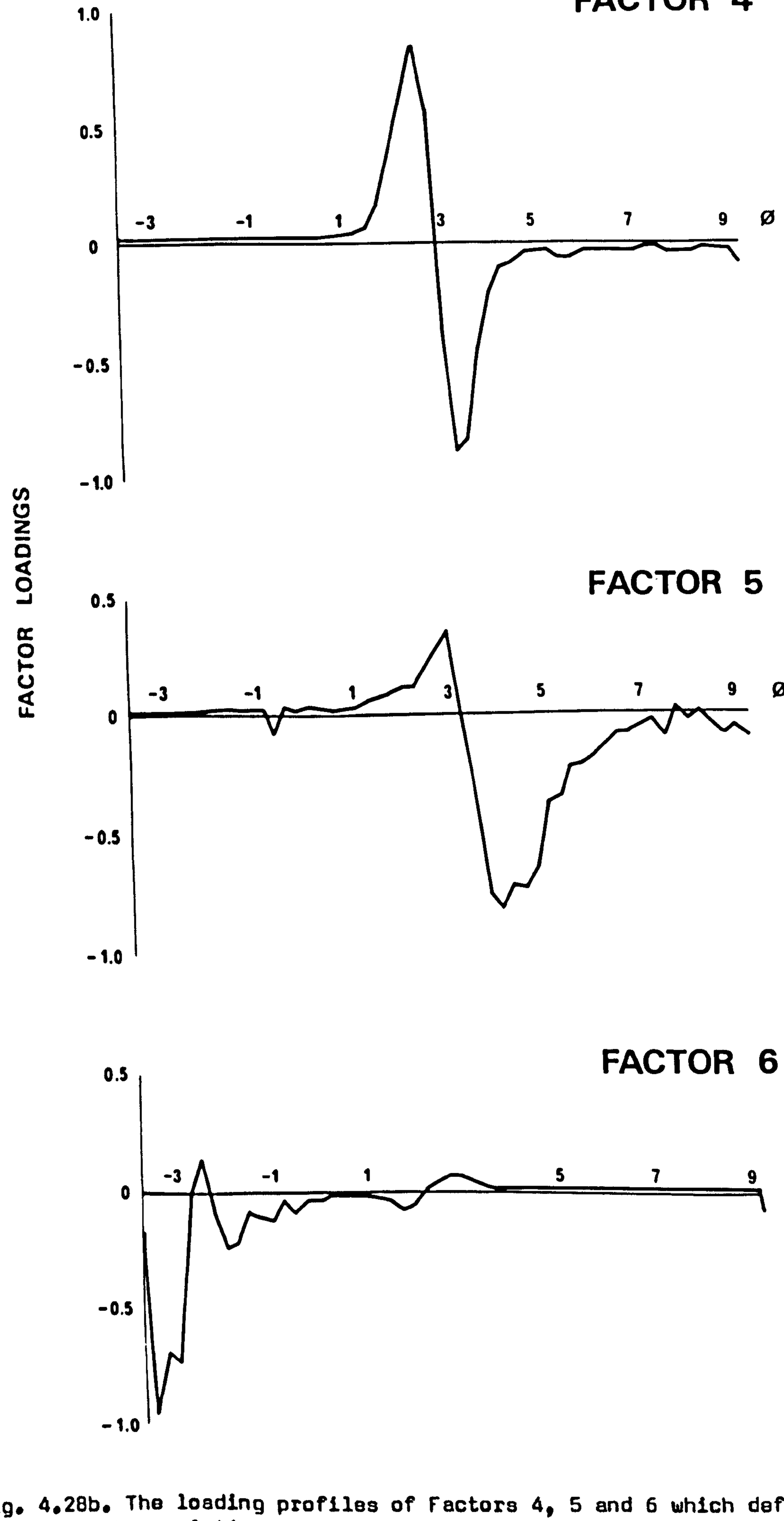

Fig. 4.28b. The loading profiles of factors 4, 5 and 6 which define sediment sub-populations 4, 5 and 6.

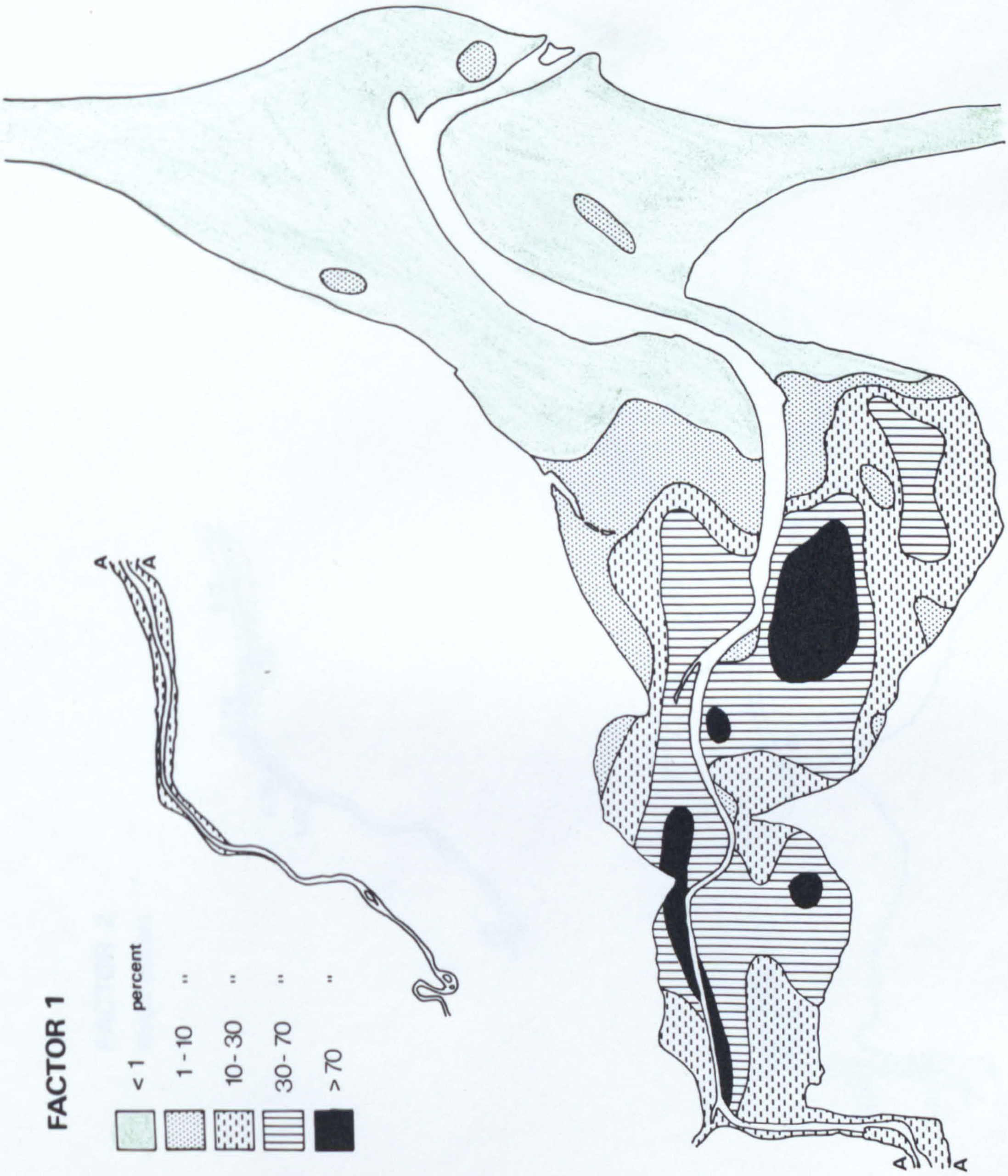

Fig. 4.29. The distribution of Factor 1, the silt and clay sub-population.

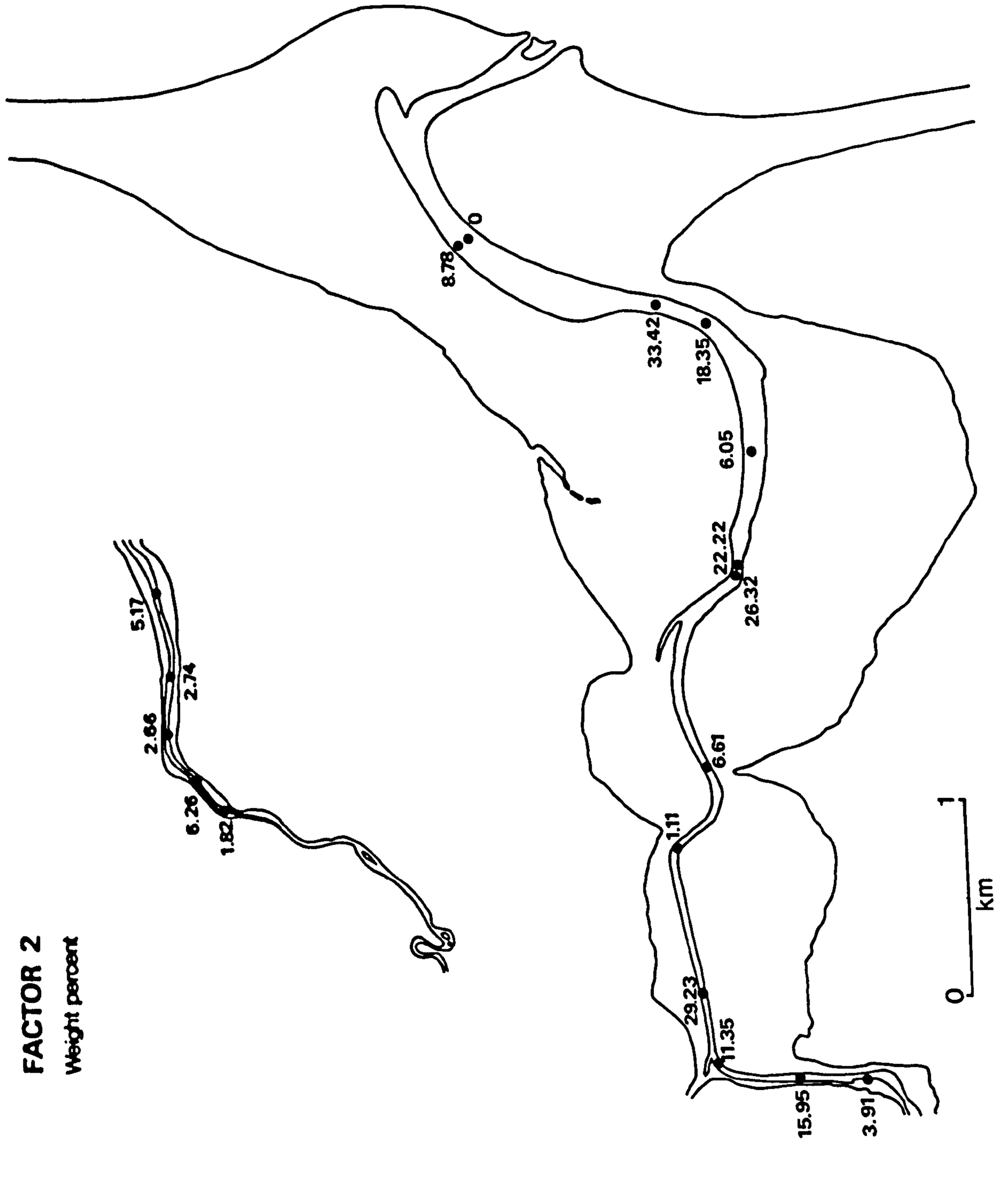

Fig. 4.30. The distribution of Factor 2, the granule and very small pebble sub-population.

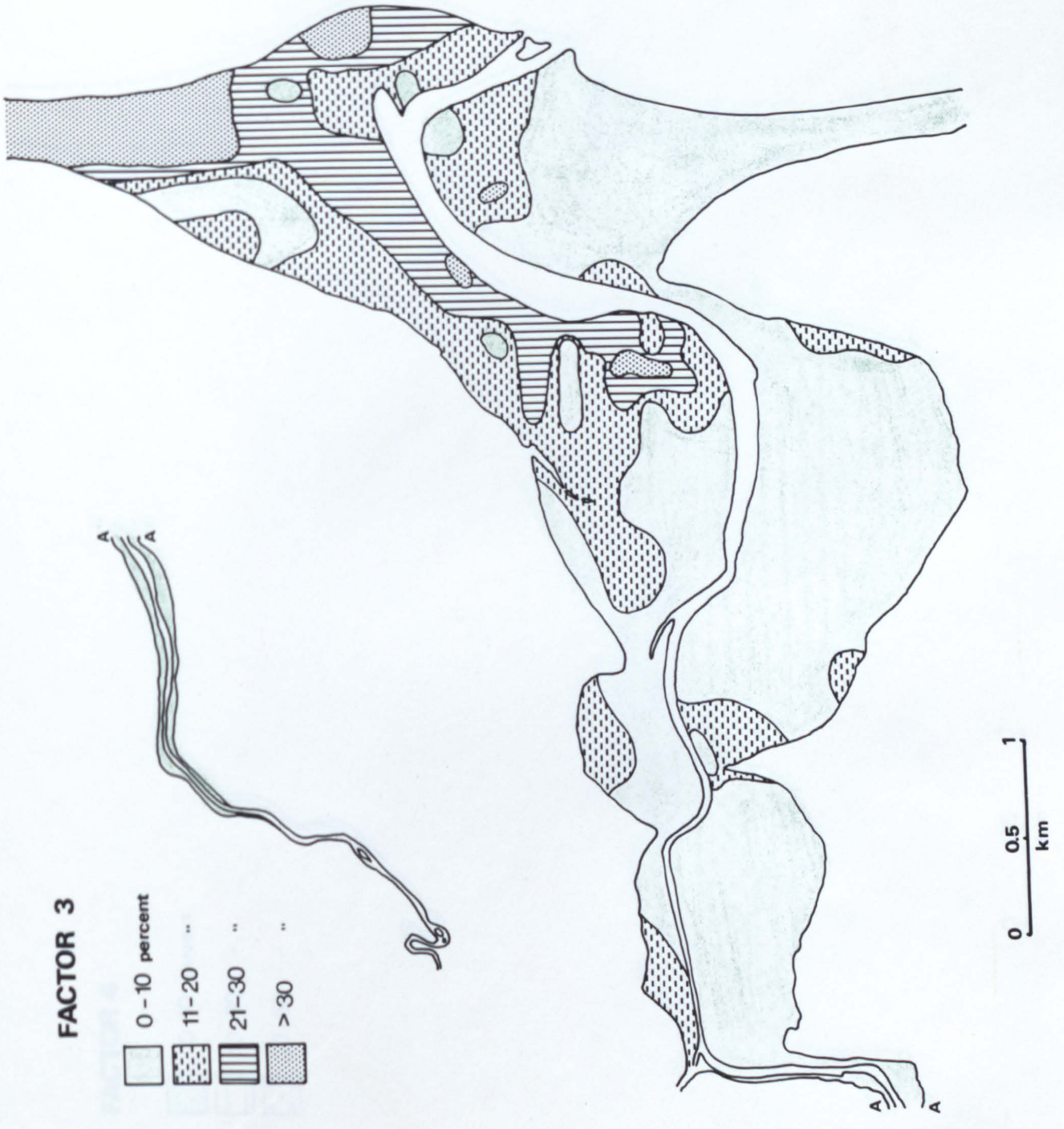

Fig. 4.31. The distribution of Factor 3, the very coarse-, coarse- and medium sand sub-population.

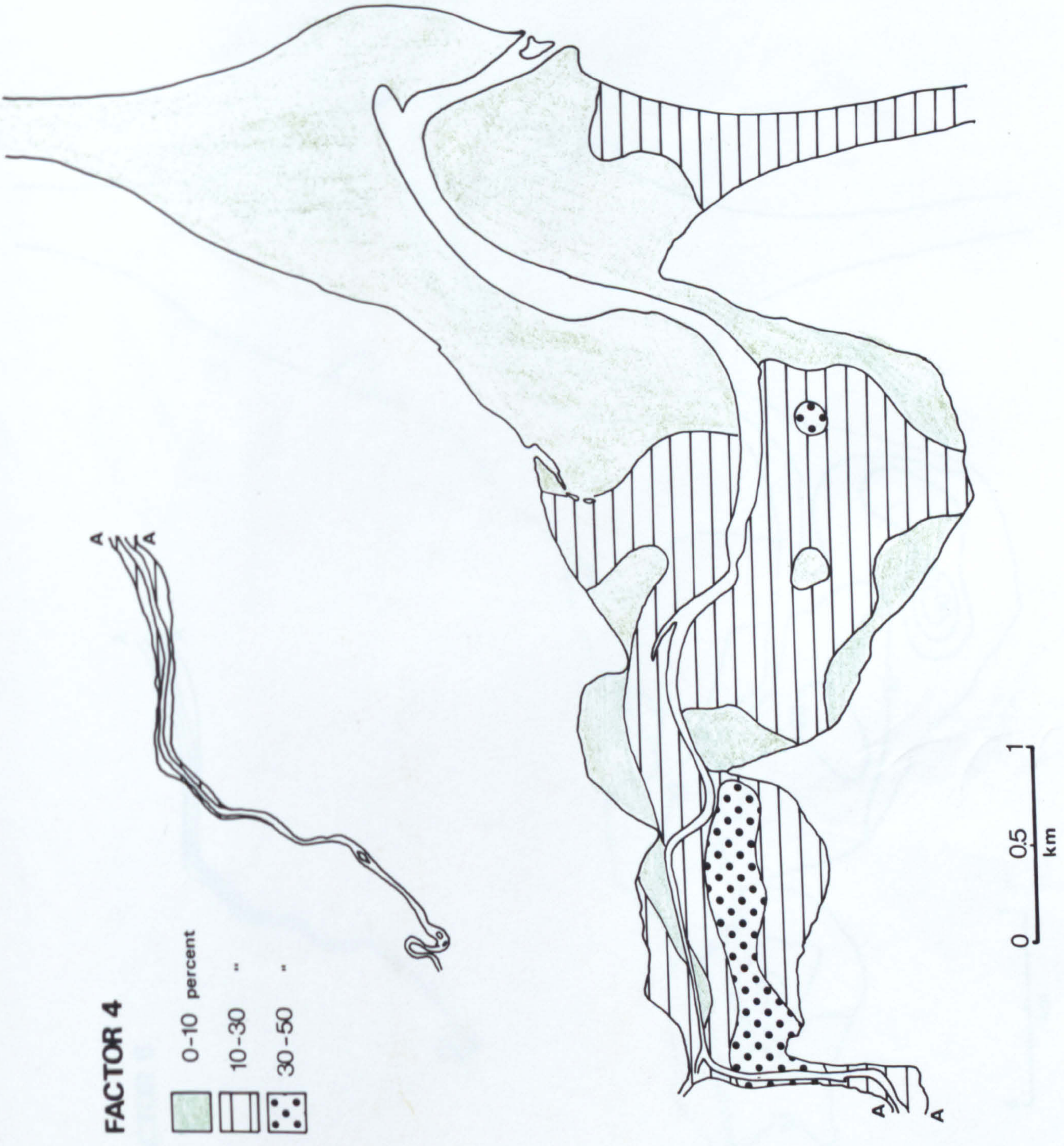

Fig. 4.32. The distribution of Factor 4, the very fine sand sub-population.

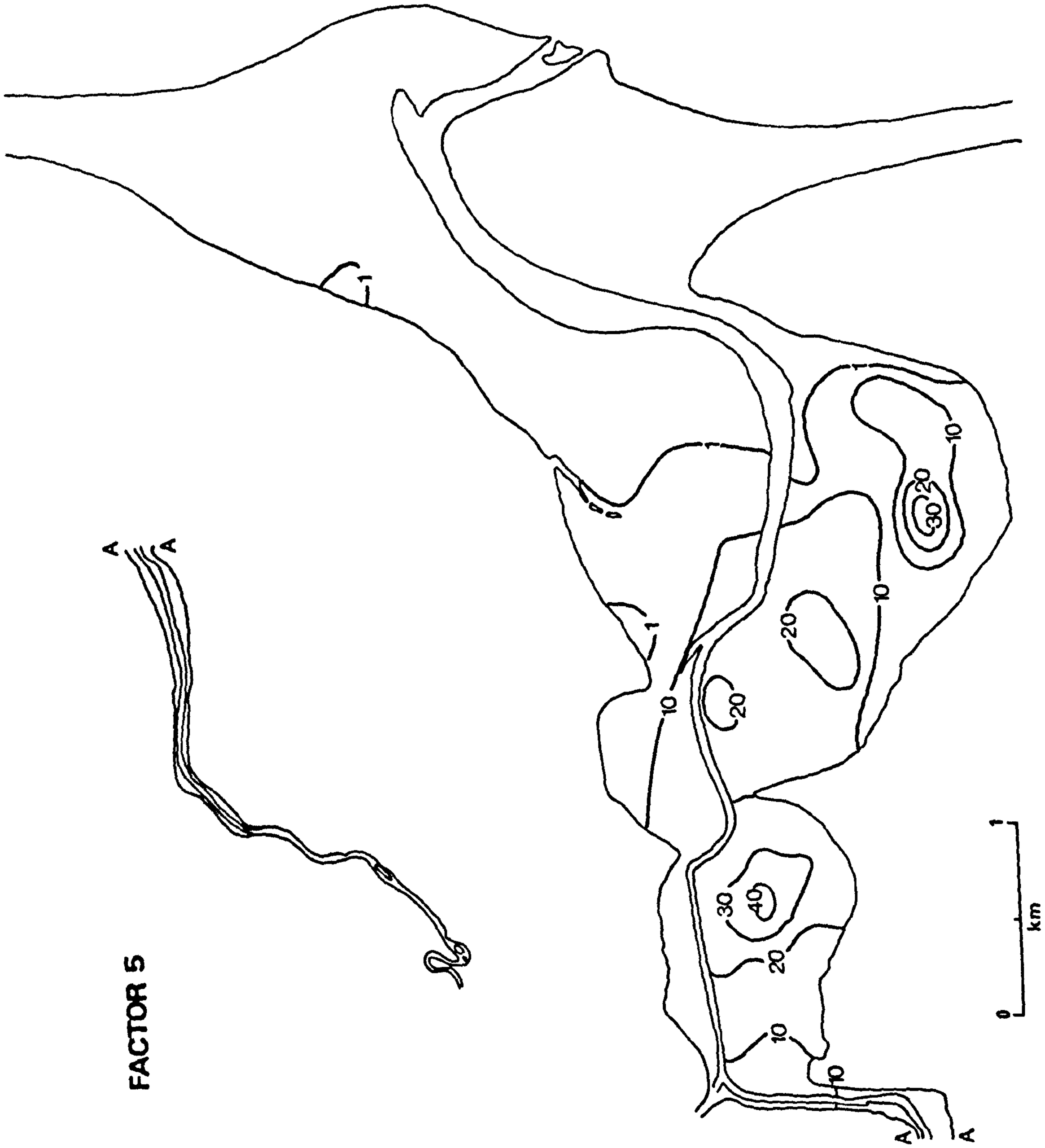

Fig. 4.33. The distribution of Factor 5, the very fine sand/very coarse silt sub-population.

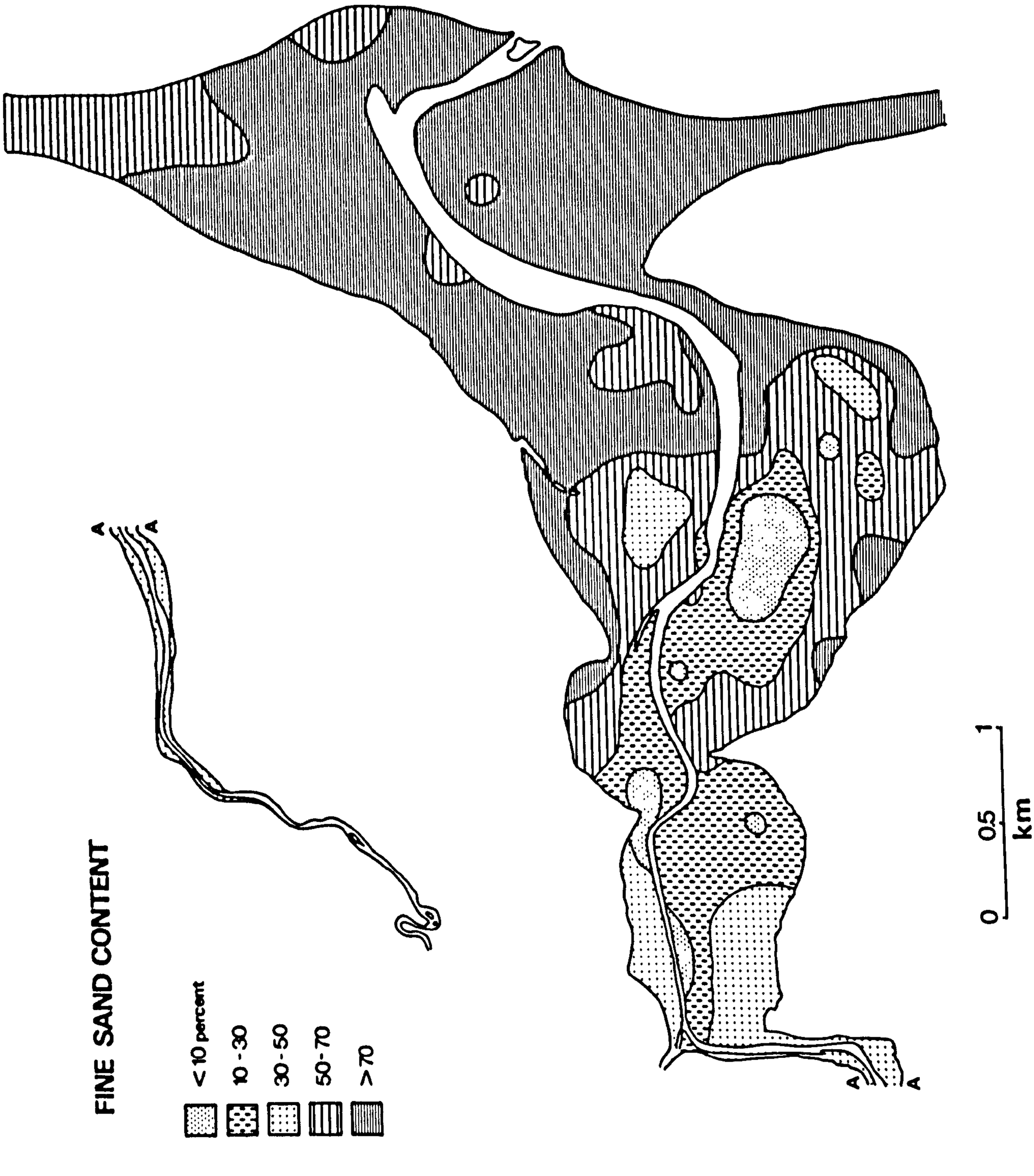

Fig. 4.34. The distribution of fine sand, the basic sediment sub-population.

V. FACIES ANALYSIS

Groups of sediments with distinct textural attributes were identified by the application of a cluster analysis (Wishart, 1970) to the raw weight percentage data obtained by sieve and pipette analysis. Each group was termed a 'textural facies'.

Integration of textural data with that obtained through the study of hydrography, bedforms, internal sedimentary and biogenic structures, and sediment composition provided a basis for the interpretation of the sedimentary processes applicable to each facies.

Techniques

Cluster Analysis

The clustering method used was that of Ward (1963). This was one of several standard methods available in the Cluston 1A computer program of Wishart (1970). The program calculates a similarity matrix for all possible pairs of samples using the Euclidean distance coefficient:

$$d_{ik}^2 = \sum_{j=1}^{n} (x_{ij} - x_{kj})^2$$

where n = number of variables

x_{ij} = the numeric value of variable j for sample i

x_{kj} = the numeric value of variable j for sample k

The coefficients are then clustered systematically by Ward's hierarchical technique. At each stage in the analysis the loss of information which results from the grouping of individuals into clusters is measured by the increase in the total sum of squared deviations of every point in the cluster from the mean of the cluster. The two individuals or individual and cluster combined at each fusion are the ones which result in the minimum increase in the error sum of squares. The clustering process ends when the initial number of samples has been

grouped into a single cluster.

The optimum number of clusters for a particular data set is determined by reference to the numeric values of the fusion coefficient. A reduction in the number of clusters beyond the optimum results in a rapid increase in the value of the coefficient.

Input for the analysis consisted of the 53 variables measured on each sample. Analyses were performed on both raw weight percentage data and standardised data; both produced the same results.

The sequence of sample clustering is expressed in dendogram form in Figure 4.35. The inset shows the rate of change of the fusion coefficient with the number of clusters formed. The first major change of slope occurs at the 7-cluster level, and this is accepted as the optimum number of facies distinguishable by grain-size attributes. The sediments comprising the seven clusters will be referred to as Textural Facies I-VII.

Of the seven facies four are groups of intertidal flat sediments and three are related to the sediments of the channel of the River Eden. The restricted areal distribution of each intertidal flat facies is shown in Figure 4.36.

C-M Analysis

C-M Analysis (Passega, 1957, 1964) was applied to the Eden estuary samples in order to determine the general modes of sediment transport associated with the sediments of each facies.

The C-M diagram is formed by plotting for each sample in a deposit the one-percentile value, C, in microns and the median value, M, in microns of the grain-size frequency distribution. Passega (1957) showed that certain segments of the C-M diagram correspond with particular transport and sedimentation mechanisms (Fig. 4.37b). The shape of the segments remains constant for a particular mechanism,

but the position and size of each segment may vary depending on the local hydraulic conditions.

The usefulness of C-M analysis, which originally only considered the coarse half of a distribution, was extended by the addition of FM, LM and AM diagrams (Passega and Byramjee, 1969). F, L and A are the percentages by weight of the fractions of the distribution finer than 125, 31 and 4 microns respectively. These parameters are plotted against the median and together with the C-M diagram form the 'grain-size image' of a deposit.

The Bed-Stage Concept of Moss (1972)

Moss (1972) showed that in the bed-load deposits of shallow unidirectional currents a textural sequence parallelled that of primary structures. With increasing grain-size and/or transporting power, sedimentary characteristics followed a stepwise pattern from five ripple bed-stage, coarse ripple bed-stage, dune bed-stage to rheologic bed-stage. It was postulated that (a) the various bed-stages differed from each other in the nature of their depositional processes, and (b) that the textural features of a bed-stage could be shown by a sediment whether or not the primary structure developed.

The identification of bed-stages in the Eden sediments, using textural (sub-population) analysis and structural data, permitted inferences to be made about sediment depositional processes. Such inferences are based on the field and experimental data of Moss.

Textural Facies I

Distribution

Textural Facies I occurs to the north of and immediately to the south of the Eden channel in the lower estuary and includes the sediments of the flood- and ebb-tidal deltas. There are also minor

occurrences on the west side of Pilmour Links and on the north and south margins of the middle estuary (Fig. 4.36).

Characteristics

The average sediment of Textural Facies I is a fine sand with a well-sorted, near symmetrical and leptokurtic grain-size distribution (Table 4.9).

Table 4.9. Textural Facies I : Folk and Ward average summary statistics.

Number of samples : 86

	Average	Min.	Max.
Mean (phi)	2.29	1.83	2.65
S. Dvn (phi)	0.42	0.27	1.18
Skewness	0.00	-0.32	+0.41
Kurtosis	1.20	0.83	5.16
Mode (phi)	2.33	1.88	2.63

Ten representative[1] cumulative grain-size frequency curves (Fig. 4.38a) show that differences between samples occur only outside the 5 to 95 cumulative weight percentage range. The samples illustrated in Figure 4.38a are end-member samples, and as such show the characteristic features of the facies developed to their fullest extent. Over 90 wt% of the sample occurs within the 1 to 3 phi size range, and there are only traces of coarse and fine tails.

Sub-population analysis (Table 4.10, p. 134) indicates that the main contributor to textural variation is medium sand which ranges from 3.5 to 66.7 wt% in individual samples, and averages 23 wt% for the facies as a whole. The sediment which forms the basic stock or frame-

---

1. A Q-mode factor analysis of the raw weight data assigned factor loadings to each sample. The ten samples with the highest factor loadings in each facies were considered to show the characteristic textural features of the facies.

work population is fine sand which averages 73 wt%. The interstitial populations, very-fine sand and silt and clay, average only 2.71 and 1.08 wt% respectively.

Table 4.10. Textural Facies I : Sub-population analysis.

Number of samples : 86

Sub-population	Average (%)	Min. (%)	Max. (%)
1. Slt + C	1.08	0.00	11.28
2. G + SP	0.09	0.00	5.17
3. VCS/CS/MS	23.07	3.46	66.74
4. VFS	2.71	0.50	8.60
5. VFS/VCSlt	0.17	0.00	3.38
Fine Sand	73.20	33.00	91.00

The sediments containing high proportions of medium sand (20-30 wt%, and occasionally up to 67 wt%) tend to exhibit large-scale asymmetric bedforms, although there are exceptions, and small-scale ripples, equally well endowed with medium sand, were encountered. Fine sand mixed with between 10 and 30 wt% of medium sand does not appear to have any bed-stage restrictions (Moss, 1972), and the development of a particular bedform is related solely to the prevalent hydraulic conditions. Sand-waves and megaripples developed in zones of strong tidal current activity, whereas small-scale ripples were ubiquitous and formed both in tidal current zones, where they were superimposed on the longer bedforms, and in wave-dominated areas, where they were the bed-response to rapid temporal variations in flow direction.

The asymmetry of bedforms and internal sedimentary structures (Chapter 3, III) reflects the importance of unidirectional currents in certain areas occupied by Facies I sediments. In the flood-tidal delta, bedforms show both flood- and ebb-orientated asymmetries, whilst internal structures are predominantly flood-orientated. The ebb-tidal

delta carries exclusively ebb-orientated bedforms.

Internal structures of Facies I sand-flats are generally sub-horizontal laminae. Heavy minerals are prominent in some laminae (Fig. 4.39). In Chapter 4,III, it was shown that the proportion of heavy minerals in the 2-3 phi size range increases rapidly as the Eden channel, in the lower estuary, is approached from both north and south. This, coupled with a commensurate increase in the hydraulically equivalent medium sand content, is taken as an indicator of the enhanced transporting power of flood- and ebb-tidal currents in the vicinity of the tidal inlet/outlet relative to other areas of the lower estuary.

Interpretation

Textural Facies I is markedly influenced by tidal currents. Flood-tidal currents which enter the estuary from both the north-east and south-east carry medium and fine sand onto and over the intertidal flats. The major part of the medium sand load is deposited in areas adjacent to the Eden channel. Ebb-tidal currents, likewise, transport sediment of the same size grades onto the ebb-tidal delta, though on the stoss-side of the structure medium sand is less abundant than in crestal areas. This may result from the intense reworking of sediments in the crestal area which concentrates the coarser fractions and removes the finer ones. The sediments of South Tentsmuir Beach are similarly reworked by wave activity.

C-M analysis produced a diagram (Fig. 4.40), which showed a considerable scatter of points, but all except one fell within Passega's fields IV and V. A single sample from the margin of the Eden channel fell in field I. The pattern may be divided into two segments which correspond with the lower part of Passega's PQ section and the upper part of his QR section. The majority of samples plot in the QR section, and there is a general proportionality between the one-

percentile value and the median grain diameter. For most values of M, however, there is a range of C values. This vertical trend may be the result of a decreasing quantity of grains of the maximum suspensive size with an increasing admixture of rolling grains.

As a group these sediments appear to be the result of deposition from graded suspensions and material carried as bed-load. The maximum suspensive size was 300 microns, and bed-load material ranged up to 720 microns in diameter.

The boundary of 300 microns for maximum suspensive size agrees well with the dividing value (250μm) between sub-population 3 and the fine sand sub-population. Fine sand may therefore be transported predominantly as a graded suspension, whereas the medium-coarse sands of sub-population 3 may be transported either by a saltation process (Moss, 1972) or by rolling on the bed. Moss (1972) found that rolling particles in the ripple and dune bed-stages were relatively few, and when they did occur they were "up to a few times the diameter of the framework particles" and readily identifiable with the contact population. The majority of medium-sand size particles would be transported by saltation under coarse-ripple and dune bed-stage conditions.

The cumulative grain-size curves (Fig. 4.38a) do not suggest that there is a definite contact population in well developed Facies I sediments. Sub-population 3 sediments appear to grade into the framework population and may have been deposited from a saltating mass contemporaneously with the deposition of fine sand from graded suspensions.

In summary, the sediments of Textural Facies I are transported and deposited in a high energy environment dominated by tidal currents. Wave action is subordinate, but important in certain areas. The sediments are, typically, fine sands with varying proportions of medium sand. The highest medium sand concentrations appear to occur in areas

influenced by both tidal current and wave activity. The observed mixture of medium and fine sand has no bed-stage restrictions, and both small and large-scale bedforms develop depending upon local hydraulic controls. The predominant modes of sediment transport appear to be graded suspensions for the fine-sand grade, and saltation (with very minor rolling) for the medium-sand grade.

Textural Facies II

Distribution

Textural Facies II occurs on the West Sands to the east of Pilmour Links, around Out Head, and in a zone which spans the Eden channel to the south-west of Out Head (Fig. 4.36). A single sample from the north shore of the estuary was also attributed to this facies.

Characteristics

The average sediment of this facies is a fine sand with a very well sorted near symmetrical and leptokurtic size distribution (Table 4.11).

Table 4.11. Textural Facies II : Folk and Ward average summary statistics.

Number of samples : 21

	Average	Min.	Max.
Mean (phi)	2.72	2.62	2.92
S. Dvn (phi)	0.33	0.24	0.81
Skewness	0.00	-0.19	+0.49
Kurtosis	1.50	1.09	3.58
Mode (phi)	2.71	2.63	2.88

Representative cumulative curves for sediments of this facies (Fig. 4.38b) show considerable variation in their constituent grain-sizes outwith the 2.5 to 3.0 phi size range.

Sub-population analysis (Table 4.12) indicates that the framework population is fine sand (up to 83 wt%) and that very fine sand (up to 12 wt%) is the interstitial population. The majority of samples are devoid of silt and clay and the values of up to 9 wt% occur only in the sediments of the westermost zone. The medium sand fraction is only present in amounts of up to 6.8 wt% and forms the contact population.

Table 4.12. Textural Facies II : Sub-population analysis.

Number of samples : 21

Sub-population	Average (%)	Min. (%)	Max. (%)
1. Slt + C	1.56	0.00	9.10
2. G + SP	0.00	-	-
3. VCS/CS/MS	2.98	0.30	6.80
4. VFS	12.27	4.60	25.00
5. VFS/VCSlt	0.37	0.00	5.00
Fine Sand	83.17	65.00	91.00

The predominant bedform was the small-scale ripple of straight to sinuous type. Ripple trains were both in- and out-of-phase and two (and rarely three) ripple trains were frequently superimposed one on the other. Internal structures were, generally, gently seaward dipping laminae.

Interpretation

The C-M diagram (Fig. 4.41) shows that the samples form a group characterised by a very restricted range of median grain-sizes from 140 to 163 microns. The size of the coarsest particles, however, varies over the complete range of medium sand size grades from 250 to 500 microns. The vertical trend, which parallels Passega's PQ section and transects his QR sections, is indicative of a predominantly suspensive form of transport.

The five samples with identical median and one-percentile values are from the sand-dunes at Out Head and are of sub-aerial origin. Their position on the diagram indicates that the maximum suspensive size for wind-blown sand is 287 microns.

Texturally and structurally Facies II sediments are analagous to the sediments of Moss's fine ripple bed stage. The ripples are produced by wave activity and in the section on wave-refraction (page 35) it was shown that interfering wave-fronts produced up to three penecontemporaneous ripple trains on the West Sands. The ripples generated under these conditions, to seaward of the breaking-wave zone, are not destroyed by the retreating water-front during the ebb-tide, but the crests of the bedforms are generally planed off. Sediment transportation in the fine ripple bed stage would be a combination of saltation and suspension.

Although the fine ripple bed stage is the one which is temporarily preserved, it probably does not reflect the conditions under which the major part of sediment transport occurs. With the rising tide, the zone of 'breaking' waves advances over the West Sands, and beneath 'breaking' waves and in the swash and backwash associated with them, sediment transport is undoubtedly in the rheologic realm. Sediments in the swash zone of the upper foreshore are generally plane-bedded and are attributable to the rheologic bed stage.

The C-M pattern, Figure 4.41, may therefore represent sediments transported by rheologic flows as well as by saltation and suspension mechanisms.

The important feature of both the fine ripple bed stage and the rheologic bed stage is the ability to incorporate substantial amounts of interstitial material in the voids in the framework population. On the West Sands this interstitial material accounts for up to 13 wt% of the sediment. Moss (1972) suggested that because grains do not

project above the viscous sublayer in the fine-ripple bed stage, microturbulence is not generated over the bed or in the open interstices, and fine material from both suspension and bed-load can pass copiously into the bed as an interstitial population. During the rheologic bed stage, dispersive pressure drives fine material into the interstices, despite microturbulence, which again results in a significant proportion of interstitial grains.

In summary, Textural Facies II sediments are transported and deposited in a high energy environment dominated by wave action. This wave action includes the oscillatory motion generated by shoaling waves and the high intensity, turbulent motions created by breaking waves. The sediments are, typically, very well sorted fine sands containing very minor amounts of medium sand but significant amounts of very fine sand. Sediment transport modes are low intensity saltation and suspension (fine ripple bed stage), and high intensity, rheologic-flow (rheologic bed stage). Both transport modes permit the retention of fine grained material in the interstices of the framework population.

Textural Facies III

Distribution

Textural Facies III (Fig. 4.36) is present over much of the middle and upper estuary, with special emphasis on Edenside Flat and the southern marginal areas of Kincaple Flat. It also occurs in an equant zone between Sanctuary Spit and the Eden channel.

Charateristics

The average sediment of this facies is a very fine sand with a poorly sorted, strongly fine skewed and very leptokurtic size distribution (Table 4.13, page 141).

Table 4.13. Textural Facies III : Folk and Ward average summary statistics.

Number of samples : 24

	Average	Min.	Max.
Mean (phi)	3.64	2.79	5.52
S. Dvn (phi)	1.97	0.65	3.53
Skewness	+0.65	+0.42	+0.83
Kurtosis	2.60	1.03	6.70
Mode (phi)	2.75	2.38	3.13

The cumulative frequency curves of 10 samples selected randomly[1] from the 24 in the facies show marked deviations from phi-normality (Fig. 4.30c). The fraction coarser than 3 phi is well-sorted, whereas that finer than 3 phi is apparently very poorly sorted.

Sub-population analysis (Table 4.14) shows that on average Facies III sediments consist mainly of fine sand (average 45 wt%) with subordinate sub-equal amounts of silt and clay, and very fine sand. Medium sand averages 5.35 wt%.

Table 4.14. Textural Facies III : Sub-population analysis.

Number of samples : 24

Sub-population	Average (%)	Min. (%)	Max. (%)
1. Slt + C	26.79	11.78	51.36
2. C + SP	0.00	0.00	0.00
3. VCS/CS/MS	5.35	0.24	18.73
4. VFS	21.37	6.87	50.40
5. VFS/VCSlt	13.89	0.00	42.92
Fine Sand	44.98	16.00	73.75

Inspection of the maximum values recorded for each sub-population (Table 4.14) shows that all groups except medium sand and very fine

---

1. Random selection was necessary because the sediments of Facies III were not identified as a separate group by the Q-mode factor analysis.

sand/very coarse silt are present in sufficient quantities to form primary modes in some samples within the facies. Silt and clay, and very fine sand can no longer be regarded as purely interstitial material, as in combination they may be more abundant than fine sand.

X-ray radiography revealed very few primary sedimentary structures in sediments of this facies (Chapter 3,III). Small-scale cross laminae were present occasionally in the more easterly areas and planar laminae in the more westerly areas, but bioturbation by a prolific in-fauna had almost completely destroyed the bedding features.

The sediment surface exhibited ripple-type bedforms only in the marginal areas of the estuary where the fine sand content was high and silt and clay content low. In the remaining areas the bed was of a cohesive sediment which normally carried only biogenic structures. Algal mats and isolated algal filaments were also locally present.

Interpretation

Because of the considerable amounts of very fine sand and silt and clay in Facies III sediments, they were not amenable to description by a C-M diagram alone, and recourse was made to FM, LM and AM diagrams to aid the interpretation (Fig. 4.42, upper diagram).

On the C-M diagram (Fig. 4.42, lower diagram) the samples plot in a broad zone parallel to the QR section of Passega. As such, the coarse half of each sample might be interpreted as a graded suspension deposit. The maximum suspensive size in this facies is shown to be 200 microns.

The FM, LM and AM diagram (Fig. 4.42, upper diagram) shows the changing proportions of very fine sand and coarse silt, silt, and clay in Facies III sediments as the median grain-size decreases. The diagram shows that as the median value decreases there is a marked increase in the very fine sand and very coarse silt content, and smaller sub-

equal increments in the silt (<31 microns) and clay content. The range of median grain-sizes in this facies is not sufficiently wide to allow a definitive FM, LM, AM diagram to be drawn, but comparison with the trends shown in Passega's schematic diagram for graded and uniform suspension deposits (Fig. 4.37a) over the same size range (200-60 microns) indicates that these sediments may be the deposits of graded suspensions.

If this is so, Facies III sediments may be viewed as the landward equivalents of Facies I sediments, that is, the two facies may be co-genetic. Such an interpretation is in agreement with the observed variation in modal grain diameter.

Whether the measured silt and clay particle sizes ever existed as single entities in nature cannot be determined from the analysis of a bottom sediment. Kranck (1975) showed that the 'tail' of fine material present in most mixed sand-mud sediments may be due to grains which were deposited as floccules, whereas the modal peak consisted of individual grains. She also showed that the change of slope which occurs when cumulative size distributions of sand-mud mixtures are plotted on probablility paper can be explained without invoking transport by several agents, and concurred with Belderson's (1964) idea that the discontinuity was due to the disaggregation during analysis of previously flocculated material.

The very small thickness of post-Carse Clay sediments present in the marginal areas of the middle estuary suggests that present-day sand deposition is virtually non-existent, and the deposition of fine grained sediments is very slow. Indeed, in the marginal areas of the middle estuary an equilibrium seems to exist between deposition and erosion. The Facies III sediments may be the product of the addition of silt and clay-size material to the sands deposited in this area during the Flandrian transgression. The fine material is rapidly and

continuously mixed with the sand by the in-fauna.

In summary, Facies III sediments occur in the low-energy marginal areas of the middle estuary. Deposition of very fine sand, silt and clay from waning tidal currents may be important. The fine sand which in nearly all cases forms the modal grain-size may be a palimpsest sediment, having been emplaced during the Flandrian transgression. The finer grained components of the sediment have been mixed into the sand by the in-fauna.

Textural Facies IV

Distribution

Textural Facies IV occupies the central part of the middle estuary (Fig. 4.36). It is distributed in the form of an elongate zone which borders the Eden channel between Guardbridge and Shelly Point and then crosses the channel and occupies the northern part of Kincaple Flat.

Characteristics

The sediments of this facies are the finest in the estuary and are medium silts with very poorly sorted, strongly fine skewed and platykurtic grain-size distributions (Table 4.15). The modal grain-size is highly variable and is typically much finer than that of the surrounding area.

Table 4.15. Textural Facies IV : Folk and Ward average summary statistics.

Number of samples : 16

	Average	Min.	Max.
Mean (phi)	6.30	4.94	7.99
S. Dvn (phi)	3.07	2.44	3.59
Skewness	+0.42	+0.25	+0.60
Kurtosis	0.88	0.58	1.24
Mode (phi)	7.84	2.63	11.50

Representative cumulative curves (Fig. 4.38d) show that fine sand is no longer the well sorted framework population and that there is a considerable spread of median grain-sizes.

Sub-population analysis (Table 4.16) showed that Facies IV is dominated by the silt and clay sub-population. Fine sand and very fine sand are subordinate and average 11.4 and 15.5 wt% respectively.

Table 4.16. Textural Facies IV : Sub-population analysis.

Number of samples : 16

Sub-population	Average (%)	Min. (%)	Max. (%)
1. Slt + C	71.71	49.62	94.92
2. G + SP	0.00	0.00	0.00
3. VCS/CS/MS	1.27	0.00	4.16
4. VFS	15.51	4.39	26.12
5. VFS/VCSlt	20.13	11.20	31.36
Fine Sand	11.44	0.69	30.14

Interpretation

These very fine grained sediments occur in seemingly anomalous positions on the intertidal flats. Between Guardbridge and Coble House Point they occur on the slope between Edenside Flat and the channel proper. The fine material presumably settles out of suspension during the still-stand period around the time of high-water and becomes sufficiently well bonded to the bed, so that it is not eroded during the ebb-tide. The area is subject to the interference of man and effluent from Guardbridge paper mill is discharged into the estuary at this location. The effluent includes unspecified chemicals, hot water and the clay-mineral Kaolinite, all of which contribute to the production of an artificial depositional environment for fine-grained sediment.

To the east of Coble House Point the fine sediments are concentrated in areas of extensive mussel bank and seaweed developments. As shown in Chapter 3,III, mussel banks are active depositional sites

for sediment, which upon size analysis appears to be very fine grained. Actual deposition probably took place with the individual particles aggregated into faecal pellets.

Fine grained sediments may also be retained on the bed by the trapping effect of filamentous green algae. Material which settles between the filaments in an algal mat is unlikely to be removed by tidal current or wave action.

In summary, Facies IV sediments are the finest in the estuary and occur in areas adjacent to the Eden channel. Sedimentation is strongly influenced by factors other than hydrodynamic ones and the role of the mussel, Mytilus edulis, in extracting particulate matter from suspension and depositing it in the form of faecal pellets is believed to be of major importance.

Textural Facies V-VII : The Eden Channel Facies

Facies V, VI and VII are groups of samples which are restricted to the channel of the River Eden. They differ from the sediments of the previous facies in that they contain significant quantities of granules and small pebbles (sub-population 2) and material coarser than -3.0 phi (sub-population 6). Twelve channel samples were included in the original cluster analysis and six additional samples have been assigned to various facies on consideration of their content of the basic sediment populations and their Folk and Ward summary statistics. Three of the original 12 channel samples were allocated to Facies I - an intertidal flat facies.

There is no uniform distribution of facies types within the channel, and samples of Facies V, for example, occur to both landward and seaward of the Facies VI sediments (Fig. 4.43).

Facies V sediments are medium sands with moderately sorted, coarse skewed and very leptokurtic grain-size distributions (Table 4.17, and Fig. 4.44a).

Table 4.17. Textural Facies V : Folk and Ward average summary statisitics.

Number of samples : 5

	Average	Min.	Max.
Mean (phi)	1.37	0.87	1.63
S. Dvn (phi)	1.05	0.80	1.57
Skewness	-0.26	-0.43	+0.03
Kurtosis	1.60	1.27	1.95
Mode (phi)	1.83	1.38	2.13

The VCS/CS/MS sub-population was predominant (Table 4.18) and, contrary to the situation on the intertidal flats, very coarse sand and coarse sand were present in significant amounts: an average 6.9 and 16.1 wt% respectively. The granule and very small pebble sub-population was a characteristic feature of Facies V sediments and averaged 4.44 wt%.

Table 4.18. Textural Facies V : Sub-population analysis.

Number of samples : 5

Sub-population	Average (%)	Min. (%)	Max. (%)
1. Slt + C	3.07	1.14	7.28
2. G + VSP	4.44	2.66	6.61
3. VCS/CS/MS	73.47	57.10	89.06
4. VFS	1.59	0.07	4.31
Fine Sand	17.43	3.12	28.64

Facies VI was represented by only two samples which came from the bed of the N-S trending stretch of the Eden channel at Guardbridge. Average summary statistics for the two samples were M_z: 0.67 phi, O_I: 3.13 phi, Sk_I: -0.23, and K_G: 0.91. The cumulative curves (Fig. 4.44b) show a moderately sorted framework population and well developed

interstitial and contact populations. Sub-population analysis showed the samples to consist of pebbles coarser than -3.0 phi (8mm), up to 40 wt% of very coarse-to medium sand, and sub-equal amounts of small pebbles, very small pebbles and granules, fine sand and silt plus clay (Table 4.19).

Table 4.19. Textural Facies VI : Sub-population analysis.

Number of samples : 2

Sub-population	Average (%)	Min. (%)	Max. (%)
1. Slt + C	15.66	8.18	23.15
2. G + VSP	13.65	11.35	15.95
3. VCS/CS/MS	36.81	33.28	40.35
4. VFS	2.45	1.75	3.15
6. SP	17.31	9.34	24.68
7. Coarser than -3.75 phi	5.32	0.00	10.65
Fine Sand	15.27	14.61	15.93

Facies VII was also represented by two samples, both of which were very coarse sands with very poorly sorted coarse skewed and platy-kurtic grain-size distributions (Fig. 4.44b). Average summary statistics were M_z: -0.21 phi, O_I: 2.13 phi, Sk_I: -0.16, and K_G: 0.78. The very coarse-to medium sand sub-population is the major constituent of the facies averaging 50.5 wt% (Table 4.20). The granule and very small pebble sub-populations attains its maximum development in this facies accounting for between 26 and 29 wt% of each distribution.

Table 4.20. Textural Facies VII : Sub-population analysis.

Number of samples : 2

Sub-population	Average (%)	Min. (%)	Max. (%)
1. Slt + C	4.62	3.74	4.77
2. G + VSP	27.77	26.32	29.23
3. VCS/CS/MS	50.50	46.49	54.61
4. VFS	1.00	0.65	1.35
Fine Sand	7.71	4.08	11.34

All the channel samples of Facies V-VII plot in field I of Passega's C-M diagram (Fig. 4.40). The distribution trends roughly parallel to the C-M line and suggests that the predominant transport mechanisms are saltation and graded suspensions. The cumulative curves shown by channel facies sediments suggest that material coarser than 1.0 phi forms a contact population which would be transported by rolling over the framework population of medium sand.

Comparison of the Intertidal Flat Facies

Comparison of the sediments of the four intertidal flat facies may be made by reference to the envelopes of the cumulative curves of the end-member samples and on the basis of the proportions of the various sub-populations (Figs. 4.45 and 4.46).

End-member samples of Textural Facies I and II show a slight overlap of distributions in the medium and very fine sand grades, but within the fine sand range the distinction between the two is very clear and may be expressed by the median grain-size values. Facies I is characterised by a median grain-size of 2.2 phi and Facies II by a median of 2.6 to 2.8 phi.

With respect to sediment sorting Facies I is, on average, more poorly sorted than Facies II[1]. Skewness values for each facies are the same (0.0), but considering the whole range of skewness values shown by these sediments, Facies I samples may show a much higher degree of negative skewness than Facies II samples. Differentiation between the two facies may also be made on Kurtosis values; Facies I sediments are mesokurtic to leptokurtic, whereas Facies II samples are very leptokurtic.

These textural attributes of sediments formed in tidal current dominated areas (Facies I) and wave dominated areas (Facies II) are in accord with those found by Allen (1971) in the Gironde estuary:

Footnote 1: this statement is based on the sediment statistics in Fig 4.38.

the sediments of tidal current areas are characteristically coarser grained, less well sorted and have a greater tendency to negative skewness than do those of wave dominated areas.

Facies II and III cumulative curves overlap considerably in the medium and fine sand grades, but differ markedly in the content of sediment finer than 3 phi. In terms of modal grain diameter the two framework populations are identical (2.73 and 2.75 phi). The incorporation of considerable amounts of silt and clay into the fine sands of Facies III distinguishes them from Facies II.

Facies IV is composed of a distinct group of sediments, the frequency distributions of which overlap with those of the other facies only in the 1 to 2 phi size range.

The distinction between the intertidal flat facies is readily made with reference to the sub-populations (Fig. 4.46).

Facies I and II are distinguishable by the size grade of sediment which is mixed with the fine sand framework population: medium sand is concentrated in Facies I and very fine sand in Facies II.

Facies III is characterised by the sub-equal development of three sub-populations: fine sand, very fine sand, and silt and clay.

Facies IV is distinguished by virtue of the dominance of silt and clay over the two subordinate size grades, fine sand and very fine sand.

Comparison of Channel and Intertidal Flat Facies

The main feature which distinguishes the channel facies from those of the intertidal flats is their content of material coarser than 0.0 phi. Sediment of the fine sand grade, so characteristic of the intertidal flat sediments, is deficient in the channel samples: a maximum of 28.64% (Facies V) was recorded. Envelopes of the cumulative frequency curves of both groups are shown in Figure 4.44d.

Anomalous Gravels on the Intertidal Flats

In certain areas of the intertidal flats pebble and cobble sized material is present. The occurrences are of two types:

(i) the inclusion of large (2 to 18cm max. diameter) tri-axial ellipsoids of clay with a surface coating of lithic fragments (armoured-mud-balls) in the arenaceous sediments at Out Head, and

(ii) areally restricted gravel deposits lying upon a surface of grey clay.

Armoured mud balls are described in Chapter 4,III.

The areally restricted gravel deposits are found in patches around the shores of the middle estuary, especially to the east of Coble Shore. The gravels rest upon a surface of grey clay which may be either exposed or covered by a thin layer of silty-sand deposited between the pebbles. The gravels are not related to the present hydrodynamic regime, but are the product of the reworking of a sandy-gravel which forms a part of the post-Glacial stratigraphy in this area (see page 5). Over much of the area of the middle estuary the gravel occurs at a depth of 20 to 25cm below the present sediment surface and is overlain by fine sands, silts and muds. In the marginal areas of the middle estuary, however, the sediment cover is thinner and locally the gravel has been exposed. The interstitial sediment has been removed, but the framework elements of the gravel have remained in place and now constitute a sediment in a totally anomalous position on the intertidal flats.

Conclusions on Textural Facies and their Depositional Environments.

The majority of Eden estuary sediments are fine sands with which are mixed varying proportions of subordinate grain-size populations, the character of which depends upon the local hydrodynamic and biologic environment. Analysis of associations between the various sub-populations defined seven textural facies, four within the sediments of the inter-tidal flats and three in the channel sediments. The relationships of these facies to their environments of deposition may be briefly summarised as follows:

Textural Facies I (for details see pages 132-137)

The sediments of this facies are fine sands with an admixture of medium sand. They are transported and deposited in a high energy environment dominated by tidal currents. Wave action is subordinate but important in such areas as the crest of the ebb-tidal delta. The observed mixture of fine and medium sand appears to have no bed-stage restrictions and both small- and large-scale asymmetrical bedforms develop depending upon very local hydrodynamic conditions. The predominant modes of sediment transport appear to be graded suspensions for the fine sand grade and saltation with minor rolling for the medium sand grade.

Textural Facies II (for details see pages 137-140)

These sediments are very well sorted fine sands containing very minor amounts of medium sand but significant amounts of very fine sand. Transport and deposition takes place in a high energy environment dominated by wave action which includes the oscillatory motion of shoaling waves and the high intensity, turbulent motions created by breaking waves. Sediment transport modes are low intensity saltation and suspension (fine ripple bed-stage) and high intensity rheologic flow (rheologic bed-stage). Both transport modes permit the retention

of fine grained material in the interstices of the framework population.

Textural Facies III (for details see pages 140-144).

These sediments occur in the low energy, marginal areas of the middle estuary and are fine sands with admixtures of very fine sand and silt and clay. Deposition of very fine sand and silt and clay from waning flood-tidal currents is believed to be of importance, as is the trapping of suspended sediment by mats of filamentous algae. An abundant mobile in-fauna has the effect of producing a texturally homogeneous sediment. The palimpsest gravels (page 151) geographically fall within this facies.

Textural Facies IV (for details see pages 144-146).

Sediments of this facies are the finest in the estuary and occur in areas marginal to the Eden channel. Deposition appears to be strongly influenced by factors other than hydrodynamic ones and the role of the mussel, Mytilus edulis, in extracting particulate matter from suspension and depositing it in the form of faecal pellets is considered to be of major importance. Artificial environmental conditions are generated by the discharge of effluent from Guardbridge papermill.

Textural Facies V-VII (for details see pages 146-149).

These sediments occur on the bed of the Eden channel and are distinguishable from the intertidal flat sediments by their high content of material coarser than the medium sand grade and by the relative scarcity of fine sand. The predominant transport mechanisms are saltation and graded suspensions. Material coarser than 1.0phi appears to form a contact population which would be transported by rolling over the framework population of medium sand.

In conclusion it may be stated that within the Eden estuary all size-grades of sediment from pebbles to clay are available for redis-

tribution and that the actual textures observed are the products of selective sediment redistribution by well-defined, geographically restricted hydrodynamic processes which, in certain areas of the estuary, combine with important biological and physico-chemical controls of sedimentation.

Fig. 4.35. The sequence of sample clustering in dendrogram form.

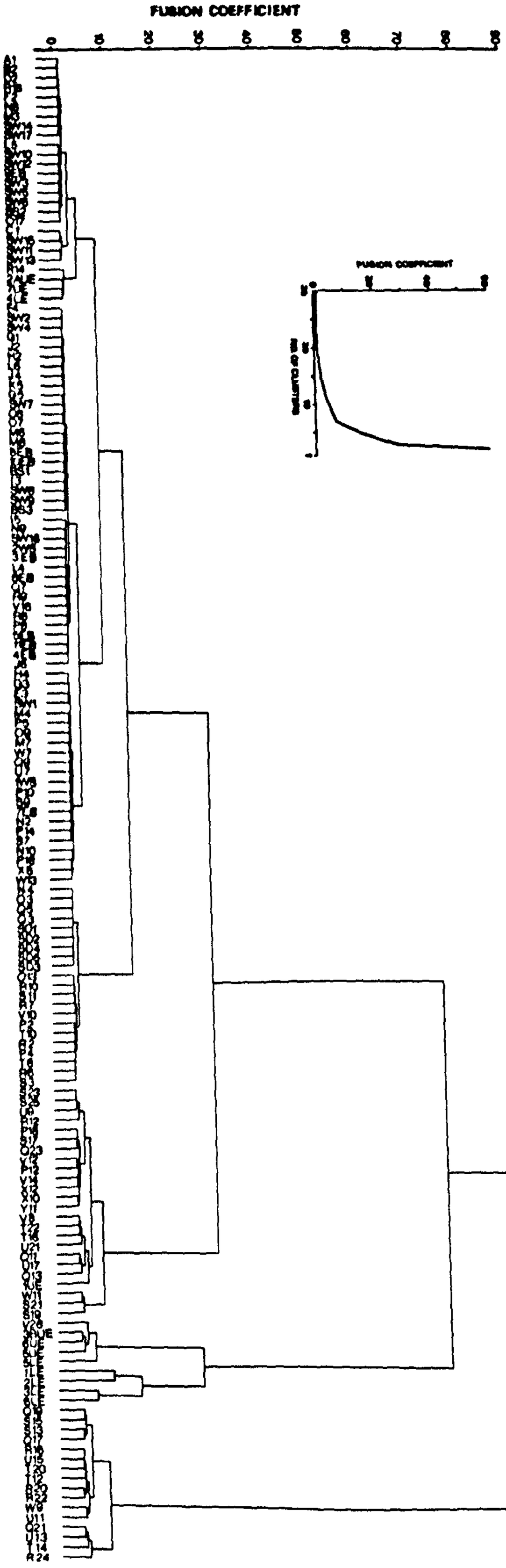

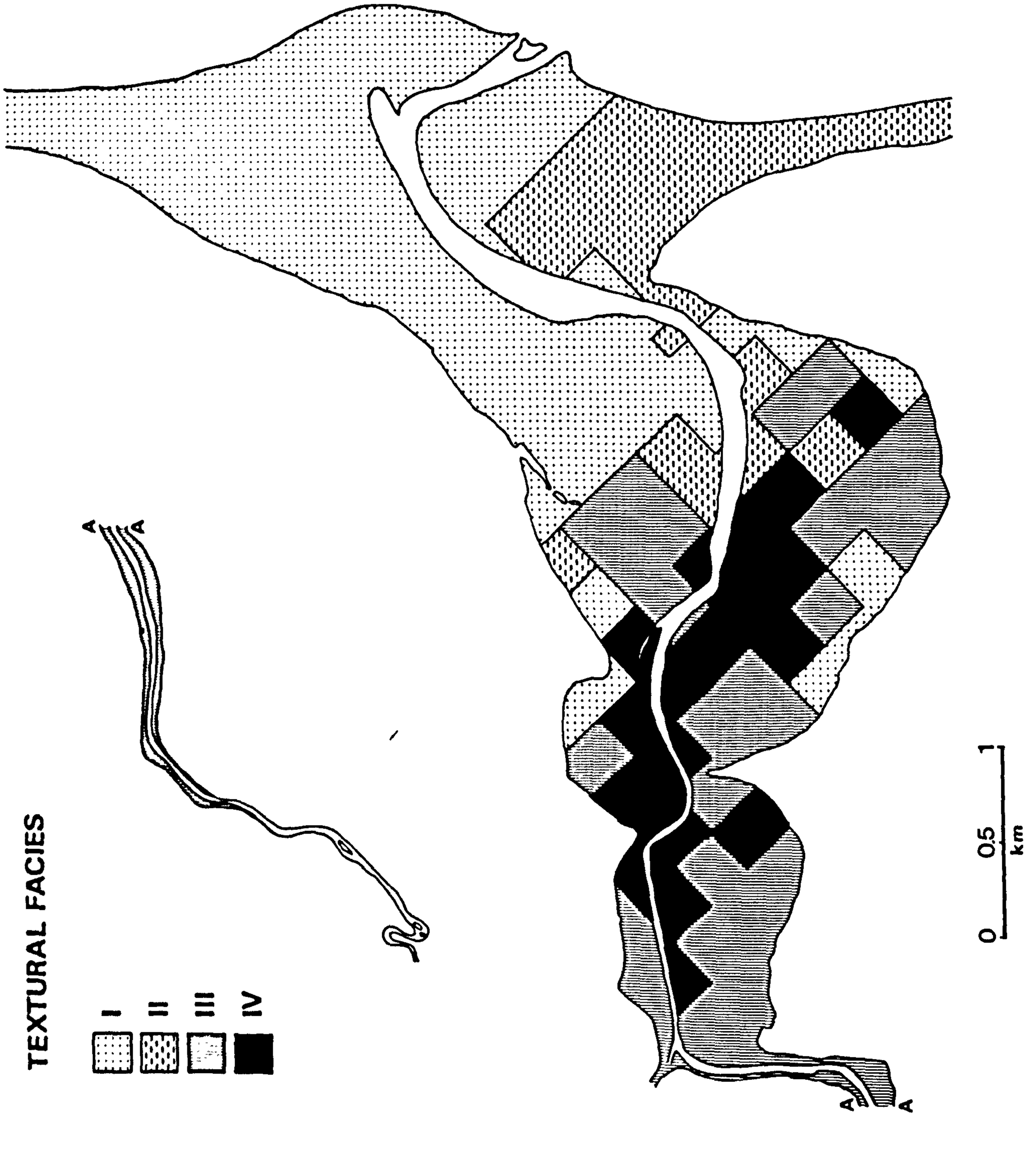

Fig. 4.36. The areal distribution of the four intertidal flat textural facies.

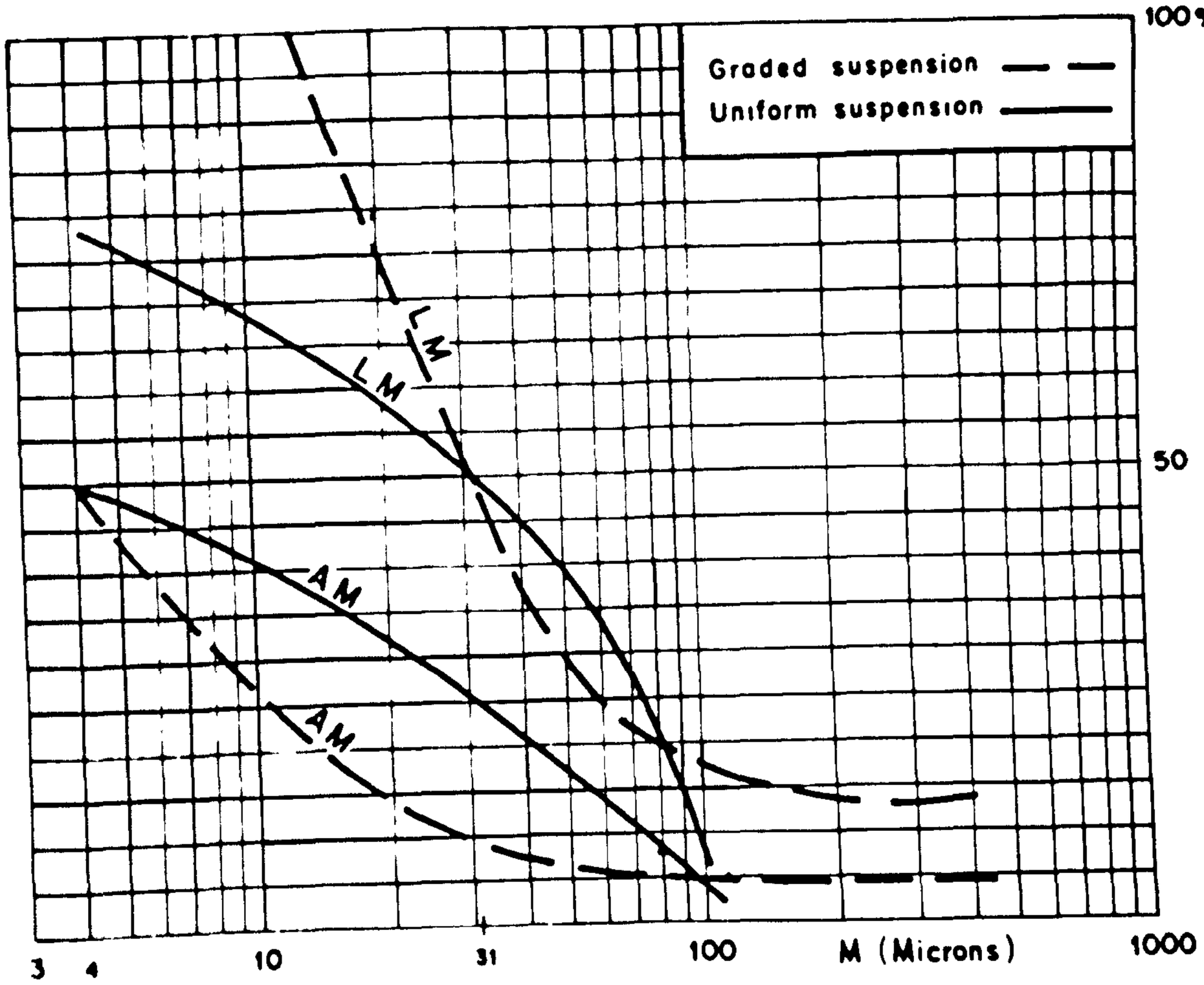

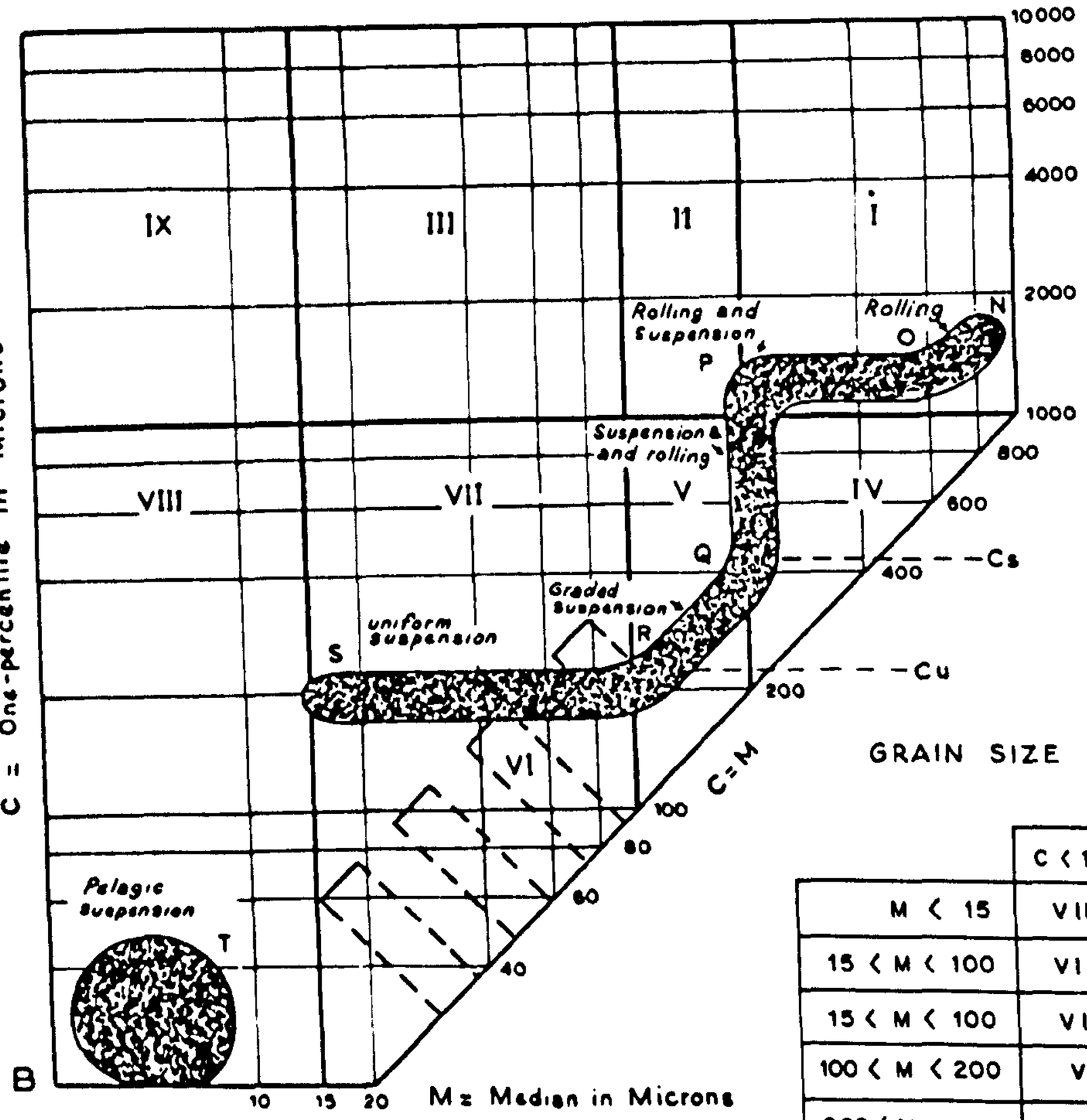

GRAIN SIZE TYPES

	C < 1000	C > 1000
M < 15	VIII	IX
15 < M < 100	VII (1)	III
15 < M < 100	VI (2)	
100 < M < 200	V	II
200 < M	IV	I

(1) Uniform suspension
(2) Graded suspension

Fig. 4.37a. Schematic LM and AM diagrams for graded and uniform suspension deposits.
b. C-M diagram and grain-size types.
From Passega and Byramjee, 1969.

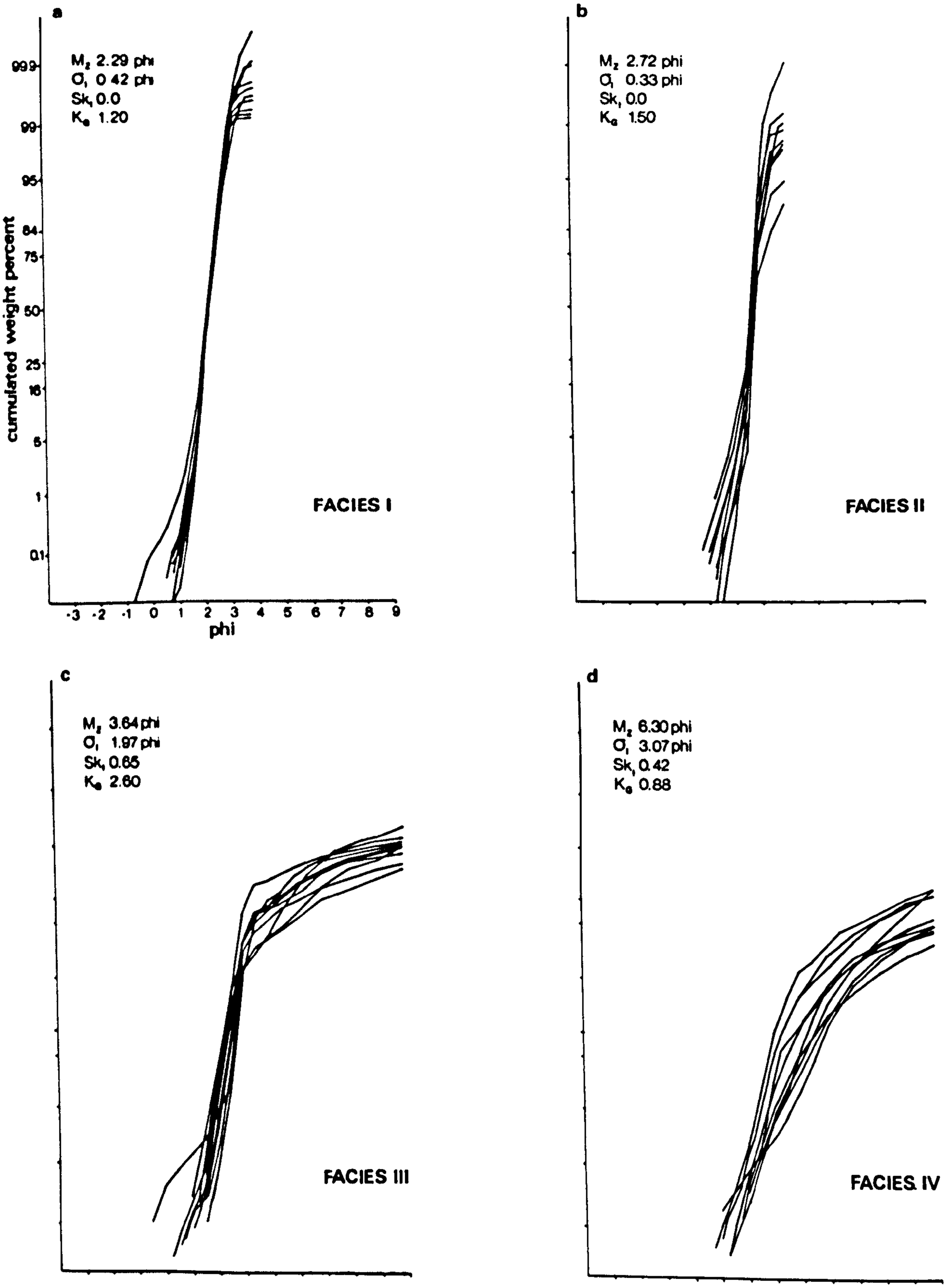

Fig. 4.38. Representative cumulative grain-size frequency curves for the four intertidal flat textural facies.

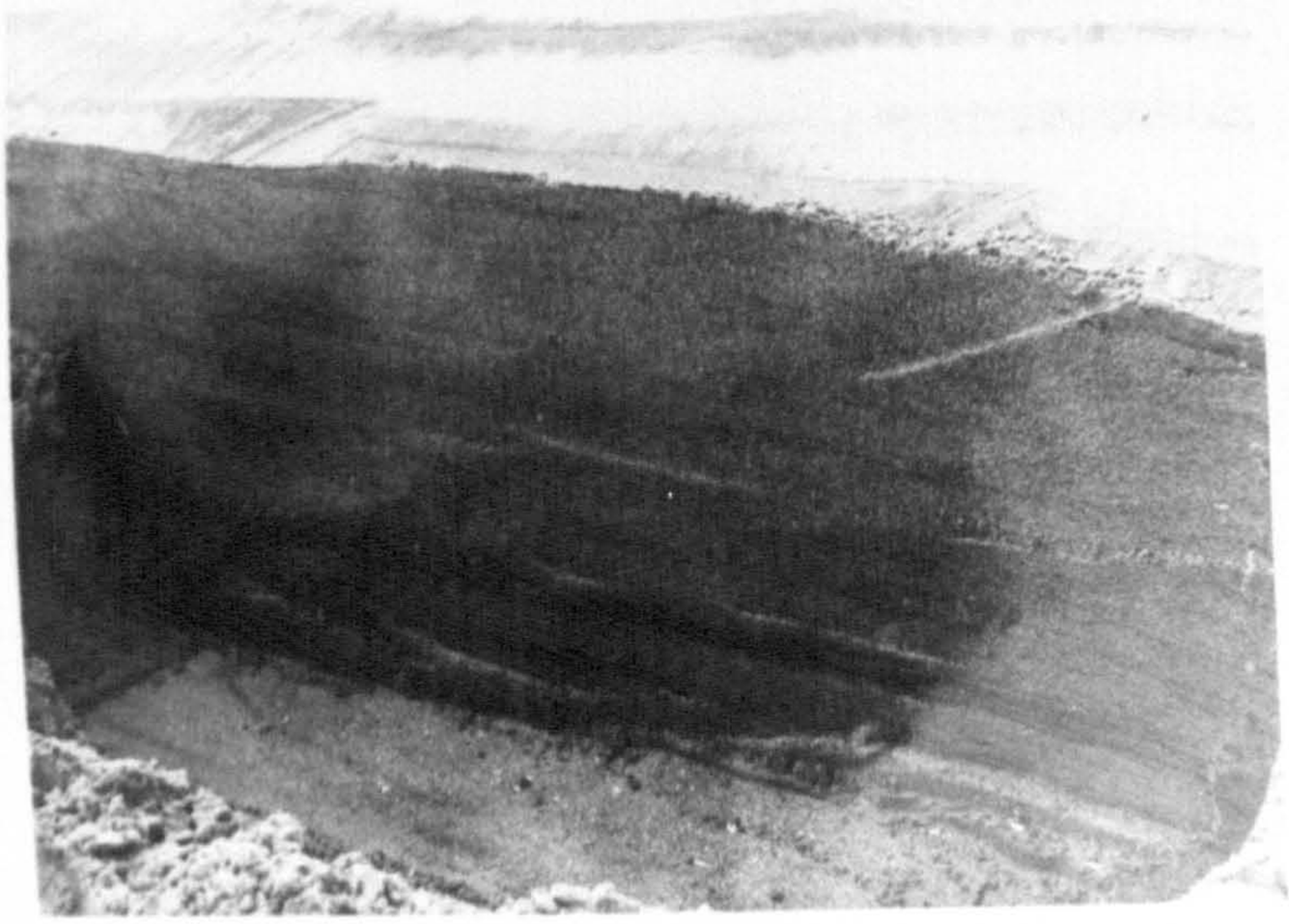

Fig. 4.39. The laminated nature of Facies I sediments. Note the heavy mineral concentrations in the lower part of the trench.

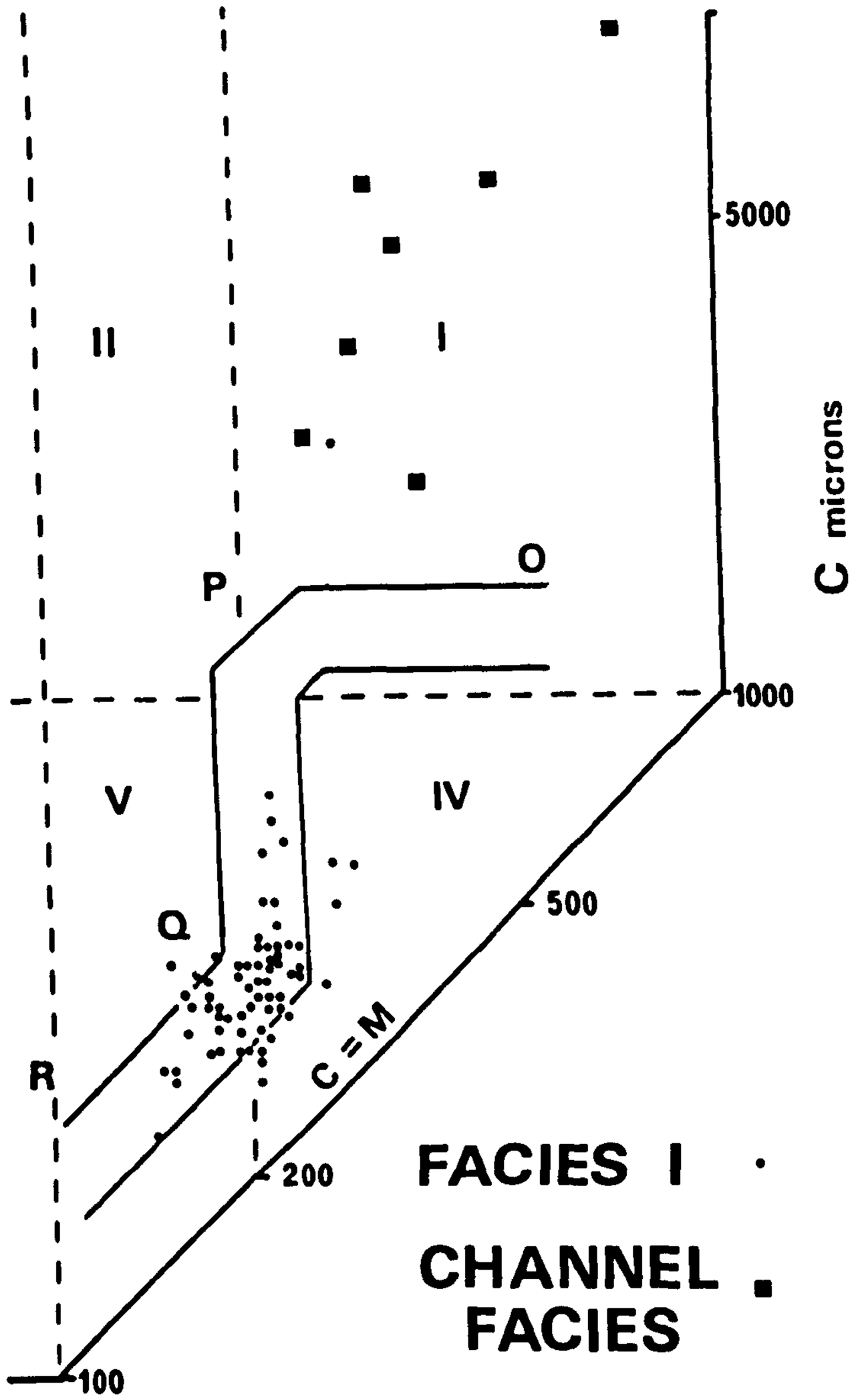

Fig. 4.40. C-M diagram of the sediments of Facies I and those of the Channel Facies V-VII.

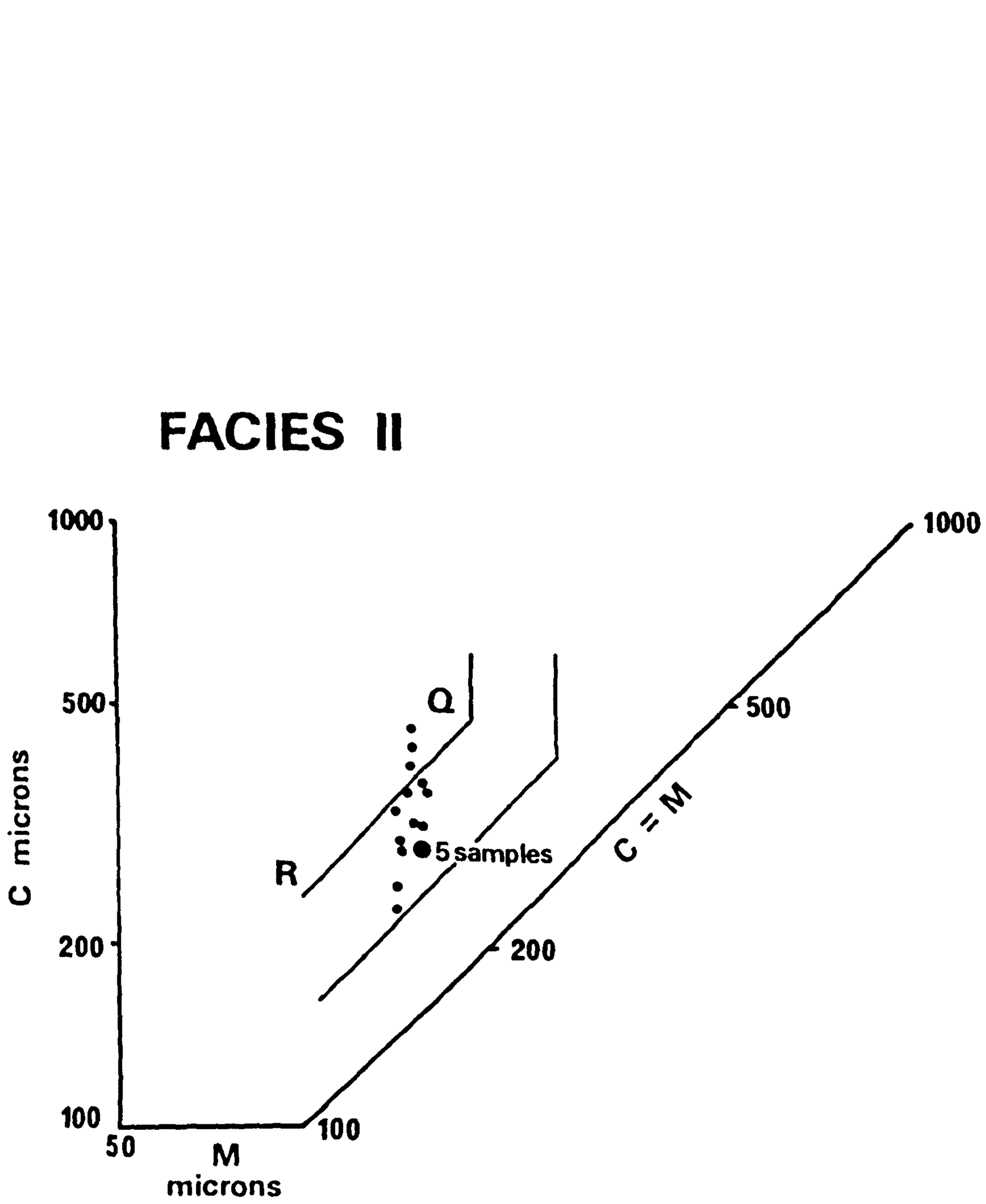

Fig. 4.41. C-M diagram of Facies II sediments.

FACIES III

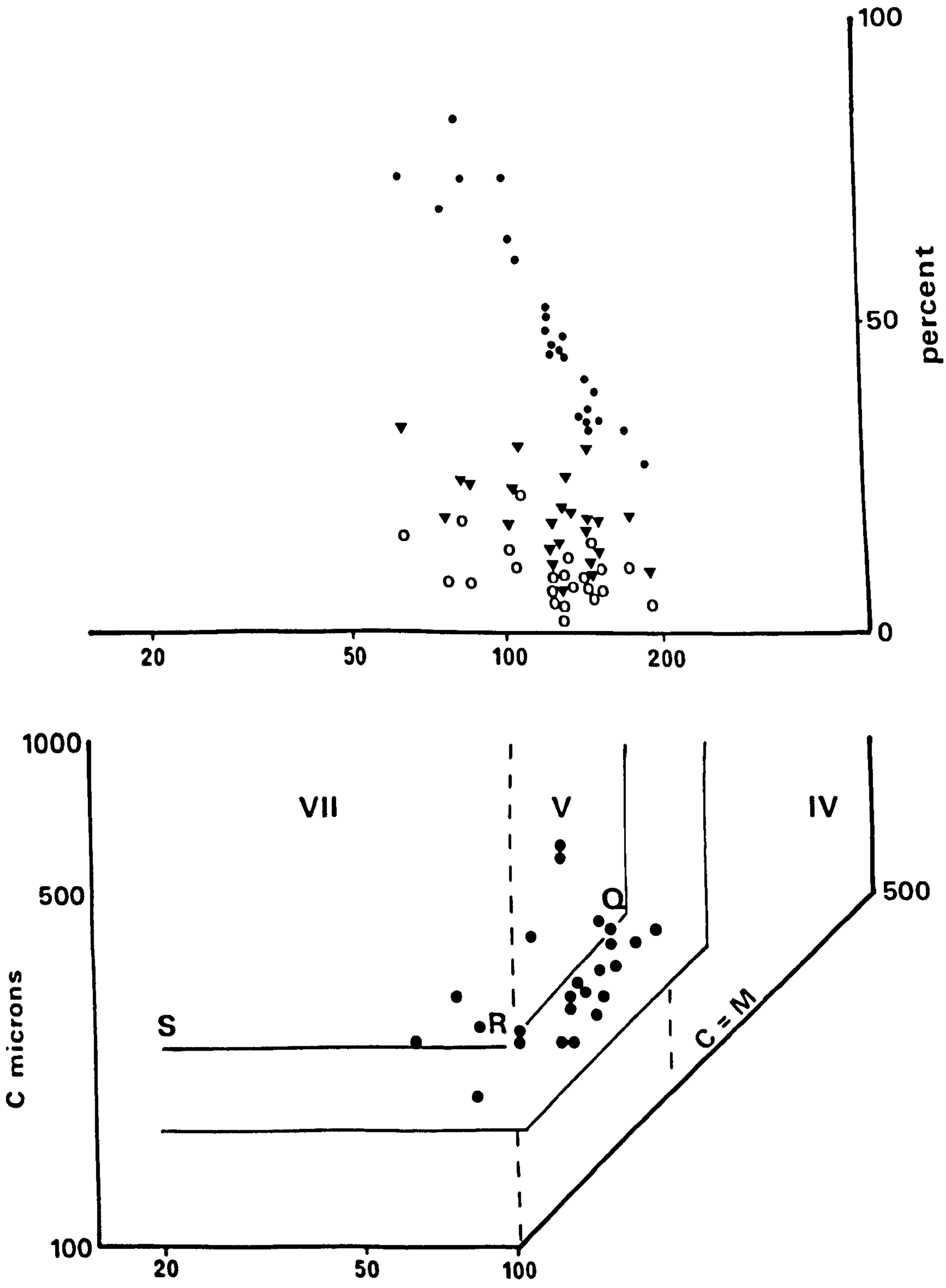

Fig. 4.42. Top: FM, LM, AM diagram for Facies III sediments.
FM: solid dots
LM: triangles
AM: open circles.
Bottom: C-M diagram for Facies III sediments.

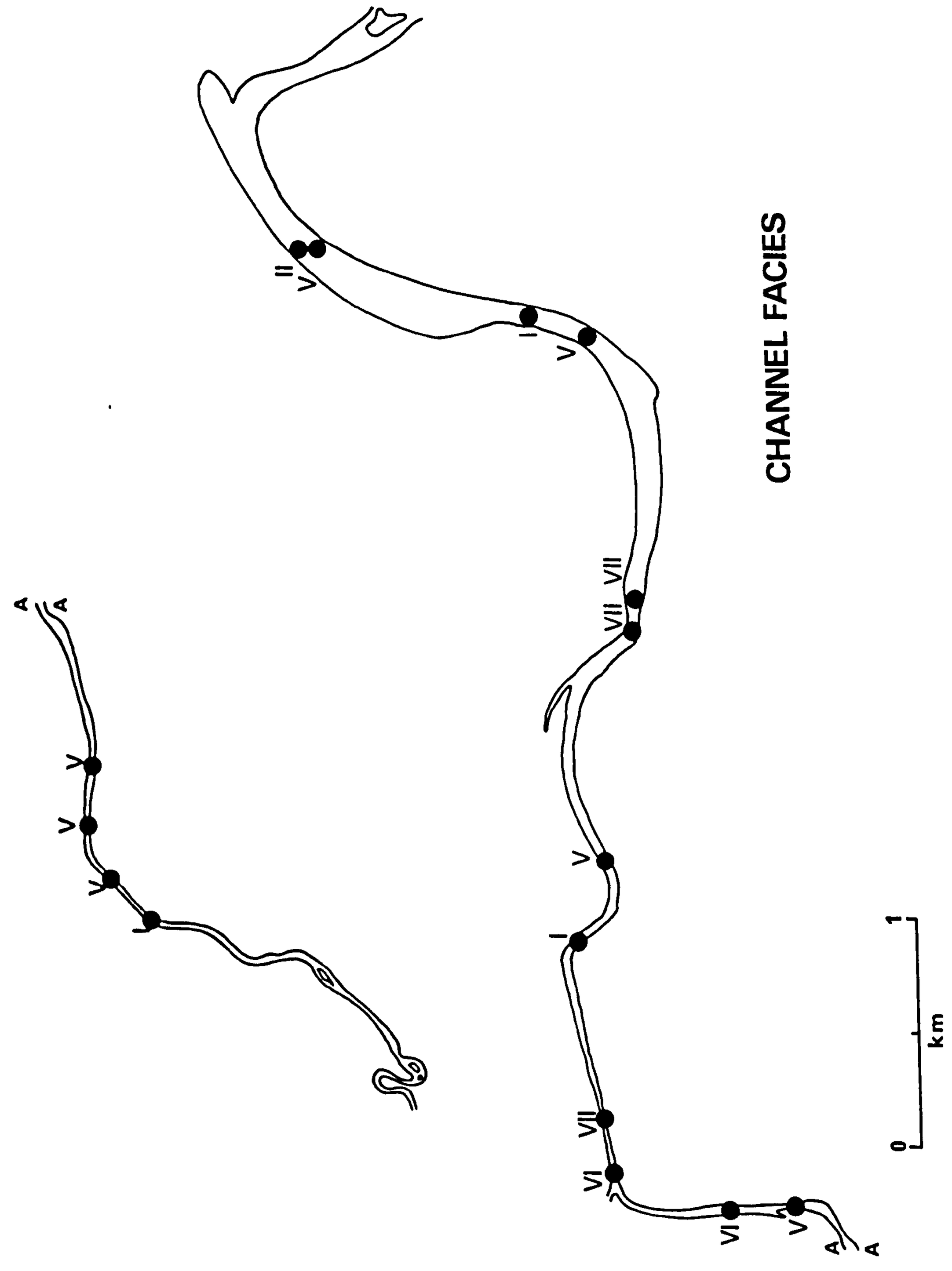

Fig. 4.43. Distribution of facies types within the channel sediments.

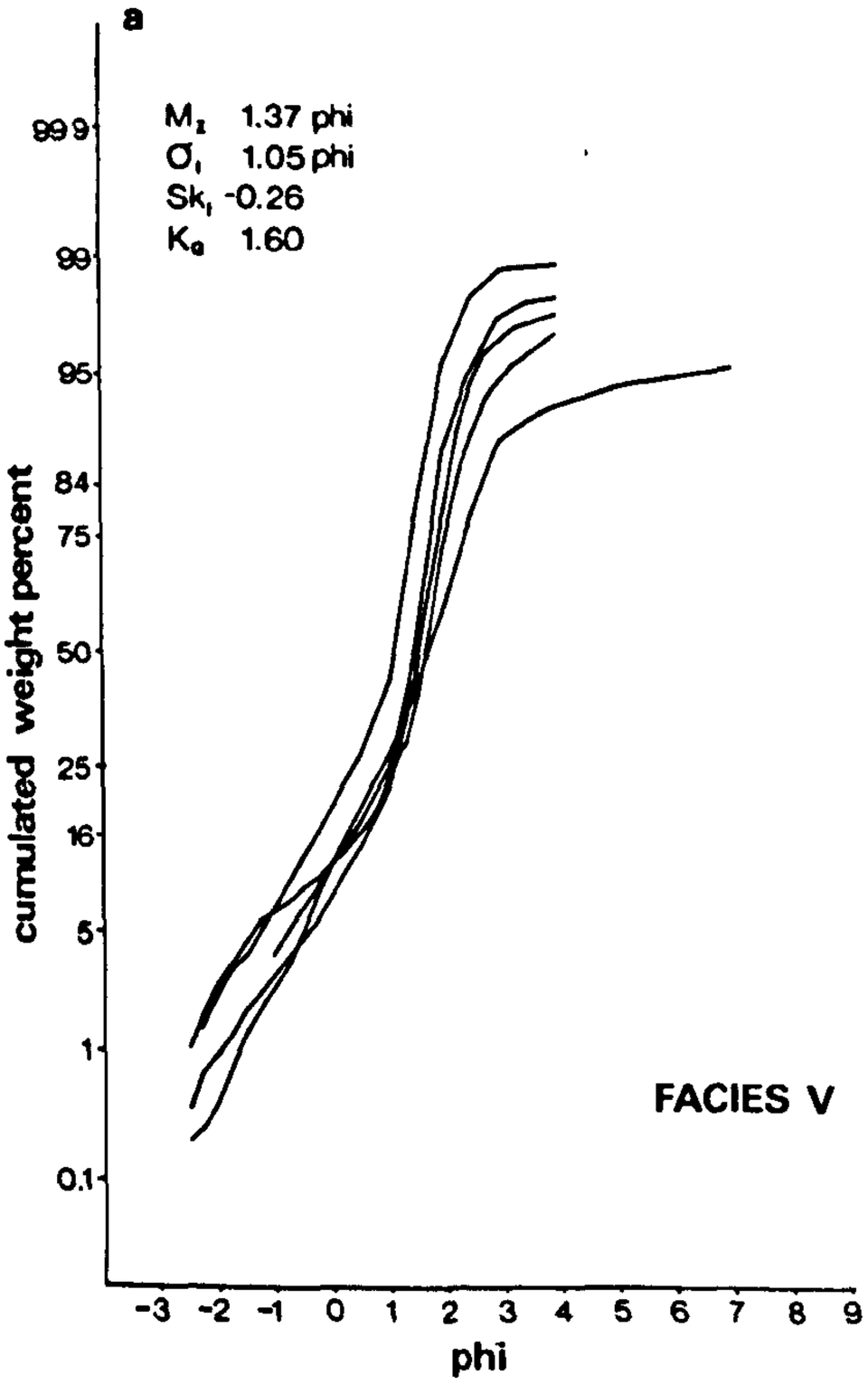

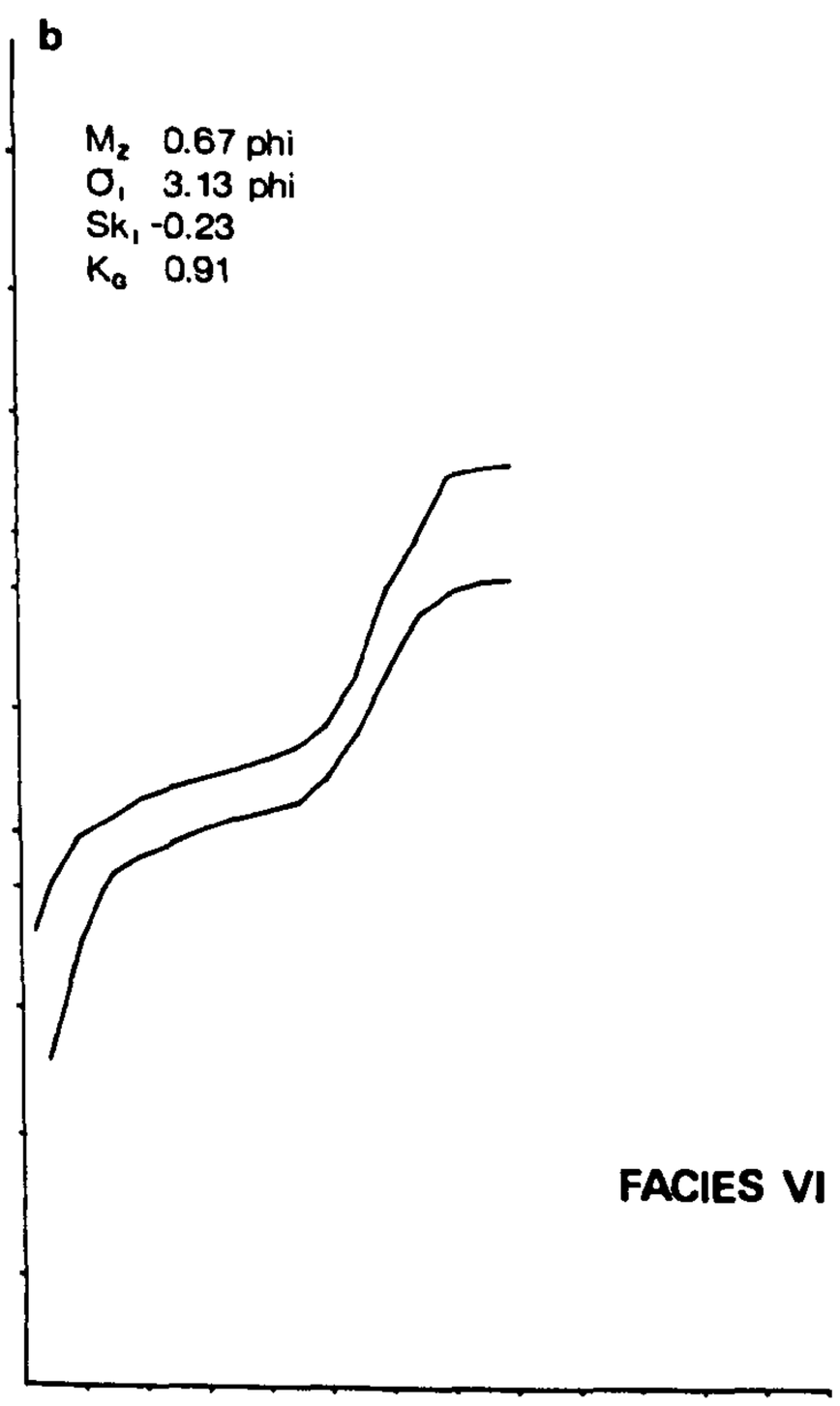

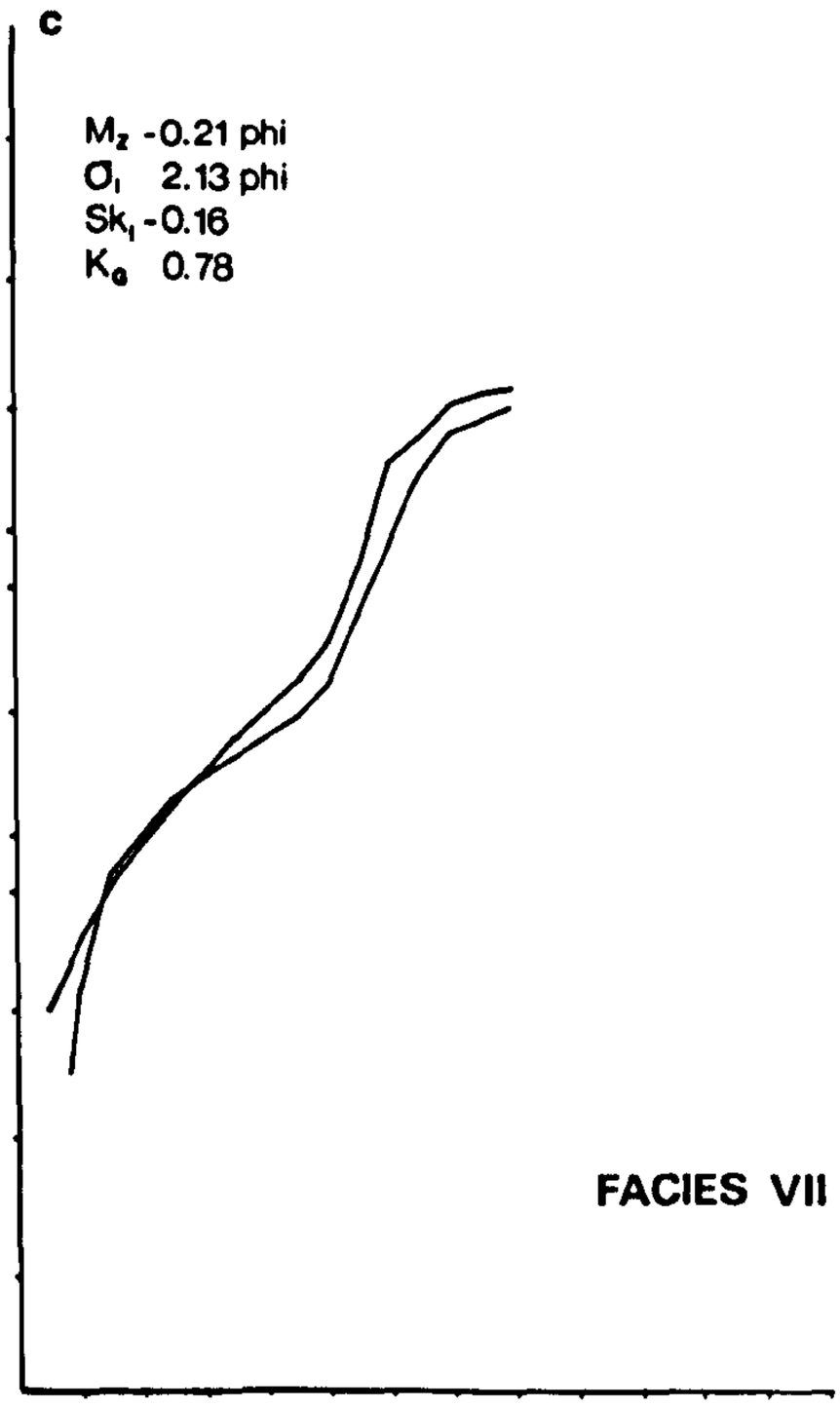

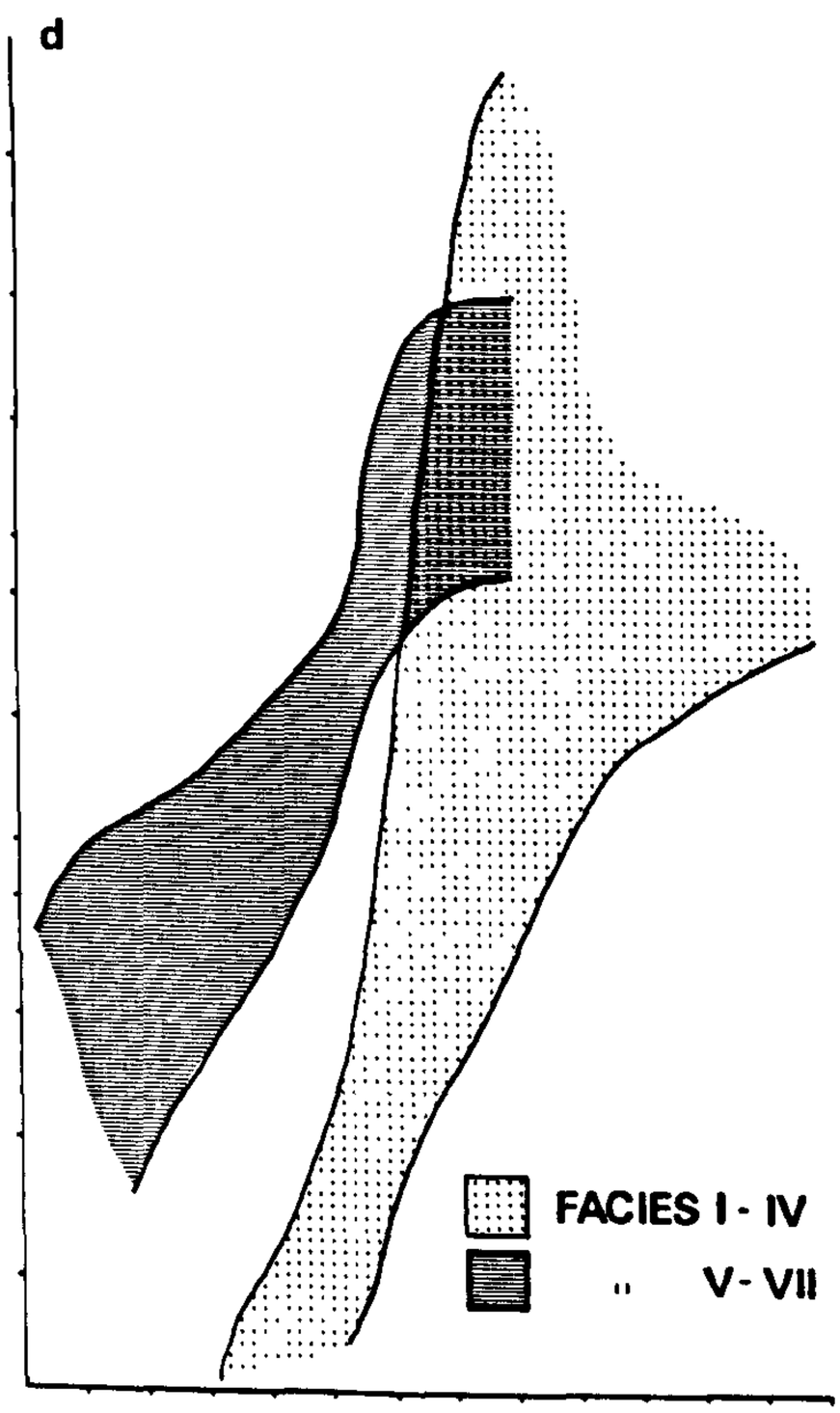

Fig. 4.44. a - c: Cumulative frequency curves of the three Eden channel textural facies.
d: A comparison of the grain-size distributions of intertidal flat and channel samples based on the envelopes of cumulative frequency curves for facies I-IV and V-VII.

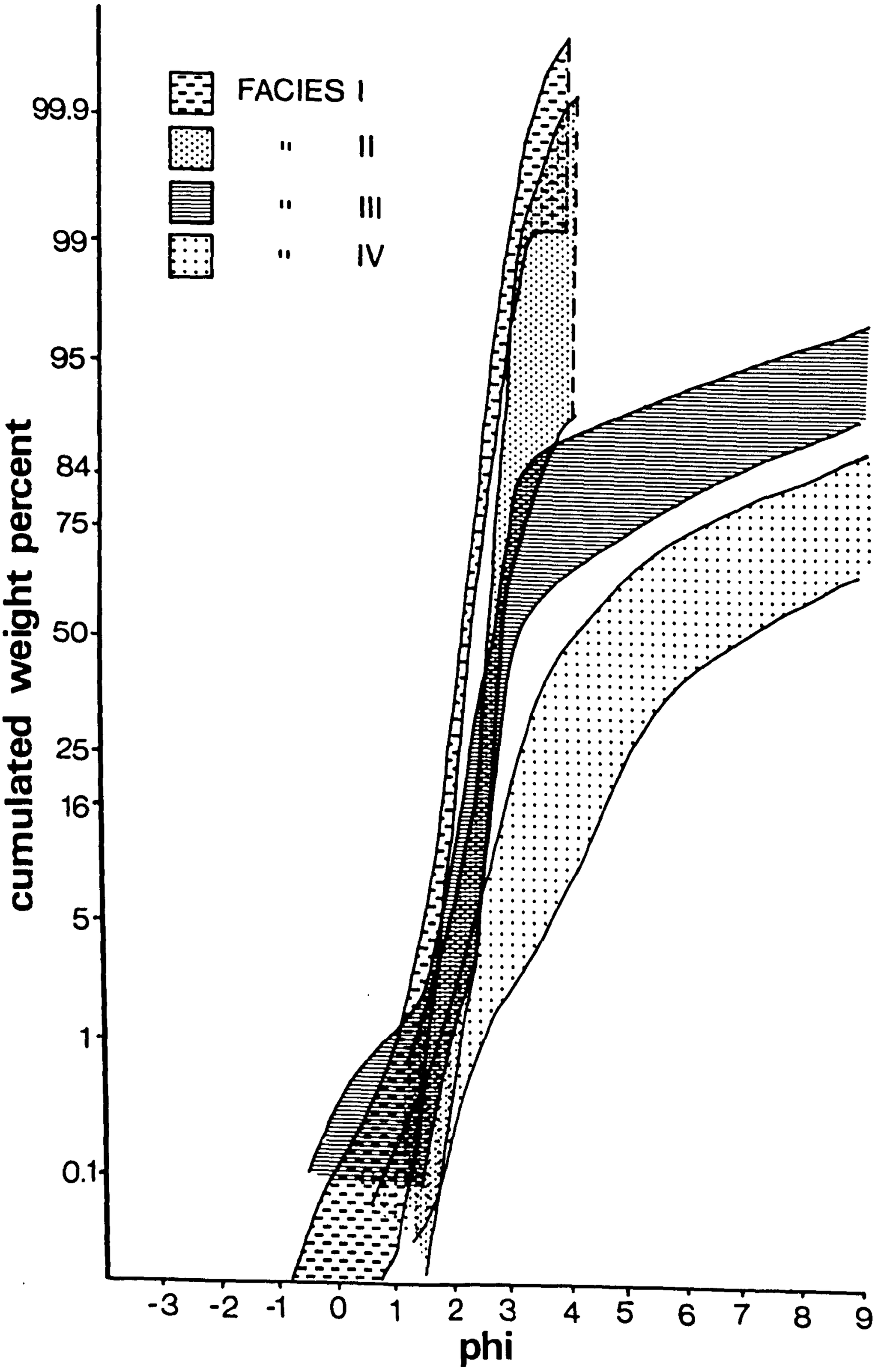

Fig. 4.45. Envelopes of the cumulative grain-size frequency curves of the end-member samples for Facies I-IV.

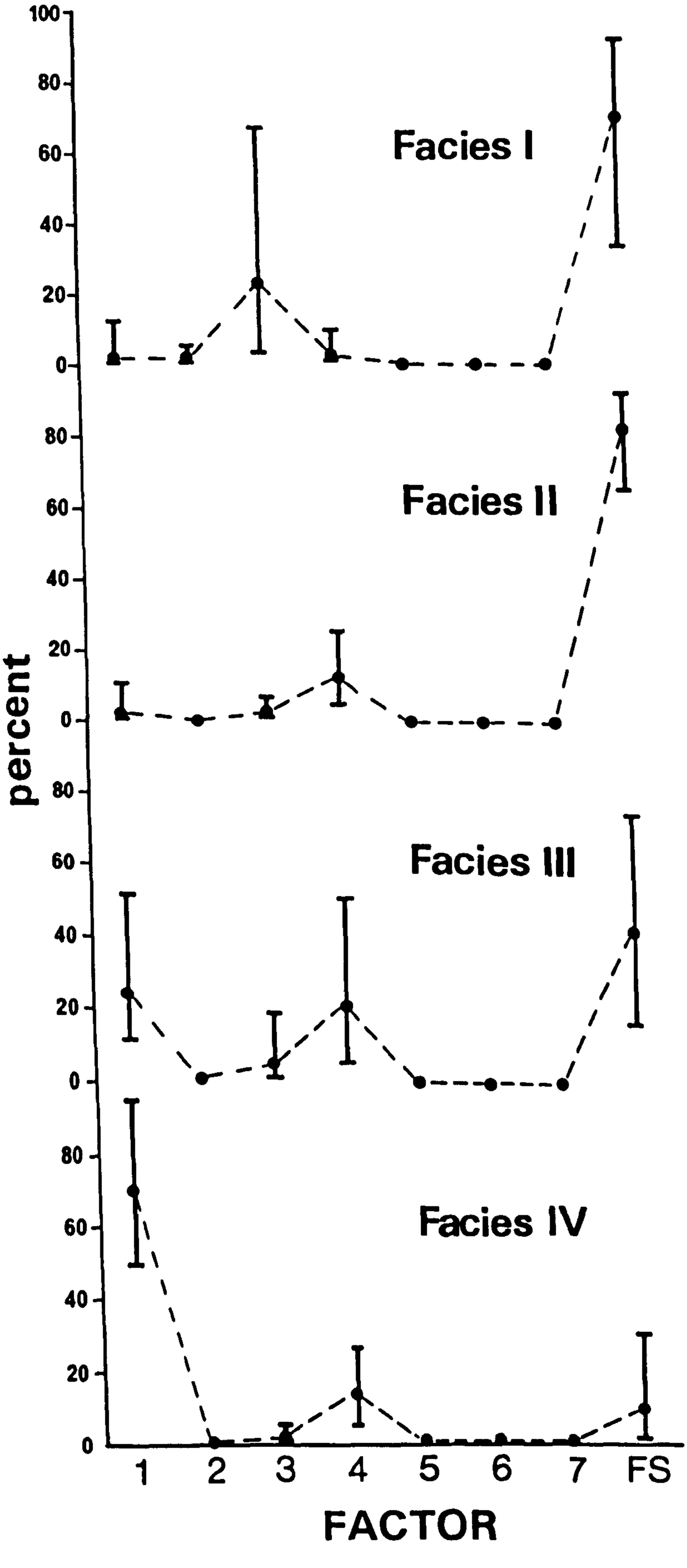

Fig. 4.46. A comparison of the intertidal flat facies I-IV on the basis of sediment sub-populations.
Dots represent average values and bars, the range of values.

APPENDIX 1

Flow Patterns - Lagrangian Data

The surveys were confined to the six hour period around high-water. Measurements could not be taken during the early flood- or late ebb-stages because of inadequate water-depth over the flats.

A. East Kincaple Flat

Flow paths were observed over the eastern part of the Kincaple intertidal flat on 6th. August 1974. Predicted time of high-water at St. Andrews was 17.34 BST. Three drogues were released between 1.5 and 2 hours before high-water. Summaries of the path-time histories are given in Table A1. The distance and velocity values are the minimum possible as the straight line distance between successive points on the curve were measured.

Table A1 Path-time histories - 6th. August 1974.

Drogue	Time BST	Flow Direction	Distance Metres	Average Velocity cm sec^{-1}
A	15.30	-	-	-
	16.10	254	518	22
	16.55	151	573	21
	17.40	057	140	6
	18.05	035	177	10
	18.30	018	238	17
			1646	15
B	15.40	-	-	-
	16.00	220	296	25
	Re-released			
	17.30	-	-	-
	17.58	053	155	9
	18.23	042	262	17
	18.47	020	299	21
	19.13	040	302	19
			1314	18
C	15.52	-	-	-
	16.22	222	220	12
	17.12	236	085	3
	17.50	078	207	9
	18.14	057	244	17
	18.44	051	381	21
	19.06	050	457	35
			1594	16

Table A2 Path-time histories - 18th. July 1974.

Drogue	Time BST	Flow Direction	Distance Metres	Average Velocity cm sec^{-1}
G	13.29	-	-	-
	13.50	144	143	11
	14.45	118	259	8
	15.05	115	162	14
	15.45	090	328	13
	16.19	097	721	36
			1610	16
G$_1$	14.17	-	-	-
	14.42	084	79	5
	15.16	112	418	20
	15.55	090	409	20
			960	16
H	13.39	-	-	-
	14.03	348	55	4
	14.35	120	454	24
	15.30	103	451	14
			960	14

Flow paths were measured over the western part of Kincaple on the 7th. August 1974. Predicted time of high-water at St. Andrews was 13.07 BST. Three drogues were released approximately two hours before high-water. A path-history summary is given in Table A3, page iv.

The three drogues followed similar paths; each was an elongate loop open to the north. Flow on the flood-tide followed a clockwise path. The lateral displacement of water decreased to the west as shown by the decreasing width of the loops. Drogues D and E showed similar patterns of flow during the ebb with the flow direction becoming more easterly as the channel was approached.

Table A3 Path-time histories - 7th. August 1974.

Drogue	Time BST	Flow Direction	Distance Metres	Average Velocity $cm\ sec^{-1}$
D	16.03	-	-	-
	16.25	230	152	11
	17.05	266	244	10
	17.45	295	82	3
	18.05	343	152	12
	18.30	123	259	13
	18.50	078	91	8
	19.20	066	183	13
	19.37	066	152	15
	19.50	070	280	36
			1595	12
E	16.11	-	-	-
	16.43	210	171	9
	17.15	280	183	10
	17.52	312	91	4
	18.10	027	122	11
	18.42	037	152	8
	19.01	059	95	8
	19.13	059	79	11
	19.37	051	201	14
	19.50	070	280	36
			1374	10
F	16.20	-	-	-
	16.53	262	177	9
	17.21	283	171	10
	17.58	-	-	-
	18.32	090	131	6
	18.51	113	134	12
	19.06	090	67	7
	19.30	060	171	12
	19.42	057	122	17
	19.55	084	396	51
			1369	11

C. Areas to the North of the Eden Channel

1. Flood-tide flow was observed in the area to the north of the Eden channel on 9th. July 1974. Time of predicted high-water at St. Andrews was 18.36 BST. The drogue was released over the area of the flood-tidal delta. The path-time history is given in Table A4, page v.

Table A4. Path-time histories - 9th. July 1974.

Drogue	Time BST	Flow Direction	Distance Metres	Average Velocity $cm\ sec^{-1}$
1	15.23	-	-	-
	15.48	233	198	16
	16.04	190	218	23
2	16.33	Re-released		
	16.51	238	247	23
	17.05	235	305	30
	17.18	300	293	30
	17.35	309	311	30
	17.50	299	282	29
	18.05	316	57	7
			1493	27

Initial flow was to the WSW at an average velocity of 16cm sec^{-1}. The direction then changed to SSW, and the drogue became grounded on the rising-bed in the western part of the southern flood-channel within the flood-tidal delta system. The drogue was re-released over the northern part of the flood-tidal delta and the flow direction was again to the south-west until the drogue came under the influence of water flowing up the channel. This caused an abrupt change in flow direction and from 17.05 to 17.18 BST the drogue followed a north-westerly path parallel to the north bank of the channel. At the point where the channel turns to the west the drogue continued on a north-westerly course and was drifted over the flat between Coble House Point and Scally Point.

2. Ebb-flow directions were observed over the area to the north of the Eden channel on 27th. August 1974 (Table A5). Predicted time of high-water at St. Andrews was 11.32 BST.

Table A5. Path-time histories - 27th. August 1974.

Drogue	Time BST	Flow Direction	Distance Metres	Average Velocity cm sec^{-1}
J	10.29	-	-	-
	11.03	023	125	6
	11.39	034	250	12
	12.15	109	193	8
	13.20	-	-	-
			568	9
K	11.15	-	-	-
	11.48	108	244	12
	12.30	074	710	25
	12.54	046	418	39
			1372	25
L	10.48	-	-	-
	11.20	-	-	-
	12.02	077	527	21
	12.44	048	826	33
			1353	27

Drogue J was released one hour before high-water to the west of a topographically high area of mussel banks and Fucus colonies. During the hour before high-water the drogue followed a clockwise path around the western margin of the high area, the flow direction changing from NNE to east. During the early part of the ebb-tide the flow was to the ESE. The drogue eventually became grounded in shallow water between the mussel banks and the sand-bank associated with the spit.

Drogues K and L were released at approximately the time of high-water. They followed parallel paths through the flood-tidal delta system. In both cases an almost easterly flow direction was followed before to the north-east.

4. The Outer Estuary east of Out Head

Three drogues were released to the north of Out Head on 14th. June 1974. Predicted time of high-water at St. Andrews was 09.43 BST. The path-time histories are given in Table A6, page vii.

Table A6. Path-time histories - 14th. June 1974.

Drogue	Time BST	Flow Direction	Distance Metres	Average Velocity $cm\ sec^{-1}$
M	09.59	-	-	-
	10.18	010	338	30
	10.44	020	465	30
	11.00	030	676	70
	11.17	070	623	61
			2102	48
N	10.07	-	-	-
	10.33	020	312	20
	10.52	008	336	30
	11.02	054	676	113
	11.22	070	623	52
			1949	54
P	10.13	-	-	-
	10.39	033	338	22
	10.59	015	549	46
	11.14	052	401	45
	11.22	070	623	130
			1911	61

The drogues were released in the thirty minute period after high-water. Drogues M and P followed very similar paths as they were both controlled by the flow in the Eden channel. The northern drogue (N) was released over the topographically high area on the channel margin. Flow was to the NNE in the early stages but later became NE to ENE as the flow was diverted by a major north-south sand bar situated to the north of the channel.

APPENDIX 2

Organic Matter (Weight percent determined by H_2O_2 oxidisation)

L3	0.88	P16	1.51	R11	2.34	S23	2.60	U17	4.36
M7	1.19	P17	1.90	R12	2.57	S24	2.62	U20	3.13
M8	1.19	P18	2.80	R13	1.73	S25	2.61	U21	3.02
M9	0.35	P19	0.84	R14	0.89	T7	1.41	V7	1.86
N2	0.73	Q2	0.75	R16	7.54	T8	1.29	V8	2.50
N3	0.81	Q3	0.95	R17	3.21	T9	1.35	V9	7.19
N4	1.17	Q4	1.29	R18	1.85	T10	1.19	V10	1.20
N5	0.64	Q5	3.08	R19	1.16	T11	1.29	V11	5.04
N7	1.22	Q7	0.34	R20	5.75	T12	5.90	V12	3.60
N9	1.13	Q8	1.07	R21	1.54	T13	4.13	V13	5.11
N10	1.20	Q11	3.73	R22	7.26	T14	6.23	V14	5.10
O2	1.25	Q12	2.01	R24	7.54	T15	1.61	V15	2.29
O3	0.80	Q13	1.72	S2	0.79	T16	5.02	V16	2.03
O4	1.23	Q14	8.26	S3	1.05	T17	3.27	V26	0.60
O9	1.23	Q16	3.91	S6	0.88	T19	5.27	W7	0.95
O10	0.67	Q17	6.16	S7	1.86	T20	4.92	W8	1.06
O12	3.85	Q18	5.11	S9	0.21	T21	4.49	W9	3.53
O13	1.54	Q19	4.38	S10	0.91	T22	2.92	W10	6.80
O17	1.29	Q20	3.67	S11	1.34	T23	3.13	W11	4.51
P2	0.90	Q21	6.11	S12	2.63	T25	4.47	W12	1.11
P3	0.75	Q22	1.58	S13	4.22	U7	0.99	W13	1.72
P4	1.06	Q23	2.93	S14	2.42	U8	1.78	W14	0.86
P5	1.31	Q24	2.68	S15	12.60	U9	1.58	W27	0.70
P7	1.22	R2	0.83	S16	5.40	U10	1.56	X8	6.36
P9	1.19	R3	0.67	S17	2.21	U11	8.50	X9	1.70
P10	1.11	R6	1.37	S18	1.55	U12	7.84	X10	2.76
P11	0.50	R7	0.19	S19	1.84	U13	2.70	X11	2.04
P12	1.67	R8	0.23	S20	4.27	U14	9.56	X12	3.95
P13	1.53	R9	0.83	S21	2.85	U15	7.90	Y10	1.86
P14	1.37	R10	0.22	S22	3.10	U16	2.70	Y11	3.38

APPENDIX 3

Example of a completed data collection sheet.

Date: 3.7 73 Sample No: N3

Tide: Wind: SW

Ripple Marks

	R1	R2	R3
Straight			
Sinuous		✓	
Catenary			
In-phase			
Out of phase		✓	
Linguoid			
Lunate			
Bow-shaped			
Height	1 3	0.9	0 2
Chord	11	11	2.7
Span	200+	>70	
Semichord	13	3.5	
Inter-saddle Dist.	12	19	
Symmetry	A/Fl.Or	A/Eb.Or	A/Ebb
Dir/Strike	27/028°	28/144°	~/106°
Crestal Platform	-	-	-

Junctures

Open			
Zig-zag			
Comp. Z-Z			
Buttress	✓		
Comp buttress	✓		

Plane-bed	
Lineations	
Firm sub.	
Soft sub.	
Cav. sand	
Sediment	
Shell frags.	
Mytilus	
A. marina	
L. conchilega	

Remarks:-

l = 4.5	l = 4.0	
S = 5.2	S = 7.0	
SL = 17°	SL = 22°	
VFI¹ = 8.46	VFI² = 12.2	VFI³ = 1.35
HFI = ±70	1 52	

The Folk and Ward (1957) formulae and Folk's (1968) verbal descriptions for the sub-divisions of the measures are as follows:

Graphic Mean (Mz)

A measure of the overall average size of a sediment.

$$M_z = \frac{(\phi 16 + \phi 50 + \phi 84)}{3} \text{ phi}$$

Verbal description:

-1.0	to 0.0 phi	Very Coarse Sand
0.0	to 1.0 phi	Coarse Sand
1.0	to 2.0 phi	Medium Sand
2.0	to 3.0 phi	Fine Sand
3.0	to 4.0 phi	Very Fine Sand
4.0	to 5.0 phi	Very Coarse Silt
5.0	to 6.0 phi	Coarse Silt
6.0	to 7.0 phi	Medium Silt
7.0	to 8.0 phi	Fine Silt
8.0	to 9.0 phi	Very Fine Silt
> 9.0	phi	Clay.

Inclusive Graphic Standard Deviation (σ_I)

The average of the standard deviations measured over the central 68% of the curve and the central 90% of the curve.

$$\sigma_I = \frac{\phi 84 - \phi 16}{4} + \frac{\phi 95 - \phi 5}{6.6} \text{ phi}$$

Verbal description:

	0.35	very well-sorted
0.36 -	0.50	well-sorted
0.51 -	0.70	moderately well-sorted
0.71 -	1.00	moderately-sorted
1.10 -	2.00	poorly-sorted
2.10 -	4.00	very poorly-sorted
	4.10	extremely poorly-sorted.

Inclusive Graphic Skewness (Sk_I)

The average of the skewness values measured over the central 68% of the curve and the central 90% of the curve.

$$Sk_I = \frac{\phi 16 + \phi 84 - 2\phi 50}{2(\phi 84 - \phi 16)} + \frac{\phi 5 + \phi 95 - 2\phi 50}{2(\phi 95 - \phi 5)}$$

Verbal description:

+1.0 to +0.3	strongly fine skewed
+0.3 to +0.1	fine skewed
+0.1 to -0.1	near symmetrical
-0.1 to -0.3	coarse skewed
-0.3 to -1.0	strongly coarse skewed.

Graphic Kurtosis (K_G)

A measure of the dispersion in the tails of the distribution compared with that in the central portion. In a phi-normal distribution the $\phi 5$ to $\phi 95$ spread should be 2.44 times that of $\phi 25$ to $\phi 75$.

$$K_G = \frac{\phi 95 - \phi 5}{2.44\ (\phi 75 - \phi 25)}$$

Verbal description:

0.67	very platykurtic
0.67 to 0.90	platykurtic
0.90 to 1.10	mesokurtic
1.10 to 1.50	leptokurtic
1.50 to 3.00	very leptokurtic
> 3.00	extremely leptokurtic.

APPENDIX 4 — Part II

Computer Program for calculation of Folk and Ward Statistical Parameters: a modified version of G.P. Allen's Fortran IV program for granulometric analysis.

```
C      PROGRAMME D'ANALYSE GRANULOMETRIQUE. LES DONNES SONTO 1) LA TAILLE
C      DES TAMIS ENUNITES PHI , ET 2) LE POID DE SEDIMENT RECEULLIS SUR
C      CHAQUE TAMIS, EXPRIME EN POURCENTAGE DU TOTAL.
C      CES DONNES DOIVENT ETRE TAPES EN F 8.2 . LA PREMIERE CARTE
C      PRECEDANT LES CONNES DOIT PORTER LE CHIFFRE  N EGALE AU NOMBRE TOTAL
C      DES TAMIS UTILISES  LA VALEUR DU POID RECEULLIS SUR LE TAMIS AU
C      AU PLUS GRANDES MAILLES DOIT ETRE ZERO  ET LA VALEER DU TAMIS DE FOND
C      DOIT ETRE  6.00 PHI.
C      LES VARIABLES SONT OPHI(N) = DONNES EN PHI  FREQ(J)= POIDS
C      APHI(I) = VALEUR MEDIANE DE L'INTERVAL DES PHI  D(N) = FREQUENCES DES
C      PERCENTILES  C(N) = LES PERCENTILES  SKEW = MOYENNE SIG = LA DEVIATION
C      STANDARD  MOM = LE SKEWNESS .
C      PROGRAMMATEURO GEORGE ALLEN
C      CONSIDERABLY MODIFIED IN WINTER 74-75 BY ED. STEPHENS  GEOLOGY  ST ANDREWS
0001          DIMENSION TITLE(5),TITL1(200),TITL2(200),FREZ(50)
0002          REAL PHI(50) ,FREQ(50),APHI(50),D(21),SKEW,SIG,MOM,SK2,
             1 MO2, C(21)/0.05,0.1,0.15,0.16,0.20,0.25,0.30,0.35,0.40,0.45,
             2 0.50,0.55,0.60,0.65,0.70,0.75,0.80,0.84,0.85,0.90,0.95 /,
             3  AMEAN,PDEV2,PDEV1,PDEV3,PDEV4,PHSK1,PHSK2,PHSK3,PHSK4,
             4AKURT,CUBE,CUBY,SDEV,AMM(50),X,Y(200),A(200),B(200),E(200),
             5  F(200),G(200),P(200),H(200)
0003          REAL ZZ(22)
0004           INTEGER N,M,I,J,LI,FRQ(50),IFR(200)
0005          READ(5,214) IEXTRA,PHIMN
0006      214 FORMAT(I1,F6.0)
0007          IF(PHIMN.EQ.0.0) PHIMN=11.5
0008          LOGICAL*1 L(80)
0009          LI=0
0010      114 FORMAT(4F8.0,I8,5A4)
0011     1992 READ(5,114) CI,QMIN,QMAX,TWEIT,N,TITLE
0012          IF(N.EQ.0)  GO TO 92
0013          M=N
0014          READ(5,215) (FREQ(I),I=1,M)
0015      215 FORMAT(10F8.0)
0016          PHI(1)=QMIN
0017          DO 216 I=2,M
0018      216 PHI(I)=PHI(I-1)+CI
0019          WRITE(6,217) TITLE
```

```
0020          217 FORMAT(' SAMPLE',2X,5A4,//)
0021              FRTOT=0.0
0022              IF(TWEIT.EQ.100.0) GO TO 115
0023              DO 116 I=1,M
0024              FREQ(I)=FREQ(I)*100.0/TWEIT
0025          116 FRTOT=FRTOT+FREQ(I)
0026          666 FORMAT(1X,F10.3)
0027              GO TO 120
0028          115 DO 121 I=1,M
0029          121 FRTOT=FRTOT+FREQ(I)
0030          120 FINES=100.0-FRTOT
0031              IF(IEXTRA.EQ.0) GO TO 117
0032              M=N+1
0033              PHIMAX=PHI(N)
0034              SDV=ABS((PHIMN-PHIMAX)/3.0)
0035              IRNG=IFIX(ABS(PHIMN-PHIMAX)*2)
0036              PI=PHIMAX
0037              DO 118 I=1,IRNG
0038              IPHI=N+I
0039              PHI(IPHI)=PI+1.0
0040              Y1=(PHIMN-PI)/SDV
0041              Y2=(PHIMN-PHI(IPHI))/SDV
0042              CALL NDTR(Y1,P1,D1)
0043              CALL NDTR(Y2,P2,D2)
0044              AREA=P1-P2
0045              FREQ(IPHI)=AREA*FINES
0046          118 PI=PHI(IPHI)
0047              M=IPHI
0048              N=M-1
0049          117 X=0
0050              LI=LI+1
0051              Y(LI)=FREQ(1)
0052              IF(PHI(1).LT.6)Y(LI)=FREQ(N)
0053              DO 93 I=1,N
0054           93     AMM(I)=2**(-PHI(I))
0055              WRITE(6,61)(AMM(I),I=1,N)
0056              WRITE(6,60)(PHI(I),I=1,M)
0057              WRITE(6,70)(FREQ(I),I=1,M)
```

```
0058                X=0
0059                J=N-2
0060                IF(FREQ(1)-FREQ(2))330,330,334
0061             334 X=1
0062                GO TO 330
0063             330 DO 335 I=2,J
0064                IF(FREQ(I)-FREQ(I+1))336,336,335
0065             336 IF(FREQ(I+1)-FREQ(I+2))335,335,338
0066             338 X=X+1
0067             335 CONTINUE
0068                IF(FREQ(N-1)-FREQ(N))339,339,340
0069             339 X=X+1
0070                GO TO 340
0071             340 DO 1 I=1,N
0072               1 APHI(I)=(PHI(I)+PHI(I+1))/2
0073                SKEW=0
0074                DO 2 I=1,N
0075               2 SKEW=SKEW+APHI(I)*FREQ(I)
0076                SKEW= SKEW/100
0077                A(LI)=SKEW
0078                SIG=0
0079                DO 3 I=1,N
0080             3  SIG=(APHI(I)-SKEW)**2*FREQ(I)+SIG
0081                SIG=SQRT(SIG/100)
0082                SDEV=SIG
0083                B(LI)=SDEV
0084                MOM=0
0085                DO 4 I=1,M
0086             4  MOM=(((APHI(I)-SKEW)**3)*FREQ(I))+MOM
0087                CUBE=MOM/100
0088                MOM=(MOM*(1/SIG**3))/100
0089                MOM=MOM/2
0090                SK2 = 2**(-SKEW)
0091                WRITE(6,80) SKEW,SIG,MOM,SK2
0092                X=0.0
0093                DO 3006 I=1,N
0094                IF(FREQ(I).LE.X) GO TO 3006
0095                HHH=(PHI(I)+PHI(I-1))/2
```

```
0096            X=FREQ(I)
0097         3006 CONTINUE
0098            DO5 I=2,M
0099          5  FREQ(I)=FREQ(I)+FREQ(I-1)
0100            DO 1999 I=1,N
0101         1999 FREZ(I)=FREQ(I)
0102            WRITE(6,90) (FREQ(I),I=1,M)
0103            SIG= FREQ(M)
0104            DO6 I=1,M
0105          6  FREQ(I)=FREQ(I)/100
0106            I=1
0107            J=0
0108            FRVL=0.0
0109           13 J=J+1
0110            IF(C(J).GT.FREQ(I)) FRVL=FREQ(I)
0111            IF(J.EQ.22) GO TO 112
0112            IF(C(J).LT.FRVL) GO TO 11
0113           14  IF(C(J).GT.FREQ(I+1)) GO TO 12
0114               D(J)=PHI(I+1)-(PHI(I+1)-PHI(I))*(FREQ(I+1)-C(J))
                  1 /(FREQ(I+1)-FREQ(I))
0115                GO TO 13
0116           11 D(J)=0
0117               GO TO 13
0118           12 I=I+1
0119               IF(I.LT.M)GO TO 14
0120          112  DO 573 I=1,21
0121          573  ZZ(I) =D(I)
               C      THIS REVERSAL OF PERCENTILES HAS BEEN ABANDONED
               C      DO 574 I=1,21
               C 574  D(I) =ZZ(22-I)
0122                WRITE(6,91)(C(J),D(J),J=1,21)
0123                AMEAN=(D(4)+D(18))/2
0124                BMEAN=(D(4)+D(11)+D(18))/3
0125                 PDEV1=(D(18)-D(4))/2
0126                 PDEV2=D(6)/D(16)
0127                PDEV3=(D(21)-D(1))/5
0128                 PDEV4=((D(18)-D(4))/4)+((D(21)-D(1))/6.6)
0129                 PDEV1=ABS(PDEV1)
```

```
0130                PCEV3=ABS(PDEV3)
0131                PDEV4=ABS(PDEV4)
0132               PHSK1=(D(21)+D(1))-(2*D(11))
0133                PHSK2= ((0.5*(D(4)+D(18)))-D(11))/(0.5*(D(18)-D(4)))
0134                PHSK3=((0.5*(D(1)+D(21)))-D(11))/(0.5*(D(18)-D(4)))
0135               PHSK4=((D(4)+D(18)-(2*D(11)))/(2*(D(18)-D(4))))+
                  1 ((D(1)+D(21)-(2*D(11)))/(2*(D(21)-D(1))))
0136               AKURT=(D(21)-D(1))/(2.44*(D(16)-D(6)))
0137               WRITE(6,200) BMEAN,PDEV1,PDEV2,PDEV3,PDEV4
0138                WRITE(6,203)CUBE
0139                WRITE(6,201) PHSK1,PHSK2,PHSK3,PHSK4
0140                WRITE(6,202) AKURT
0141               E(LI)=0.
0142               IF(Y(LI).LT.5)E(LI)=PHSK1
0143               IF(Y(LI).GT.5)E(LI)=PHSK2
0144               IF(Y(LI).GT.15.999)E(LI)=99.99
0145                 F(LI)=D(11)
0146                 G(LI)=CUBE
0147                 H(LI)=AKURT
0148              P(LI)=D(1)
0149                   FREQ(1)=FREQ(1)*100
0150                IF(X-2)1870,1872,1873
0151          1870    WRITE(6,870)
0152                  GO TO 58
0153          1872    WRITE(6,872)
0154                  GO TO 58
0155          1873    WRITE(6,873)
0156                  GO TO 58
0157            58     IF(SDEV.LT.0.35) GO TO 1860
0158                 IF(SDEV.LT.0.5)GO TO 1861
0159                 IF(SDEV.LT.0.8)GO TO 1862
0160                 IF(SDEV.LT.1.4) GO TO 1863
0161                 IF(SDEV.LT.2.00)GO TO 1864
0162                 IF(SDEV.LT.2.6) GO TO 1865
0163                 IF(SDEV.GT.2.6)GO TO 1866
0164          1860 WRITE(6,860)
0165                GO TO 67
0166          1861 WRITE(6,861)
```

```
0167                GO TO 67
0168             1862 WRITE(6,862)
0169                GO TO 67
0170             1863 WRITE(6,863)
0171                GO TO 67
0172             1864 WRITE(6,864)
0173                GO TO 67
0174             1865 WRITE(6,865)
0175                GO TO 67
0176             1866 WRITE(6,866)
0177                GO TO 67
                 C   FRIEDMAN TEST
0178             67 IF(CUBE.LT.-2.00) GO TO 992
0179                IF(SDEV.GT.0.6) GO TO 500
0180                IF(CUBE.LT.0.05) GO TO 600
0181                GO TO 650
0182             500 IF(SDEV.GT.0.84) GO TO 501
0183                CUBY = 1.15-(1.83*SDEV)
0184                IF(CUBE.LT.CUBY) GO TO 600
0185                GO TO 650
0186             501 IF(SDEV.GT.1.0) GO TO 650
0187                CUBY=8-(10*SDEV)
0188                IF(CUBE.LT.CUBY) GO TO 600
0189                GO TO 650
0190             600 WRITE(6,602)
0191                IFR(LI)=2
0192                GO TO 992
0193             650 WRITE(6,603)
0194                IFR(LI)=1
0195                GO TO 992
0196             992 J=0
0197                DO 1073 I=1,21
0198                IF(I.EQ.4) GO TO 1073
0199                IF(I.EQ.18) GO TO 1073
0200                J=J+1
0201                FREQ(J)=D(I)
0202            1073 CONTINUE
0203                N=19
```

```
0204                WRITE(6,333)(L(I),I=1,78)
                C   CALL GRAPH(FREQ,FRQ,N)
0205                TITL1(LI)=TITLE(4)
0206                TITL2(LI)=TITLE(5)
0207                DO 1995 I=1,N
0208                IF(PHI(I).NE.4.0) GO TO 1995
0209                FINES=100.0-FREZ(I)
0210                GO TO 1996
0211             1995 CONTINUE
0212             1996 Y(LI)=FINES
0213                A(LI)=BMEAN
0214                B(LI)=PDEV4
0215                E(LI)=PHSK4
0216                F(LI)=AKURT
0217                H(LI)=HHH
0218                G(LI)=D(11)
0219                GO TO 1992
                C  92 READ(5,412)
                C     WRITE(7,402)(Y(I),A(I),B(I),E(I),F(I),G(I),H(I),
                C    1P(I),IFR(I),I=1,LI)
0220               92 WRITE(7,409)(TITL1(I),TITL2(I),Y(I),A(I),B(I),E(I),F(I),P(I),G(I),
                   1H(I),I=1,LI)
0221              409 FORMAT(2A4,8F6.2)
0222                  WRITE(6,2005)
0223                  DO 2006 I=1,LI
0224                  IF(IFR(I).EQ.1) GO TO 2007
0225                  WRITE(6,2002)TITL1(I),TITL2(I),Y(I),A(I),B(I),E(I),F(I),P(I) ,G(I)
                     1,H(I)
0226                  GO TO 2006
0227             2007 WRITE(6,2008)TITL1(I),TITL2(I),Y(I),A(I),B(I),E(I),F(I),P(I),G(I),
                     1H(I)
0228             2006 CONTINUE
0229                  IUYT=KLOCK(JHGF,LLA)
0230                  LLA=LLA-LLB
0231                  WRITE(6,9995) LLA
0232                  STOP
0233              402 FORMAT(23X,8F6.2,I2)
0234              222 FORMAT(I2,78A1)
```

```
0235          333 FORMAT('1',T20,78A1,//)
0236           30 FORMAT(10F8.4)
0237          412 FORMAT(' ')
0238           60 FORMAT(' DIAMETERES PHI '(T20,12F8.4))
0239         9995 FORMAT(' TEMPS DE CALCUL EN SECONDS',F8.2)
0240           61 FORMAT(' DIAMETERES MM'(T20,12F8.4))
0241           70 FORMAT(' FREQUENCES 0'(T20,12F8.4))
0242           80 FORMAT('0'T20,'MOYENNE',T40,'ECART TYPE',T60,'SKEWNESS'
                 1/T10,'PHI',T20,F8.4,T40,F8.4,T60,F8.4,/T10,'MM',T20,F8.4)
0243           90 FORMAT ('OCUMULS 0'(T20,12F8.4))
0244           91 FORMAT(/(7(F11.4,F6.2)))
0245          200 FORMAT('OMOYENNE PHI =',F8.4,///,' DEVIATION PHI =',F8.4
                 1,4X,' TRASK SORTING =',F8.4,4X,' SORTING SIMPLE = ',F8.4,
                 24X,' INCLUSIVE GRAPHIC ST DEV =',F8.4)
0246          201 FORMAT('OSKEWNESS SIMPLE =',F8.4,4X,' SKEWNESS PHI =',
                 1F8.4,4X,' DEUXIEME PHI SKEWNESS =',F8.4,4X,
                 2//' INCLUSIVE GRAPHIC SKEWNESS =',F8.4)
0247          203 FORMAT(//' MEAN CUBED DEVIATION =', F8.4)
0248          202 FORMAT('OKURTOSIS GRAPHIQUE ='F8.4)
0249           870 FORMAT(//,3X,' SABLE UNIMODAL')
0250           872 FORMAT(///,3X,' SABLE BIMODAL')
0251           873 FORMAT(///,3X,' SABLE MULTIMODAL')
0252           861 FORMAT(3X,' SABLE BIEN CLASSE')
0253           860 FORMAT(3X,' SABLE TRES BEIN CLASSE')
0254           862 FORMAT(3X,'SABLE MODERAMENT BEIN CLASSE')
0255           863 FORMAT(3X,' SABLE MODERAMENT CLASSE')
0256           864 FORMAT(3X,' SABLE MAL CLASSE')
0257           865 FORMAT(3X,' SABLE TRES MAL CLASSE')
0258           866 FORMAT(3X,' SABLE EXTREMEMENT MAL CLASSE')
0259           602 FORMAT(   ///' SELON LES TRAVAUX DE FREIDMAN, CE SABLE EST PROBABI
                 1LEMENT DORIGINE PLAGE MARINE')
0260           603 FORMAT(/,4X,' SELON LES TRAVAUX DE FRIEDMAN, CE SABLE EST PROBABIL
                 1EMENT DORIGINE ALLUVIALE ')
0261          2005 FORMAT('1LISTING DES RESULTAS GRANULOMETRIQUES',
                 1////,' SAMPLE   FINES     MEAN      S.DEV.   SKEWNESS  KURTOSIS
                 1P(5)      P(50)    MODE',4X ,' FRIEDMAN',//)
0262          2002 FORMAT(' ',2A4,8F10.3,3X,'PLAGE')
0263          2008 FORMAT(' ',2A4,8F10.3,3X,' ALLUVIAL')
```

```
0264          1070 FORMAT(' ',100A1,//)
0265               END


0001               SUBRCUTINE NDTR(X,P,D)
0002               AX=ABS(X)
0003               T=1.0/(1.0+0.2316419*AX)
0004               D=0.3989423*EXP(-X*X/2.0)
0005               P=1.0-D*T*((((1.330274*T-1.821256)*T+1.781478)*T-0.3565638)*T+0.31
                  193815)
0006               IF(X) 1,2,2
0007             1 P=1.0-P
0008             2 RETURN
0009               END
```

Folk & Ward Statistical Parameters

	Mz	σ_I	Sk_I	K_G
A1	2.17	0.48	-0.27	1.09
B2	2.18	0.45	-0.20	1.02
C1	1.95	0.51	-0.04	0.86
D2	2.13	0.46	-0.15	1.07
E3	2.46	0.29	-0.12	1.11
F2	2.15	0.38	-0.08	0.98
F4	2.32	0.33	-0.04	1.06
G1	2.25	0.37	-0.06	1.01
G3	2.42	0.31	-0.09	1.07
G5	2.32	0.28	0.08	0.97
H2	2.24	0.35	-0.05	1.03
H4	2.43	0.31	-0.07	1.13
I3	2.21	0.33	0.09	1.02
I5	2.36	0.42	0.10	1.21
J2	2.23	0.36	-0.18	1.07
J4	2.23	0.32	-0.01	1.04
J6	2.43	0.39	0.05	1.06
K5	2.26	0.36	-0.09	1.02
L4	2.35	0.36	-0.05	0.94
L5	2.13	0.37	0.10	0.97
L6	2.25	0.34	-0.00	0.97
M3	2.20	0.46	-0.02	0.93
M4	2.45	0.32	-0.28	0.97
M6	2.22	0.34	0.08	0.96
M7	2.45	0.34	-0.23	1.06
M8	2.29	0.35	0.11	0.94
N2	2.55	0.34	-0.22	1.27
N4	2.63	0.29	-0.16	1.29
N8	2.20	0.38	0.00	0.99
N9	2.31	0.39	0.00	0.96
N10	2.52	1.18	0.41	5.16
O3	2.63	0.31	-0.10	1.43
O7	2.33	0.27	0.16	0.83
O8	2.36	0.31	0.17	0.86
O9	2.48	0.35	-0.15	1.12
O13	2.79	0.31	0.02	1.22
O17	2.44	0.69	0.33	2.29
P2	2.76	0.24	-0.09	1.14
P4	2.67	0.33	-0.19	1.45
P5	2.43	0.36	-0.29	1.21
P8	2.27	0.39	-0.07	0.92
P10	2.49	0.40	-0.09	1.14
P12	3.12	1.87	0.66	3.22
P14	2.53	0.38	-0.17	1.22
P16	2.62	0.93	0.40	3.66
P18	3.37	2.33	0.77	2.09
Q3	2.67	0.30	-0.07	1.44
Q5	2.67	0.29	-0.06	1.29
Q7	2.36	0.38	-0.10	1.06
Q9	2.51	0.35	-0.15	1.24
Q11	3.91	2.49	0.73	1.59
Q13	4.13	2.83	0.76	1.16

	Mz	σ_I	Sk_I	K_G
Q17	5.45	2.90	0.49	1.02
Q19	7.38	3.36	0.25	0.63
Q21	7.36	3.03	0.44	0.68
Q23	3.41	2.31	0.70	2.38
R2	2.78	0.24	-0.13	1.17
R6	2.73	0.31	-0.11	1.28
R7	2.76	0.35	0.18	1.19
R8	2.28	0.43	-0.09	0.93
R9	2.37	0.41	-0.10	0.96
R10	2.83	0.53	0.31	2.52
R12	5.52	3.53	0.83	1.03
R14	1.83	0.75	-0.12	1.52
R16	6.73	3.43	0.48	0.63
R18	2.22	0.49	-0.09	1.04
R20	4.94	2.74	0.60	1.24
R22	5.34	2.84	0.53	1.15
R24	7.99	2.99	0.26	0.62
S3	2.71	0.33	-0.15	1.44
S7	2.59	0.34	-0.08	1.13
S9	2.43	0.35	-0.10	1.10
S11	2.92	0.81	0.49	3.58
S13	5.21	2.79	0.42	1.08
S15	6.59	3.59	0.32	0.74
S17	2.86	1.43	0.65	2.06
S19	3.84	2.02	0.71	3.66
S21	3.71	1.29	0.42	2.32
S23	3.32	1.21	0.64	2.80
S25	3.37	1.70	0.67	5.02
T8	2.66	0.37	-0.16	1.30
T10	2.77	0.25	-0.02	1.09
T12	6.59	3.40	0.43	0.84
T14	6.12	2.44	0.33	1.19
T16	4.77	2.52	0.57	1.31
T20	6.80	3.23	0.58	0.65
T22	3.96	2.11	0.75	1.86
U7	2.49	0.38	-0.20	1.20
U9	3.09	0.65	0.54	2.66
U11	6.83	3.56	0.37	0.58
U13	7.22	3.13	0.42	0.72
U15	5.24	2.76	0.42	1.21
U17	3.67	1.84	0.72	1.29
U21	4.08	2.04	0.59	1.73
V8	3.41	1.37	0.62	1.19
V10	2.89	0.24	0.11	1.47
V12	3.12	1.77	0.65	4.24
V14	3.69	2.13	0.78	2.08
V16	2.38	0.68	0.28	2.66
V26	1.37	0.88	-0.30	1.45
W7	2.44	0.37	-0.22	1.08
W9	5.02	2.95	0.44	1.12
W11	3.88	1.98	0.44	2.10
W13	2.62	0.71	0.38	3.36
X8	2.65	0.94	0.41	3.89
X10	2.79	1.28	0.49	6.70
X12	3.53	2.22	0.76	1.95
Y11	3.43	1.92	0.80	5.44

	Mz	σ_I	Sk_I	K_G
1WS	2.93	0.28	-0.14	1.09
2WS	2.32	0.38	-0.02	0.91
3EB	2.34	0.37	0.07	0.88
4EB	2.43	0.36	-0.01	0.91
5EB	2.42	0.37	-0.04	0.93
6EB	2.37	0.36	-0.06	0.91
7EB	2.49	0.36	-0.04	1.10
8EB	2.25	0.35	0.07	0.92
9EB	2.15	0.36	0.12	0.92
10EB	2.27	0.36	0.10	0.87
11EB	2.41	0.37	0.06	0.93
BS1	2.25	0.36	0.11	0.94
BS2	2.18	0.43	0.19	0.94
BS3	2.19	0.32	0.18	0.92
SD1	2.71	0.24	0.20	1.28
SD2	2.66	0.27	-0.01	1.41
SD3	2.65	0.31	-0.02	1.43
SD4	2.64	0.29	-0.06	1.49
SD5	2.63	0.28	-0.07	1.49
SW1	2.39	0.32	-0.08	0.99
SW2	2.32	0.33	0.00	0.94
SW3	2.13	0.35	0.11	0.98
SW4	2.34	0.32	-0.02	0.94
SW5	2.13	0.34	0.08	0.95
SW6	2.15	0.35	0.06	0.93
SW7	2.29	0.28	0.12	0.96
SW8	2.19	0.29	0.10	0.99
SW9	2.19	0.29	0.13	0.99
SW10	2.14	0.36	0.02	0.96
SW11	1.99	0.38	0.09	1.10
SW12	2.12	0.36	0.03	0.99
SW13	1.87	0.39	0.07	1.11
SW14	2.19	0.47	-0.06	0.86
SW15	1.99	0.48	0.03	0.96
SW16	2.32	0.39	-0.03	0.94
SW17	2.25	0.43	0.00	0.91
1UE	3.48	2.39	0.50	2.63
2UE	1.88	1.06	-0.32	1.73
3BUE	1.47	0.80	-0.30	1.46
5UE	1.63	1.57	0.03	1.87
6UE	1.51	1.05	-0.33	1.95
7UE	2.03	0.65	-0.14	1.13
1LE	1.30	3.44	-0.08	1.05
2LE	0.03	2.82	-0.38	0.77
3LE	-0.05	2.23	-0.21	0.76
4LE	2.02	0.87	-0.06	1.52
5LE	0.87	0.93	-0.44	1.27
6LE	-0.36	2.02	-0.12	0.80
7LE	0.50	1.56	-0.44	0.82
8LE	1.53	0.85	-0.21	1.95
9LE	1.00	1.89	-0.55	1.02
10LE	0.03	2.08	-0.24	0.72
11LE	2.53	0.35	0.12	1.13
12LE	1.90	1.42	-0.32	2.20

APPENDIX 5

Percentage content of the basic factor groupings.

	FACTOR 1	FACTOR 2	FACTOR 3	FINE SAND	FACTOR 4	FACTOR 5	FACTOR 6	FACTOR 7
A1	0.72		30.79	67.94	0.54			
B2	0.27		31.83	67.25	0.64			
C1	0.32		53.05	46.10	0.53			
D2	0.13		34.46	63.82	1.58			
E3	0.01		6.23	91.07	2.68			
F2	0.27		32.68	66.52	0.53			
F4	0.72		14.82	83.23	1.22			
G1	0.08		23.71	74.57	1.64			
G3	0.20		7.71	89.53	2.55			
G5	0.05		9.48	89.17	1.30			
H2	0.41		22.64	75.74	1.21			
H4	0.25		6.84	89.95	2.95			
I3	0.31		24.06	74.21	1.42			
I5	4.30		16.35	76.72	2.63		1.18	
J2	0.71		24.41	74.38	0.50			
J4	0.60		20.91	77.84	0.65			
J6	0.20		10.85	80.30	8.64			
K5	0.81		22.40	75.94	0.84			
L4	0.17		17.05	80.29	2.48			
L5	0.20		39.68	59.36	0.76			
L6	0.60		21.97	76.53	0.90			
M3	0.05		32.78	65.01	2.16			
M4	0.04		8.33	89.68	1.94			
M6	0.02		24.07	74.93	0.97			
M7	0.75		9.84	85.50	3.92			
M8	0.11		18.90	78.91	2.06			
N2	0.65		9.58	85.13	4.66			
N4	0.73		4.72	90.00	4.55			
N8	0.37		29.44	68.98	1.21			
N9	0.36		20.26	76.33	3.05			
N10	7.98		10.45	76.13	5.44		1.03	
O3	1.04		4.75	87.27	6.95			
O7	0.27		6.72	91.98	1.04			
O8	0.48		7.43	89.85	2.22			
O9	1.06		8.42	85.49	5.05			
O13	1.79		2.13	77.17	18.94			
O17	7.72		13.50	73.65	5.18		3.38	
P2	0.72		2.08	86.11	11.07			
P4	1.18		6.26	85.08	7.48			
P5	0.05		11.94	85.34	2.67			
P8	1.13		27.10	70.30	1.47			
P10	1.43		12.03	80.48	6.06			
P12	20.80		10.30	55.71	13.19		9.67	
P14	1.45		10.17	83.14	5.25			
P16	10.77		7.32	75.61	6.28		3.33	
P18	25.57		14.43	53.11	6.87		8.72	
Q3	0.86		4.58	86.43	8.13			
Q5	0.08		3.10	87.97	8.86			
Q7	0.22		16.64	79.20	3.94			
Q9	1.58		7.01	86.13	5.27			
Q11	32.25		6.25	45.55	15.94		10.39	

	F1	F2	F3	FS	F4	F5	F6	F7
Q13	33.68		11.42	47.54	7.37	6.96		
Q17	56.10		1.77	16.78	25.36	18.89		
Q19	82.95		0.69	5.19	11.16	16.55		
Q21	91.55		0.78	1.72	5.96	17.75		
Q23	24.21		12.69	48.42	14.69	10.45		
R2	1.28		2.08	84.33	12.31			
R6	2.00		3.92	80.94	13.13			
R7	0.96		1.77	76.11	21.15			
R8	0.04		27.72	69.72	2.51			
R9	1.54		19.89	74.12	4.47			
R10	5.68		2.65	73.46	18.20	2.87		
R12	33.24		3.62	35.58	27.55	10.09		
R14	2.96		64.17	30.69	2.20			
R16	72.95		0.67	7.85	18.52	23.62		
R18	2.25		32.58	60.92	2.62			
R20	49.62		1.80	22.47	26.12	23.31		
R22	59.51		1.50	15.77	23.22	27.95		
R24	94.92			0.69	4.39	11.20		
S3	0.82		5.91	80.38	12.88			
S7	0.41		5.21	86.42	7.99			
S9	0.75		9.89	84.26	5.12			
S11	9.07		0.91	65.04	24.98	4.96		
S13	59.52		0.60	19.86	19.94	20.88		
S15	65.66		3.60	14.53	16.22	12.89		
S17	18.15		18.73	54.64	8.49	10.52		
S19	25.23		0.91	24.79	49.07	23.70		
S21	33.60		0.24	15.74	50.43	42.92		
S23	19.71		1.12	47.48	31.68	12.87		
S25	18.76		4.02	42.65	34.58	9.54		
T8	2.09		6.80	80.06	11.05			
T10	1.77		0.32	83.95	13.96			
T12	72.32		0.56	9.24	17.88	18.44		
T14	85.28		0.43	4.05	10.23	23.30		
T16	51.36		1.01	24.38	23.24	19.81		
T20	81.36		0.37	3.42	14.84	31.36		
T22	37.67		0.95	35.32	26.07	18.56		
U7	0.58		10.90	82.34	6.21			
U9	13.00		0.96	53.91	32.11			
U11	71.04		0.52	10.61	17.82	17.70		
U13	87.98		0.30	3.65	8.07	17.92		
U15	62.98		2.56	17.16	17.30	22.22		
U17	33.65		3.18	52.09	11.07	11.07		
U21	44.28		1.18	25.73	28.80	21.95		
V8	31.90		3.14	50.14	14.82	20.04		
V10	2.18		0.66	74.26	22.90			
V12	19.06		7.54	58.08	15.32	9.25		
V14	29.49		3.17	51.13	16.21	9.87		
V16	6.12		15.18	75.73	2.97	1.18		
V26	1.82	3.91	76.98	16.78	0.51			
W7	0.99		12.05	82.43	4.53			
W9	54.44		4.16	30.14	11.27	18.17		
W11	41.48		2.40	28.31	27.81	35.09		
W13	8.21		3.46	81.89	6.44	1.95		
X8	11.28		6.53	76.12	6.06	2.17		
X10	11.78		3.46	73.75	10.99	2.92		
X12	27.30		6.53	57.88	8.30	7.92		
Y11	20.66		1.51	63.79	14.05	5.75		

	F1	F2	F3	FS	F4	F5	F6	F7
1WS	0.23		4.29	92.01	3.47			
2WS	0.14		19.70	78.05	2.11			
3EB	1.26		17.70	77.93	3.11			
4EB	0.14		8.81	85.31	5.24			
5EB	0.44		11.92	82.48	5.15			
6EB	0.13		15.71	81.42	2.75			
7EB	0.22		7.65	84.91	7.21			
8EB	0.16		22.51	76.37	5.56			
9EB	0.38		37.70	61.04	0.88			
10EB	0.20		22.73	75.35	1.72			
11EB	0.41		10.64	83.02	5.93			
BS1	0.16		24.26	73.68	1.90			
BS2	0.42		39.31	56.64	3.63			
BS3	0.04		27.92	70.87	1.17			
SD1	0.22		0.86	88.72	10.19			
SD2	0.06		2.29	90.51	7.14			
SD3	0.16		2.27	87.64	9.92			
SD4	0.27		2.20	90.39	7.13			
SD5	0.29		2.42	90.76	6.52			
SW1	0.29		10.48	87.38	1.85			
SW2	0.20		16.20	82.49	1.10			
SW3	0.35		38.85	60.30	0.50			
SW4	0.08		13.44	85.27	1.20			
SW5	0.03		37.79	61.55	0.64			
SW6	0.22		35.76	63.10	0.86			
SW7	0.04		12.80	86.11	1.05			
SW8	0.22		23.56	75.63	0.59			
SW9	0.12		24.67	74.53	0.68			
SW10	0.09		35.10	64.18	0.63			
SW11	0.08		54.75	44.89	0.28			
SW12	0.16		37.27	61.89	0.66			
SW13	0.06		64.74	32.98	0.22			
SW14	0.12		34.51	63.06	2.31			
SW15	0.09		53.05	46.03	0.83			
SW16	0.09		19.66	77.33	2.92			
SW17	0.39		28.90	67.78	2.93			
1UE	26.09	3.58	9.74	38.97	23.62	15.32		
2UE	0.93	5.17	45.90	42,48	5.50			
3BUE	2.25	2.74	76.80	17.30	0.91			
5UE	7.29	2.66	57.09	28.64	4.32	2.50		
6UE	2.88	6.26	67.40	21.32	2.13			
7UE	1.76	1.82	43.34	50.16	2.92			
1LE	23.15	15.95	33.29	15.92	1.75	9.94		
2LE	8.18	11.35	40.37	14.60	1.52	13.33	10.65	
3LE	4.77	29.23	46.49	11.33	1.35	6.82		
4LE	4.54	1.11	43.98	45.47	4.69			
5LE	1.14	6.61	89.05	3.12	0.07			
6LE	3.74	26.32	54.59	4.08	0.65	10.61		
7LE	0.04	22.22	65.31	11.83	0.28			
8LE	0.06	6.05	76.73	15.20	0.82			
9LE	0.11	18.35	41.29	36.35	3.29			
10LE	0.19	33.42	48.44	16.40	1.60			
11LE	0.02		3.48	88.09	8.35			
12LE	1.31	8.78	35.13	42.23	12.56			

REFERENCES CITED

ADAMS, J.A. & GRIERSON, R.J. (1974) The Eden Estuary. Marine Laboratory, Aberdeen. Internal Report New Series No. 4. 6pp.

ALLEN, G.P. (1970) Presentation d'un programme d'analyse granulometrique en Fortran IV. Bull. Inst. Geol. Bassin Aquitaine 8, 253-260.

ALLEN, G.P. (1971) Relationship between grain size parameter distribution and current patterns in the Gironde Estuary (France). J. sedim. Petrol. 41, 74-88.

ALLEN, G.P., CASTAING, P. & KLINGEBIEL, A. (1972) Distinction of elementary sand populations in the Gironde Estuary (France) by R-mode factor analysis of grain size data. Sedimentology 19, 21-35.

ALLEN, J.R.L. (1963) The classification of cross-stratified units, with notes on their origin. Sedimentology 3, 93-114.

ALLEN, J.R.L. (1968) Current Ripples. North Holland Pub. Co. Amsterdam.

BANKS, N.L. (1973) Origin and significance of some down-current dipping cross-stratified sets. J. sedim. Petrol. 43, 423-427.

BARR, J.L. DINKELMAN, M.G. & SANDUSKY, C.L. (1970) Large epoxy peels. J. sedim. Petrol. 40, 445-448.

BATES, C.C. (1953) Rational theory of delta formation. Bull. Am. Ass. Petrol. Geol. 37, 2119-2162.

BELDERSON, R.H. (1964) Holocene sedimentation in the Irish Sea. Mar. Geol. 2, 147-163.

BELT, E.S. (1975) Scottish Carboniferous cyclothem patterns and their palaeoenvironmental significance. In: Deltas, models for exploration. (Ed. by M.L.S. Broussard), pp. 427-449. Houston Geol. Soc. Texas.

BISCAYE, P.E. (1964) Mineralogy and sedimentation of the deep sea fine fraction in the Atlantic Ocean and adjacent seas and oceans. Dept. Geol. Yale Univ. Geochem. Tech. Rep. 8: 86 pp.

BODINE, M.W. & FERNALLD, T.H. (1973) EDTA dissolution of gypsum, anhydrite and Ca-Mg carbonates. J. sedim. Petrol. 43, 1152-1156.

BOUMA, A.H. (1969) Methods for the study of sedimentary structures. Wiley.

BRAITHWAITE, C.J.R. (1973) Settling behaviour related to sieve analysis of skeletal sands. Sedimentology 20, 251-262.

BREZINA, J. (1963) Classification and measures of grain size distribution (preliminary report). Vestnik UUG 409-414.

BURGER, J.A., KLEIN, G. de V. & SANDERS, J.E. (1969) A field technique for making epoxy relief-peels in sandy sediments saturated with salt water. J. sedim. Petrol. 39, 338-341.

CARVER, R.E. (1971) Procedures in sedimentary petrology. Wiley Interscience, New York.

CHISHOLM, J.I. (1964) In: Sum. Prog. geol. Surv. U.K. for 1964.

CHISHOLM, J.I. (1966) An association of raised beaches with glacial deposits near Leuchars, Fife. Bull. geol. Surv. Gt. Br. No. 24, 163-174.

CHISHOLM, J.I. (1971) The stratigraphy of the post-Glacial marine transgression in NE Fife. Bull. geol. Surv. Gt. Br. No. 37, 91-107.

CHISHOLM, J.I. & DEAN, J.M. (1974) The Upper Old Red Sandstone of Fife and Kinross: a fluviatile sequence with evidence of marine inclusion. Scott. J. Geol. 10, 1-30.

CHMELIK, F.B. (1967) Electro-osmotic core cutting. Mar. Geol. 5, 321-325.

CLIFTON, H.E., HUNTER, R.E. & PHILLIPS, R.L. (1971) Depositional structures and processes in the non-barred high-energy nearshore. J. sedim. Petrol. 41, 651-670.

COLLINSON, J. (1970) Bedforms of the Tana River, Norway. Geogr. Annlr. 52, 31-56.

CURRAY, J.R. (1960) Tracing sediment masses by grain size modes. 21st. Intern. Geol. Cong. Copenhagen. Proc. pt 23, 119-130.

DAVIS, J.C. (1973) Statistics and data analysis in geology. John Wiley, New York.

DOEGLAS, D.J. (1948) Interpreting the results of mechanical analysis. J. sedim. Petrol. 16, 19-40.

DOEGLAS, D.J. (1968) Grain size indices, classification and environment. Sedimentology 10, 83-100.

DOTT, R.L. (1964) Wacke, greywacke and matrix - what approach to immature sandstone classification? J. sedim. Petrol. 34, 625-632.

EMERY, K. (1945) Entrapment of air in beach sand. J. sedim. Petrol. 15, 39-49.

FOLK, R.L. (1954) The distinction between grain size and mineral composition in sedimentary rock nomenclature. J. Geol. 62, 344-359.

FOLK, R.L. (1966) A review of grain size parameters. Sedimentology 6, 73-93.

FOLK, R.L. (1968) Petrology of Sedimentary Rocks. Austin, Texas. Hemphills Book Store.

FOLK, R.L. & WARD, W.C. (1957) Brazos River bar - a study in the significance of grain size parameters. J. sedim. Petrol. 27, 3.26.

FRANK, W.M. & FRIEDMAN, G.M. (1973) Continental shelf sediments off New Jersey. J. sedim. Petrol. 43, 224-237.

GEIKIE, A. (1902) The Geology of Eastern Fife. Mem. geol. Surv. Gt. Br.

GIBBS, R.J. (1968) Clay mineral mounting techniques for X-ray diffraction analysis: a discussion. J. sedim. Petrol. 38, 242-243.

GLOVER, E.D. (1961) Method of solution of calcareous materials using the complexing agent EDTA. J. sedim. Petrol. 31, 622-626.

GREENSMITH, J.T. (1965) Calciferous Sandstone Series sedimentation at the eastern end of the midland valley of Scotland. J. sedim. Petrol. 35, 223-242.

GRIFFITHS, J.C. (1967) Scientific Method in the Analysis of Sediments. McGraw-Hill, New York.

GROSS, D.L. & MORAN, S.R. (1970) A technique for the rapid determination of light minerals in detrital sands. J. sedim. Petrol. 40, 759-761.

HAILS, J.R., SEWARD-THOMPSON, B. & CUMMINGS, Lynne (1973) An appraisal of the significance of sieve intervals in grain size analysis for environmental interpretation. J. sedim. Petrol. 43, 889-893.

HAMBLIN, W.K. (1971) 'X-ray radiography' in: Procedures in Sedimentary Petrology (Ed. by R.E. Carver). Wiley Interscience, New York.

HANSEN, D.V. & RATTRAY, M. (1966) New dimensions in estuary classification. Limnol. Oceanogr. 11, 319-326.

HARBAUGH, J.W. & MERRIAM, D.F. (1968) Computer Applications in Stratigraphic Analysis. John Wiley & Sons Inc., New York.

HARTWELL, A.D. (1970) Hydrography and Holocene sedimentation in the Merrimack River estuary. Dept. Geol. Univ. Mass. Pub. No. 5 - CRG.

HAYES, M.O. (1971) Geomorphology and sedimentation in New England estuaries. In: The Estuarine Environment (Ed. by J.R. Schubel). AGI.

HOYT, J.H. & VERNON, J.H. (1964) Development and geologic significance of soft beach sand. Sedimentology 3, 44-51.

INMAN, D.L. (1952) Measures for describing the size distribution of sediments. J. sedim. Petrol. 22, 125-145.

IRANI, R.R. & CALLIS, C.F. (1967) Particle Size, Measurement, Interpretation and Application. John Wiley & Sons Inc., New York.

JACKSON, WHITTING & PENNINGTON (1949) In: Procedures in Sedimentary Petrology (Ed. by R.E. Carver). Wiley Interscience, New York.

JONES, T.A. (1970) Comparison of descriptors of sediment grain size distributions. J. sedim. Petrol. 40, 1204-1215.

JOPLING, A.V. & WALKER, R.G. (1968) Morphology and origin of ripple-drift cross-lamination, with examples from the Pleistocene of Massachussetts. J. sedim. Petrol. 38, 971-984.

KLEIN, G. de V. (1970) Depositional and dispersal dynamics of intertidal sand bars. J. sedim. Petrol. 40, 1095-1127.

KLEIN, G. de V. (1971) Peels and Impressions. In: Procedures in Sedimentary Petrology (Ed. by R.E. Carver). Wiley Interscience, New York.

KLOVAN, J.E. (1975) R and Q-Mode Factor Analysis. In: Concepts in Geostatistics (Ed. by R.B. McCammon). Springer-Verlag, Berlin.

KNAUSS, J.A. (1963) Drogues and neutral-buoyant floats. In: The Sea, vol. 2 (Ed. by M.N. Hill). Interscience, New York.

KRANCK, Kate (1975) Sediment deposition from flocculated suspensions. Sedimentology 22, 111-123.

KRINITZSKY, E.L. (1970) Radiography in the Earth Sciences and Soil Mechanics. Plenum Press, New York.

KRINSLEY, D. & DONAHUE, J. (1968) Environmental interpretation of sand grain surface textures by electron microscopy. Bull. geol. Soc. Am. 79, 743-748.

KRINSLEY, D. & MARGOLIS, S.V. (1971) Grain Surface Texture. In: Procedures in Sedimentary Petrology (Ed. by R.E. Carver), pp. 151-180. Wiley Interscience, New York.

KRUMBEIN, W.C. & PETTIJOHN, F.J. (1938) Manual of Sedimentary Petrography. Appleton-Century-Crofts, New York.

MacGREGOR, A.R. (1968) Fife and Angus Geology. Blackwood and Sons Ltd., Edinburgh.

MAIKLEM, W.R. (1968) Some hydraulic properties of bioclastic carbonate grains. Sedimentology 10, 101–109.

MATHER, P.M. (1972) Study of factors influencing variation in size characteristics of fluvioglacial sediments. Math. Geol. 4, 219–234.

McCAMMON, R.B. (1962) Efficiencies of percentile measures for describing the mean size and sorting of sedimentary particles. J. Geol. 70, 453–465.

MEISTRELL, F.J. (1972) The spit-platform concept: Laboratory observation of spit development. In: Spits and Bars (Ed. by M.L. Schwartz), pp. 225–283. Dowden, Hutchinson and Ross, Stroudsberg, Pa.

MOSS, A.J. (1962) The physical nature of common sandy and pebbly deposits, 1. Am. J. Sci. 260, 337–373.

MOSS, A.J. (1963) The physical nature of common sandy and pebbly deposits, 2. Am. J. Sci. 261, 297–343.

MOSS, A.J. (1972) Bed-load sediments. Sedimentology 18, 159–219.

MÜLLER, G. (1967) Sedimentary Petrology. Part 1: Methods in Sedimentary Petrology (translated by Schminke). Hafner Pub. Co.

OERTEL, G.F. (1972) Sediment transport in estuary entrance shoals and the formation of swash platforms. J. sedim. Petrol. 42, 858–863.

ONDRICK, C.W. & SRIVASTAVA, G.S. (1970) CORFAN-FORTRAN IV Computer program for correlation, factor analysis (R and Q-mode) and varimax rotation. Kansas geol. Surv. Computer Contr. 42.

PASSEGA, R. (1957) Texture as a characteristic of clastic deposition. Bull. Am. Ass. Petrol. Geol. 41, 1952–1984.

PASSEGA, R. (1964) Grain size representation by CM patterns as a geologic tool. J. sedim. Petrol. 34, 830–847.

PASSEGA, R. & BYRAMJEE, R. (1969) Grain-size image of clastic deposits. Sedimentology 13, 233–252.

PATERSON, I.B. (1974) The supposed Perth Readvance in the Perth district. Scott. J. Geol. 10, 53–66.

PERKINS, E.J. (1960) The diurnal rhythm of the littoral diatoms of the River Eden estuary, Fife. J. Ecol. 48, 725–728.

PRICE, W.A. (1963) Patterns of flow and channelling in tidal inlets. J. sedim. Petrol. 33, 279–290.

PRITCHARD, D.W. (1955) Estuarine circulation patterns. Proc. Am. Soc. Civ. Eng. 81, 717-

REINECK, H.E. & SINGH, I.B. (1973) Depositional Sedimentary Environments, pp. 439. Springer-Verlag, Berlin.

ROBINSON, A.H.W. (1960) Ebb-flood channel systems in sandy bays and estuaries. Geography 45, 183–199.

ROYAL COMMISSION ON COASTAL EROSION, 1907.

SCHÄFER, W. (1972) Ecology and Paleoecology of Marine Environments (translated by I. Oertel). Ed. by G.Y. Craig. Oliver & Boyd, Edinburgh.

SCHÜBEL, J.R. (1971) The Estuarine Environment. AGI.

SCULL, B.J. (1960) Removal of heavy liquid separates from glass centrifuge tubes – alternate method. J. sedim. Petrol. 30, 626.

SETLOW, L.W. & KARPOVITCH, R.P. (1972) 'Glacial' microtextures on quartz and heavy mineral sand grains from the littoral environment. J. sedim. Petrol. 42, 864–875.

SISSONS, J.B. (1967) The Evolution of Scotland's Scenery. Oliver & Boyd, Edinburgh.

SISSONS, J.B. SMITH, D.E. & CULLINGFORD, R.A. (1966) Late Glacial and Post-Glacial Shorelines in S.E. Scotland. Inst. Br. Geog. Trans. 39, 9–18.

SNEED, E.D. & FOLK, R.L. (1958) Pebbles in the lower Colorado River, Texas, a study in particle morphogenesis. J. Geol. 66, 114–150.

STANLEY, D.J. (1969) Armoured mud balls in an intertidal environment, Minas Basin, south-east Canada. J. Geol. 77, 683–693.

SWALLOW, J.C. (1955) A neutral-buoyant float for measuring deep currents. Deep-Sea Research 3, 74–81.

TAY ESTUARY RESEARCH CENTRE (1971) Investigations in the estuarine environments of the Tay: Physical aspects:- an interim report (Ed. by A.T. Buller, J. McManus, D.J.A. Williams).

TRASK, P.D. (1932) Origin and environment of source sediments of petroleum. Gulf Pub. Co., Houston.

VAN STRAATEN, L.M.J.U. (1954) Composition and structure of recent marine sediments in the Netherlands. Leid. geol. Meded. 19, 1–110.

VAN STRAATEN, L.M.J.U. & KUENEN, PH. (1958) Tidal action as a cause clay accumulation. J. sedim. Petrol. 28, 406.

VISHER, G.S. (1965) Fluvial processes as interpreted from ancient and recent fluvial deposits. In: Primary Sedimentary Structures and their Hydrodynamic Interpretation (Ed. by G.V. Middleton). Spec. Publ. Soc. Econ. Palaeont. Miner., Tulsa, 12, 116–132.

VISHER, G.S. (1969) Grain size distributions and depositional processes. J. sedim. Petrol. 39, 1074–1106.

WARD, (1963) cited in Wishart, D. (1970) Fortran IV programs for eight methods of Cluster Analysis (Clustan 1). Computer Contrib. 38, State geol. Surv. Kansas, Lawrence.

WENTWORTH, C.K. (1922) A scale of grade and class terms for clastic sediments. J. Geol. 30, 377.

WILSON, J.H. (1910) Nature Study Rambles Around St. Andrews. W.C. Henderson, Univ. Press, St. Andrews.

WISHART, D. (1970) FORTRAN IV programs for eight methods of cluster analysis (Clustan 1). Computer Contrib. 38, State geol. Surv. Univ. Kansas, Lawrence.

Additional Reference

JOPLING, A.V. (1965) Laboratory Study of the Distribution of Grain Sizes in Cross-Bedded Deposits. In: Primary Sedimentary Structures and their Hydrodynamic Interpretation (Ed. by G.V. Middleton). Spec. Publ. Soc. Econ. Palaeont. Miner., Tulsa, 12, 53–65.